



uOttawa

L'Université canadienne
Canada's university

**FACULTÉ DES ÉTUDES SUPÉRIEURES
ET POSTDOCTORALES**



uOttawa

L'Université canadienne
Canada's university

**FACULTY OF GRADUATE AND
POSTDOCTORAL STUDIES**

Jennifer L. Thropp

AUTEUR DE LA THÈSE / AUTHOR OF THESIS

M.Sc. (Geography)

GRADE / DEGREE

Department of Geography

FACULTÉ, ÉCOLE, DÉPARTEMENT / FACULTY, SCHOOL, DEPARTMENT

Spatial and Temporal Variability in Permafrost Conditions, Northern Canada

TITRE DE LA THÈSE / TITLE OF THESIS

Antoni Lewkowicz

DIRECTEUR (DIRECTRICE) DE LA THÈSE / THESIS SUPERVISOR

Sharon Smith

CO-DIRECTEUR (CO-DIRECTRICE) DE LA THÈSE / THESIS CO-SUPERVISOR

Bernard Lauriol

Christophe Burn

Gary W. Slater

Le Doyen de la Faculté des études supérieures et postdoctorales / Dean of the Faculty of Graduate and Postdoctoral Studies

**SPATIAL AND TEMPORAL VARIABILITY IN
PERMAFROST CONDITIONS, NORTHERN CANADA**

Jennifer Throop

Thesis submitted to the
Faculty of Graduate and Postdoctoral Studies
In partial fulfillment of the requirements
For the Master of Science degree in Geography

Department of Geography
Faculty of Arts
University of Ottawa

© Jennifer Throop, Ottawa, Canada, 2010



Library and Archives
Canada

Published Heritage
Branch

395 Wellington Street
Ottawa ON K1A 0N4
Canada

Bibliothèque et
Archives Canada

Direction du
Patrimoine de l'édition

395, rue Wellington
Ottawa ON K1A 0N4
Canada

Your file *Votre référence*
ISBN: 978-0-494-69102-1
Our file *Notre référence*
ISBN: 978-0-494-69102-1

NOTICE:

The author has granted a non-exclusive license allowing Library and Archives Canada to reproduce, publish, archive, preserve, conserve, communicate to the public by telecommunication or on the Internet, loan, distribute and sell theses worldwide, for commercial or non-commercial purposes, in microform, paper, electronic and/or any other formats.

The author retains copyright ownership and moral rights in this thesis. Neither the thesis nor substantial extracts from it may be printed or otherwise reproduced without the author's permission.

In compliance with the Canadian Privacy Act some supporting forms may have been removed from this thesis.

While these forms may be included in the document page count, their removal does not represent any loss of content from the thesis.

AVIS:

L'auteur a accordé une licence non exclusive permettant à la Bibliothèque et Archives Canada de reproduire, publier, archiver, sauvegarder, conserver, transmettre au public par télécommunication ou par l'Internet, prêter, distribuer et vendre des thèses partout dans le monde, à des fins commerciales ou autres, sur support microforme, papier, électronique et/ou autres formats.

L'auteur conserve la propriété du droit d'auteur et des droits moraux qui protègent cette thèse. Ni la thèse ni des extraits substantiels de celle-ci ne doivent être imprimés ou autrement reproduits sans son autorisation.

Conformément à la loi canadienne sur la protection de la vie privée, quelques formulaires secondaires ont été enlevés de cette thèse.

Bien que ces formulaires aient inclus dans la pagination, il n'y aura aucun contenu manquant.


Canada

ABSTRACT

The data from nine permafrost thermal monitoring sites at widely separated locations across northern Canada were examined individually, spatially, and temporally. Three sites are in Nunavut (Alert, Iqaluit, and Baker Lake), two in the Northwest Territories (Table Mountain and Wrigley), and four in the Yukon Territory (Wolf Creek, Sixty Mile, Alpine Burwash, and Red Creek). The sites have between one and five boreholes that are instrumented to between 3 and 60 m with records of varying durations. Most of the boreholes are co-located with weather stations recording air temperatures and snow depths.

A comprehensive analysis of each site is presented assessing the relations between climate and permafrost temperatures, both in the near surface and at depth. The local characteristics at each site, and among sites, were assessed using various methods including mean annual temperatures, surface and thermal offsets, n-factors, and the apparent thermal diffusivity. Time series analyses were conducted at sites with longer air and ground temperature data records.

Regional mean annual air temperatures were defined as the primary determinant of permafrost temperatures at the study sites, but this relationship is modulated by snow (depth, duration, and timing) and vegetation characteristics, the substrate material, and the moisture content, both frozen and unfrozen, within the active layer and the permafrost. Of the study sites, permafrost temperatures at Iqaluit are the most sensitive to changes in climate due to little buffering between the air and the permafrost, and permafrost temperatures at Wrigley, Table Mountain, and Wolf Creek are the least sensitive to changes in climate due to the significant latent heat effects in this isothermal permafrost associated with high amounts of ice and unfrozen moisture.

Climatic cooling was observed in the earlier part of the record at Iqaluit from the late 1940's until the early 1990's, and at Alert between the early 1950's and the mid 1970's. Climatic warming was observed in mean annual and winter average temperatures at Alert, Baker Lake, Iqaluit, Table Mountain, and Wrigley in recent decades. This was reflected in warming permafrost temperatures at all of the long-term thermal monitoring sites. The greatest magnitude of ground temperature warming occurred at Iqaluit (+1.6 to +1.9°C/decade), then Alert (+0.2 to +0.6°C/decade), and Baker Lake (+0.3°C/decade). Ground temperatures at Table Mountain warmed the least (+0.1 to +0.2°C/decade), but the warming at this site is important because it represents a progressive change in unfrozen moisture in the fine-grained, ice rich permafrost.

ACKNOWLEDGEMENTS

Most importantly I must thank my two supervisors, Dr. Antoni G. Lewkowitz and Dr. Sharon L. Smith, for all of their guidance and support over the past few years. I would like to express my appreciation for the valuable time and energy they have spent helping to improve my work, and for inspiring me with their knowledge and enthusiasm on permafrost science. I am extremely grateful for the experience that I have gained while working with Toni and Sharon.

This research would not have been possible without the financial assistance provided by the International Polar Year program, the Geological Survey of Canada, and the Northern Scientific Training Program. My field season in the Yukon was a success thanks to the generous “donations” of boreholes from Doug, Lorna, and Heather at Archer Cathro & Associates, Scott at Western Copper Corporation, and Kevin at Largo Resources Ltd. I would also like to express my appreciation to the Geological Survey of Canada and Environment Canada for supplying much of the data used in this thesis.

I must acknowledge my field companions, Amaris Page, Natasha Harvey, and Debi Wickham. During my two field seasons I was fortunate to have helpful and competent individuals whose company I enjoyed very much. An extra thanks to Debi and Mark, who let us pitch our tents on their beautiful property in West Dawson on numerous occasions.

I am also very thankful to many other students who have provided both emotional and intellectual support along the way. I would like to express my gratitude to these individuals in particular: Philip Bonnaventure, Marian Kremer, and Tara Paull. Many other individuals along the way have provided inspiration and advice, and have shared stories of similar challenges.

And finally, to my family, who have supported me immensely since I began my master’s degree in 2007. I am thankful for their continued understanding and patience. In particular I am grateful to my grandmother, Charlotte Orton, and my partner, Ryan Christie.

TABLE OF CONTENTS

<i>Abstract</i>	ii
<i>Acknowledgements</i>	iii
<i>Table of Contents</i>	iv
<i>List of Figures</i>	vi
<i>List of Tables</i>	xii
<i>Definitions and Symbols</i>	xv
1. INTRODUCTION	1
1.1 BACKGROUND	1
1.2 RESEARCH OBJECTIVES	3
1.3 STRUCTURE OF THE THESIS	4
2. BACKGROUND: CLIMATE – PERMAFROST INTERACTIONS	5
2.1 INTERACTIONS BETWEEN THE AIR AND THE GROUND SURFACE	5
2.1.1 <i>Snow</i>	5
2.1.2 <i>Surface Offset</i>	6
2.1.3 <i>Thawing and Freezing Degree Days</i>	7
2.1.4 <i>N-factors</i>	8
2.2 GROUND SURFACE AND PERMAFROST INTERACTIONS	10
2.2.1 <i>Thermal Offset</i>	10
2.2.2 <i>Unfrozen Moisture and Latent Heat</i>	11
2.2.3 <i>The Zero-Curtain Effect</i>	12
2.3 THERMAL STATE AND CHANGES OF PERMAFROST	13
2.3.1 <i>Amplitude, Thermal Diffusivity, ZAA, and Phase Lag</i>	13
2.3.2 <i>Permafrost Thickness</i>	17
2.3.3 <i>Changes over time – Climate and Permafrost</i>	18
3. METHODOLOGY	20
3.1 METHODS USED FOR INDIVIDUAL SITE ANALYSIS	20
3.1.1 <i>MAAT, MAGST, TTOP, Surface Offset and Thermal Offset</i>	20
3.1.2 <i>TDD, FDD, and N-factors</i>	21
3.1.3 <i>Snow Data Analysis</i>	22
3.1.4 <i>Temperature Envelopes</i>	23
3.1.5 <i>Amplitude, Apparent Thermal Diffusivity, and Phase Lags</i>	23
3.2 TEMPORAL ANALYSIS	25
3.2.1 <i>Hind-casting Air Temperature ‘Record’</i>	25
3.2.2 <i>Standardization of Ground Temperature ‘Record’</i>	29
4. SITE DESCRIPTIONS AND RESULTS	34
4.1 ALERT, NUNAVUT	35

4.1.1 Alert BH1 and BH2	40
4.1.2 Alert BH3	43
4.1.3 Alert BH4	49
4.1.4 Alert BH5	53
4.1.5 Regional Climatic Trends at Alert, Nunavut.....	60
4.1.6 Synthesis of Alert Boreholes	63
4.2 IQALUIT, NUNAVUT	67
4.3 BAKER LAKE, NUNAVUT	78
4.3.1 Influence of a snow-fence induced snow drift at Baker Lake, Nunavut	89
4.4 SIXTY MILE, YUKON	92
4.5 RED CREEK, YUKON.....	97
4.6 ALPINE BURWASH – KLUANE RANGE, YUKON	103
4.7 TABLE MOUNTAIN, NORTHWEST TERRITORIES	108
4.8 WRIGLEY, NORTHWEST TERRITORIES.....	116
4.9 WOLF CREEK, YUKON	124
4.9.1 Wolf Creek Aggradational Permafrost Mound.....	126
4.9.2 Wolf Creek Palsa 25	130
5. DISCUSSION.....	135
5.1 INTER-SITE COMPARISONS	135
5.1.1 MAAT.....	135
5.1.2 MAGT.....	138
5.1.3 Apparent Thermal Diffusivity	140
5.1.4 n_r	142
5.1.5 n_f	145
5.1.6. Moisture Content	148
5.1.7 Site Typology.....	150
5.2 CHANGES OVER TIME.....	156
5.2.1 Response of the ground to air temperature trends.....	156
5.2.2 Seasonal Correlations.....	162
5.3 LIMITATIONS OF THE STUDY	165
5.4 FUTURE RECOMMENDATIONS	165
6. CONCLUSION	167
REFERENCES	172
APPENDIX A.....	180
APPENDIX B	181
APPENDIX C.....	185

LIST OF FIGURES

Figure 1.1: Location map of the thermal monitoring sites in relation to the permafrost zones across Canada.	3
Figure 3.1: Ground temperature time series at Alert BH3.....	24
Figure 3.2: Relationship between monthly average air temperatures at the Alert BH3 on-site weather station and the Alert ECCS from 2000 to 2006.....	26
Figure 3.3: Hind-cast MAATs at Alert BH3 from correlated Alert ECCS data between 1950 and 2006, and actual measured on-site MAAT between 2000 and 2008.....	28
Figure 3.4: Hind-cast seasonal average air temperatures at Alert BH3 between 1950 and 2006 from correlated ECCS data, and actual measured seasonal average air temperatures between 2000 and 2008.	28
Figure 3.5: The average deviations from the MAGT for each 10-day period at depths above ZAA at Alert BH3.	32
Figure 4.1: Location map of five boreholes at Alert, Nunavut.....	36
Figure 4.2: Photograph of Alert BH1 taken in August, 2001.	37
Figure 4.3: Photograph of Alert BH2 taken in August, 2001.	37
Figure 4.4: Photograph of Alert BH3 weather station and borehole, taken in August, 2002.....	38
Figure 4.5: Photograph of weather station at Alert BH4, taken in August 2002.....	38
Figure 4.6: Photograph taken from Alert BH5 looking toward Alert BH4 at the shore of the lake, taken in August, 2002.	39
Figure 4.7: Photograph of weather station and borehole at Alert BH5, taken in August 2002.....	39
Figure 4.8: Mean ground temperature profiles at Alert, Nunavut, BH1 and BH2 for the Years 1978-79, 1979-80, 1990-91 and 2005-06.	41
Figure 4.9: MAGTs at Alert BH1, from 18.3 m and deeper, between 1978 and 2007...42	42
Figure 4.10: MAGTs at Alert BH2, from 18.3 m and deeper, between 1978 and 2007.42	42
Figure 4.11: Air, ground surface, and 2.4 m temperatures, and snow depths between 2000 and 2005 at Alert BH3.	43
Figure 4.12: Relationship between SDD and surface offsets at Alert BH3 between 2002 and 2008.....	45
Figure 4.13: Relationship between average snow depths and n_f at Alert BH3 between 2002 and 2008.....	46
Figure 4.14: Temperature envelope at Alert BH3 for the year 2003-04.....	48
Figure 4.15: Time series of MAGTs from Alert BH3 and MAAT calculated using Alert ECCS data between 1978 and 2004.....	49
Figure 4.16: Air temperatures, ground surface temperatures, and snow depths at Alert BH4 between 2002 and 2008.....	50
Figure 4.17: Temperature envelopes at Alert BH4 for (A) 2001-02, and (B) 2007-08. .53	53
Figure 4.18: MAAT and MAGST trends at Alert BH5 between 2000 and 2008 from continuously logged on-site data.	55

Figure 4.19: MAGTs between 2000 and 2008 at Alert BH5 from continuously logged data.....	58
Figure 4.20: MAGT depth profiles at Alert BH5, Nunavut, from 2000 to 2008.....	58
Figure 4.21: Temperature envelope at Alert BH5, Nunavut, for 2000-01.....	59
Figure 4.22: MAGTs calculated from manual measurements and correlated MAATs from ECCS data from 1978 to 2000 at Alert BH5.....	60
Figure 4.23: Hind-cast MAATs at Alert BH3, BH4 and BH5 from correlated Alert, Nunavut, ECCS data between 1950 and 2006.....	61
Figure 4.24: Comparison of measured on-site MAAT from 2000 to 2008 with the values calculated from correlations with the Alert ECCS data between 2001 and 2006 for Alert BH3, BH4, and BH5.	61
Figure 4.25: Seasonal average air temperatures at Alert BH3, BH4, and BH5 from hind-cast monthly Alert ECCS data.....	62
Figure 4.26: MAGT profiles at the five borehole sites in Alert, Nunavut; one from early in the record, and one from recent years.....	64
Figure 4.27: MAGTs at all of the boreholes and MAAT from BH3, BH4 and BH5 using correlated ECCS data between 1978 and 2008.	65
Figure 4.28: Photograph of the weather station at the Iqaluit permafrost thermal monitoring site in Nunavut.	68
Figure 4.29: Photograph of the weather station at the Iqaluit permafrost thermal monitoring site in Nunavut.	68
Figure 4.30: Relationships at Iqaluit (A) BH1 and (B) BH2 between MAAT and the corresponding MAGT at 5 m based on phase lags from 1988 to 2004 ..	70
Figure 4.31: Temperature envelopes at Iqaluit (A) BH1 and (B) BH2 for the year 2002-03.	73
Figure 4.32: MAGTs and MAATs at Iqaluit BH1 from 1989-2004.....	74
Figure 4.33: MAGTs and MAATs at Iqaluit BH2 from 1988-2004.....	74
Figure 4.34: Hind-cast values of MAGT for 5 m depth at Iqaluit BH2 between 1948 and 2007 plotted alongside the measured MAGT at 5 m from 1988 to 2004.....	75
Figure 4.35: Hind-cast MAAT at the Iqaluit borehole sites from 1948 to 2007.	76
Figure 4.36: Hind-cast seasonal air temperatures at the Iqaluit borehole sites between 1947 and 2007.....	77
Figure 4.37: Photograph of Baker Lake BH2, looking away from the town and towards the snow fence (upwind).	79
Figure 4.38: Photograph of Baker Lake BH4 (undisturbed site) and the weather station, looking towards the snow fence and the lake (down wind).	80
Figure 4.39: Temperature time-series from manual measurements taken at 3 m depth for all four boreholes, and the average winter air temperatures at Baker Lake, Nunavut, from correlated ECCS data between 1997 and 2005.	81
Figure 4.40: Air and ground surface temperatures, and snow depths at Baker Lake BH4 between July 2002 and March 2008.....	82
Figure 4.41: Monthly average air and ground surface temperatures at BH2 and BH4 from 2002 to 2008 at Baker Lake, Nunavut.	83
Figure 4.42: Temperature envelope at Baker Lake BH4, Nunavut, 2005-06.....	86

Figure 4.43: Changes in MAGTs from manual measurements at Baker Lake BH4 and MAAT from correlated ECCS data between 1997 and 2007.	86
Figure 4.44: A) Relationship between MAGTs at 3 m, based on the September 1 to August 31 year, and MAAT, based on the June 1 to May 31 year, between 1997 and 2007 at Baker Lake BH4, and B) Hind-cast 3 m MAGTs based on the best-fit equation from 1951 to 2007, plotted with MAGTs from manual and continuous measurements.	87
Figure 4.45: MAATs from correlated ECCS data between 1951 and 2007 at Baker Lake, Nunavut.	88
Figure 4.46: Trends in the seasonal average air temperatures at Baker Lake, Nunavut, between 1952 and 2008, derived from correlated ECCS data.	89
Figure 4.47: Air and ground surface temperature at Baker Lake BH2 and BH4.	90
Figure 4.48: Temperature envelopes at Baker Lake BH2 and BH4, taken from manual measurements between 1997 and 2005.	91
Figure 4.49: Thaw depths at Baker Lake BH2 and BH4 between 1997 and 2005.	92
Figure 4.50: Photograph of the weather station at Sixty Mile, Yukon Territory, taken on July 17, 2008.	93
Figure 4.51: Depth profile of the Sixty Mile borehole showing the location of the thermistors in relation to the overlying terrain.	93
Figure 4.52: Air and ground surface temperatures with snow depths at Sixty Mile, Yukon, between August 20, 2007 and September 2, 2009.	94
Figure 4.53: Shallow ground temperatures at the Sixty Mile borehole between July 17, 2008 and September 3, 2009.	96
Figure 4.54: Deeper ground temperatures from the Sixty Mile borehole between July 17, 2008 and September 3, 2009.	96
Figure 4.55: Temperature envelope at the Sixty Mile borehole for the 2008-09 year.	97
Figure 4.56: Photograph of the Red Creek borehole, Yukon Territory, taken on July 19, 2008.	98
Figure 4.57: Temperatures at the ground surface, 10, 25, and 50 cm deep, and snow depths at Red Creek, Yukon, from August 28, 2007 to July 19, 2008.	99
Figure 4.58: Ground temperatures at 0.5 m at Red Creek between August 2007 and August 2009.	101
Figure 4.59: Ground temperature time series at Red Creek, Yukon, between October 3, 2007 and September 4, 2009.	102
Figure 4.60: Temperature envelopes at Red Creek, Yukon, for the years October 3, 2007 to October 2, 2008, and September 1, 2008 to August 31, 2009.	103
Figure 4.61: Photograph of the Alpine Burwash borehole during drilling, taken on August 16, 2008.	104
Figure 4.62: Depth profile of the Alpine Burwash borehole showing the location of the thermistors in relation to the overlying terrain.	104
Figure 4.63: Daily air, ground surface, and 60 cm temperature, and snow depths at Alpine Burwash, Kluane Range, from August 18, 2008 to September 14, 2009.	106
Figure 4.64: Daily ground temperatures at the Alpine Burwash, Kluane Range, borehole between August 18, 2008 and September 14, 2009.	107

Figure 4.65: Monthly average temperature profiles from September 2008 to August 2009 at the Alpine Burwash – Kluane Range borehole.	107
Figure 4.66: Photograph of the weather station and borehole at Table Mountain, taken in September, 2003.	108
Figure 4.67: Daily air temperature, ground surface temperature, and snow depth trends at Table Mountain, NWT, between September 2002 and September 2006.	110
Figure 4.68: TTOP at Table Mountain, NWT, between 1996 and 2007.	112
Figure 4.69: Temperature Envelope at Table Mountain, NWT, in 1998-99.	113
Figure 4.70: MAGTs at Table Mountain, NWT, at all depths below ZAA between 1985 and 2007.	114
Figure 4.71: MAATs at Table Mountain, NWT, calculated from Fort Simpson ECCS data between 1964 and 2008, and the on-site measured values between 2001 and 2008.	115
Figure 4.72: Seasonal average air temperatures at Table Mountain, NWT, from correlated Fort Simpson ECCS data between 1963 and 2008, and on-site measured air temperatures from 2001 to 2008.	116
Figure 4.73: Photo of weather station at Wrigley borehole site, taken in August, 2002.	117
Figure 4.74: Air and ground surface temperatures, and snow depths at Wrigley, NWT, between June 2001 and September 2008.	118
Figure 4.75: Temperature envelope at Wrigley, NWT, for 2005-06.	121
Figure 4.76: MAGTs at 1.5, 2.5, and 3.5 m depth at Wrigley, NWT, between 2003 and 2008.	122
Figure 4.77: MAAT at Wrigley, NWT, hind-cast from Fort Simpson ECCS between 1964 and 2008, and on-site MAAT from 2001 to 2008.	123
Figure 4.78: Seasonal average air temperatures at Wrigley, NWT, from correlated Fort Simpson ECCS data from 1963 to 2008, and on-site seasonal averages between 2001 and 2008.	124
Figure 4.79: Photographs of the Wolf Creek Aggradational Permafrost Mound borehole site.	125
Figure 4.80: Photographs of Wolf Creek Palsa 25 borehole site.	125
Figure 4.81: Air and ground surface temperatures with snow depths at the Wolf Creek APM site between August 2004 and August 2008.	127
Figure 4.82: Ground surface and 25 cm temperature trends at Wolf Creek APM site, between July 2005 and July 2008.	129
Figure 4.83: Temperature envelope at Wolf Creek APM between June 1, 2007 and May 31, 2008.	130
Figure 4.84: Air and ground surface temperatures and snow depths from Palsa 25 in Wolf Creek, Yukon, between September 2006 and July 2008.	131
Figure 4.85: Ground temperature trends at 0.5 and 1 m from Palsa 25, Wolf Creek, Yukon Territory.	133
Figure 4.86: Ground temperature time series in borehole at Wolf Creek Palsa 25 below the active layer between August 2004 and July 2008.	134
Figure 4.87: Temperature envelope at Palsa 25, Wolf Creek, Yukon, for the year 2007-08.	134

Figure 5.1: Relationship between MAGTs and MAATs from all of the boreholes.136

Figure 5.2: Relationship between average MAAT with thaw depth at both the bedrock and sediment sites.138

Figure 5.3: The apparent thermal diffusivity against depth at each borehole.....141

Figure 5.4: The relationship between MAGTs from each site and the depth of ZAA. ..142

Figure 5.5: The relation between SDD and n_f for individual years for sites Alert, Baker Lake, Sixty Mile, Alpine Burwash, Table Mountain, Wrigley, and Wolf Creek APM and Palsa 25.147

Figure 5.6: Permafrost temperatures at A) Red Creek between 2007 and 2009, B) Wolf Creek Palsa 25 between 2006 and 2008 and C) Wolf Creek APM between 2006 and 2008.149

Figure 5.7: Relationship between the annual range of monthly average air temperatures and ground temperatures near 1.0 m depth.151

Figure 5.8: Range of temperatures at Alert BH5 for both the air and the ground at 0.8 m between July 17, 2002 and September 2, 2003.....153

Figure 5.9: Range of temperatures at Baker Lake BH4 for both the air and the ground at 1.0 m between July 17, 2002 and September 2, 2003.....153

Figure 5.10: Range of temperatures at Sixty Mile for both the air and the ground at 1.5 m between July 17, 2008 and September 2, 2009.....154

Figure 5.11: Range of temperatures at Wolf Creek Palsa 25 for both the air and the ground at 1.0 m between July 17, 2005 and September 2, 2006.155

Figure 5.12: Range of temperatures at Table Mountain for both the air and the ground at 1.0 m between July 17, 2002 and September 2, 2003.....156

Figure 5.13: MAGT profiles at all sites that warmed over the monitoring period: A – Alert BH1; B – Alert BH2; C – Alert BH4; D – Alert BH5; E – Iqaluit BH1 and BH2; F – Table Mountain.....158

Figure 5.14: MAAT trends at Table Mountain and Wrigley, Baker Lake, Iqaluit and Alert BH3, BH4 and BH5, all from correlated ECCS data.159

Figure 5.15: December to May average temperatures at Iqaluit between 1948 and 1993.....161

Figure 5.16: The three significant correlations between the residuals of (A) summer ground temperatures and 2 year lagged spring air temperatures at Alert BH2; (B) summer ground temperatures and autumn air temperatures, no lag, at Alert BH5; and (C) summer ground temperatures and summer air temperatures, no lag, at Table Mountain.164

Figure B-1: Relationship between monthly average air temperatures at the Alert BH4 on-site weather station and the Alert ECCS (Environment Canada, 2008) from 2000 to 2006.181

Figure B-2: Relationship between monthly average air temperatures at the Alert BH5 on-site weather station and the Alert ECCS (Environment Canada, 2008) from 2000 to 2006.181

Figure B-3: Relationship between monthly average air temperatures at the Baker Lake on-site weather station and the Baker Lake ECCS (Environment Canada, 2009) from 2002 to 2006.182

Figure B-4: Relationship between monthly average air temperatures at the Iqaluit on-site weather station and the Iqaluit ECCS (Environment Canada, 2009) from 2000 to 2004.....	182
Figure B-5: Relationship between the average air temperatures during the spring months (March, April, and May) at the Table Mountain on-site weather station and the Fort Simpson ECCS (Environment Canada, 2009) from 2002 to 2008.	183
Figure B-6: Relationship between the average air temperatures during the summer months (June, July, and August) at the Table Mountain on-site weather station and the Fort Simpson ECCS (Environment Canada, 2009) from 2002 to 2008.	183
Figure B-7: Relationship between the average air temperatures during the autumn months (September, October, and November) at the Table Mountain on-site weather station and the Fort Simpson ECCS (Environment Canada, 2009) from 1999 to 2007.	184
Figure B-8: Relationship between the average air temperatures during the winter months (December, January, and February) at the Table Mountain on-site weather station and the Fort Simpson ECCS (Environment Canada, 2009) from 1999 to 2008.	184
Figure C-1: The average deviations from the MAGT for each 10-day period at Alert BH4.....	186
Figure C-2: The average deviations from the MAGT for each 10-day period at Alert BH5.....	188
Figure C-3: The average deviations from the MAGT for each 10-day period at Baker Lake BH4.....	190

LIST OF TABLES

Table 3.1: Table of average deviations from MAGT at Alert BH3 based on data from 2000 to 2004.	31
Table 3.2: Manual measurements at Alert BH3 between September 1982 and August 1983.....	32
Table 3.3: Calculated values from manual measurements at Alert BH3 between September 1982 and August 1983, and final MAGT for the year.....	32
Table 3.4: MAGTs at Alert BH3 calculated from discontinuous manual measurements between 1978 and 2000.....	33
Table 4.1: Summary table of the data used in the analysis of the five boreholes at Alert, Nunavut, and the depths of thermistors within the boreholes.	35
Table 4.2: Summary table of on-site data at Alert BH3, including FDD _a , FDD _s , TDD _a , TDD _s , SDD, n _f and n _t	44
Table 4.3: Summary table of continuously logged on-site data at Alert BH3, including the MAAT, MAGST, surface offset, TOP, TTOP, and the thermal offset.	45
Table 4.4: Summary table of on-site data at Alert BH4, including FDD _a , FDD _s , TDD _a , TDD _s , SDD, n _f and n _t	50
Table 4.5: Summary table of continuously logged on-site data at Alert BH4, including the MAAT, MAGST, surface offset, TOP, TTOP, and the thermal offset.	51
Table 4.6: Summary table of continuously logged on-site data at Alert BH5, including the MAAT, MAGST, surface offset, TOP, TTOP, and the thermal offset.	55
Table 4.7: Summary table of on-site data at Alert BH5, including FDD _a , FDD _s , TDD _a , TDD _s , SDD, n _f and n _t	56
Table 4.8: Summary table of n _f , n _t , and SDD at Alert BH3, BH4 and BH5 between 2000 and 2008.	66
Table 4.9: Summary table of surface and thermal offsets at Alert BH3, BH4 and BH5 between 2000 and 2008.	66
Table 4.10: Summary table of the data used in the analysis of the two boreholes at Iqaluit, Nunavut, and the depths of the thermistors within the boreholes.....	69
Table 4.11: Summary table of continuously logged on-site data at Iqaluit BH1 and BH2, including the MAAT, MAGST, surface offset, TOP, TTOP, and the thermal offset.	71
Table 4.12: Summary table of on-site data at Iqaluit, including FDD _a , FDD _s , TDD _a , TDD _s , n _f and n _t	71
Table 4.13: Summary table of the data used in the analysis of the four boreholes at Baker Lake, Nunavut, and the depths of the thermistors within the boreholes.....	80
Table 4.14: Summary table of on-site data at Baker Lake BH4, including FDD _a , FDD _s , TDD _a , TDD _s , SDD, n _f and n _t	82

Table 4.15: Summary table of continuously logged on-site data at Baker Lake BH2 and BH4, including the MAAT, MAGST, surface offset, TOP, TTOP, and the thermal offset.....	83
Table 4.16: Summary table of on-site data at Baker Lake BH2, including FDD _a , FDD _s , TDD _a , TDD _s , n _f and n _t	84
Table 4.17: Summary table of the data used in the analysis of the Sixty Mile borehole and the vertical depths of the thermistors from the surface.	94
Table 4.18: Summary table of the data used in the analysis of the Red Creek borehole and the depths of the thermistors from the surface.	98
Table 4.19: Summary table of the data used in the analysis of the Alpine Burwash borehole and the vertical depths of the thermistors from the surface.	105
Table 4.20: Summary table of the data used in the analysis of the Table Mountain borehole and the depths of the thermistors within the borehole.	109
Table 4.21: Summary table of continuously logged on-site data at Table Mountain, including the MAAT, MAGST, surface offset, TOP, TTOP, and the thermal offset.	111
Table 4.22: Summary table of on-site data at Table Mountain, including FDD _a , FDD _s , TDD _a , TDD _s , SDD, n _f and n _t	111
Table 4.23: Summary table of the data used in the analysis of the Wrigley borehole and the depths of the thermistors within the borehole.	117
Table 4.24: Summary table of continuously logged on-site data at Wrigley, including the MAAT, MAGST, surface offset, TOP, TTOP, and the thermal offset.	119
Table 4.25: Summary table of on-site data at Wrigley, including FDD _a , FDD _s , TDD _a , TDD _s , SDD, n _f and n _t	119
Table 4.26: Summary table of the data used in the analysis of the Wolf Creek boreholes and the depths of the thermistors.....	126
Table 4.27: Summary table of on-site data at Wolf Creek APM, including FDD _a , FDD _s , TDD _a , TDD _s , SDD, n _f and n _t	127
Table 4.28: Summary table of continuously logged on-site data at Wolf Creek APM, including the MAAT, MAGST, surface offset, TOP, TTOP, and the thermal offset.	128
Table 4.29: Summary table of continuously logged on-site data at Wolf Creek Palsa 25, including the MAAT, MAGST, surface offset, TOP, TTOP, and the thermal offset.	131
Table 4.30: Summary table of on-site data at Wolf Creek Palsa 25, including FDD _a , FDD _s , TDD _a , TDD _s , SDD, n _f and n _t	132
Table 5.1: Table of average values of MAAT, MAGST, and MAGT over the monitoring period at all sites, the depth that the MAGT represents, and if the permafrost is considered cold (C) or warm (W).....	136
Table 5.2: Table of average apparent thermal diffusivities at thermal monitoring sites and the depth of ZAA.	141
Table 5.3: Average values of n _f , SDD, and n _t at all sites, and the length of the record in years used to obtain each average value.	143

Table 5.4: Table of r^2 values from seasonal correlations at the five boreholes at Alert and the one at Table Mountain.....	163
Table A-1: Resolution and accuracy of monitoring equipment used at sites in this study.....	180
Table C-1: Table of average deviations from MAGT at Alert BH4 based on data from 2000 to 2002 and 2007 to 2008.....	185
Table C-2: MAGTs at Alert BH4 calculated from discontinuous manual measurements between 1978 and 1988.	186
Table C-3: Table of average deviation from MAGT at Alert BH5 based on data from 2000 to 2008.	187
Table C-4: MAGTs at Alert BH5 calculated from discontinuous manual measurements between 1978 and 2000.	188
Table C-5: Table of average deviations from MAGT at Baker Lake BH4 based on data from 2002 to 2003 and 2005 to 2006	189
Table C-6: MAGTs at Baker Lake BH4 calculated from discontinuous manual measurements between 1997 and 2005.....	190

DEFINITIONS AND SYMBOLS

Autumn – September, October, November (SON)
A – amplitude
A_{ZAA} – amplitude at zero annual amplitude, or 0.1°C
A_(z) – amplitude at z depth
BH – borehole
ECCS – Environment Canada Climate Station
FDD – freezing degree-days (°C day)
FDD_a – freezing degree days of the air (°C day)
FDD_s – freezing degree-days of the ground surface (°C day)
κ – apparent thermal diffusivity
MAAT – mean annual air temperature
MAGST – mean annual ground surface temperature
MAGT – mean annual ground temperature
maxT – maximum annual temperature at z depth
minT – minimum annual temperature at z depth
n_f – freezing n-factor
n_t – thawing n-factor
P – period
SDD – snow-depth days (cm day)
Spring – March, April, May (MAM)
Summer – June, July, August (JJA)
TDD – thawing degree-days (°C day)
TDD_a – thawing degree-days of the air (°C day)
TDD_s – thawing degree-days of the ground surface (°C day)
TOP – depth of the top of permafrost (m)
TTOP – temperature at the top of permafrost
Winter – December, January, February (DJF)
z – depth
ZAA – zero-annual amplitude
z_{ZAA} – depth of zero annual amplitude

1. INTRODUCTION

1.1 BACKGROUND

Permafrost is defined as earth materials that remain at or below 0°C for 2 years or more (van Everdingen, 2005). More than 20% of Earth's total land area is within the four permafrost zones defined by Brown et al. (1997): relatively warm, isolated patches (0-10% coverage); sporadic discontinuous (10-50% coverage); extensive discontinuous (50-90% coverage); and continuous permafrost (>90% coverage). The full range of permafrost zones are observed over approximately 50% of Canada, including alpine and sub-sea permafrost (Heginbottom et al. 1995; French, 2007). In mountainous regions it is possible that all of the permafrost zones may be observed over limited horizontal distances due to changes in elevation.

Climate is a first-order control on permafrost temperatures with local microclimate also substantially affecting ground surface temperatures, and therefore the thermal regime of the permafrost. At a local scale, ground surface and permafrost temperatures are affected by the characteristics of the snowpack, the type and height of vegetation, moisture content in the ground, topography, the geothermal flux, and the thermal conductivity of the earth materials (Judge, 1973). Consequently, the relation between air and ground temperatures is not straightforward (Brown, 1960; Williams and Smith, 1989; Zhang et al., 2005).

Future climate change, particularly air temperature and precipitation, will likely be enhanced in the high latitudes over the next century (ACIA, 2005; IPCC, 2007). These changes will greatly affect permafrost characteristics and distribution across the polar and alpine regions of the world. The warming or thawing of permafrost will affect

and possibly change hydrological processes that are at the base of aquatic and terrestrial ecosystems, having an impact on the traditional lifestyles of northerners. Infrastructure design in permafrost environments will also have to take these changing conditions into account to ensure structural integrity over time. Such changes are already underway, as revealed by a northward migration of the southern boundary of permafrost (Brown, 1960; Kwong and Gan, 1994), warming ground temperatures throughout most of the permafrost regions (Lachenbruch and Marshall, 1986; Osterkamp and Romanovsky, 1999; Osterkamp, 2005; Smith et al., 2005; Isaksen et al., 2007), increases in active layer thickness, and permafrost degradation (Jorgenson et al., 2001; Jorgenson et al., 2006; Pullman et al., 2007).

Given the clear need to improve our understanding of the relationship between climate and permafrost, this thesis examines the spatial and temporal variability in permafrost conditions at nine sites in three of the permafrost zones in northern Canada. It looks in detail at the relations between air and ground temperatures, both in the near surface and at depth within the permafrost. Observational data from widely separated sites across Canada are described and analyzed in order to reveal the range of permafrost conditions, changes that have occurred in permafrost, and how these changes vary based on location.

A total of nine sites across northern Canada are examined in this thesis (Figure 1.1): three in Nunavut (Alert, Iqaluit, and Baker Lake), two in the Northwest Territories (Table Mountain and Wrigley), and four in the Yukon Territory (Wolf Creek, Sixty Mile, Alpine Burwash, and Red Creek). Detailed descriptions of each site are presented later in the thesis.

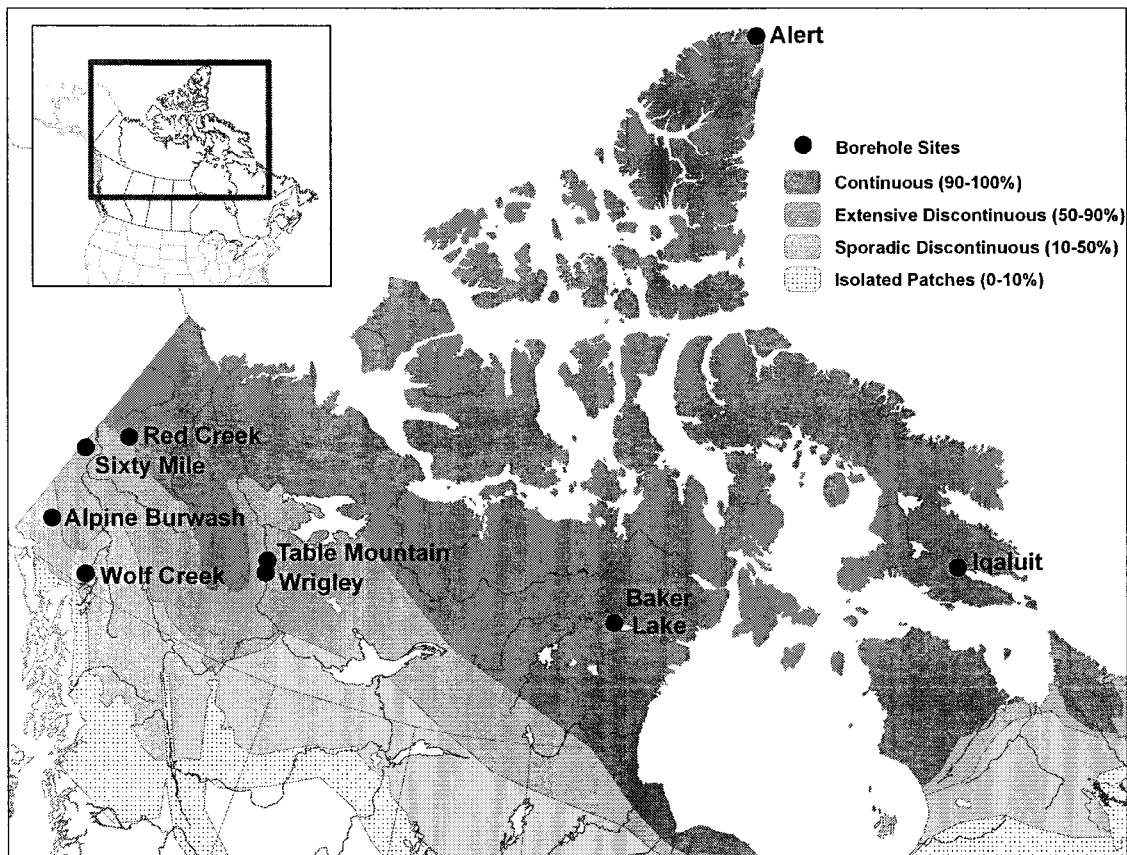


Figure 1.1: Location map of the thermal monitoring sites in relation to the permafrost zones across Canada (Heginbottom et al., 1995).

1.2 RESEARCH OBJECTIVES

The two main goals of this research were 1) to assess permafrost conditions across a variety of environments in northern Canada, and 2) to evaluate climatic influences on permafrost conditions at these sites over space and through time. The goals were achieved through meeting three objectives. The first was to identify site-specific relations between climate and permafrost, and was achieved by analysing interactions between the air and the ground surface, between the ground surface and the top of permafrost, and at various depths within the permafrost. The second objective was to examine the trends in annual and seasonal climate, and to identify the impacts they had

on permafrost conditions. The final objective was to determine and describe the variable influence of snow-pack characteristics (timing, duration, and depth) on temperatures at the ground surface and within the permafrost.

1.3 STRUCTURE OF THE THESIS

This thesis is composed of six sections. Section two presents background on relations between climate and permafrost. Section three outlines the analytical methods used. Section four presents a site description followed by a comprehensive set of results for each site. Section five examines and discusses inter-site comparisons and changes that occurred over time, and suggests opportunities for future research. Section six presents the conclusions of the research.

2. BACKGROUND: CLIMATE – PERMAFROST INTERACTIONS

Numerous interactions must be understood in order to analyze the relationship between climate and permafrost. The interactions between climate and near-surface permafrost can be examined using the relations between three mean annual temperatures. These are the mean annual air temperature (MAAT), the mean annual ground surface temperature (MAGST), and the mean annual temperature at the top of permafrost (TTOP; Smith and Riseborough, 2002). These relations are controlled mainly by conditions immediately above the ground surface and the thermal properties within the ground. Within the permafrost, temperatures are controlled predominantly by the amount of heat exchange flowing into and out of the ground seasonally. This is dependent on the thermal conductivity of the earth materials and past thermal history, and is reflected in the geothermal gradient (Williams and Smith, 1989; French, 2007). The following sections outline the essential components involved in climate-permafrost relations.

2.1 INTERACTIONS BETWEEN THE AIR AND THE GROUND SURFACE

2.1.1 Snow

Snow is a very effective insulator due to its low thermal conductivity, and therefore has a strong influence on the thermal regime of the ground (Williams and Smith, 1989). Snow primarily affects winter ground temperatures: where snow cover is thick, it reduces heat loss from the ground thus limiting the magnitude of ground cooling (Goodrich, 1978); where it is thin or absent, greater heat loss occurs, increasing cooling (Ishikawa, 2002). Snow can also affect ground temperatures during the spring and summer at sites where deep and late-lying accumulations occur; this situation may alter

the depth of thaw, and decrease the magnitude of warming that would otherwise occur. Long-term changes in the accumulation of snow can affect the temperature of the ground without changes occurring in air temperature (Goodrich, 1982), and can actually counteract the effects of changes in air temperature on ground surface temperatures (Gruber et al., 2004; Taylor et al., 2006).

Significant factors that influence the ground thermal regime are the timing of the first accumulation of snow on the surface, the duration of snow cover, and the maximum thickness reached during the winter (Goodrich, 1982). If snow arrives late in autumn the cool air temperatures will have a more direct impact on the ground surface than if the snow had arrived earlier (Ishikawa, 2002). Once air temperatures rise above 0°C in the spring, the snow begins to melt, and once it has melted, the near-surface temperatures begin to rise. The lag in time between air temperatures rising above 0°C and ground surface temperatures rising above 0°C can be used to represent the duration of the snowmelt (Woo et al., 2007). An effective method that is used to observe both the depth and duration of snow with one value is snow depth-days (SDD), which is a cumulative total of daily average snow depths over the winter (Karunaratne and Burn, 2003).

2.1.2 Surface Offset

The surface offset is defined as the difference in temperature between the MAAT and the MAGST (Smith and Riseborough, 2002), and is calculated by:

$$\text{Surface Offset} = \text{MAGST} - \text{MAAT} \quad (1)$$

The size of this offset is dependent upon conditions at the ground surface that act as a buffer between the atmosphere and the ground surface. The main factors that control the surface offset are (1) the snow cover that insulates the ground surface and reduces heat

loss during the winter; (2) the vegetation cover that shades the ground surface from direct insolation during the summer (Williams and Smith, 1989; Smith and Riseborough, 2002); and (3) the presence or absence of permafrost (Karunaratne and Burn, 2004).

Vegetation is an effective buffer in the summer causing ground temperatures to be cooler than the air, and can aid the accumulation of snow in the winter causing warmer ground temperatures than in the air (Smith, 1975; French and Slaymaker, 1993), and overall leading to smaller amplitudes of ground temperature waves. Depending on the type, vegetation, such as conifers, can also intercept snow leading to a thinner snow cover on the ground.

Ground surface temperatures have the potential to vary significantly more across a local area than air temperatures. Karunaratne and Burn (2004) measured similar air temperatures at five sites near Mayo, Yukon Territory, with distinctly different ground surface temperatures. The observed surface offsets varied by as much as 3.6°C as a result of spatial variations in winter snow depths and vegetation characteristics (i.e. canopy cover and surface albedo), illustrating the importance of such variables.

2.1.3 Thawing and Freezing Degree Days

Thawing degree-days (TDD) are the sum of daily mean temperatures above 0°C during the thawing season, and freezing degree-days (FDD) are the sum of daily mean temperatures below 0°C during the freezing season. TDD and FDD can be calculated for both air and ground surface temperatures (Klene et al., 2001). They are used to indicate temporal changes in air-to-ground surface temperature relations, as well as for seasonal analysis and comparisons between sites. These values are also used to calculate n-

factors, which represent air-to-surface relations (Taylor, 1995) and will be described in the next section.

Changes in climate over time can be examined through a seasonal perspective: one season may have a higher year-to-year variability or a stronger trend than another. Kwong and Gan (1994) observed more warming in minimum monthly temperatures than in maximum monthly temperatures, and greater changes in some months than others. In general, an increase in winter minimum air temperatures would decrease the amount of heat that escapes from the ground, and an increase in summer maximum air temperatures would increase the amount of heat that enters the ground (Kwong and Gan, 1994). However, the influence of changing winter air temperatures on ground temperatures also depends on snow cover. TDD and FDD can also be used, both in the ground surface and the air, to indicate variations in climate-permafrost relations across space. Klene et al. (2001) found that surface degree-day sums can vary greatly as a response to microclimatic influences over areas as small as 1 ha.

2.1.4 N-factors

An n-factor is a ratio of the seasonal ground surface temperature index to the seasonal air temperature index, using a degree-day sum to calculate each (Lunardini, 1978; Taylor, 1995; Klene et al., 2001). N-factors are calculated using:

$$n_t = \frac{TDD_s}{TDD_a} \quad (2)$$

$$n_f = \frac{FDD_s}{FDD_a} \quad (3)$$

where n_t and n_f are the thawing and freezing n-factors, respectively; TDD_s and TDD_a are the sums of the thawing degree-days of the ground surface and the air, respectively; TDD_a is calculated based on the timing of the thawing season of the ground surface; FDD_s and FDD_a are the sums of the freezing degree-days of the ground surface and the air, respectively; and FDD_a is calculated based on the timing of the freezing season of the ground surface (Klene et al., 2001; Karunaratne and Burn, 2003).

The closer the value of n_f or n_t is to 1.0, the more similar the air temperature index is to the ground surface temperature index, and the lower the value, the greater the buffering between the air and the surface. Air temperatures are highly variable and reach great extremes which are attenuated at the ground surface by vegetation cover during summer and snow cover during winter (Taylor, 1995). Values of n_t tend to be higher in open areas, and lower in areas with greater shading (Taylor, 1995). Values of n_t were observed as greater than 1.0 for surfaces such as gravel, sand or pavement, whereas lower values were observed in forested sites with shading at the surface (Taylor, 1995). High values of n_t suggest direct exposure to sun, which results in higher ground surface temperatures than air temperatures (Taylor, 1995). For example, an n_t value of 1.25 was reported for a bare rock and gravel site in the Kuparuk River basin of north-central Alaska (Klene et al., 2001). The most important factors that determine n_t are the near-surface thermal diffusivity and subsurface conditions (Karunaratne and Burn, 2004), vegetation or canopy cover, and soil moisture. Karunaratne and Burn (2004) found that when the thermal diffusivity in the near-surface was high, the thaw front would progress rapidly, allowing the ground surface to warm almost as much as the air and resulting in values of n_t close to 1.0.

Values of n_f are controlled mainly by snow cover and the thermal conditions of the subsurface material (Karunaratne and Burn, 2004). The buffering effects of snow cover on air-to-ground surface temperatures are reflected in values of n_f being less than 1.0 for most natural areas (Taylor, 1995). Karunaratne and Burn (2003) found that as SDD increase, values of n_f decrease. N-factors can be highly variable spatially and temporally due to the variability of surface conditions in natural environments; thus lengthy observation periods are needed to ensure accuracy (Klene et al., 2001). Karunaratne and Burn (2004) calculated n_f for five sites near Mayo, Yukon Territory, and found that the n_f values from one year were lower than those from a second year at all five sites, a difference they attributed to variations in snow conditions between the two years.

2.2 GROUND SURFACE AND PERMAFROST INTERACTIONS

2.2.1 Thermal Offset

The thermal offset is defined as the difference between the MAGST and TTOP (Smith and Riseborough, 2002), and is calculated using:

$$\text{Thermal Offset} = \text{TTOP} - \text{MAGST} \quad (4)$$

This offset is caused by the changes in thermal conductivity of the active layer during thawed and frozen periods (Burn and Smith, 1988; Smith and Riseborough, 2002). At sites where moisture is present in the ground, the thermal conductivity is higher when the site is frozen than when thawed; this allows heat to move more easily up through the active layer in the winter than down through the active layer in the summer (Judge, 1973; Taylor et al., 2000). The difference in the ground thermal conductivity is a result of ice being four times more conductive than water (Smith and Riseborough, 2002).

Bedrock and dry earth materials tend to have very low or no thermal offset as a result of minor seasonal changes in thermal conductivity (Burn and Smith, 1988; Romanovsky and Osterkamp, 1995; Smith and Riseborough, 2002). Larger thermal offsets occur in soils with higher moisture content due to the significant seasonal changes in thermal properties (Burn, 2004). A thermal offset exists when the mean annual ground temperature (MAGT) profile decreases with depth from the ground surface to the base of the active layer (Goodrich, 1978). Consequently, it is possible for equilibrium permafrost, and even aggrading permafrost, to exist where MAGST are above 0°C (Burn and Smith, 1988; Williams and Smith, 1989; Smith and Riseborough, 1996). Another important point is that the ground surface temperature does not necessarily define the characteristics of the permafrost, or its presence or absence, since thermal offsets vary significantly between sites (Burn and Smith, 1988).

The depth of the top of permafrost (TOP) is often difficult to define. Where there are enough temperature measurements within the active layer, TOP can be determined by extrapolating from above (Riseborough, 2008). Interpolation is another method used when there are records for temperatures above and below TOP (Nelson and Hinkel, 2003). A third technique is selecting a standard depth below the maximum observed thaw depth during the monitoring period, since temperatures within the first few meters of permafrost are usually quite similar to temperatures at the top of permafrost (Karunaratne et al., 2008).

2.2.2 Unfrozen Moisture and Latent Heat

Unfrozen moisture is present in many soils at temperatures several degrees below 0°C. This causes the release or absorption of latent heat over a range of temperatures

during phase change (Riseborough, 1990). Non-conductive heat flow has been observed beneath the active layer, in the near-surface permafrost, indicating that unfrozen moisture is present at sub-zero temperatures (Outcalt and Hinkel, 1996). The amount of unfrozen moisture decreases along with decreasing ground temperatures, yet this occurs at different rates depending on soil type (Williams and Smith, 1989). In general, fine-grained soils contain more unfrozen moisture than coarse-grained soils, and bedrock sites may contain almost none. Simulations conducted by Riseborough (1990) showed that different types of sediment thaw in different ways due to unfrozen moisture. He found that coarse-grained soils with no fines thawed over a small range of temperatures and had lesser latent heat effects than fine-grained sediments, in which latent heat effects were evident over several degrees. Romanovsky and Osterkamp (2000) found that the effects of unfrozen moisture affected the ground thermal regime the most during freeze-up and shortly afterwards. They also observed the effects lasting a few weeks in cold permafrost, and often most of the winter in warm permafrost.

Latent heat effects should be large at permafrost sites with ground temperatures that are very close to 0°C where unfrozen moisture is present, especially during periods of freezing and thawing, and therefore may lessen the thermal response of the ground to changes in surface conditions (Riseborough, 1990). The propagation of surface temperatures decreases in magnitude as permafrost temperatures approach 0°C (Burgess and Riseborough, 1990). Consequently, warmer permafrost sites may be weak indicators of climate change due to large latent heat requirements inhibiting the ground from warming or thawing completely.

2.2.3 The Zero-Curtain Effect

In autumn, as the ground begins to freeze, the freezing front progresses from the ground surface downward through the active layer. As moisture in the ground freezes, latent heat is released, maintaining temperatures near 0°C. When temperatures within the active layer reach 0°C or slightly below, they remain there until all the moisture has frozen and the latent heat has been released; once this occurs the ground can cool further (French, 2007). A similar pattern is observed in the spring when ice that is present within the active layer thaws (Outcalt and Hinkel, 1996). The extended period when the ground remains close to 0°C, while moisture is freezing or thawing, is known as the ‘zero-curtain’ effect (Williams and Smith, 1989; French, 2007). The zero-curtain effect can only occur where moisture is present within the ground (Outcalt et al., 1990), and at some sites may occur at lower temperatures, indicating that the soil moisture may have lower freezing points than 0°C (Williams and Smith, 1989). An extended zero-curtain indicates that a significant amount of frozen or unfrozen moisture is present in the active layer (Isaksen et al., 2007), or that the temperature gradient is weak. The variability of the zero-curtain from year-to-year can give an indication of how moisture conditions change at a site (Outcalt et al., 1990), and it can also be used to examine more extreme climatic events: e.g., Isaksen et al. (2007) observed an extended zero-curtain during one year of monitoring due to an exceptional amount of rainfall prior to freeze-back.

2.3 THERMAL STATE AND CHANGES OF PERMAFROST

2.3.1 Amplitude, Thermal Diffusivity, ZAA, and Phase Lag

The amplitude of the ground temperature wave reflects attenuated seasonal fluctuations with depth. A depth is eventually reached where seasonal fluctuations are no

longer evident and only gradual long-term changes occur; this is known as the depth of zero annual amplitude (ZAA; Williams and Smith, 1989), discussed in detail later in this section. Below this depth these gradual long-term changes occur over multiple years or decades and are typically associated with long-term changes in surface conditions, e.g. a warming climate, changes in snow characteristics, or an extreme event such as a fire that destroys the vegetation and surface organic layer. The amplitude is calculated for each depth using:

$$A_{(z)} = \frac{\max T - \min T}{2} \quad (5)$$

where $A_{(z)}$ is the amplitude at z depth, $\max T$ and $\min T$ are the maximum and minimum temperatures reached over one year at z depth, respectively (Williams and Smith, 1989).

Temperature envelopes are a visual representation of the annual range of temperatures at each depth. They can be used to portray changes in the range of temperatures from one year to the next, to assess changes in active-layer thicknesses, and for comparisons of conditions between sites. The maximum and minimum temperature profiles define the temperature envelope at a site (Brown, 1978). In deeper profiles, temperature envelopes can indicate whether the permafrost is in equilibrium or disequilibrium with the surface, or if it is relict. Deviations in the near-surface profile can indicate climatic warming or cooling trends (Harris et al., 2003).

The thermal diffusivity is the rate at which temperatures are able to propagate with depth (Williams and Smith, 1989). The thermal diffusivity is dependent upon the thermal conductivity and heat capacity of the material, and is driven by thermal gradients (Hinkel, 1997). The thermal diffusivity can be calculated at sites with a sinusoidal temperature wave using:

$$\kappa = \frac{\pi}{P} \left(\frac{z_2 - z_1}{\ln A_1/A_2} \right)^2 \quad (6)$$

where κ is the thermal diffusivity (m^2s^{-1}) and P is the period of the wave, usually in seconds, either over one day (86400) or one year (3.15×10^7) depending on the period in which the amplitude represents (Williams and Smith, 1989). This calculated value for thermal diffusivity is considered “apparent” because it includes non-conductive heat transfer within the soil, e.g. the latent heat effects involved with phase change (Hinkel, 1997). Obtaining a value for the apparent thermal diffusivity using this method can be problematic if soil moisture contents fluctuate over time.

ZAA occurs at some depth below which annual fluctuations diminish to less than 0.1°C , usually located between 10 and 20 m depth (Williams and Smith, 1989; Gruber et al., 2004; Isaksen et al., 2007). The temperature at ZAA relates directly to TTOP (Smith and Riseborough, 2002). In general, the greatest depths of ZAA are observed in areas with colder surface conditions and particularly thermally conductive material, such as bedrock; the shallowest depths are observed where ground temperatures are close to 0°C and phase change is taking place (Riseborough, 1990), often in fine-grained material. Surface temperatures propagate faster at sites where the ground is frozen, versus unfrozen, due to higher apparent thermal diffusivities (Riseborough, 1990), resulting in reduced attenuation of the amplitude with depth and a greater depth of ZAA. At sites where the apparent thermal diffusivity is low, possibly due to high amounts of unfrozen moisture, the amplitude will dampen rapidly with depth and ZAA will be shallower.

The apparent thermal diffusivity can be used to determine an approximate depth of ZAA in shallow boreholes. The depth of ZAA is calculated using the deepest known

apparent thermal diffusivity in a borehole that is shallower than ZAA. The following was adapted from the equation for thermal diffusivity from Williams and Smith (1989):

$$z_{ZAA} = \sqrt{\frac{\kappa P}{\pi} \left(\ln \frac{A_1}{A_{ZAA}} \right)^2} + z_1 \quad (7)$$

where z_{ZAA} is the depth of ZAA, A_1 is the amplitude at the second deepest thermistor, and A_{ZAA} is the amplitude at ZAA, or 0.1°C. The amplitude at the second deepest thermistor is used because it will not be affected by the phase changes that may occur within the active layer.

The phase lag is also determined using the apparent thermal diffusivity. The phase lag indicates the length of time it takes for a temperature wave to reach a particular depth. The phase lag can be calculated using:

$$t = \frac{z}{2} \left(\frac{P}{\pi \kappa} \right)^{1/2} \quad (8)$$

where t is the time starting from the date the surface temperature wave passes through the mean annual value in the spring to the date the temperature wave passes through the mean at z depth (Williams and Smith, 1989). Seasonal fluctuations will propagate more rapidly downwards through material with a higher thermal diffusivity, producing a shorter lag than in material with low thermal diffusivity, and a deeper ZAA. For example, bedrock generally has a high thermal diffusivity and ZAA can attain depths greater than 20 m (Williams and Smith, 1989). The thermal diffusivity and phase lag vary based on site-specific conditions and can explain some of the variability in air-to-ground temperature relations.

Permafrost thermal profiles below ZAA usually indicate warming with depth, known as the geothermal gradient (French, 2007). The geothermal gradient is a result of

heat from the centre of the earth flowing toward the surface, known as the geothermal heat flux (French, 2007). The geothermal gradient varies across space and is controlled by the thermal conductivity of the earth materials and the geothermal heat flux (Judge, 1973). Each ground thermal profile is unique, and is based on the history of on-site climatic and surface conditions. Thermal profiles can be examined for changes in climatic conditions (Taylor et al., 2006). Warming climatic conditions can be observed when permafrost that is very close to 0°C thaws. Cold permafrost is well below 0°C and has little risk of thaw, but climatic changes are observed through changes in the thermal profile. A curve towards warmer temperatures in the upper portions of permafrost would indicate warming ground surface conditions, perhaps caused by climate warming, increases in snow depths, or changes in other surface conditions, and a curve toward colder temperatures would indicate ground surface cooling.

2.3.2 Permafrost Thickness

The thickness of permafrost is a function of the ground surface and air temperature histories, the thermal properties of the ground over the previous decades to thousands of years, and the geothermal gradient (Williams and Smith, 1989; Taylor et al., 2000). The thickest permafrost should have a combination of low ground surface temperatures, high thermal conductivity, and low heat flow (Williams and Smith, 1989).

Thicknesses can be estimated if temperature measurements extend below ZAA. Below this depth the thermal profile generally follows the geothermal gradient to the base of the permafrost, assuming that the permafrost is in equilibrium with current climatic conditions. There are two possible methods of estimating the thickness of permafrost. One method uses the surface temperature, heat flow, and thermal conductivity of the

earth material (Judge, 1973). A second method is the downward extrapolation of the geothermal gradient from below ZAA (Gruber et al., 2004), but deep profiles are needed for this. The assumption that the ground warms by 1°C per 30-60 m can be used when the geothermal gradient is unknown, and from this a very general range of possible thicknesses can be derived (French, 2007). However, the values obtained using this method are only estimates, as geothermal gradients vary regionally along with differences in geology and tectonics (Jessop et al., 1984; Williams and Smith, 1989). These methods can be problematic at sites with ground temperatures that are close to 0°C, in which case the gradient may be extremely small due to the influence of unfrozen moisture and latent heat effects.

2.3.3 Changes over time – Climate and Permafrost

An increasing or decreasing trend in MAAT must be observed over a long enough time span to be considered significant. These trends can occur through warming or cooling across all seasons, or changes in one or two seasons, such as warming summers or cooling winters (Osterkamp, 2007). Trends in air temperatures are easy to detect when long enough data records exist, but the case is not as simple for permafrost temperature trends. The surface of the ground is affected not only by air temperatures, but also microclimate influences, such as snow and vegetation. Significant amounts of snow can act to offset the influence of an increasing or decreasing trend in winter air temperatures (Smith, 1975; Throop et al., 2008).

Changes in climate and permafrost temperatures can be observed at sites over long time periods. The ground is a filter for minor fluctuations in air temperatures, allowing the broad climatic signal to be stored in the ground. This signal of climatic

warming or cooling is observed in permafrost temperature changes at depths below ZAA. Greater depths in the thermal profile represent larger scale events further back in time (Lachenbruch and Marshall, 1986). Increases in permafrost temperatures and changes in thermal profiles have been observed in a number of studies which have been used as indicators of past climatic warming (Lachenbruch and Marshall, 1986; Harris et al., 2003; Taylor et al., 2006; Osterkamp, 2008). The clearest climate change signal will be observed at exposed bedrock sites (Smith and Riseborough, 1996), where vegetation, snow cover, and ground moisture have minimal effects.

3. METHODOLOGY

The data used in this thesis are from a range of thermal monitoring sites that were collected over varying time periods; therefore the instruments used for data collection and the methods of analysis varied for each site. Refer to Appendix A for the types of instruments used in data collection at each site, and the resolution and accuracy of these. In general, September 1 to August 31 was used as the annual cycle, unless otherwise stated. All recognizable erroneous data were removed from the datasets before analysis began (e.g. missing values and obvious logger inaccuracies). Trends or relations identified in this thesis were analyzed using linear regression or correlation and were tested for statistical significance.

3.1 METHODS USED FOR INDIVIDUAL SITE ANALYSIS

3.1.1 MAAT, MAGST, TTOP, Surface Offset and Thermal Offset

Air temperatures were measured between 1 and 2 m above the ground surface, and ground surface temperatures were measured with sensors placed between 2 and 5 cm below the surface. MAAT and MAGST were obtained by calculating the average of all daily temperatures each year. A slightly different range of dates were used when gaps were present in the air or ground surface data.

TOP was located by interpolating between the two depths where the maximum temperatures bracket 0°C to determine the maximum depth of 0°C penetration (Nelson and Hinkel, 2003). TTOP was calculated by interpolating between the MAGTs at these same depths. For sites where interpolation of TOP was not possible, a fixed depth was

selected beneath the depth where maximum temperatures reached 0°C over the monitoring period (e.g. Alert BH5) (Karunaratne et al., 2008).

The surface offset was calculated by subtracting the MAAT from the MAGST of the same year (Eq. 1; Smith and Riseborough, 2002). Positive values of the surface offset indicate that the ground surface is warmer than the air, which is most often the case. The thermal offset was calculated by subtracting the MAGST from TTOP (Eq. 4; Romanovsky and Osterkamp, 1995; Smith and Riseborough, 2002). The thermal offset is represented as a negative value, as the ground usually cools with depth within the active layer, and the values are positive in the rare cases when TTOP is warmer than the MAGST.

3.1.2 TDD, FDD, and N-factors

TDD and FDD were calculated for both the air and the ground surface. TDD are the sum of temperatures above 0°C during the thawing season, and FDD are the sum of the temperatures below 0°C during the freezing season. The freezing season is determined by the ground surface, as once it passes the 0°C threshold, it fluctuates above and below less frequently than the air. For calculating TDD, the thawing season begins when the ground surface temperature remains above 0°C and ends when it goes below 0°C, and the days included are only the ones where the air and ground surface are both above 0°C (Karunaratne and Burn, 2003). For calculating FDD, the freezing season begins when the ground surface temperature remains below 0°C and ends when it goes back above 0°C, and the days included are only the ones where the air and ground surface are both below 0°C (Karunaratne and Burn, 2003). The ground surface temperature sometimes fluctuates above and below 0°C at the beginning or end of both seasons.

When this occurs during the thawing season, the latter begins when the sum of the temperatures above 0°C exceed the sum of the subsequent temperatures below 0°C, and vice-versa during the freezing season.

Thawing and freezing n-factors (n_t and n_f , respectively) were calculated using the sums of TDD and FDD. Values of n_t were calculated using Equation 2, and values of n_f were calculated using Equation 3 (Klene et al., 2001).

3.1.3 Snow Data Analysis

Daily snow depth data were collected using two methods at the nine sites. At Wolf Creek Palsa 25, Red Creek, Sixty Mile, and Alpine Burwash it was collected using miniature data loggers called iButtons, and employing the method described in Lewkowicz (2008). The miniature data loggers were positioned vertically along a post at 5, 10, 20, 30, 40, 50, 60, 80, and 100 cm above the ground surface. Snow depths were interpreted by assessing the differences in temperatures between iButtons. At the other sites, Alert, Table Mountain, Wrigley, Wolf Creek APM, Baker Lake, and Iqaluit, the snow data was collected hourly using the SR50M acoustic snow sensor made by Campbell Scientific. The resolution and accuracy of these instruments is provided in Appendix A.

Snow depths were plotted against air and ground surface temperatures to investigate the lag between air and ground surface temperature changes, and the inter-annual variability of snow characteristics. These graphs were also used to examine the effect that the timing of the snow's arrival and departure had on the length of the zero-curtain.

An annual average snow depth was calculated for each year using daily averages, and the maximum depth was identified. SDD were calculated by adding together each daily snow depth value throughout the season. This value takes into account both the depth and duration of snow accumulation, and therefore encapsulates inter-annual variability (Karunaratne and Burn, 2003).

SDD values were correlated against surface offsets and freezing n-factors (Riseborough and Smith, 1998) to investigate the impact of snow on ground surface temperatures, and to determine the importance of snow in air to ground surface temperature relations at each site.

3.1.4 Temperature Envelopes

Maximum and minimum temperatures at each borehole were extracted for each depth's annual ground temperature cycle. MAGTs were calculated by averaging the daily values at each depth for every year. These values were then plotted to determine the annual range of temperatures throughout the borehole. The MAGT values plotted on this graph reveal the characteristics of the thermal profile.

3.1.5 Amplitude, Apparent Thermal Diffusivity, and Phase Lags

The amplitude of the annual temperature wave was calculated by subtracting the minimum ground temperature from the maximum ground temperature and dividing by two, half of the range, at each depth for all years (Eq. 5). In order to encompass the entire thermal year within the ground, taking into account the time it takes for the temperature wave to propagate to depth, the dates for each site were selected according to their unique characteristics. For example, the propagation of the maximum and minimum

temperature waves at Alert BH3 are longer than a single 12-month period, so the dates used for acquisition of the maximum and minimum ranges were customized according to each site's thermal characteristics (Fig. 3.1). The amplitude was then used to calculate the apparent thermal diffusivity between depths over one year (Eq. 6; Williams and Smith, 1989). An approximate depth of ZAA was then calculated, particularly for boreholes that did not reach this depth, from the average apparent thermal diffusivity near the bottom of the borehole (Eq. 7). Even though Eq. 6 is intended for sites with sinusoidal ground temperature waves, it is useful for sites with asymmetric temperature waves. A comparison of measured ZAA and the calculated depth from the apparent thermal diffusivities was conducted at the Wrigley and Wolf Creek sites. Even though the ground temperature wave was asymmetric, the calculated ZAA fell between the thermistors above and below the observed ZAA. Therefore, the apparent thermal diffusivity can be calculated for sites with asymmetric ground temperature waves using Eq. 6.

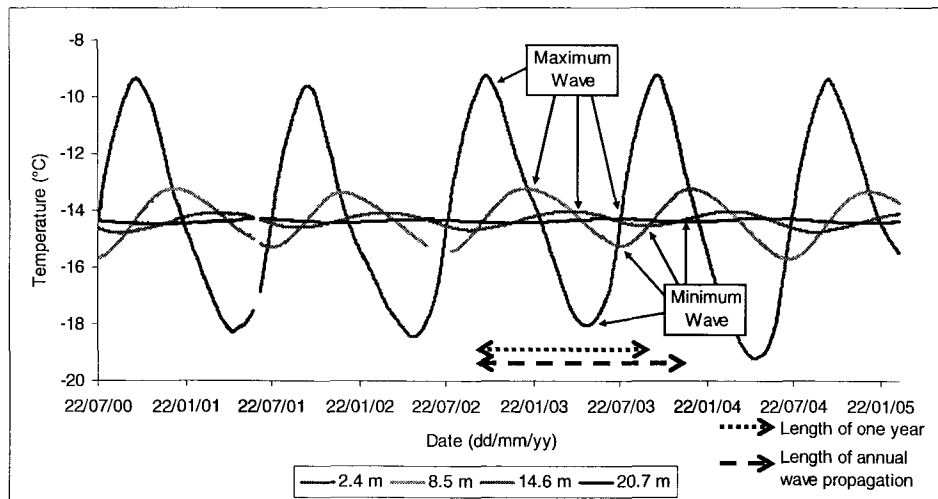


Figure 3.1: Ground temperature time series at Alert BH3. The maximum and minimum temperature waves take longer than one calendar year to propagate to 20.7 m, so the maximum values for each year at this site were obtained between September 1 and August 31, and the minimum values were obtained between March 1 and February 28.

Phase lags were calculated using the apparent thermal diffusivity to indicate the length of time that the annual temperature wave takes to propagate through the ground (Eq. 8; Williams and Smith, 1989). The calculated phase lags were used to ensure that the correct measurements were being correlated with one another when assessing the air to ground temperature relations. The apparent thermal diffusivity and phase lags were calculated for all sites, with the exception of Table Mountain because of the site's high inter-annual variability in near-surface amplitude, and its shallow depth of ZAA.

3.2 TEMPORAL ANALYSIS

The temporal component of the project involved only the datasets with longer ground temperature time series: Alert, Baker Lake, Iqaluit, Table Mountain, and Wrigley. The first stage in this analysis was to standardize the data and obtain a comparable continuous record of air and ground temperatures. The methods used to standardize this data are outlined in the following sections.

The standardization produced a continuous 'record' consisting of hind-cast MAGTs and monthly air temperatures stretching back to the beginning of the monitoring period at each site. The next stage of the research was to analyze the data, assess the inter-annual variability in seasonal air temperatures, and observe the presence or absence of trends and their magnitudes.

3.2.1 Hind-casting Air Temperature 'Record'

Four of the sites (Alert, Baker Lake, Iqaluit, and Table Mountain) had ground temperature monitoring instrumentation in place before on-site air temperature and snow depth sensors were installed. Each of the four sites is close to an Environment Canada

Climate Station (ECCS) which collects high frequency, quality controlled, meteorological variables. The four nearest ECCSs to the sites mentioned above are Alert, Baker Lake, Iqaluit, and Fort Simpson, respectively. Continuous records of hind-cast air temperatures for the measurement sites were produced for the period prior to the start of ground temperature monitoring through correlation of overlapping monthly on-site and ECCS data (Fig. 3.2). Data from the on-site weather stations were used, and when this data was unavailable, the gaps were filled using Vemco logger data also recording air temperatures on-site. The correlations from all of the sites can be found in Appendix B.

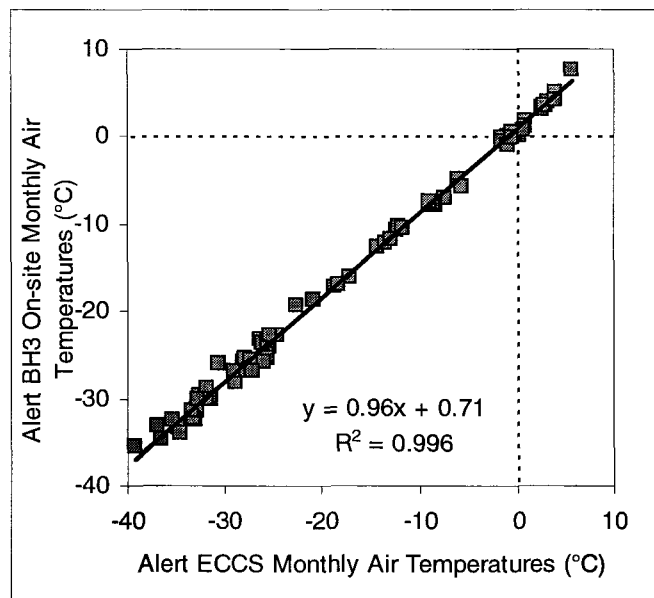


Figure 3.2: Relationship between monthly average air temperatures at the Alert BH3 on-site weather station and the Alert ECCS (Environment Canada, 2009) from 2000 to 2006. The correlation is significant at $p < 0.001$.

The following is an explanation of the method used to hind-cast the air temperature record for Alert BH3, and a brief note about Table Mountain. Monthly average air temperatures were acquired from the Alert ECCS overlapping the period of on-site measurements at the Alert BH3 weather station. The ECCS and on-site data were correlated to observe the strength of the relationship and to determine the line-of-best-fit

equation ($r^2=0.996$; $p<0.001$; Fig. 3.2). Historical monthly air temperatures from the Alert ECCS were input to the best-fit equation ($y = 0.96x + 0.71$) to hind-cast on-site monthly air temperatures between July 1950 and September 2006. Four seasonal relationships were plotted at Table Mountain because they varied considerably between the Fort Simpson ECCS and the thermal monitoring site (Appendix B). Each line of best-fit equation was used to hind-cast monthly values and calculate seasonal average temperatures based on the specific months defined by Camill (2005), and Popova and Shmakin (2009): autumn – September to November; winter – December to February; spring – March to May; and summer – June to August.

MAATs and seasonal average temperatures at Alert BH3 (Figs. 3.3 and 3.4) were calculated using the hind-cast monthly average temperatures. The hind-cast air temperatures were visually assessed for warming or cooling trends. Regression analyses were then conducted on the trends to test whether or not they were statistically significant. Trend-lines are plotted only when they are considered statistically significant. The hind-cast MAAT values for Alert BH3 show a statistically significant warming trend of 0.4°C per decade between 1976 and 2006 (Fig. 3.3; $p<0.01$), and the hind-cast seasonal values show significant warming trends in both winter and autumn ($p<0.05$; Fig. 3.4).

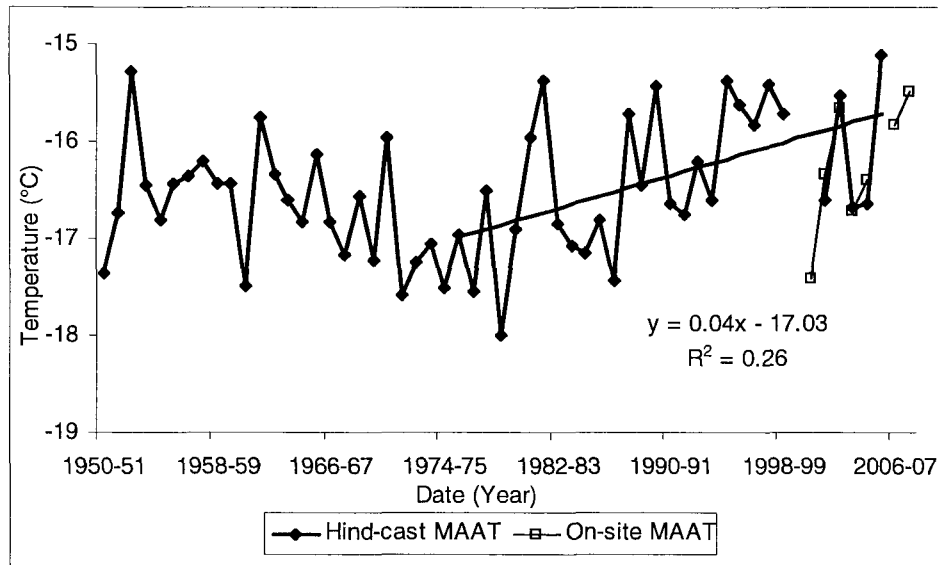


Figure 3.3: Hind-cast MAATs at Alert BH3 from correlated Alert ECCS data (Environment Canada, 2009) between 1950 and 2006, and actual measured on-site MAAT between 2000 and 2008. The warming trend between 1976 and 2006 is significant at $p < 0.01$.

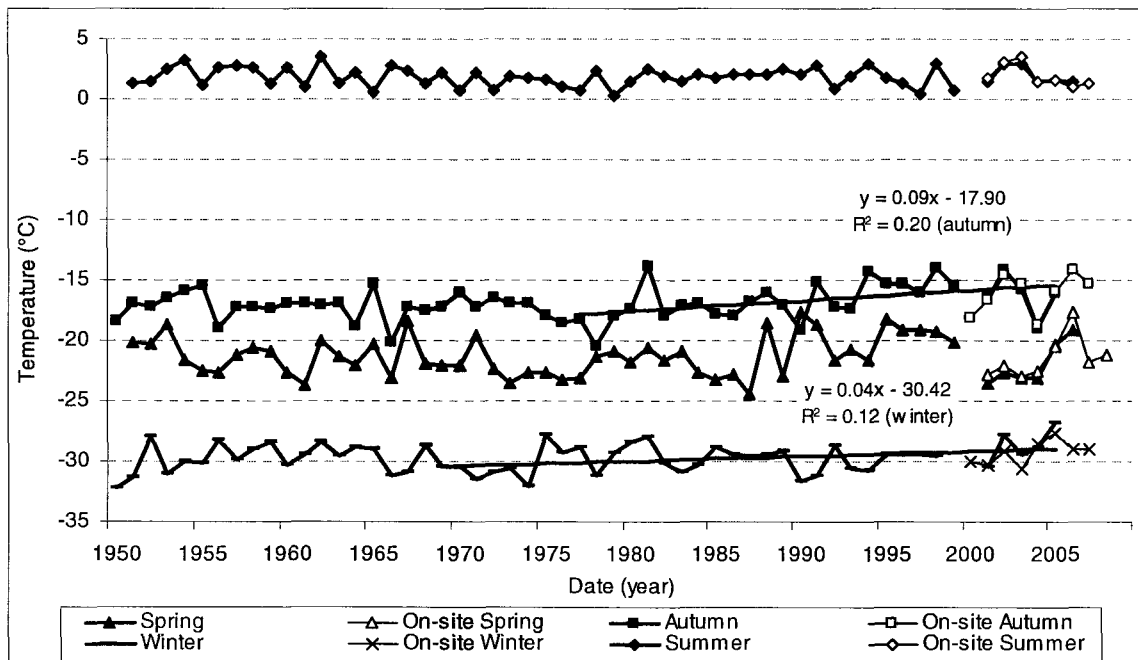


Figure 3.4: Hind-cast seasonal average air temperatures at Alert BH3 between 1950 and 2006 from correlated ECCS data (Environment Canada, 2009), and actual measured seasonal average air temperatures between 2000 and 2008. Warming trends in the autumn and winter are statistically significant at $p < 0.05$.

3.2.2 Standardization of Ground Temperature 'Record'

Ground temperature data were collected manually in the earlier years of monitoring and automatically in more recent years at Alert, Baker Lake, and Table Mountain (Tables 4.1, 4.13, and 4.20). The manual data produced a discontinuous record of ground temperatures with one or two measurements per month, and sometimes missing months entirely. The following method was developed to calculate the MAGT at each depth for the years with episodic manual data, and was applied to Alert BH3, BH4, and BH5, and Baker Lake BH4. At Table Mountain a simple average was taken from the manual measurements because most of the readings are from below the depth of ZAA.

This method is an important component of this research, enabling MAGTs to be extracted from sporadic measurements. The cubic spline interpolation method tested by Riseborough and Burgess (1996) was inappropriate for use with the manual data for a large portion of the data records in this study due to infrequent and inconsistent data collection. The following describes the method used in this study to calculate MAGTs during the period of manual measurements at Alert BH3. The data from the other sites where MAGTs were calculated using this method is given in Appendix C.

The method begins by calculating MAGTs at each depth above ZAA from all years of continuous data. The depths above ZAA at Alert BH3 are 2.4, 8.5, 14.6, and 20.7 m, and continuous measurements exist for 2000 to 2004. Next, three sets of averages were calculated per month consisting of approximately 10-day intervals (this is dependent upon how many days in each month, e.g. September 1-10, 11-20, 21-30, and August 1-10, 11-20, 21-31; Table 3.1). For every year of continuous data the 10-day average was subtracted from its corresponding MAGT to obtain the deviation of each 10-

day period from the mean. An average deviation for each 10-day period was calculated from all years to produce a standard value for those dates (Fig. 3.5 and Table 3.1). The calculated 10-day deviation for the corresponding date and depth were subtracted from each manually collected temperature value (Tables 3.2 and 3.3). These values, representing an indication of the MAGT from each manual reading, were averaged to obtain a calculated MAGT for the entire year (Table 3.4). In this way, all the data were used, but the MAGT was not weighted by changes in the frequency of sampling. In order to calculate the MAGT at depths below ZAA, a simple average was taken from the manual measurements over the course of one year between September 1 and August 31.

Table 3.1: Table of average deviations from MAGT at Alert BH3 based on data from 2000 to 2004; these values are subtracted from the corresponding manual reading to obtain an expected MAGT for each reading.

10-day Intervals	2.4m	8.5m	14.6m	20.7m
Sept 1-10	3.7	-0.7	-0.3	0.0
Sept 11-20	4.2	-0.5	-0.3	0.0
Sept 21-30	4.6	-0.3	-0.3	0.0
Oct 1-10	4.9	-0.1	-0.3	0.0
Oct 11-20	4.8	0.1	-0.2	0.0
Oct 21-31	4.5	0.3	-0.2	0.0
Nov 1-10	4.0	0.5	-0.2	-0.1
Nov 11-20	3.4	0.7	-0.1	-0.1
Nov 21-30	2.8	0.8	-0.1	-0.1
Dec 1-10	2.1	0.9	-0.1	-0.1
Dec 11-20	1.4	1.0	0.0	-0.1
Dec 21-31	0.8	1.0	0.0	-0.1
Jan 1-10	0.2	1.0	0.1	-0.1
Jan 11-20	-0.2	0.9	0.1	-0.1
Jan 21-31	-0.7	0.8	0.2	-0.1
Feb 1-10	-1.2	0.7	0.2	0.0
Feb 11-20	-1.6	0.6	0.2	0.0
Feb 21-28/29	-2.0	0.5	0.3	0.0
Mar 1-10	-2.4	0.4	0.3	0.0
Mar 11-20	-2.8	0.3	0.3	0.0
Mar 21-31	-3.2	0.2	0.3	0.0
Apr 1-10	-3.6	0.0	0.3	0.0
Apr 11-20	-3.9	-0.1	0.3	0.0
Apr 21-30	-4.1	-0.3	0.2	0.0
May 1-10	-4.1	-0.5	0.2	0.0
May 11-20	-4.1	-0.6	0.2	0.1
May 21-31	-4.0	-0.7	0.1	0.1
June 1-10	-3.7	-0.8	0.1	0.1
June 11-20	-3.3	-0.9	0.0	0.1
June 21-30	-2.7	-1.1	0.0	0.1
July 1-10	-1.9	-1.1	-0.1	0.1
July 11-20	-0.8	-1.1	-0.1	0.1
July 21-31	0.4	-1.1	-0.2	0.1
Aug 1-10	1.4	-1.1	-0.2	0.0
Aug 11-20	2.3	-1.0	-0.3	0.0
Aug 21-31	3.1	-0.9	-0.3	0.0

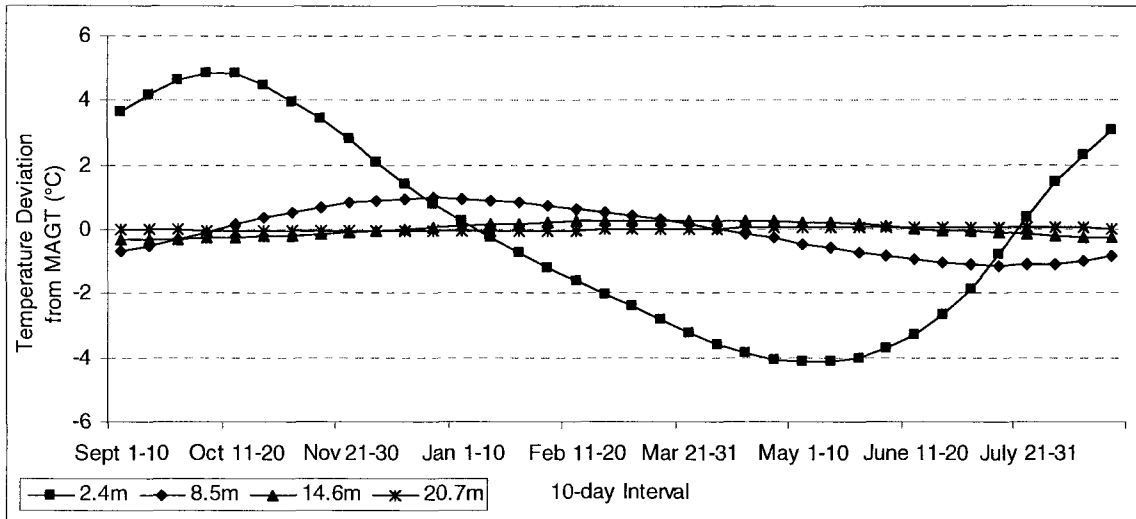


Figure 3.5: The average deviations from the MAGT for each 10-day period at depths above ZAA at Alert BH3.

Table 3.2: Manual measurements at Alert BH3 between September 1982 and August 1983.

1982-83	2.4m	8.5m	14.6m	20.7m
26-Oct-82	-10.2	-13.8	-14.7	-14.4
4-Jan-83	-14.1	-13.3	-14.2	-14.4
31-Jan-83	-15.1	-13.4	-14.1	-14.4
24-Feb-83	-16.2	-13.8	-14.0	-14.4
25-Apr-83	-17.4	-14.4	-14.1	-14.3
3-Jun-83	-17.5	-14.8	-14.2	-14.3
27-Jun-83	-16.7	-15.0	-14.2	-14.3
27-Jul-83	-14.3	-15.2	-14.4	-14.3

Table 3.3: Calculated values from manual measurements at Alert BH3 between September 1982 and August 1983, and final MAGT for the year.

1982-83	2.4m	8.5m	14.6m	20.7m
26-Oct-82	-14.6	-14.1	-14.5	-14.4
4-Jan-83	-14.4	-14.2	-14.3	-14.3
31-Jan-83	-14.4	-14.3	-14.3	-14.3
24-Feb-83	-14.2	-14.3	-14.3	-14.3
25-Apr-83	-13.4	-14.1	-14.3	-14.3
3-Jun-83	-13.8	-14.0	-14.2	-14.3
27-Jun-83	-14.0	-13.9	-14.1	-14.3
27-Jul-83	-14.7	-14.1	-14.2	-14.3
MAGT1982-83	-14.2	-14.1	-14.3	-14.3

Table 3.4: MAGTs at Alert BH3 calculated from discontinuous manual measurements between 1978 and 2000.

Year	2.4	8.5	14.6	20.7	26.8	32.9	39.0	51.2	57.3
1978-79	-14.8	-14.5	-14.5	-14.5	-14.2	-14.1	-13.9	-13.7	-13.6
1979-80	-15.7	-14.8	-14.5	-14.4	-14.2	-14.2	-13.9	-13.8	-13.7
1980-81	-15.1	-15.0	-14.8	-14.5	-14.2	-14.2	-14.0	-13.8	-13.7
1981-82	-14.4	-14.7	-14.7	-14.4	-14.3	-14.2	-14.0	-13.8	-13.7
1982-83	-14.2	-14.1	-14.3	-14.3	-14.2	-14.2	-14.0	-13.8	-13.7
1983-84	-15.5	-14.6	-14.4	-14.3	-14.1	-14.1	-14.0	-13.8	-13.7
1984-85	-14.2	-14.7	-14.7	-14.5	-14.2	-14.2	-14.0	-13.9	-13.7
1985-86	-16.5	-14.8	-14.6	-14.4	-14.2	-14.2	-14.0	-13.8	-13.7
1986-87	-14.2	-16.0	-14.9	-14.6	-14.3	-14.2	-14.0	-13.8	-13.7
1987-88	-15.7	-15.0	-14.8	-14.6	-14.3	-14.2	-14.0	-13.8	-13.7
1988-89	-14.3	-14.7	-14.8	-14.7	-14.4	-14.3	-14.1	-13.8	-13.7
1989-90	-13.8	-14.3	-14.6	-14.6	-14.4	-14.4	-14.1	-13.9	-13.7
1990-91	-15.2	-14.7	-14.6	-14.5	-14.3	-14.3	-14.1	-13.9	-13.7
1991-92	-14.3	-14.6	-14.6	-14.5	-14.3	-14.3	-14.1	-13.9	-13.7
1992-93	-15.1	-14.8	-14.5	-14.5	-14.3	-14.3	-14.1	-13.9	-13.7
1993-94	-15.2	-14.9	-14.7	-14.5	-14.3	-14.3	-14.1	-13.9	-13.8
1994-95	-15.5	-14.9	-14.9	-14.7	-14.4	-14.3	-14.1	-13.9	-13.7
1995-96	-14.4	-15.9	-14.8	-14.6	-14.4	-14.3	-14.1	-13.9	-13.8
1996-97	-13.5	-14.2	-14.5	-14.6	-14.4	-14.4	-14.1	-13.9	-13.8
1997-98	-13.3	-13.9	-14.2	-14.5	-14.3	-14.3	-14.1	-13.9	-13.8
1999-00	-14.7	-14.3	-14.3	-14.3	-14.1	-14.2	-14.0	-13.9	-13.8

4. SITE DESCRIPTIONS AND RESULTS

This section describes the results from the analysis of nine thermal monitoring sites from widely separated locations in Canada (Fig. 1.1). The results are presented beginning with the site that has the lowest ground temperatures at Alert, Nunavut, and ending with the site that has the highest ground temperatures at Wolf Creek, in the southern Yukon Territory. Site descriptions are presented immediately before the results for each site. A significant portion of the site descriptions for the boreholes at Alert, Iqaluit, Baker Lake, Wrigley and Table Mountain comes from metadata sheets on the Global Terrestrial Network for Permafrost (GTN-P, 2009) website.

The results are presented for each site beginning with the relationship between temperatures in the air and at the ground surface. This relationship is examined through the on-site characteristics of snow, the surface offset and its controls, and the n-factors relating to the FDD and TDD of the air and the ground surface. Next, the relationship between the ground surface and the top of permafrost is described through the conditions at the top of permafrost and the thermal offset, and the magnitude of latent heat and zero-curtain effects within the active layer. Thirdly, the thermal conditions within the permafrost are examined using temperature envelopes, the temperature and depth of ZAA, the thermal gradient, the apparent thermal diffusivity and phase lags, the thickness of the permafrost, and how ground temperatures have changed over time. Intra-site comparisons at Alert and Baker Lake, the sites with multiple boreholes, are included in this section. Lastly, the climatic conditions and trends are described through changes in MAATs and seasonal averages over the monitoring period.

4.1 ALERT, NUNAVUT

The permafrost thermal monitoring sites at Alert, Nunavut, are the most northerly monitoring sites in the world (Smith et al., 2005). They are located at the northernmost point of Ellesmere Island (82°30'N and 62°25'W) within the zone of continuous permafrost (Fig. 1.1). The area is a cold and dry polar desert, with little to no vegetation (Smith et al., 2003, 2005). There are five boreholes at varying elevations and depths (up to 60 m), and measurements have been recorded manually since 1978. Borehole depth and record length are provided in Table 4.1. The distribution of the five boreholes within the local area is shown in Fig. 4.1.

Table 4.1: Summary table of the data used in the analysis of the five boreholes at Alert, Nunavut, and the depths of thermistors within the boreholes.

Alert	BH1	BH2	BH3	BH4	BH5
Manual Ground Temperature Data	1978-2007	1978-2007	1978-2000	1978-2000	1978-2000
Logger Ground Temperature Data	N/A	N/A	2000-2004	2000-2002, 2007-2008	2000-04, 2006-08
Air Temperature	N/A	N/A	2000-2008	Jul00-05, Aug06-08	2000-2008
Ground Surface Temperature	N/A	N/A	2000-2005, 2006-08	Jul00-05, Aug06-08	2000-05, 2006-08
Near Surface Temperature	N/A	N/A	2001-2005	2001-2005	2001-2005
Snow	N/A	N/A	2002-2008	2002-2008	2002-2005
Manual Snow Surveys	1979-2003	1979-2003	1979-2003	1979-2003	1979-2003
Air Temperature (ECCS)	N/A	N/A	1950-2006	1950-2006	1950-2006
Distance to water body (km)	< 0.1	~ 1.0	~ 1.5	< 0.1	~ 0.4
Thermistor Depths (m)	1.5, 3.0, 6.1, 12.2, 18.3, 24.4, 30.5, 36.6, 42.7, 48.8, 54.9, 61.0	1.5, 3.0, 6.1, 12.2, 18.3, 24.4, 30.5, 36.6, 42.7, 48.8, 54.9, 61.0	2.4, 8.5, 14.6, 20.7, 26.8, 32.9, 39.0, 51.2, 57.3	0.8, 1.5, 2.3, 3.0, 3.8, 4.6, 7.6, 9.1, 12.2, 15.2	0.8, 1.5, 2.3, 3.0, 4.6, 7.6, 9.1, 15.2

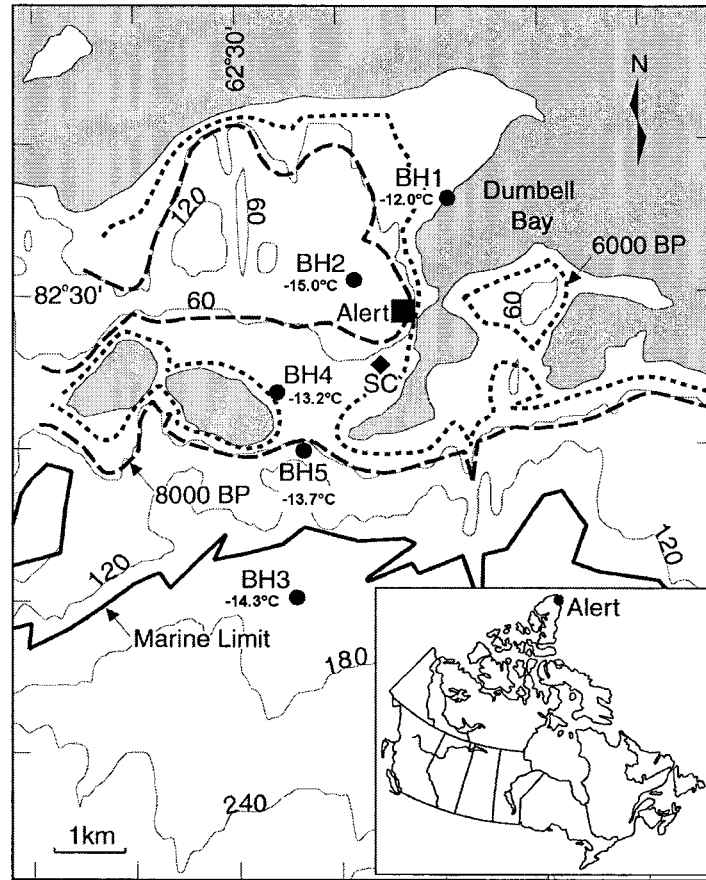


Figure 4.1: Location map of five boreholes at Alert, Nunavut (Smith et al., 2003). Temperature values represent the MAGT at the borehole for the following depths and years: BH1 and BH2 are for 12.2 m in 2005-06; BH3 is for 14.6 m in 2003-04; BH4 is for 9.1 m in 2007-08; and BH5 is for 15.2 m in 2007-08. The dashed lines represent the approximate shoreline 6000 and 8000 years ago (from England, 1976), the contour lines represent 60 m intervals, and SC is the Environment Canada snow course. BH3 lies above the marine limit.

BH1 is located at about 5 m elevation (Taylor et al., 2006) along the east coast of Dumbell Bay (Figs. 4.1 and 4.2). There is approximately 4 m of overburden composed of silt, sand and shattered rock, over argillite. BH2 is further inland at 77 m elevation (Taylor et al., 2006) on a gentle east-facing slope (Figs. 4.1 and 4.3). The overburden is about 3 m thick and composed of till and shattered rock, infilled with ice, and over top of argillite that is cemented with ice between 30 and 48 m. BH1 and BH2 have been monitored manually since 1978.



Figure 4.2: Photograph of Alert BH1 taken in August, 2001 (photo is courtesy of the Geological Survey of Canada).



Figure 4.3: Photograph of Alert BH2 taken in August, 2001 (photo is courtesy of the Geological Survey of Canada).

Measurements were also recorded manually at BH3, BH4, and BH5 since 1978, but these boreholes were instrumented with automatic data-loggers in 2000 and weather stations and ground surface loggers were installed in 2002. BH3 is the furthest inland, located on a plateau at about 170 m elevation (Taylor et al., 2006; Figs. 4.1 and 4.4). The overburden is 2.4 m thick and composed of till and shattered rock and infilled with ice. Below 2.4 m there is argillite to 13 m, then greywacke to the bottom of the borehole at 60 m. BH4 is at 38 m elevation (Taylor et al., 1982) in a valley on a south-facing slope on

the shore of a lake (Figs. 4.1, 4.5 and 4.6). The overburden is 3 m deep and composed of till and shattered rock, overlying greywacke to 8 m, and argillite to 15.2 m at the bottom of the borehole. Lastly, BH5 is at 69 m elevation on an exposed north-facing slope (Figs. 4.1, 4.6 and 4.7) aligned with the prevailing winds (Smith et al., 2003). The overburden is composed of 2.4 m of till and shattered rock and is infilled with ice, overlying argillite to the bottom of the borehole at 15.2 m.

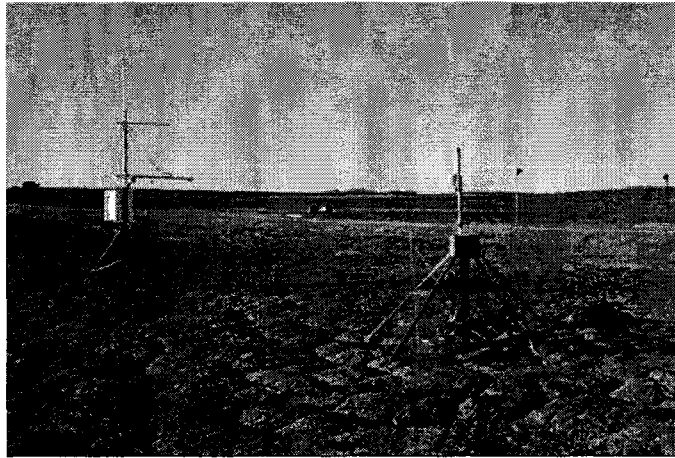


Figure 4.4: Photograph of Alert BH3 weather station and borehole, taken in August, 2002 (photo is courtesy of the Geological Survey of Canada).



Figure 4.5: Photograph of weather station at Alert BH4, taken in August 2002 (photo is courtesy of the Geological Survey of Canada).



Figure 4.6: Photograph taken from Alert BH5 looking toward Alert BH4 at the shore of the lake, taken in August, 2002 (photo is courtesy of the Geological Survey of Canada).

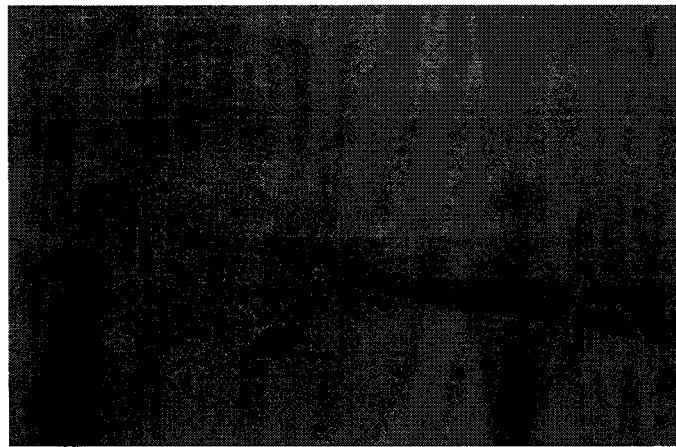


Figure 4.7: Photograph of weather station and borehole at Alert BH5, taken in August 2002 (photo is courtesy of the Geological Survey of Canada).

The closest ECCS is in Alert at $82^{\circ}31'N$ and $62^{\circ}16'W$, approximately 2.8 km from the borehole sites, though it is closer to some than to others (Fig. 4.1). The Alert boreholes are monitored by the Geological Survey of Canada, with data collected by on-site staff from Environment Canada and the Department of National Defense. Previous analyses conducted on data from this site, up to 2002 at BH5 and 2004 at BH1, BH2 and BH3, are given in Smith et al. (2003; 2005) and Taylor et al. (1982; 2006).

4.1.1 Alert BH1 and BH2

The datasets at Alert BH1 and BH2 are comprised of almost 30 years of manually collected ground-temperature and snow-depth data from 1978 to 2007. Snow depths were measured manually at four places near each borehole on every visit during the winter (Smith et al., 2003). Temperatures below ZAA were averaged to obtain MAGTs for each year, and MAGTs above ZAA were calculated using weighted averages. To calculate the shallower MAGTs, each manual reading was used to represent half of the number of days between it and the previous reading, and half of the number of days until the next reading. The temperature values from each manual reading over a September to August year were multiplied by the appropriate number of days, then added together, and lastly divided by 365 to obtain an approximate MAGT.

The snow survey data indicates that more snow usually accumulates at BH1 than at BH2 (Smith et al., 2003). Maximum snow depths at BH1 ranged between 10 and 80 cm, and max snow depths at BH2 ranged between 5 and 50 cm. Ground temperatures at depth at BH1, located along the coast of Dumbell Bay, are between 3 and 5°C warmer than that at BH2 (Fig. 4.8), which lies further inland and is at a higher elevation. Coastal warming effects due to its location are suggested by the steep geothermal gradient in comparison to that at BH2, which is likely caused by higher ground surface temperatures beneath the bay, adjacent to the borehole. Permafrost at BH1 would be significantly shallower than the permafrost at BH2 because of its warmer temperatures and steeper geothermal gradient. The ground temperature profiles at BH1 and BH2 indicate that warming has occurred by the curvature toward warmer temperatures in the near-surface in the year 2005-06 (Fig. 4.8).

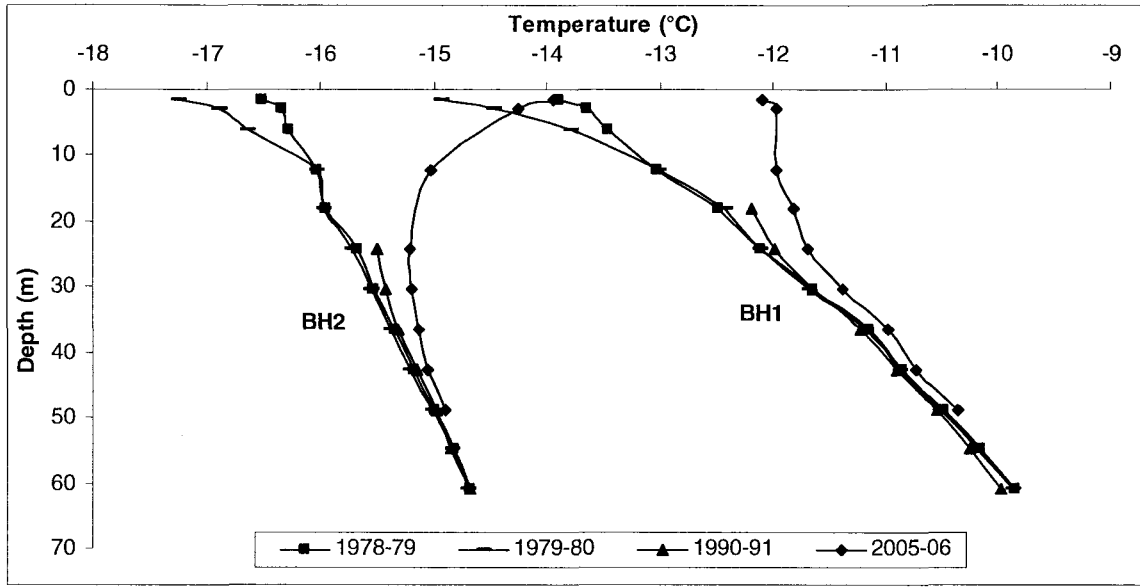


Figure 4.8: Mean ground temperature profiles at Alert, Nunavut, BH1 and BH2 for the years 1978-79, 1979-80, 1990-91 and 2005-06. BH1 warms faster with depth than BH2 due to its proximity to the coast. BH2 remains colder throughout the profile, except near the surface in 2005-06. Both sites show warming over the 27 year period.

Ground temperatures at 36.6 m and shallower have warmed since the beginning of monitoring in 1978 at both BH1 and BH2 (Figs. 4.9 and 4.10, respectively). Temperatures at 30.5 m have increased by 0.1°C per decade at both BH1 and BH2, and these trends are statistically significant ($p < 0.001$). The warming accelerated around the early 1990's, with a dip in temperatures occurring in the mid 1990's at both sites. Cooling occurred in the deepest ground temperatures until the early 1990's. The overlapping of some shallower ground temperatures in Fig. 4.10 indicates that warming has occurred from the surface downwards. This is also indicated by temperatures increasing more rapidly at the shallower depths than at deeper ones (Figs. 4.9 and 4.10).

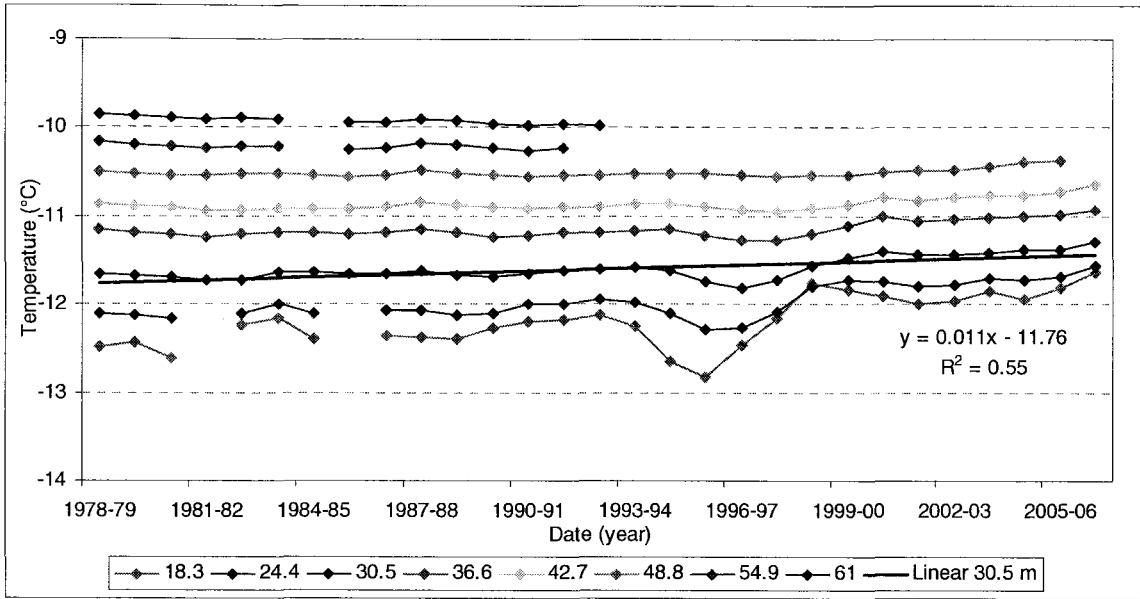


Figure 4.9: MAGTs at Alert BH1, from 18.3 m and deeper, between 1978 and 2007. The warming trend at 30.5 m is statistically significant ($p < 0.001$). Deeper ground temperatures, below 42.7 m, continued to cool until the early 1990's while the shallower temperatures warmed.

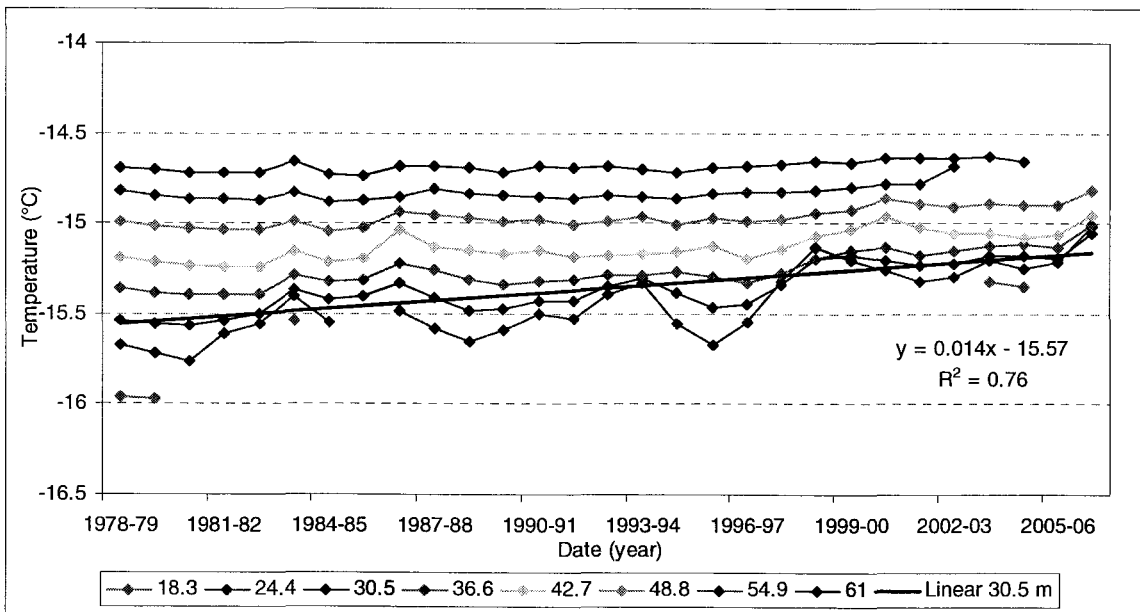


Figure 4.10: MAGTs at Alert BH2, from 18.3 m and deeper, between 1978 and 2007. The warming trend at 30.5 m deep is statistically significant ($p < 0.001$). The overlap in the shallower temperatures near the end of the record indicates that the warming has occurred from the surface downwards.

4.1.2 Alert BH3

BH3 at Alert had moderate amounts of snow during the winter between 2002 and 2008, with maximum values ranging between 37 and 76 cm, and it typically remained on the ground from the end of August or September until the end of June or July (Fig. 4.11). Thus the ground is typically snow-free for only two to four months of the year. The average snow depths ranged between 21 and 50 cm, and SDD ranged between 5212 and 15130 (Table 4.2), reflecting the high inter-annual variability in the depth and duration of snow. Manual snow surveys indicate that maximum depths reached up to 90 cm between 1979 and 2003, thicker than at any of the other sites in the area.

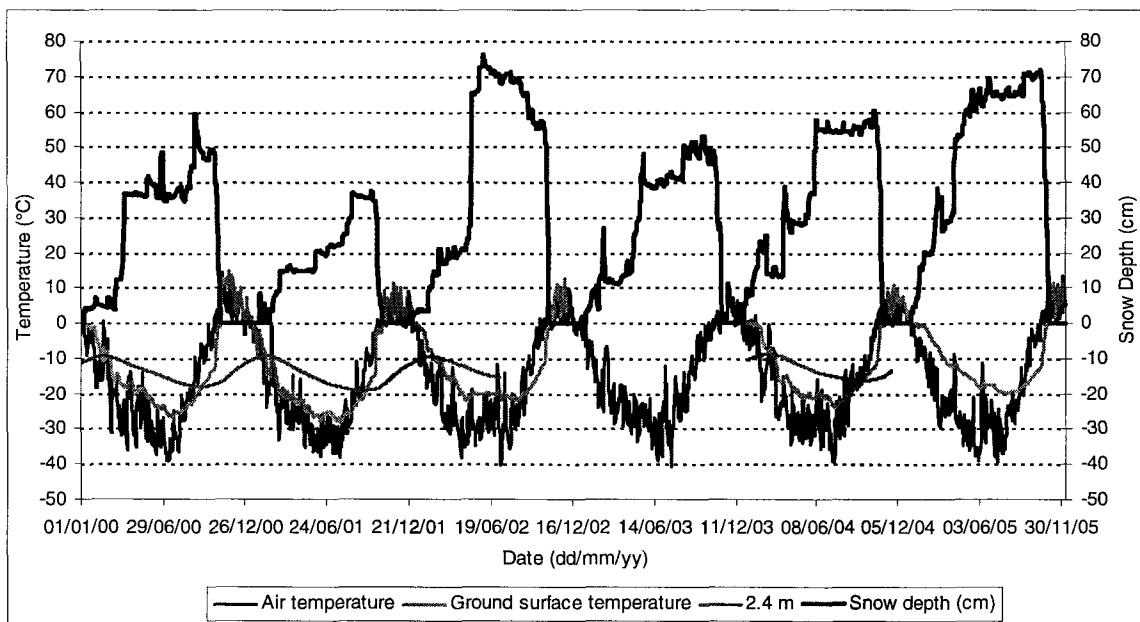


Figure 4.11: Air, ground surface, and 2.4 m temperatures, and snow depths between 2000 and 2005 at Alert BH3. When the snow accumulates at this site it tends to persist for the entire season, and the snow-free period is quite short, lasting a maximum of 2 months.

Table 4.2: Summary table of on-site data at Alert BH3, including FDD_a, FDD_s, TDD_a, TDD_s, SDD, n_f and n_t.

Year	FDD _a	FDD _s	n _f	SDD	Year	TDD _a	TDD _s	n _t
2000-01	6494.0	5312.7	0.82	<i>M</i>	2001	179.1	288.4	1.6
2001-02	6268.3	5713.0	0.91	<i>M</i>	2002	294.0	422.8	1.4
2002-03	6058.3	5014.3	0.83	9013	2003	347.8	480.7	1.4
2003-04	6274.0	5515.8	0.88	5267	2004	171.2	359.3	2.1
2004-05	6166.4	4641.1	0.75	12890	2005	<i>M</i>	<i>M</i>	<i>M</i>
2005-06	<i>M</i>	<i>M</i>	<i>M</i>	9348	2006	<i>M</i>	<i>M</i>	<i>M</i>
2006-07	5926.2	4529.7	0.76	11524	2007	155.8	281.8	1.8
2007-08	5979.6	3820.0	0.64	15130	2008	<i>M</i>	<i>M</i>	<i>M</i>
CV	0.03	0.13	0.11	0.33	CV	0.37	0.23	0.18

The coefficient of variation (CV) is presented to show the relative variability over the monitoring period. Missing data is represented by *M*.

MAATs between 2000 and 2008 were calculated using the air temperature data at the on-site weather station, and missing data were filled in using the on-site Vemco air temperature data. The MAAT ranged between -14.9 and -17.4°C and the MAGST ranged between -9.3 and -14.5°C between 2000 and 2008 (Table 4.3). The short record of MAAT shows an increase of about 0.2°C per year, but the trend is not statistically significant. The surface offsets are highly variable from year-to-year, ranging between 1.9 and 6.2°C. This variability is mostly due to the inter-annual differences in the duration and depth of snow at the site (Fig. 4.11). The relationship between SDD and surface offsets is statistically significant at $p < 0.05$ and has an r^2 value of 0.90, indicating the importance of snow at the site (Fig. 4.12).

Table 4.3: Summary table of continuously logged on-site data at Alert BH3, including the MAAT, MAGST, surface offset, TOP, TTOP, and the thermal offset.

Date	MAAT (°C)	MAGST (°C)	Surface Offset (°C)	TOP (m)	TTOP (°C)	Thermal Offset (°C)
2000-01	-17.4*	-13.9	3.5	1.4	-14.0	0.0
2001-02	-16.3*	-14.5	1.9	1.0	-14.6	-0.1
2002-03	-15.3	-12.4	3.2	1.1	-13.1	-0.7
2003-04	-16.3	-14.1	2.6	1.0	-14.4	-0.4
2004-05	-16.2	-11.7	4.7	<i>M</i>	<i>M</i>	<i>M</i>
2005-06	-14.9	<i>M</i>	<i>M</i>	<i>M</i>	<i>M</i>	<i>M</i>
2006-07	-15.3	-11.6	4.2	<i>M</i>	<i>M</i>	<i>M</i>
2007-08	-15.5	-9.3	6.2	<i>M</i>	<i>M</i>	<i>M</i>

* Values of MAAT were calculated from the Vemco loggers recording air temperature at the borehole site when weather station data was unavailable.

Missing data is represented by *M*.

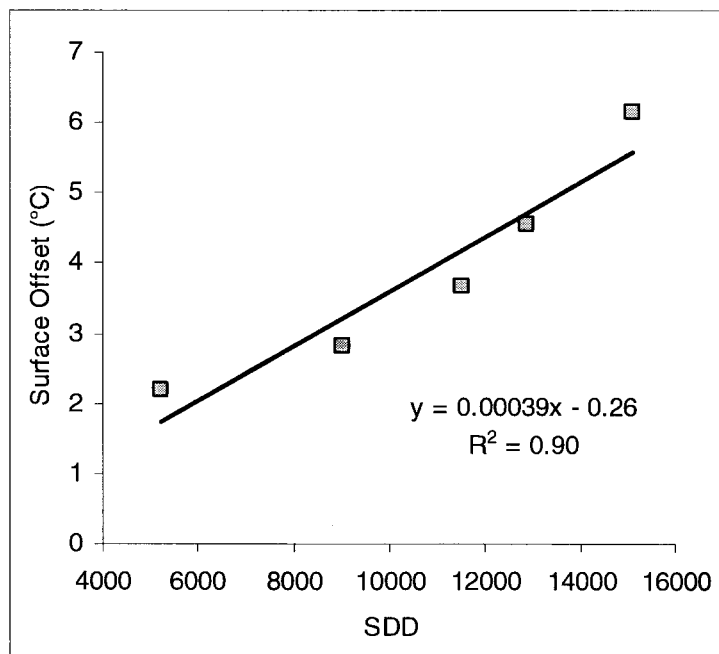


Figure 4.12: Relationship between SDD and surface offsets at Alert BH3 between 2002 and 2008. The trend line is significant at $p < 0.05$.

FDD of the air ranged between 5926 and 6494 and that of the ground surface ranged between 3820 and 5713 (Table 4.2). Values of n_f ranged between 0.64 and 0.91. Again, the inter-annual variability of air to surface relations is largely dependent on the variability in snow characteristics. The relationship between n_f and average snow depth

has a strong negative correlation with an r^2 value of 0.94 (Fig. 4.13), and is statistically significant ($p < 0.01$).

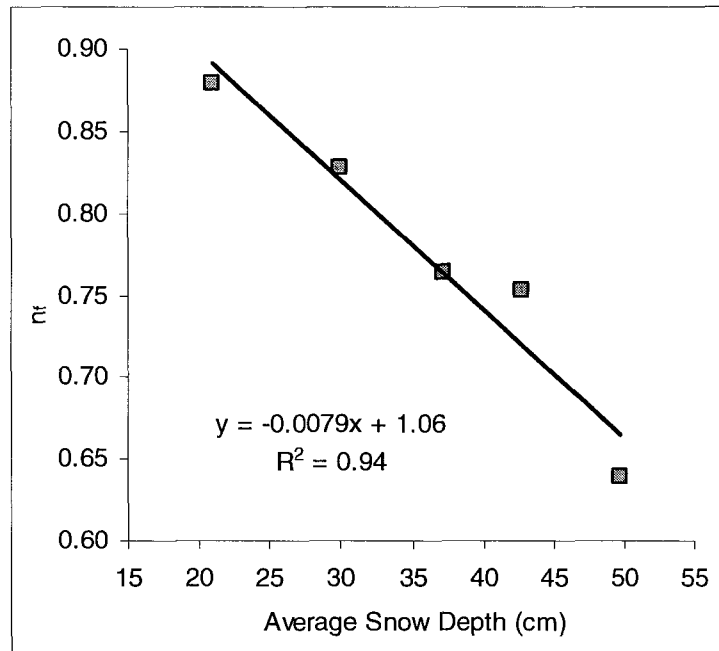


Figure 4.13: Relationship between average snow depths and n_f at Alert BH3 between 2002 and 2008. The trend line is significant at $p < 0.01$.

TDD of the air ranged between 156 and 347, and that of the ground surface ranged between 282 and 481 (Table 4.2). Values of n_t ranged between 1.4 and 2.1. The high values of n_t may be due to the minute amounts of vegetation and dark exposed surfaces, allowing the ground surface to warm more easily than the air during periods of direct solar radiation (Klene et al., 2001). In addition, air temperatures at Alert are influenced by the coast, and most likely nearby snow and ice, creating relatively colder air temperatures compared to the ground surface, which is warmed by 24 hours of daylight during the summer.

TOP and TTOP were calculated for the four thaw seasons between 2000 and 2004 (Table 4.3). TOP ranged between 0.95 and 1.40 m, and TTOP ranged between -13.1 and

-14.6°C. MAGST and TTOP were very similar over the four years, with low thermal offsets ranging from 0.0 to -0.7°C (Table 4.3).

The zero-curtain is limited at this site. It lasts between 8 and 12 days during freeze-back at 18 cm, and a shorter time at the ground surface. The latent heat effects are associated with the moisture present from melting snow during the spring, and the small amounts of precipitation the site receives over the summer. The apparent thermal diffusivity is at its lowest near the ground surface, $0.2 \times 10^{-6} \text{ m}^2\text{s}^{-1}$ compared to 1.7×10^{-6} to $3.4 \times 10^{-6} \text{ m}^2\text{s}^{-1}$ between 2.4 and 20.7 m depth, indicating that this small amount of moisture does have an effect on the propagating temperatures, causing them to dampen more rapidly near the surface than deeper in the ground.

The temperature envelope (Fig. 4.14) shows that the depth of ZAA is just above 20.7 m as the amplitude at this depth ranges between 0.08 and 0.09°C. Using the apparent thermal diffusivity to calculate a more accurate depth resulted in an estimate of 19.9 m. The average temperature at ZAA is about -14.3°C. Over the four years of continuous ground temperature monitoring, the entire profile of MAGTs has apparently warmed each year by about 0.02°C, but this is within the potential error of the instrumentation. The apparent thermal diffusivity at depths between 2.4 and 20.7 m is fairly high, and hence it takes between 10 and 10.5 months for the ground surface temperature wave to propagate to 20.7 m.

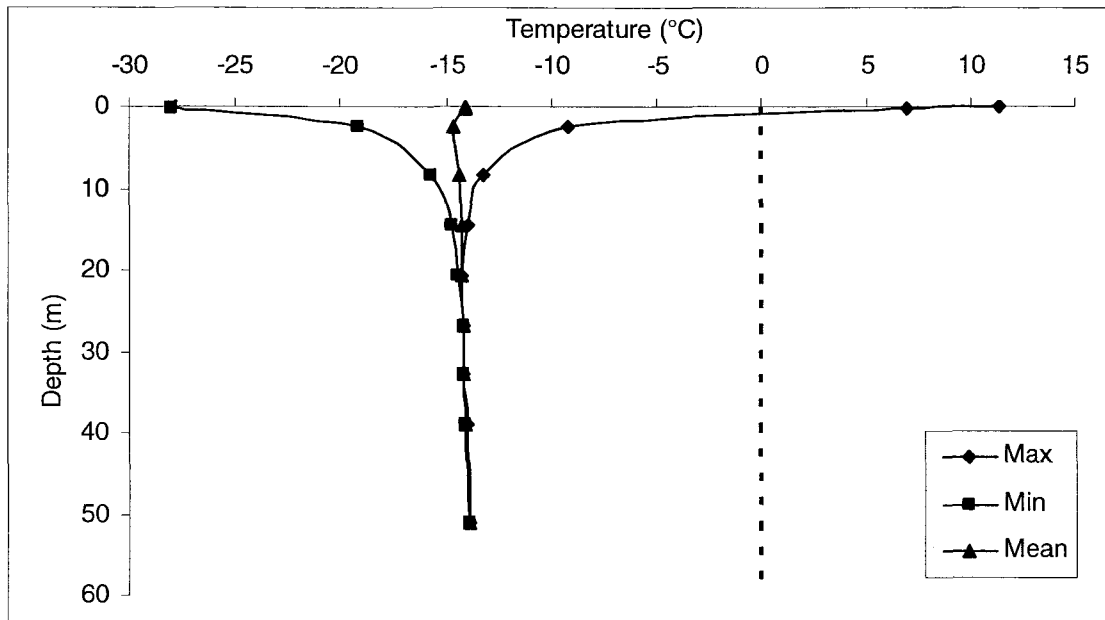


Figure 4.14: Temperature envelope at Alert BH3 for the year 2003-04.

Temperatures warm with depth by 0.4°C over 30 m below the depth of ZAA, which is just outside the range of geothermal gradients of 1°C of warming every 30-60 m depth (French, 2007). Based on the range of geothermal gradients ($1^{\circ}\text{C}/30\text{-}60\text{ m}$), the thickness of permafrost would be between 420 and 840 m.

Ground temperatures at 2.4 m warmed since the start of monitoring in 1978 by about 0.4°C per decade, but because of the considerable inter-annual variability at this depth, the trend is not statistically significant. The deep ($> 20.7\text{ m}$) ground temperatures cooled between 0.01 and 0.06°C per decade between the late 1970's and the late 1990's (Fig. 4.15). This cooling trend is statistically significant at depths 32.9 ($p<0.05$), 39.0, 51.2 and 57.3 m ($p<0.001$). However, these cooling trends are within the accuracy of the instrumentation. Since the late 1990's, ground temperatures show evidence of warming from the surface downwards (Fig. 4.15).

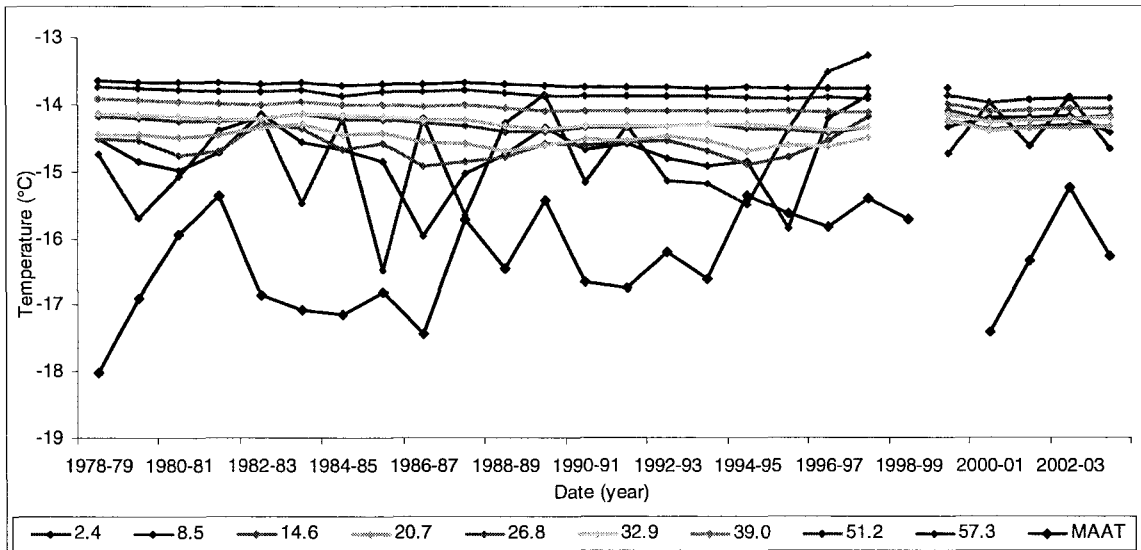


Figure 4.15: Time series of MAGTs from Alert BH3 and MAAT calculated using Alert ECCS data (Environment Canada, 2009) between 1978 and 2004.

4.1.3 Alert BH4

Continuous snow data exists for Alert BH4 between 2002 and 2008 (Fig. 4.16). The depth and duration of snow is highly variable inter- and intra-annually. SDD ranged between 2078 and 5682 (Table 4.4), the average snow depth ranged between 8.2 and 22.0 cm, and the maximum ranged between 18.7 and 48.3 cm. When the snow at this site is deeper than 20 cm for extended periods of time, the ground surface temperature fluctuations are dampened in relation to air temperature fluctuations (Fig. 4.16). The snow surveys conducted between 1979 and 2003 indicate that maximum annual snow depths ranged between 5 and 60 cm, though they are often less than 30 cm.

Table 4.4: Summary table of on-site data at Alert BH4, including FDD_a, FDD_s, TDD_a, TDD_s, SDD, n_f and n_t.

Year	FDD _a	FDD _s	n _f	SDD	Year	TDD _a	TDD _s	n _t
2000-01	6618.3	6238.0	0.94	<i>M</i>	2001	212.8	565.0	2.7
2001-02	6548.5	5973.4	0.91	<i>M</i>	2002	334.5	665.6	2.0
2002-03	6197.3	6341.0	1.02	2810	2003	354.0	632.7	1.8
2003-04	6489.4	6177.3	0.95	2234	2004	192.3	447.8	2.3
2004-05	6360.3	5587.5	0.88	2262	2005	<i>M</i>	<i>M</i>	<i>M</i>
2005-06	<i>M</i>	<i>M</i>	<i>M</i>	2078	2006	<i>M</i>	<i>M</i>	<i>M</i>
2006-07	-5955.6	-5255.1	0.88	3407	2007	213.0	444.0	2.1
2007-08	-6124.5	-4983.0	0.81	5682	2008	<i>M</i>	<i>M</i>	<i>M</i>
CV	0.04	0.09	0.07	0.44	CV	0.29	0.19	0.42

The coefficient of variation (CV) is presented to show the relative variability over the monitoring period. Missing data is represented by *M*.

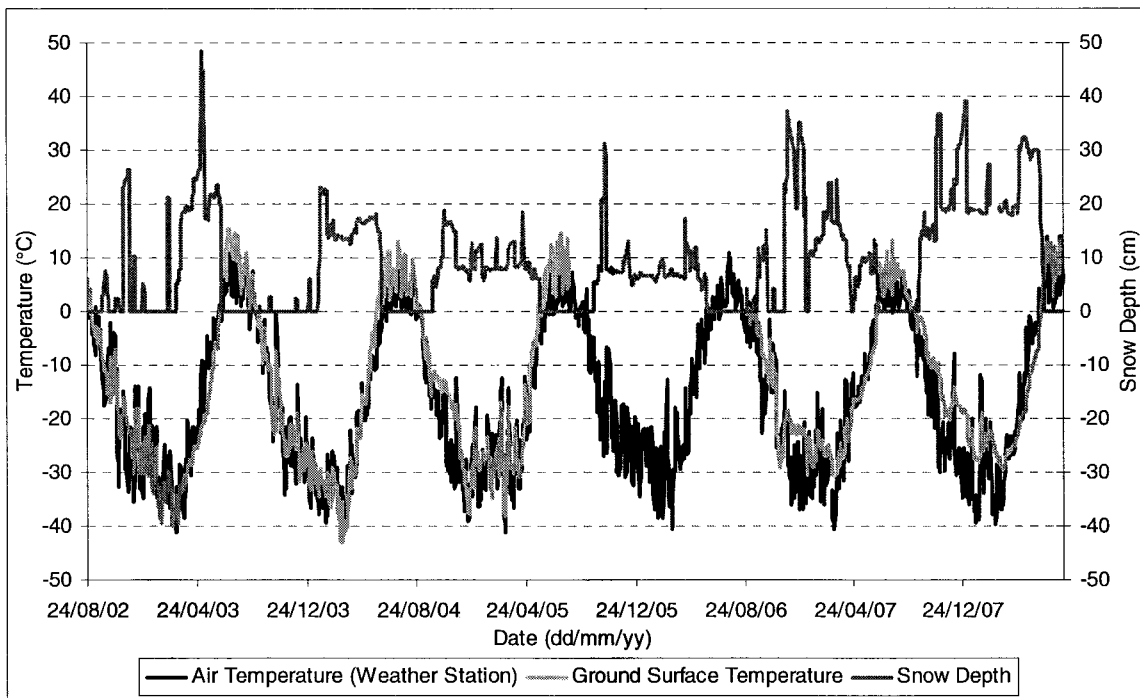


Figure 4.16: Air temperatures, ground surface temperatures, and snow depths at Alert BH4 between 2002 and 2008.

The MAAT ranged between -15.8 and -17.9°C, and the MAGST ranged between -12.1 and -15.6°C between 2000 and 2008 (Table 4.5). The surface offset ranged between 0.4 and 3.7°C. The largest surface offset occurred in 2007-08, the year that had the highest SDD value of 5682. Higher than normal ground surface temperatures

combined with the deepest snow depths on record are shown in Fig. 4.16 during the winter of 2007-08.

Table 4.5: Summary table of continuously logged on-site data at Alert BH4, including the MAAT, MAGST, surface offset, TOP, TTOP, and the thermal offset.

Date	MAAT (°C)	MAGST (°C)	Surface Offset (°C)	TOP (m)	TTOP (°C)	Thermal Offset (°C)
2000-01	-17.7*	-15.5	2.1	<i>M</i>	<i>M</i>	<i>M</i>
2001-02	-17.0*	-14.5	2.5	1.2	-14.3	0.2
2002-03	-16.0*	-15.6	0.4	<i>M</i>	<i>M</i>	<i>M</i>
2003-04	-17.4*	-15.4	2.0	<i>M</i>	<i>M</i>	<i>M</i>
2004-05	-16.6	-14.9	1.7	<i>M</i>	<i>M</i>	<i>M</i>
2005-06	-15.3	<i>M</i>	<i>M</i>	<i>M</i>	<i>M</i>	<i>M</i>
2006-07	-15.8*	-13.2	2.6	<i>M</i>	<i>M</i>	<i>M</i>
2007-08	-15.8*	-12.1	3.7	1.2	-12.2	-0.1

* Values of MAAT were calculated from the Vemco loggers recording air temperature at the borehole site when weather station data was unavailable.

Missing data is represented by *M*.

FDD of the air ranged between 5956 and 6618, and that of the ground surface ranged between 4983 and 6341 (Table 4.4). Values of n_f ranged between 0.81 and 1.02, reflecting the low influence of snow. The lowest n_f value of 0.81 occurred in 2007-08, corresponding with the greatest snow values. The two winters with highest n_f values were in 2002-03 and 2003-04; during these two winters snow accumulated on the ground later in the season, allowing the ground surface to become almost as cold as temperatures in the air, and the ground surface temperature followed air temperatures closely (Fig. 4.16).

TDD of the air ranged between 192 and 354, and that of the ground surface ranged between 444 and 666 (Table 4.4). Values of n_t are high at this site and range between 1.8 and 2.7. The ground surface is dark, dry, and has very little vegetation, allowing the surface to heat significantly more than the air during periods of direct insolation, especially since the air temperature are affected by snow and ice in the vicinity, and the cold coastal air.

TOP and TTOP were calculated for the years 2001-02 and 2007-08 (Table 4.5). During both years TOP was at approximately 1.2 m, and TTOP were -14.3 and -12.2°C, respectively. The thermal offsets were very low at 0.2 and -0.1°C, respectively. These low values indicate that the soil is very dry and the thermal conductivity therefore remains similar in both frozen and thawed states (Burn and Smith, 1988; Smith and Riseborough, 2002). The dryness of the site is also indicated by the absence of a zero-curtain effect in the near-surface temperature trends.

Although the borehole is 15.2 m deep, ground temperatures are continually recorded to a depth of 9.1 m, which is above the depth of ZAA. The temperature envelopes for the three years of continuous data, 2000-01, 2001-02, and 2007-08, are variable from year-to-year. The most recent year, 2007-08, was warmer than the two earlier ones. The temperature envelopes for 2001-02 and 2007-08 are plotted in Fig. 4.17. The maximum temperatures were comparable over the 3 years, but MAGTs and minimum temperatures were warmer in 2007-08, likely due to the large amount of snow present that winter. The annual temperature amplitude also decreased at each depth over the 3 years. Based on the average apparent thermal diffusivity at the bottom of the temperature envelope the depth of ZAA would be approximately 18.2 m. The permafrost at this site is estimated at between 430 and 860 m thick, depending on the actual geothermal gradient at the site.

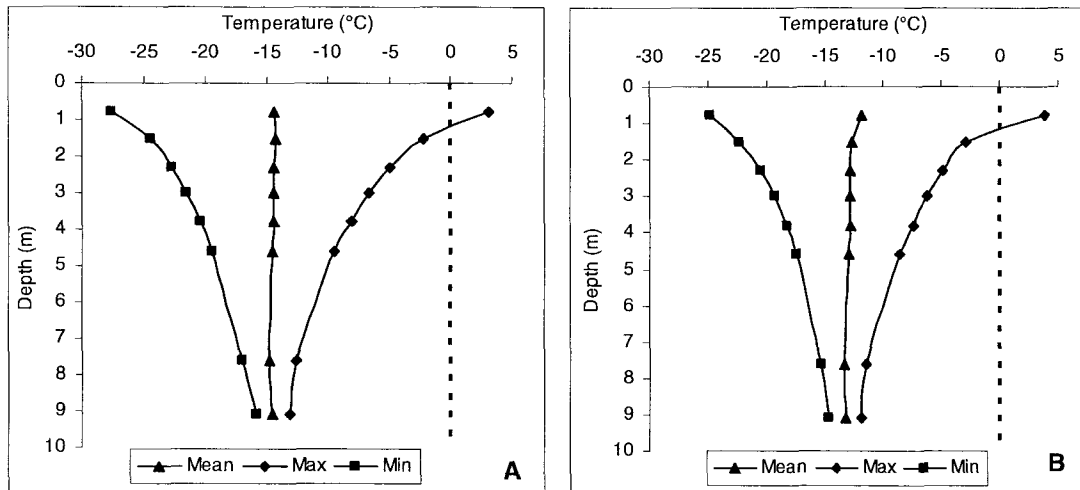


Figure 4.17: Temperature envelopes at Alert BH4 for (A) 2001-02, and (B) 2007-08.

There is no warming or cooling trend evident in the shallow ground temperature data collected manually between 1978 and 1988, although the temperatures at each depth during this period are less than they were in 2007-08. The continuous temperature record gives an indication of how the thermal wave propagated with depth using the apparent thermal diffusivity of about $1.5 \times 10^{-6} \text{ m}^2\text{s}^{-1}$. The temperature wave would take about 120 days to propagate from 1.5 to 9.1 m.

4.1.4 Alert BH5

Alert BH5 is on an exposed north-facing slope (Figs. 4.1, 4.6 and 4.7), and is prone to wind scouring, clearing the site of snow throughout most of the winter. The lack of vegetation associated with this polar desert site also reduces the possibility of snow accumulation.

Snow depths at Alert BH5 were monitored continuously between 2002 and 2005, and are the shallowest of the Alert boreholes (Smith et al., 2003). There were 3 short events where small amounts of snow remained on the ground. For about one month between April and May 2003 there was between 10 and 16 cm of snow on the ground.

The next event only lasted 4 days at the beginning of October 2003. The last event where snow remained on the ground was between the end of September and mid-November 2004, with depths between 2 and 10 cm. During these events, the ground surface temperature fluctuated less than during much of the rest of the record when it varied with almost the same magnitude as the air temperature. The maximum snow depths indicated from snow surveys ranged between 2 and 60 cm, though most often the maximum depth measured was less than 20 cm. Overall, snow appears to have very little influence on ground temperatures at this site because the pack remains very thin through the winter.

The MAAT ranged between -14.5 and -17.2°C , and the MAGST ranged between -12.9 and -15.5°C from 2000 to 2008 (Fig. 4.18; Table 4.6). Both the MAAT and MAGST were coldest in the earlier part of the record and warmer in more recent years. MAAT increased at a rate of 0.3°C per year over this period, and the trend is statistically significant ($p < 0.05$). The warming trend in MAGST was also statistically significant ($p < 0.01$) with the same rate of 0.3°C warming per year. The surface offset ranged between 0.2 and 1.9°C . These low values are due to the ground surface temperatures remaining very close to, or slightly colder than, air temperatures in the winter, and almost always remaining warmer than the air in the summer.

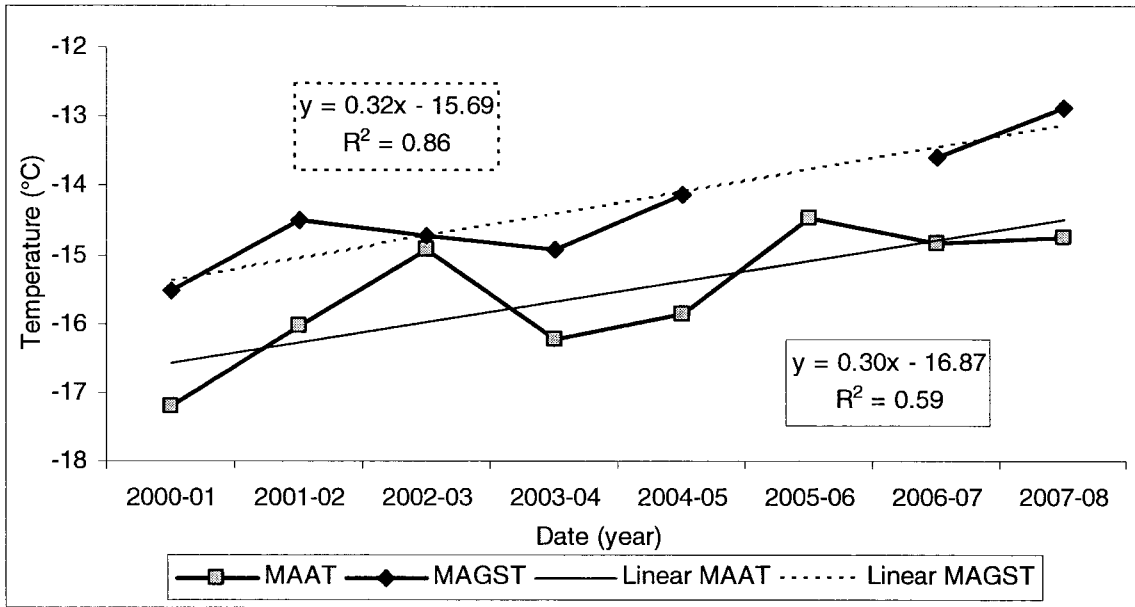


Figure 4.18: MAAT and MAGST trends at Alert BH5 between 2000 and 2008 from continuously logged on-site data. Both trends are statistically significant ($p < 0.05$ and $p < 0.01$, respectively).

Table 4.6: Summary table of continuously logged on-site data at Alert BH5, including the MAAT, MAGST, surface offset, TOP, TTOP, and the thermal offset.

Date	MAAT (°C)	MAGST (°C)	Surface Offset (°C)	TOP (m)	TTOP (°C)	Thermal Offset (°C)
2000-01	-17.2*	-15.5	1.7	0.8	-15.7	-0.2
2001-02	-16.0*	-14.5	1.5	0.8	-14.8	-0.3
2002-03	-14.9	-14.7	0.2	0.8	-14.6	0.1
2003-04	-16.2	-14.9	1.3	0.8	-14.9	0.1
2004-05	-15.9	-14.1	1.7	M	M	M
2005-06	-14.5	M	M	M	M	M
2006-07	-14.8	-13.6	1.2	0.8	-14.3	-0.7
2007-08	-14.8	-12.9	1.9	0.8	-13.6	-0.7

* Values of MAAT were calculated from the Vemco loggers recording air temperature at the borehole site when weather station data was unavailable.

Missing data is represented by *M*.

FDD of the air ranged between 5570 and 6420, and that of the ground surface ranged between 5190 and 6080 from 2000 to 2008 (Table 4.7). Values of n_f remained very close to 1.0, with a range between 0.91 and 1.03. These high values are due to the thin snow cover during the winter, as shown by the very low values of SDD (Table 4.7). The year-to-year variability of FDD is similar for both the air and ground surface.

Table 4.7: Summary table of on-site data at Alert BH5, including FDD_a, FDD_s, TDD_a, TDD_s, SDD, n_f and n_t.

Year	FDD _a	FDD _s	n _f	SDD	Year	TDD _a	TDD _s	n _t
2000-01	6421.0	6080.3	0.95	<i>M</i>	2001	168.9	445.3	2.6
2001-02	6170.9	5845.8	0.95	<i>M</i>	2002	308.3	566.1	1.8
2002-03	5780.5	5950.5	1.03	367	2003	324.2	571.9	1.8
2003-04	6051.7	5965.3	0.99	14	2004	170.7	414.2	2.4
2004-05	5913.9	5739.2	0.97	201	2005	<i>M</i>	<i>M</i>	<i>M</i>
2005-06	<i>M</i>	<i>M</i>	<i>M</i>	<i>M</i>	2006	<i>M</i>	<i>M</i>	<i>M</i>
2006-07	5567.7	5345.0	0.96	<i>M</i>	2007	170.1	414.4	2.4
2007-08	5720.5	5191.5	0.91	<i>M</i>	2008	<i>M</i>	<i>M</i>	<i>M</i>
CV	0.05	0.06	0.04	0.91	CV	0.35	0.17	0.18

The coefficient of variation (CV) is presented to show the relative variability over the monitoring period. Missing data is represented by *M*.

TDD of the air ranged between 169 and 324, and TDD of the ground surface ranged between 414 and 572 (Table 4.7). Values of n_t ranged between 1.8 and 2.6. The ground surface thermistor was observed sticking out of the ground on June 6, 2007, and was replaced on July 19, 2007. This may have caused higher than normal summer surface temperatures prior to the correction. The highest n_t after the logger was replaced was 2.4 and does not seem to be a problem since it is within the range of the preceding years. Values of n_t exceeded 1.0 for the entire monitoring period and are likely due to direct insolation on the exposed shattered bedrock surface, with little vegetation and low moisture and evaporation, in combination with the cold coastal effects on air temperatures in summer.

The borehole temperature record shows that TOP fluctuated just above and below 0.8 m throughout the monitoring period. Since temperatures within a few meters of TOP do not vary greatly as warming occurs very slowly with depth (Karunaratne and Burn, 2008), and this is especially true for a site in shattered bedrock, 0.8 m was used at this site as TOP. TTOP ranged between -13.6 and -15.7°C from 2000 to 2008 (Table 4.6),

with the coldest values occurring in 2000 and the warmest in 2008. The thermal offset ranged between -0.1 and 0.7°C , indicating that TTOP is very similar to MAGST.

There is very little moisture at this site, making it highly responsive to air temperature changes. The zero-curtain effect was only observed near the ground surface and lasted for a maximum of 7 days. The apparent thermal diffusivity within the active layer is lower than in the rest of the profile at about $2.8 \times 10^{-6} \text{ m}^2\text{s}^{-1}$.

At all of the measurement depths (down to 15.2 m) MAGT followed similar warming trends (Fig. 4.19). At 0.8 and 15.2 m depths temperatures have been warming since 2000 at a rate of 2.3°C and 1.6°C per decade, respectively. Both of these trends are statistically significant ($p < 0.05$ and $p < 0.001$, respectively) even though the record is short and 2 years of data are missing from the 8 years. The temperatures at 15.2 m depth ranged between -13.7 and -14.9 , and each year the entire depth profile of MAGTs warmed (Fig. 4.20). The large range at the top of the temperature envelope is due to the small amounts of snow at this site (Fig. 4.21), allowing the ground to cool along with winter air temperatures, while the dark surface in the summer allows high absorption of incoming solar radiation. The annual temperature range at the ground surface often exceeds 50°C , while at 4.6 m the annual range is about 10°C , and at 15.2 m it decreases to about 1°C (Fig. 4.21). Due to the lack of unfrozen moisture at the site, the range in ground temperatures dampens slowly with depth.

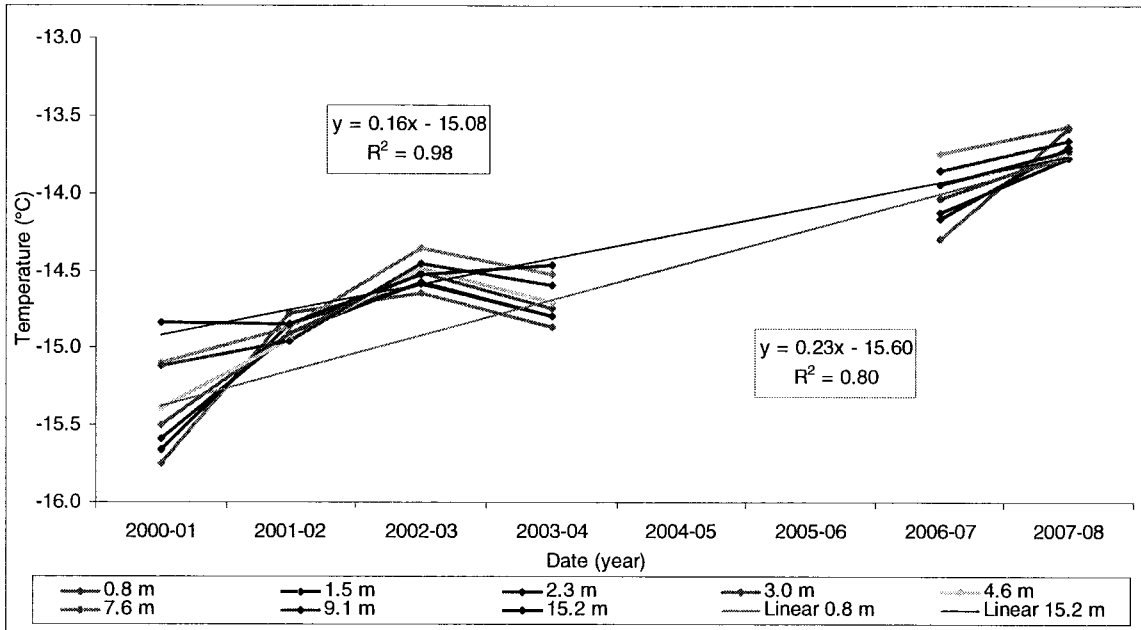


Figure 4.19: MAGTs between 2000 and 2008 at Alert BH5 from continuously logged data. Significant warming trends occurred at 0.8 and 15.2 m depths ($p < 0.05$ and $p < 0.001$, respectively).

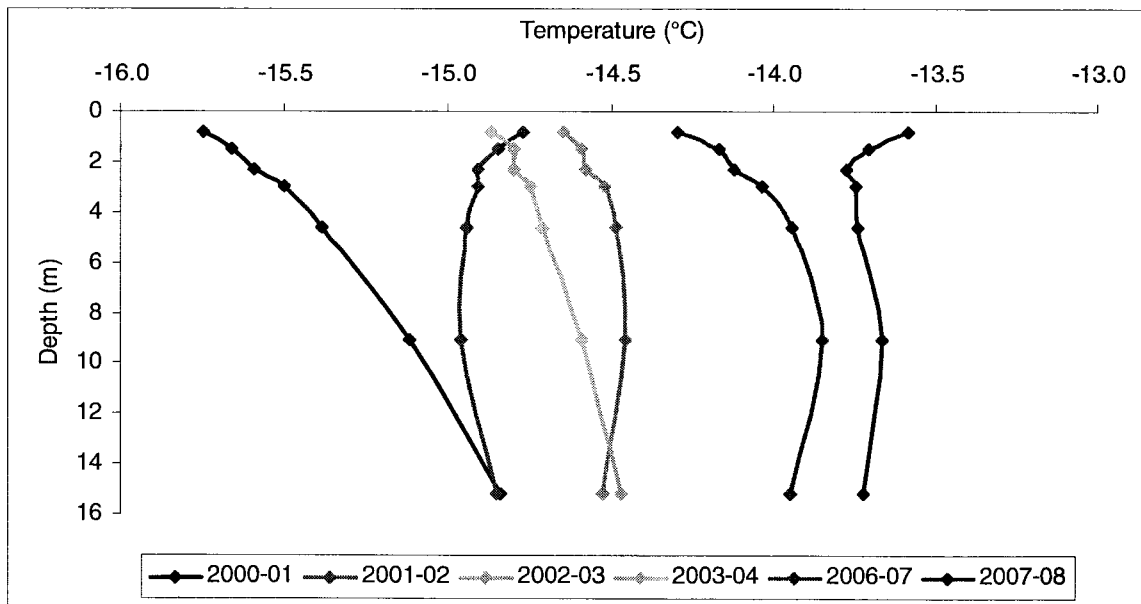


Figure 4.20: MAGT depth profiles at Alert BH5, Nunavut, from 2000 to 2008, showing warming through the entire profile each year. Note: sensor at 7.6 m depth has been removed from this figure due to drifting, and it is likely that 2.3 m has drifted as well, but to a smaller degree, and so it has not been removed.

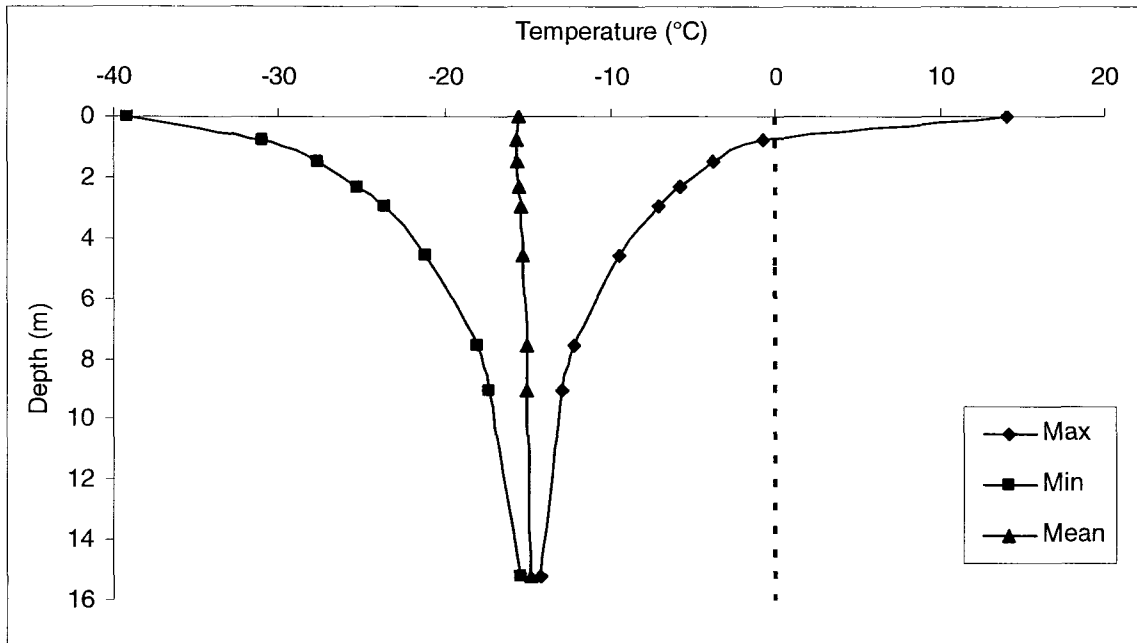


Figure 4.21: Temperature envelope at Alert BH5, Nunavut, for 2000-01.

The depth of ZAA is deeper than the base of the borehole at 15.2 m. Using the apparent thermal diffusivity near the bottom of the borehole, the depth of ZAA is approximately 23.8 m. The apparent thermal diffusivity is high compared to the other sites, and the temperature wave propagates relatively rapidly with depth. It would take between 180 and 195 days for the temperature at 0.8 m to propagate to 15.2 m. The thickness of the permafrost at this site, based on TTOP, is estimated to be between 500 and 800 m.

The extended record derived from the manual measurements shows that MAGTs at each depth warmed between 1978 and 2000 (Fig. 4.22). MAGTs at 0.8 m and 7.6 m warmed over the period by about 0.5°C and 0.3°C per decade, respectively, but they are not statistically significant due to the large inter-annual variation. MAGTs at 15.2 m warmed significantly by 0.2°C per decade ($p < 0.05$).

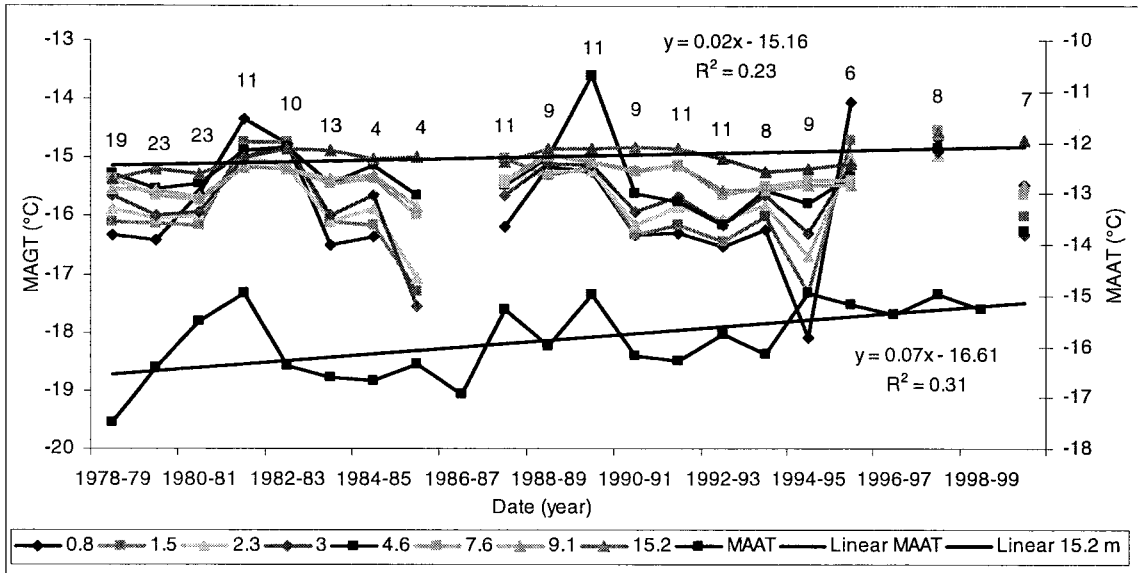


Figure 4.22: MAGTs calculated from manual measurements and correlated MAATs from ECCS data (Environment Canada, 2009) from 1978 to 2000 at Alert BH5. The warming trends in MAAT and MAGT at 15.2 m are both statistically significant ($p < 0.001$ and $p < 0.05$, respectively). The number values above each MAGT represent the number of manual measurements recorded that year. Note: Values from 1994-95 were skewed by readings taken during colder than normal periods, so they are probably not an accurate estimate of values closer to the surface.

4.1.5 Regional Climatic Trends at Alert, Nunavut

The air temperature records at Alert BH3, BH4, and BH5 were hind-cast to 1950 through correlations using monthly ECCS air temperature data (Fig. 4.23). The three sites have slight climatic differences due to the local topography of the area (Figs. 4.23 and 4.24): Alert BH5 is the warmest, BH3 is slightly colder, and BH4 experiences the coldest MAAT of the three. A climatic cooling trend is observed between the start of the record in 1950 until about 1975 (Fig. 4.23). The cooling trend was consistent at all three sites, cooling at a rate of 0.3°C per decade, and is significant at $p < 0.05$. This is followed by a significant warming trend between about 1976 to the end of the record in 2006 ($p < 0.01$; Fig. 4.23). MAAT warmed at a rate of 0.4 or 0.5°C per decade, and BH4 experienced a slightly higher magnitude of warming than the other two sites.

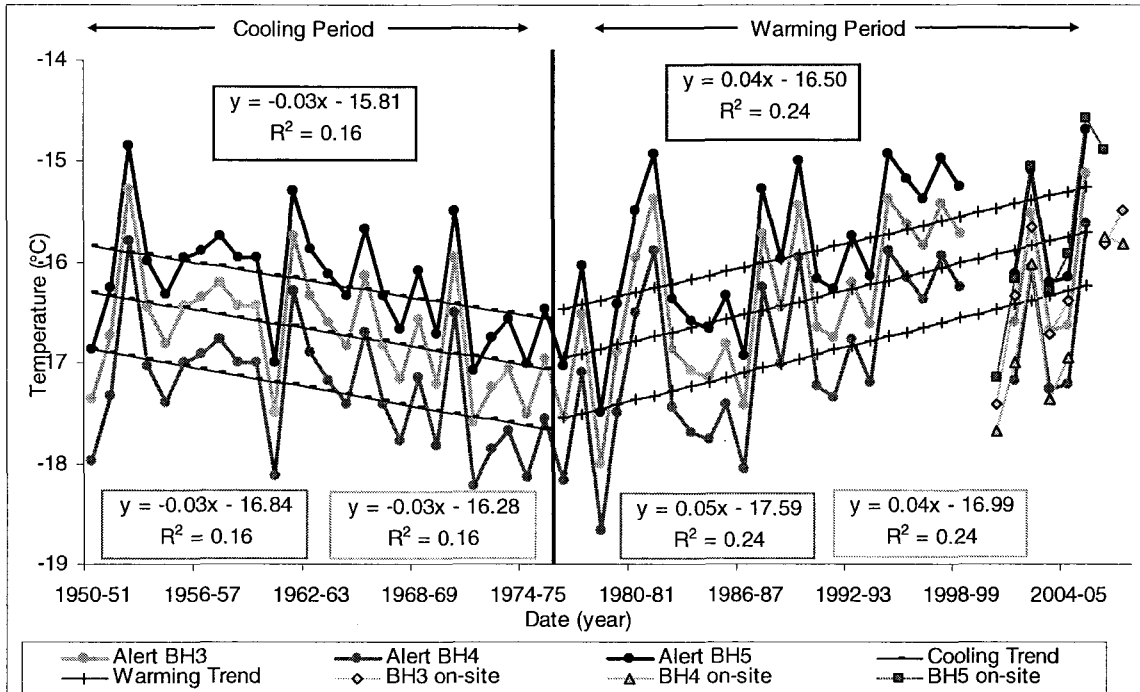


Figure 4.23: Hind-cast MAATs at Alert BH3, BH4 and BH5 from correlated Alert, Nunavut, ECCS data (Environment Canada, 2009) between 1950 and 2006. Cooling trends from 1950 to 1975 and warming trends from 1976 to 2006 are observed at all three boreholes, and are significant at $p < 0.05$ and 0.01 , respectively.

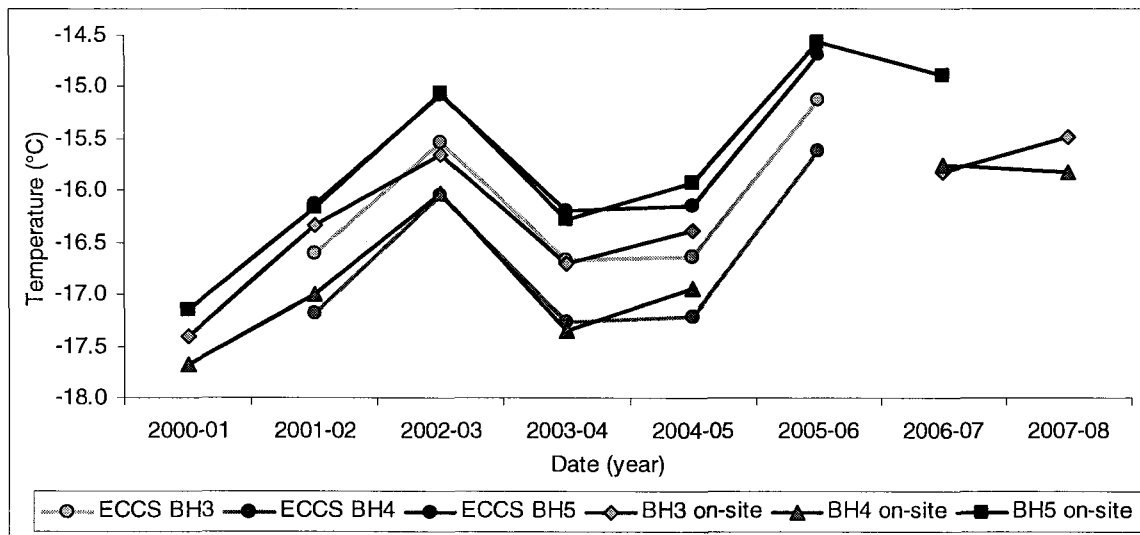


Figure 4.24: Comparison of measured on-site MAAT from 2000 to 2008 with the values calculated from correlations with the Alert ECCS data between 2001 and 2006 (Environment Canada, 2009) for Alert BH3, BH4, and BH5. The figure also illustrates the differences in MAAT between the three sites.

Seasonal average temperatures between 1950 and 2007 at Alert BH3, BH4, and BH5 are plotted in Figure 4.25. Spring and autumn temperatures are the most variable inter-annually. Although the spring warmed by about 0.3 to 0.4°C per decade since the 1970's, it was not significant. Autumn, on the other hand, warmed with significance by 0.9°C per decade since the late 1970's ($p < 0.05$; Fig. 4.25). Winter also warmed significantly by 0.4°C per decade which began in 1970 and continued until the end of the record in 2006 ($p < 0.05$; Fig. 4.25). Summer was the least variable inter-annually, and remained relatively constant over the period, fluctuating around a mean of 1.7°C for the entire period (Fig. 4.25). The local variation between the thermal monitoring sites is visible in Fig. 4.25, although autumn and summer temperatures are most similar between the sites, whereas greater differences are observed during spring and winter.

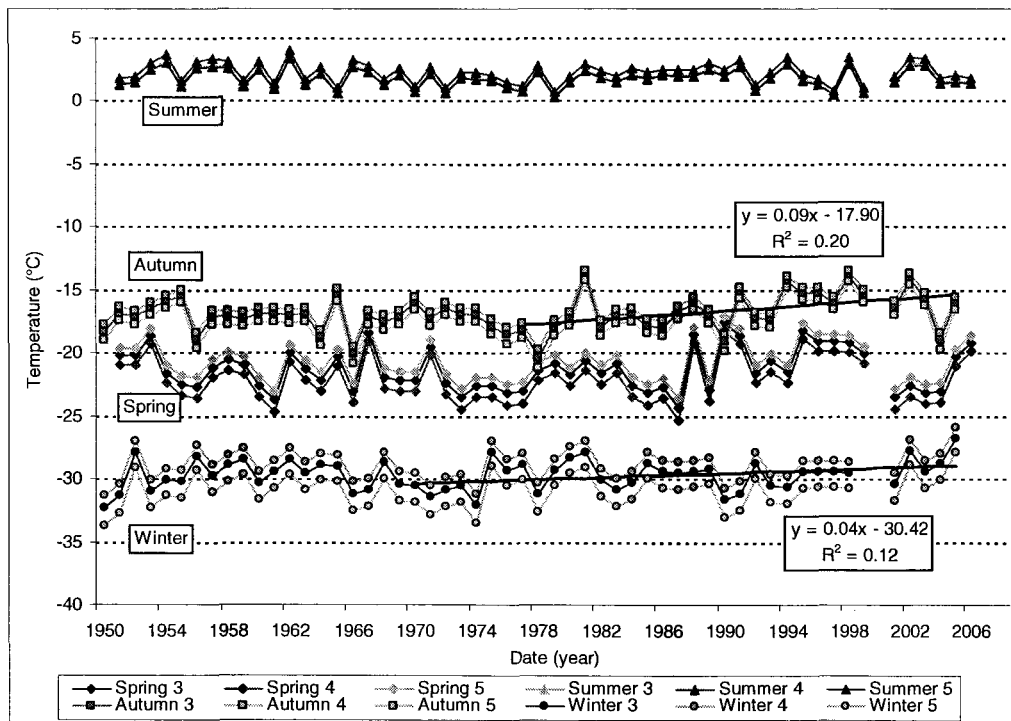


Figure 4.25: Seasonal average air temperatures at Alert BH3, BH4, and BH5 (labeled by season and number of borehole) from hind-cast monthly Alert ECCS data (Environment Canada, 2009). Statistically significant trends are observed in the winter and autumn at the sites ($p < 0.05$); the trend-lines are plotted for BH3.

4.1.6 Synthesis of Alert Boreholes

The five boreholes at Alert, Nunavut, are all within 7 km from one another. BH1 and BH3 are the furthest apart, with the former located along the coast of Dumbell Bay at 5 m elevation, and the latter located furthest from the coast at 170 m elevation (Fig. 4.1). The ground temperatures at all of the sites have been influenced by similar air temperature trends, but variations in micro-climatic factors have resulted in different thermal responses of the ground. The main cause of the variations in ground temperatures is the variable snow conditions among the sites, and the length of time that the ground surface is exposed to air temperatures (Smith et al., 2003).

MAGTs at BH1 are the mildest, and the thermal profile exhibits the steepest gradient of the other four boreholes (Fig. 4.26). These characteristics are attributed to the borehole's proximity to the coast. The thermal profile at BH2 is the coldest of all the boreholes, though the reason for this is unknown due to the lack of micro-climate data at the site. Taylor et al. (2006) suggested that winter atmospheric temperature inversions may be the cause of colder temperatures at BH2, as the strength of these are +1.7K per 100 m elevation at Alert. MAGTs at all of the boreholes warmed at all depths between the late 1970's and the mid-to-late 2000's, with the exception of BH3, which did not warm at depths greater than 20 m (Fig. 4.26). MAGTs shallower than 16 m at BH3 were warmer than those at BH4 and BH5 at the beginning of monitoring. Since less warming occurred at BH3, MAGTs are colder than those at BH4 and BH5 in recent years (Fig. 4.26).

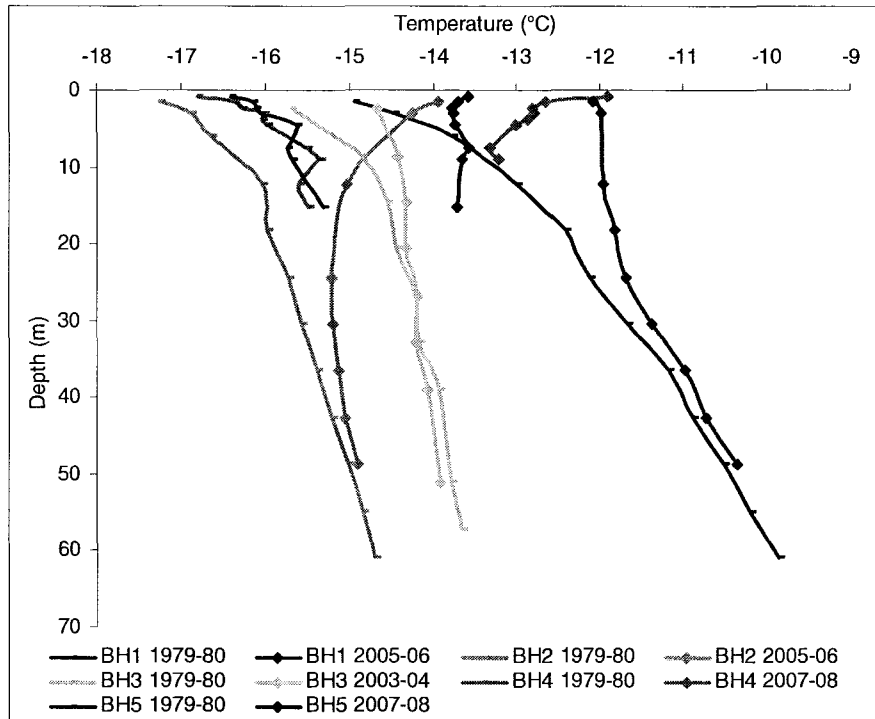


Figure 4.26: MAGT profiles at the five borehole sites in Alert, Nunavut. There are two profiles for each borehole site; the first is from 1979-80 near the beginning of monitoring, and the second is from 2005-06 at BH1 and BH2, 2003-04 at BH3, and 2007-08 at BH4 and BH5. The graph shows that significant warming has occurred at all of the borehole sites throughout the MAGT profile except at BH3 where a lesser warming has occurred only in the top 20 m.

Statistically significant warming trends ($p < 0.001$) are shown in Fig. 4.27 for BH1, BH2, BH4 and BH5. BH3 is the only site where significant warming did not occur. The ground at BH4 warmed the most at 9.1 m depth by about 0.6°C per decade, although there is a sizeable gap in the data between 1988 and 2000, followed by BH5 at 15.2 m depth which warmed by about 0.4°C per decade. At BH1 and BH2 MAGTs increased at a rate of about 0.2°C per decade at 24.4 m depth. MAATs at Alert also warmed significantly between 1979 and 2008 by about 0.4°C per decade ($p < 0.05$; Fig. 4.27).

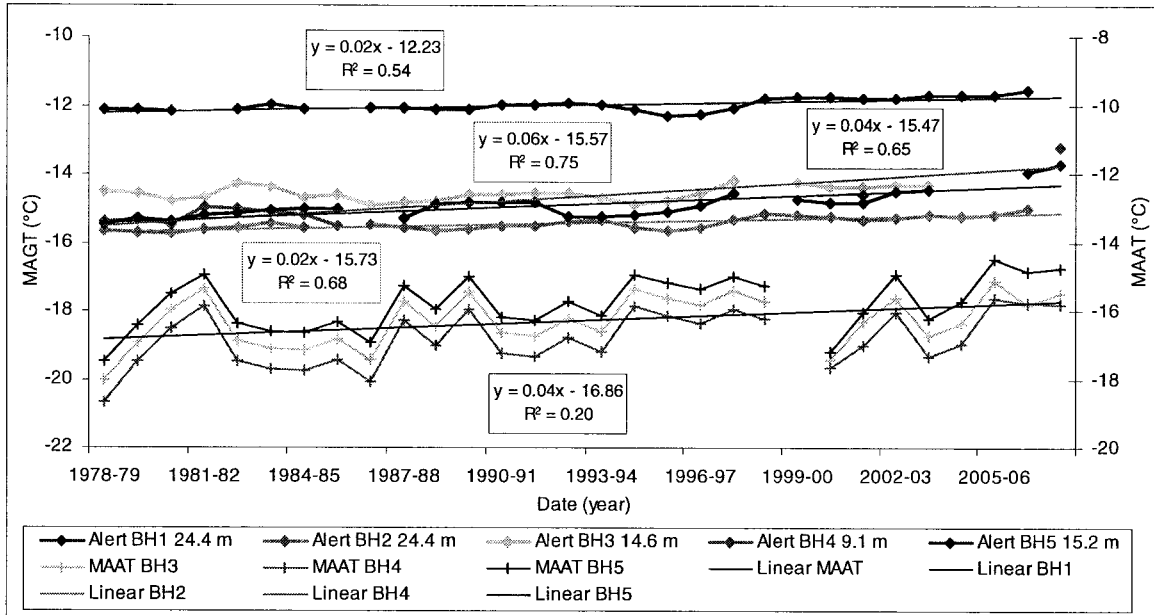


Figure 4.27: MAGTs at all of the boreholes and MAAT from BH3, BH4 and BH5 using correlated ECCS data (Environment Canada, 2009) between 1978 and 2008. Statistically significant warming trends ($p < 0.001$) are present in MAGT at BH1, BH2, BH4 and BH5. MAAT also warmed significantly at $p < 0.05$. Note: MAAT is on a secondary axis.

MAGT warming at BH3 was less than that at the other four boreholes, and is likely due to the significant amount of snow that typically accumulates at BH3 during the winter each year. Over the six years of snow depth monitoring SDD averaged 10519 at BH3, 3079 at BH4, and 194 at BH5 (Table 4.8). The effect of snow at BH3 is also reflected in both n_f and the surface offset; the n_f value is consistently lower, and the surface offset is consistently higher, than at BH4 and BH5 (Tables 4.8 and 4.9). 2001-02 is the only year when the surface offset is lower at BH3 than BH4, and n_f is the same. Unfortunately no snow data exists for this year at the borehole sites or at the ECCS climate station, but based on the n_f value of 0.91, BH3 likely had less snow than usual and was more similar to what BH4 received.

Table 4.8: Summary table of n_f , n_t , and SDD at Alert BH3, BH4 and BH5 between 2000 and 2008.

Year	n_f			n_t			SDD		
	BH3	BH4	BH5	BH3	BH4	BH5	BH3	BH4	BH5
2000-01	0.82	0.94	0.95	1.6	2.7	2.6	<i>M</i>	<i>M</i>	<i>M</i>
2001-02	0.91	0.91	0.95	1.4	2.0	1.8	<i>M</i>	<i>M</i>	<i>M</i>
2002-03	0.83	1.02	1.03	1.4	1.8	1.8	9013	2810	367
2003-04	0.88	0.95	0.99	2.1	2.3	2.4	5212	2234	14
2004-05	0.75	0.88	0.97	<i>M</i>	<i>M</i>	<i>M</i>	12890	2262	201
2005-06	<i>M</i>	<i>M</i>	<i>M</i>	<i>M</i>	<i>M</i>	<i>M</i>	9342	2078	<i>M</i>
2006-07	0.76	0.88	0.96	1.8	2.1	2.4	11524	3407	<i>M</i>
2007-08	0.64	0.81	0.91	<i>M</i>	<i>M</i>	<i>M</i>	15130	5682	<i>M</i>
Average	0.80	0.91	0.97	1.7	2.2	2.2	10519	3079	194
CV	0.11	0.07	0.04	0.18	0.15	0.18	0.33	0.44	0.91

The coefficient of variation (CV) is presented to show the relative variability over the monitoring period.

Table 4.9: Summary table of surface and thermal offsets at Alert BH3, BH4 and BH5 between 2000 and 2008.

Year	Surface Offset (°C)			Thermal Offset (°C)		
	BH3	BH4	BH5	BH3	BH4	BH5
2000-01	3.5	2.1	1.7	0.0	<i>M</i>	-0.2
2001-02	1.9	2.5	1.5	-0.1	-0.2	-0.3
2002-03	3.2	0.4	0.2	-0.7	<i>M</i>	0.1
2003-04	2.6	2	1.3	-0.4	<i>M</i>	0.1
2004-05	4.7	2.1	1.6	<i>M</i>	<i>M</i>	<i>M</i>
2005-06	<i>M</i>	<i>M</i>	<i>M</i>	<i>M</i>	<i>M</i>	<i>M</i>
2006-07	4.2	2.6	1.2	<i>M</i>	<i>M</i>	-0.7
2007-08	6.2	3.7	1.9	<i>M</i>	0.1	-0.7
Average	3.8	2.2	1.3	-0.3	-0.1	-0.3

BH5 is almost completely windswept during the winter causing n_f to be very close to 1.0 each year. The surface offset is the lowest at BH5 and is controlled mainly by the summer air-surface interactions. The ground surface and the air are very close in temperature during the winter; therefore the offset must be created by the ground warming more than the air during summer.

The thermal offset is low at all three sites, BH3, BH4 and BH5. Alert is an arid environment, classified as a polar desert, and the latent heat effects associated with the freezing and thawing of the active layer are minimal. Since the thermal offset is negligible, permafrost temperatures at Alert are controlled primarily by the buffering

between the air and the surface temperature. Therefore the most important variables controlling the permafrost temperatures at Alert are primarily air temperatures, followed by the thickness and duration of snow in the winter, amount of direct insolation in the summer, and the proximity to a water or ice-covered body year round. As a consequence, BH3 may have warmed less than the other sites because the significant air temperature warming that occurred during winter was partially dampened by a thicker snow-pack. The differences in ground temperatures at this site illustrate the potential for variability in other areas. Variations in ground temperatures of up to 4°C occur across less than 7 km near Alert, Nunavut.

4.2 IQALUIT, NUNAVUT

The permafrost thermal monitoring site at Iqaluit, Nunavut, lies within the zone of continuous permafrost at 63°44'N and 68°28'W, at an estimated elevation of 109 m (Figs. 1.1, 4.28, and 4.29). It lies in the southern part of Baffin Island just over 1 km north of the coast of Frobisher Bay. Information about this site was extracted from the GTN-P Iqaluit metadata sheet (GTN-P, 2009). This exposed tundra site is on massive bedrock, overlain by a thin till veneer with fairly well developed soil and sparse vegetation. The tides along the coast of Frobisher Bay can reach heights of up to 9 m, causing a reduced ice-cover season.

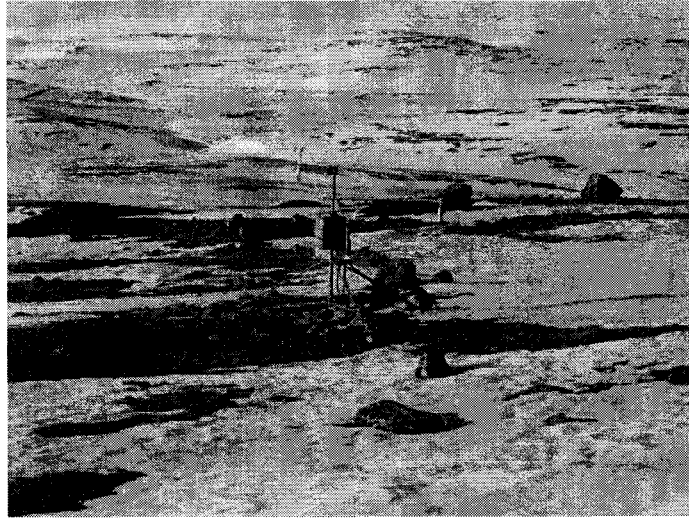


Figure 4.28: Photograph of the weather station at the Iqaluit permafrost thermal monitoring site in Nunavut, taken in May, 2004 (Eley, 2005).

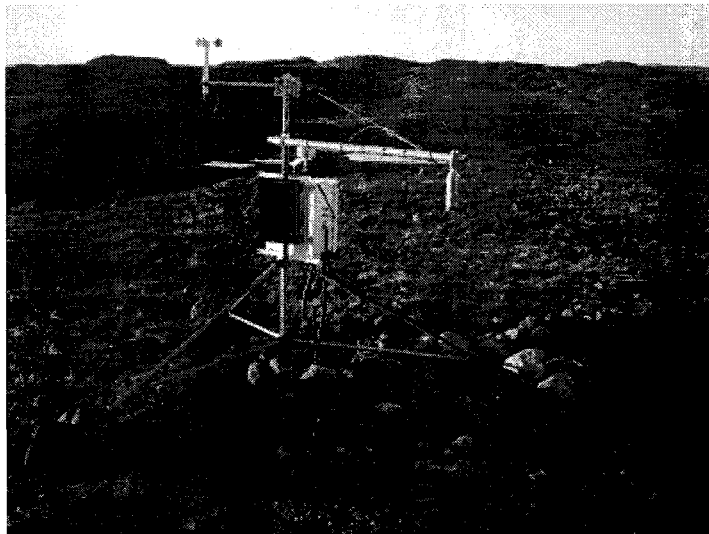


Figure 4.29: Photograph of the weather station at the Iqaluit permafrost thermal monitoring site in Nunavut, taken in September, 2002 (Eley, 2005).

There are two 5 m boreholes at this site that were drilled in 1988 and lie on either side of a weather station. The length of the records and depths of thermistors are given in Table 4.10. Each borehole has a logger that has recorded temperatures daily; BH2 since 1988 and BH1 since 1989. Air temperatures have been recorded every 3 hours since 1997, and ground temperatures at the surface and 20 cm depth have been recorded every

3 hours since 2000. This borehole site is maintained by Environment Canada and the data utilized are from Eley (2005). The closest ECCS is in Iqaluit at 63°45'N and 68°33'W, approximately 4.1 km from the borehole site. A brief analysis of ground temperatures at this site up to 2002 can be found in Smith et al. (2005).

Table 4.10: Summary table of the data used in the analysis of the two boreholes at Iqaluit, Nunavut, and the depths of the thermistors within the boreholes.

Iqaluit	BH1	BH2
Manual Borehole Data	N/A	N/A
Logger Borehole Data	1989-2004	1988-2004
Air Temperature	Nov97-May00, Nov00-Dec00, Jun01-Oct04	
Ground Surface Temperature	Nov00-Dec00, Jun01-Oct04	
20 cm	Nov00-Dec00, Jun01-Oct04	
Snow	Snow Surveys and ECCS 1947-2004	
Air Temperature (ECCS)	Dec 1947 – Sept 2007	
Calculated MAGT from ECCS	1948-2006	
Distance to nearest water body	~ 1.5 km	
Thermistor Depths (m)	0.5, 1.0, 1.5, 2.0, 3.0, 4.0, 5.0	

The borehole site at Iqaluit is subject to wind scouring and snow redistribution. The snow accumulation is minimal overall, varies spatially and is discontinuous through time (Eley, 2005). The statistically significant relationship (Fig. 4.30; $r^2 = 0.89, 0.90$; $p < 0.001$) between MAAT and MAGT at 5 m depth at both BH1 and BH2 provide evidence that snow has minimal influence on ground temperatures at this site.

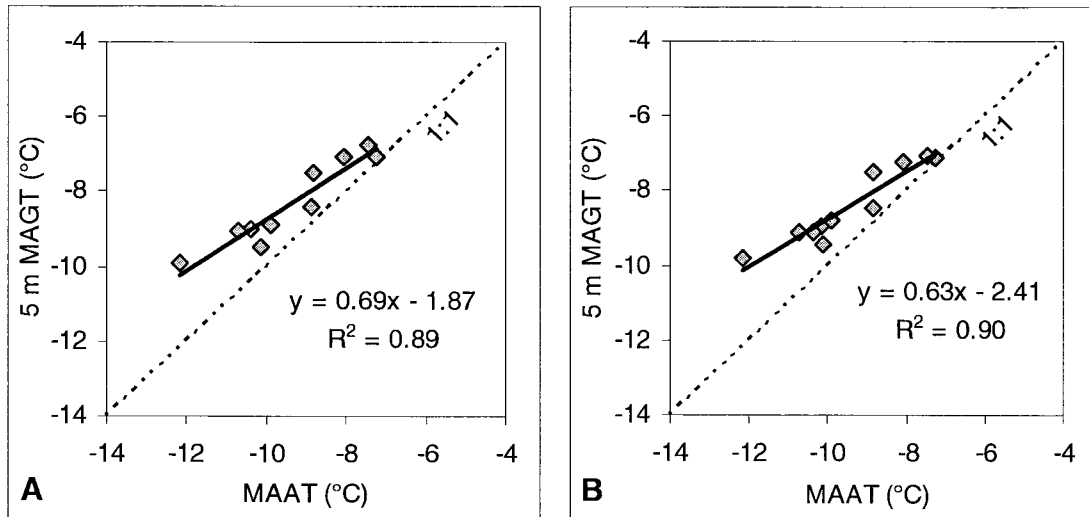


Figure 4.30: Relationships at Iqaluit (A) BH1 and (B) BH2 between MAAT and the corresponding MAGT at 5 m based on phase lags from 1988 to 2004. The strong relationship between these variables is illustrated by the high r^2 values and statistically significant relationships ($p < 0.001$) at both sites.

Three years of ground surface data between 2001 and 2004 were used to calculate the surface offset (Table 4.11). MAGST ranged between -5.0 and -6.5°C , and MAAT measured at the borehole site ranged between -7.6 and -8.9°C over the same period. From these values the surface offsets ranged between 2.1 and 2.8°C .

Table 4.11: Summary table of continuously logged on-site data at Iqaluit BH1 and BH2, including the MAAT, MAGST, surface offset, TOP, TTOP, and the thermal offset.

Date	MAAT (°C)	MAGST (°C)	Surface Offset (°C)	TOP (m)		TTOP (°C)		Thermal Offset (°C)	
				BH1	BH2	BH1	BH2	BH1	BH2
1988-89	-10.3*	M	M		1.5		-9.7	M	M
1989-90	-10.3*	M	M	1.5	1.4	-10.0	-9.4	M	M
1990-91	-10.4*	M	M	1.6	1.4	-9.3	-9.5	M	M
1991-92	-10.7*	M	M	1.7	1.6	-9.0	-8.8	M	M
1992-93	-11.7*	M	M	1.4	1.4	-10.7	-10.8	M	M
1993-94	-10.0*	M	M	1.5	1.4	-9.0	-9.4	M	M
1994-95	-8.5*	M	M	1.5	1.4	-7.9	-7.9	M	M
1995-96	-7.8*	M	M	M	M	M	M	M	M
1996-97	M	M	M	1.8	1.7	-7.4	-7.6	M	M
1997-98	M	M	M	2.1	2.1	-7.4	-7.7	M	M
1998-99	-7.8	M	M	2.0	2.1	-6.6	-6.7	M	M
1999-00	-8.8*	M	M	2.0	2.0	-7.6	-7.9	M	M
2000-01	-7.5*	M	M	M	M	M	M	M	M
2001-02	-8.9	-6.5	2.4	2.2	2.2	-7.5	-7.7	-1.0	-1.2
2002-03	-7.7	-4.9	2.8	2.1	2.0	-6.6	-7.0	-1.7	-2.1
2003-04	-7.6	-5.5	2.1	2.3	2.2	-6.4	-6.9	-0.9	-1.4

* Values of MAAT were calculated using correlated ECCS data (Environment Canada, 2009). Missing data is represented by *M*.

FDD of the air ranged between 3445 and 3893, and that of the ground surface ranged between 2732 and 3287. Values for n_f ranged between 0.79 and 0.88 (Table 4.12). TDD of the air ranged between 667 and 793, and that of the ground surface ranged between 898 and 971 (Table 4.12). Values of n_t ranged between 1.2 and 1.4, remaining above 1.0 throughout monitoring. These high values of n_t are due to the lack of vegetation at the surface, allowing direct solar radiation to warm the ground surface more than the air (Klene et al., 2001).

Table 4.12: Summary table of on-site data at Iqaluit, including FDD_a, FDD_s, TDD_a, TDD_s, n_f and n_t .

Year	FDD _a	FDD _s	n_f	Year	TDD _a	TDD _s	n_t
2001-02	3893.3	3287.0	0.84	2002	696.7	898.0	1.3
2002-03	3478.0	2732.2	0.79	2003	792.9	971.1	1.2
2003-04	3444.8	3042.7	0.88	2004	667.1	967.2	1.4
CV	0.07	0.09	0.05	CV	0.09	0.04	0.09

The coefficient of variation (CV) is presented to show the relative variability over the monitoring period.

TOP increased significantly from approximately 1.4 m to 2.3 m at both boreholes during the monitoring period from 1989 to 2004 ($p < 0.001$; Table 4.11). TTOP ranged between -6.4 and -10.7°C at BH1, and between -6.7 and -10.8 at BH2, and increased by about 3.5°C over the 15 year period, or at a rate of 2.3°C per decade ($p < 0.001$). The thermal offset was calculated for the three years corresponding with ground surface temperatures. It ranged between 1.2 and 2.1°C at BH1 and between 0.9 and 1.7°C at BH2.

The zero-curtain effect is longer during freeze-back than during thaw in the spring. There is also a period of time during freeze-back where the temperature at depths 1, 1.5, and 2 m remain below -1°C for slightly longer than a month. This may be due to saline conditions in the ground, creating a lowered freezing point.

These boreholes do not reach the depth of ZAA. Over the monitoring period the average range in ground temperatures at 0.5 m depth was 33.6°C , diminishing to 7.7°C at 5 m depth. BH1 and BH2 have similar ground temperature profiles, with slight differences likely due to moisture content of the ground and snow characteristics (Fig. 4.31). Based on the apparent thermal diffusivity between 4 and 5 m, the depth of ZAA for BH1 is estimated at 18.8 m, and ZAA at BH2 is estimated at 21.4 m.

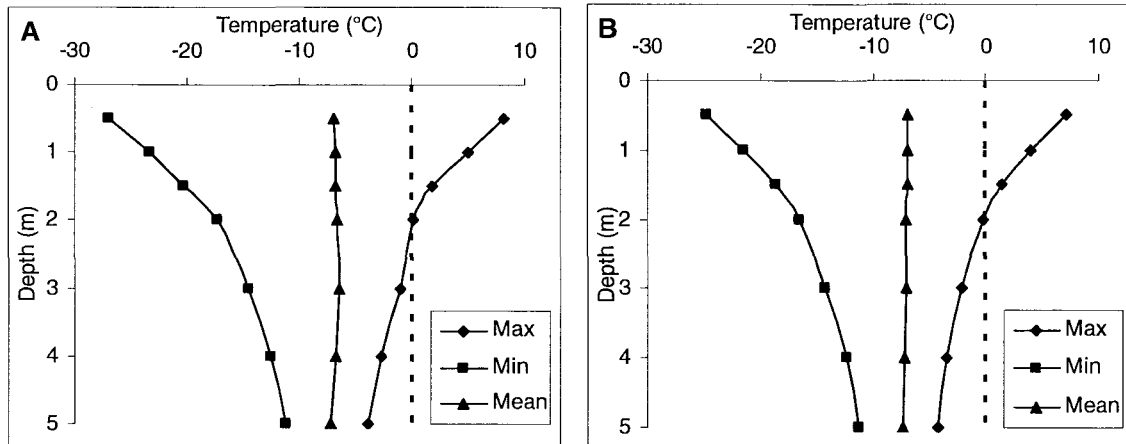


Figure 4.31: Temperature envelopes at Iqaluit (A) BH1 and (B) BH2 for the year 2002-03. BH1 reaches slightly lower minimum temperatures than BH2, and the latent heat effects in the active layer appear to be stronger at BH1.

In 1989 the MAGT was -10°C at 5 m. Based on this temperature the permafrost is estimated to be between 300 and 600 m thick. The direction of the geothermal gradient cannot be accurately assessed at this site due to the shallow depth of the boreholes.

Warming trends were observed at all depths at both of the Iqaluit boreholes (Figs. 4.32 and 4.33). At BH1 the MAGT at 5 m depth warmed by 1.9°C per decade, 3 m warmed by 2.3°C per decade, and 0.5 m warmed by 2.6°C per decade. At BH2 the MAGT at 5 m depth warmed at a rate of 1.6°C per decade, 3 m warmed by 1.9°C per decade, and 0.5 m warmed by 2.3°C per decade. These trends are all statistically significant ($p < 0.001$). BH1 warmed slightly more overall than BH2. The dip in temperatures in 1992-93, observed both in the air and the ground, was likely a result of the Mount Pinatubo eruption that occurred in June 1991 and ejected large quantities of aerosols into the atmosphere, causing a temporary cooling of air temperatures around the globe (Bassett and Lin, 1993; Hansen et al., 1996).

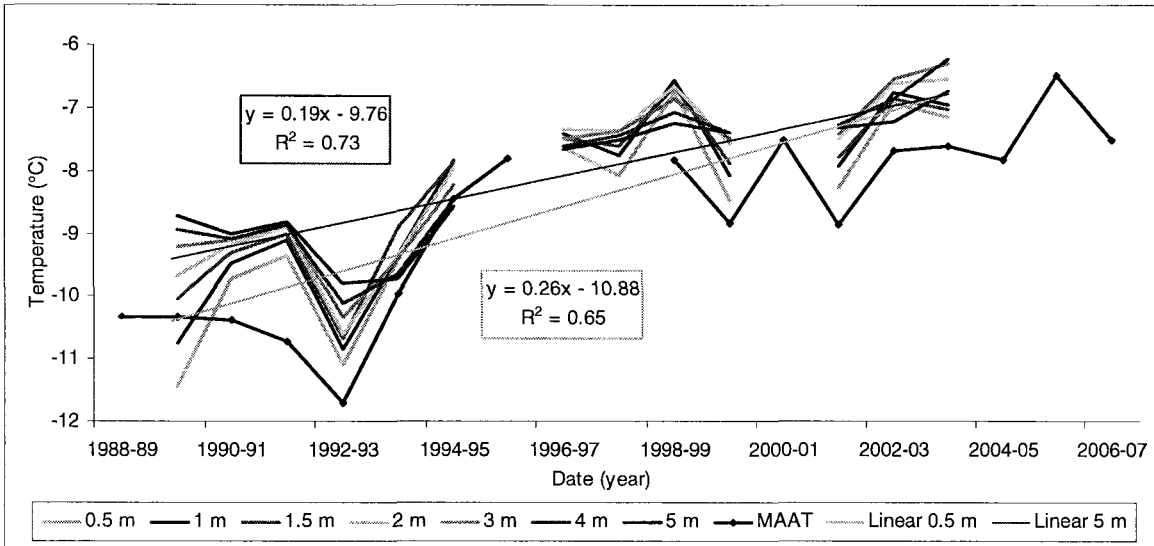


Figure 4.32: MAGTs and MAATs at Iqaluit BH1 between 1989 and 2004, showing warming temperatures at all depths, and the linkages between air and ground temperature trends. MAAT were calculated using correlated ECCS data (Environment Canada, 2009). The trends are significant at $p < 0.001$.

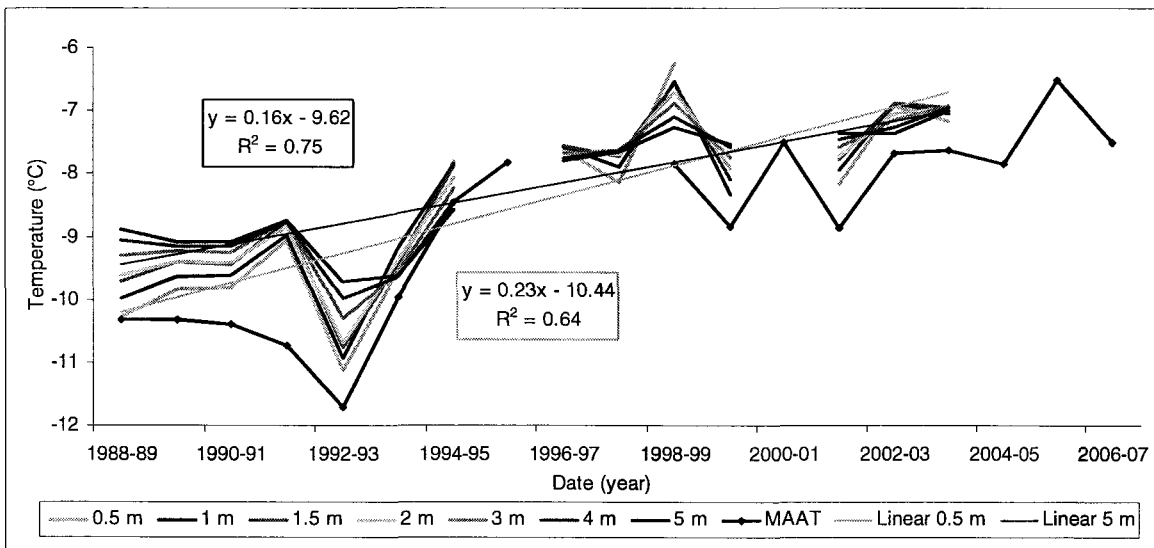


Figure 4.33: MAGTs and MAATs at Iqaluit BH2 between 1988 and 2004, showing warming temperatures at all depths, and the linkages between air and ground temperature trends. MAAT were calculated using correlated ECCS data (Environment Canada, 2009). The trends are significant at $p < 0.001$.

The strength of the relationship between MAAT and the corresponding 5 m MAGTs (Fig. 4.30) allowed the hind-casting of MAGTs at this depth back to 1948 for both boreholes. Assuming that snow has remained an insignificant variable at the

borehole site since 1948, these values of 5 m MAGT should be accurate. The hind-cast MAGTs at BH2 are plotted in Fig. 4.34 alongside the measured MAGTs at 5 m depth to illustrate the accuracy of the hind-cast method. The hind-cast record shows a cooling trend from 1948 to 1993 at a rate of about 0.2°C per decade, and a warming trend from 1993 to 2007 at a rate of 0.9°C per decade. These trends are both statistically significant ($p < 0.01$ and $p < 0.05$, respectively).

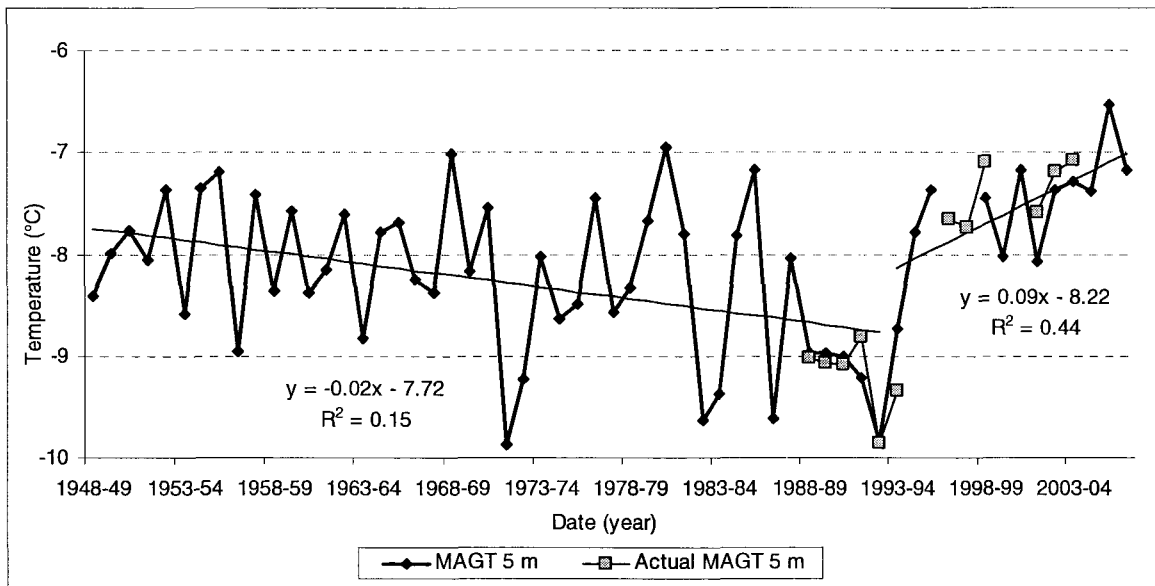


Figure 4.34: Hind-cast values of MAGT for 5 m depth at Iqaluit BH2 between 1948 and 2007, calculated using correlated Iqaluit ECCS air temperature data (Environment Canada, 2009), plotted alongside the measured MAGT at 5 m from 1988 to 2004. The cooling trend is significant at $p < 0.01$, and the warming trend is significant at $p < 0.05$.

Hind-cast MAATs derived from the correlated Iqaluit ECCS data ranged between -6.5 and -11.8°C from 1948 to 2006 (Fig. 4.35). The coldest MAAT on record occurred in the 1971-1972 year and the warmest occurred in 2005-2006. Inter-annual variability in MAAT increased from around 1970 to the mid-1990s. A statistically significant cooling trend of 0.4°C per decade occurred at Iqaluit between 1948 and 1993 ($p < 0.01$). MAAT then increased significantly between 1993 and 2006 by about 1.4°C per decade ($p < 0.05$).

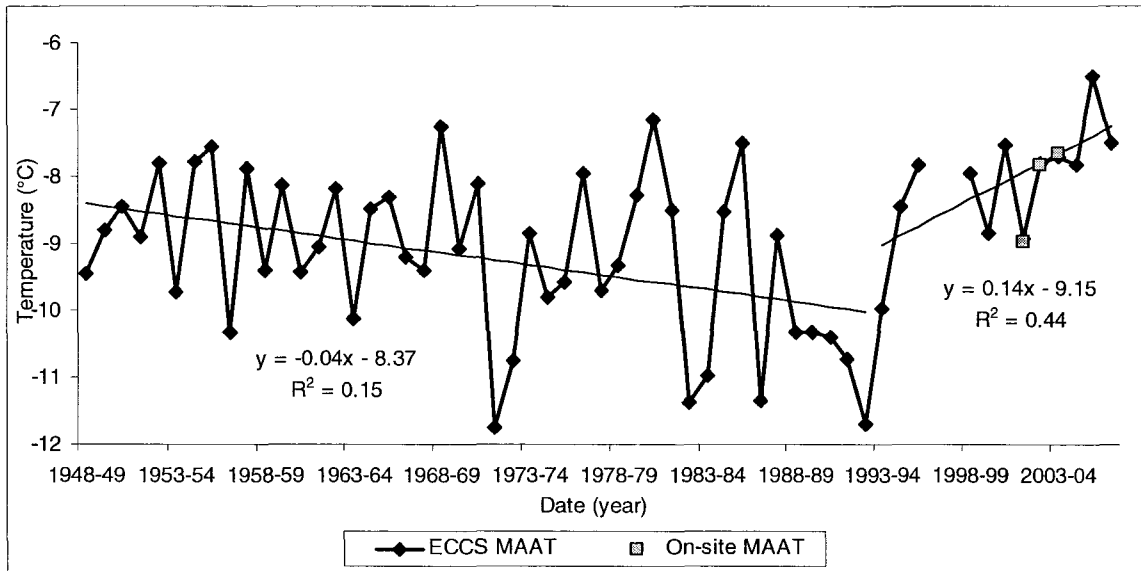


Figure 4.35: Hind-cast MAAT at the Iqaluit borehole sites between 1948 and 2007, obtained from correlated Iqaluit ECCS data (Environment Canada, 2009) plotted alongside on-site measured MAAT. The cooling trend observed from 1948 to 1993 is significant at $p < 0.01$, and the warming trend between 1993 and 2007 is significant at $p < 0.05$.

Seasonal air temperatures were analyzed based on the timing of cooling and warming trends in the MAAT. The period of cooling took place from the beginning of the record in 1947 to 1992, and the period of warming took place between 1993 and 2007. Summer air temperatures decreased by about 0.1°C per decade between 1948 and 1992, then increased by about 0.5°C per decade until 2007, but neither of these trends are statistically significant (Fig. 4.36). Air temperatures in the summer changed little overall and had the lowest inter-annual variability of all four seasons. Summer air temperatures may be prevented from increasing or decreasing dramatically due to the buffering effect of cold waters in Frobisher Bay.

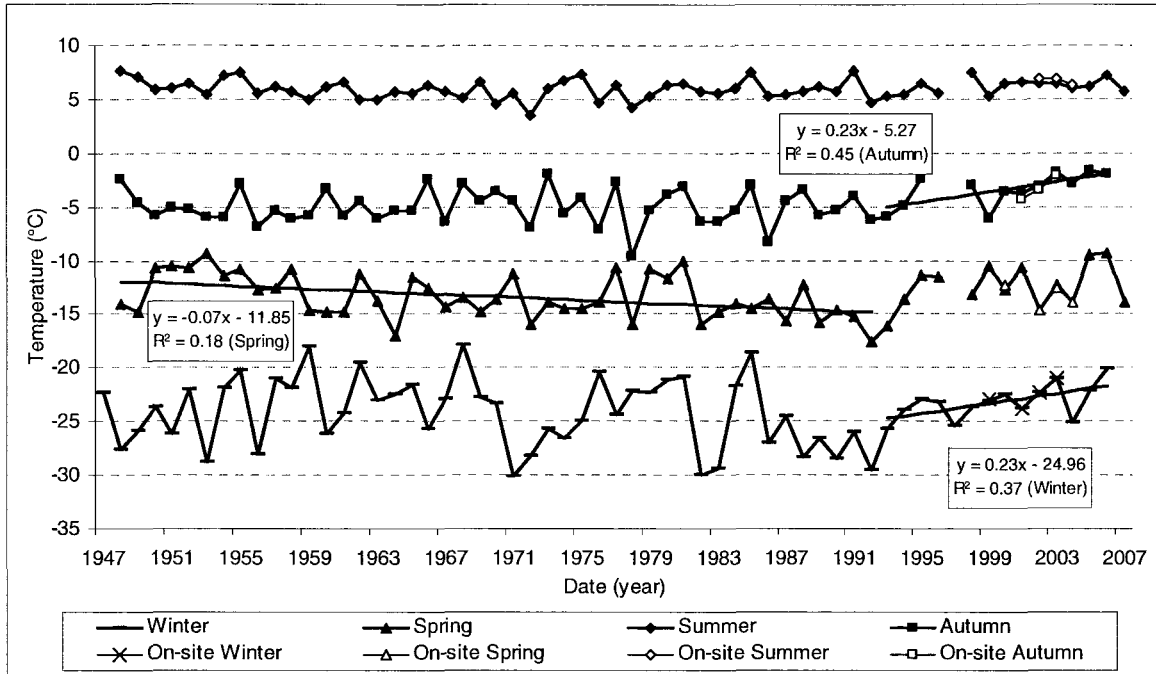


Figure 4.36: Hind-cast seasonal air temperatures at the Iqaluit borehole sites between 1947 and 2007, obtained from correlated ECCS data (Environment Canada, 2009). The cooling trend in the spring is significant at $p < 0.01$. The warming trends in autumn and winter are also significant at $p < 0.05$.

Winter air temperatures were the most variable inter-annually of all the seasons in the earlier part of the record, but variability decreased around the late 1980's (Fig. 4.36). Winter air temperatures increased with statistical significance by about 2.3°C per decade during the recent warming period ($p < 0.05$; Fig. 4.36). During the cooling period between 1947 and 1992 winter air temperatures cooled by 0.6°C per decade, but the trend is not statistically significant due to the high inter-annual variability.

Spring air temperatures cooled with statistical significance between 1948 and 1992 by about 0.7°C per decade ($p < 0.01$; Fig. 4.36). During more recent years spring air temperatures warmed by about 1.4°C per decade, but the trend was not significant. Autumn air temperatures did warm with statistical significance between 1993 and 2006 at a rate of about 2.3°C per decade (Fig. 4.36; $p < 0.05$). Autumn air temperatures cooled

by about 0.1°C per decade during the earlier part of the record, but the trend was not statistically significant.

The climate patterns at Iqaluit changed around 1993 with autumn and winter air temperatures both warming by 2.3°C per decade. Since air temperatures and ground temperatures are closely linked at this site (Fig. 4.30) climate warming results in permafrost warming. Figures 4.32 and 4.33 show the increases in ground temperatures at all depths in BH1 and BH2 that follow changes in air temperature trends. This permafrost thermal monitoring site is therefore a sensitive indicator of changes in climate and a deeper borehole that extends below the depth of ZAA would be a useful addition at this site.

4.3 BAKER LAKE, NUNAVUT

The permafrost thermal monitoring site at Baker Lake, Nunavut, lies within the zone of continuous permafrost at 64°19'N and 96°2' W (Fig. 1.1). Elevation has not been measured at the borehole sites, but it would be comparable to the Baker Lake ECCS elevation of 18 m (Environment Canada, 2009). The area has permafrost thicknesses of up to 200 m (Smith et al., 2005), and is an arctic tundra site with moderate vegetation. There are four boreholes at this site that were drilled to 3 m in 1997, forming a transect perpendicular to a snow fence that was installed in 1981. The boreholes are located in till composed of coarse gravels and sands with a peat layer at the surface that is less than 15 cm thick, and the materials have low ice contents (GTN-P, 2009).

BH1 is located 135 m downwind from the snow fence; BH2 is 45 m downwind from the snow fence (Fig. 4.37), and is beneath the large snow drift that forms each winter; BH3 is 180 m upwind of the snow fence; and BH4 is 400 m upwind of the snow

fence and is the least affected (Fig. 4.38), representing natural conditions. Each borehole has thermistors at 50 cm intervals to a maximum depth of 3 m. The length of the records and depths of the thermistors are given in Table 4.13. Manual ground temperature readings were taken on a monthly or bimonthly basis from 1997-2005. A logger was attached at BH4 in 2002 to record temperatures three times per day. A weather station was set up at BH4 in 2002 and ground surface temperature sensors were installed at BH2 and BH4. This site provides the opportunity to look at the effects of snow cover variation in a tundra environment.

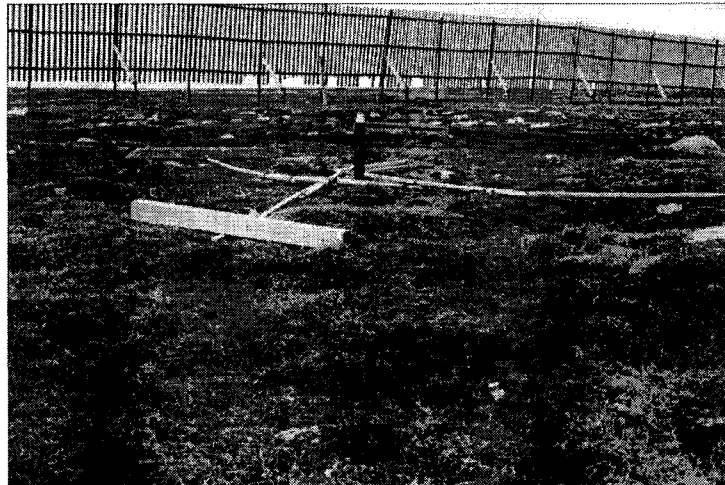


Figure 4.37: Photograph of Baker Lake BH2, looking away from the town and towards the snow fence (upwind). Note the brown vegetation from the long-lasting snow drift. Photo was taken on July 30, 2002, one week after the end of snowmelt (photo is courtesy of the Geological Survey of Canada).

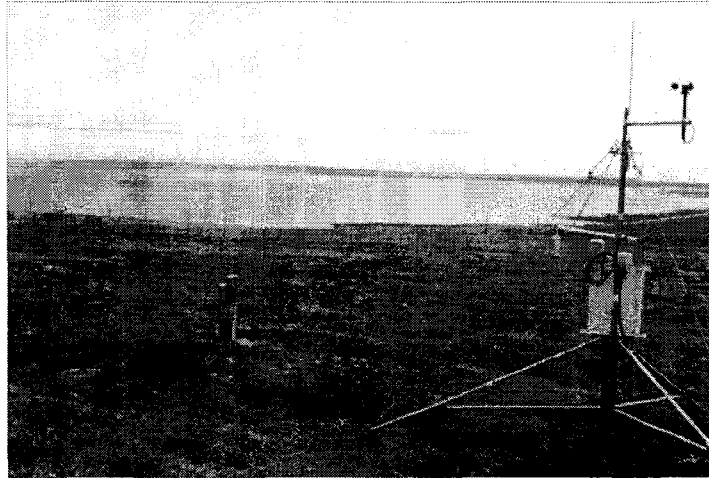


Figure 4.38: Photograph of Baker Lake BH4 (undisturbed site) and the weather station, looking towards the snow fence and the lake (down wind). Photo was taken July 30, 2002 (photo is courtesy of the Geological Survey of Canada).

Table 4.13: Summary table of the data used in the analysis of the four boreholes at Baker Lake, Nunavut, and the depths of the thermistors within the boreholes.

Baker Lake	BH1	BH2	BH3	BH4
Manual Borehole Data	1997-2005	1997-2005	1997-2005	1997-2006
Logger Borehole Data	N/A	N/A	N/A	Aug02-Nov03, Aug04-Mar05, Sept05-Apr07
Ground Surface Temperature	N/A	2002-2008	N/A	2002-2008
Snow	N/A	N/A	N/A	2002-2006
Air Temperature (on-site)	2002-2007			
Air Temperature (ECCS)	1946-2008			
Distance to nearest water body (km)	< 1.0 km			
Thermistor Depths (m)	0.5, 1.0, 2.0, 2.5, 3.0 (Note: 1.5 m sensor drifted, so data were removed)			

The Baker Lake permafrost monitoring site is maintained by the Geological Survey of Canada and the Baker Lake community, and was established in partnership with Environment Canada and the University of Toronto. The closest ECCS is in Baker Lake, Nunavut, at 64°18'N and 96°4'W, approximately 3 km from the borehole sites. Previous analyses of site data to 2003 can be found in Smith et al. (2005), and to 2007 in Throop et al. (2008).

Temperatures at BH2 are significantly affected by the snow drift, resulting in higher winter ground temperatures than at the other three boreholes (Fig. 4.39). BH1, further downwind from the snow fence, has been affected by the snow fence in a different way. BH1 receives less snow as a result of the fence, making ground temperatures colder than those at BH3 and BH4 (Fig. 4.39). BH3 appears most similar to BH4, showing only limited effects from its proximity to the snow fence. The inter-annual variability in temperatures at 3 m depth appears to be somewhat dependent upon winter average temperatures, but must also be somewhat attributed to snow characteristics (Fig. 4.39).

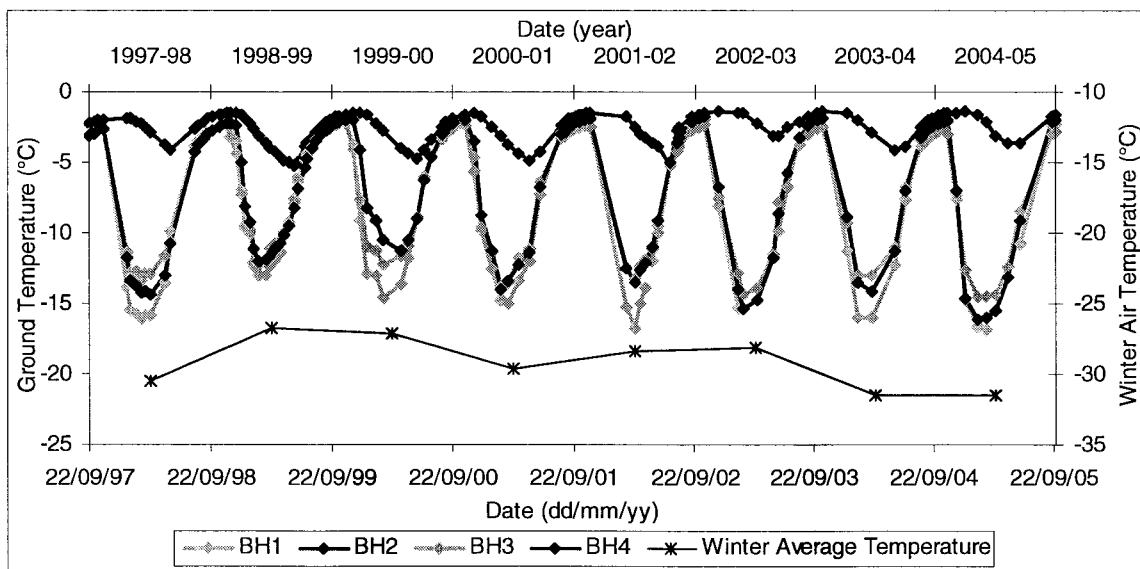


Figure 4.39: Temperature time-series from manual measurements taken at 3 m depth for all four boreholes, and the average winter air temperatures at Baker Lake, Nunavut, from correlated ECCS data (Environment Canada, 2009) between 1997 and 2005. The effects of the large snow drift are particularly evident in winter ground temperatures at BH2. Temperatures at 3 m seem to be somewhat dependent upon winter average air temperatures, especially at BH1.

Snow cover at BH4 varied significantly inter and intra-annually (Fig. 4.40). This site has low tundra vegetation, and is prone to drifting snow. Between 2002 and 2006 the average snow depth ranged between 13 and 28 cm, the maximum depth ranged between 25 and 56 cm, and the SDD ranged between 3004 and 7282 (Table 4.14). Snow

accumulated at BH4 between the end of September and the end of October, and melted between the end of May and the middle of June, resulting in a snow-free period of up to 4.5 months.

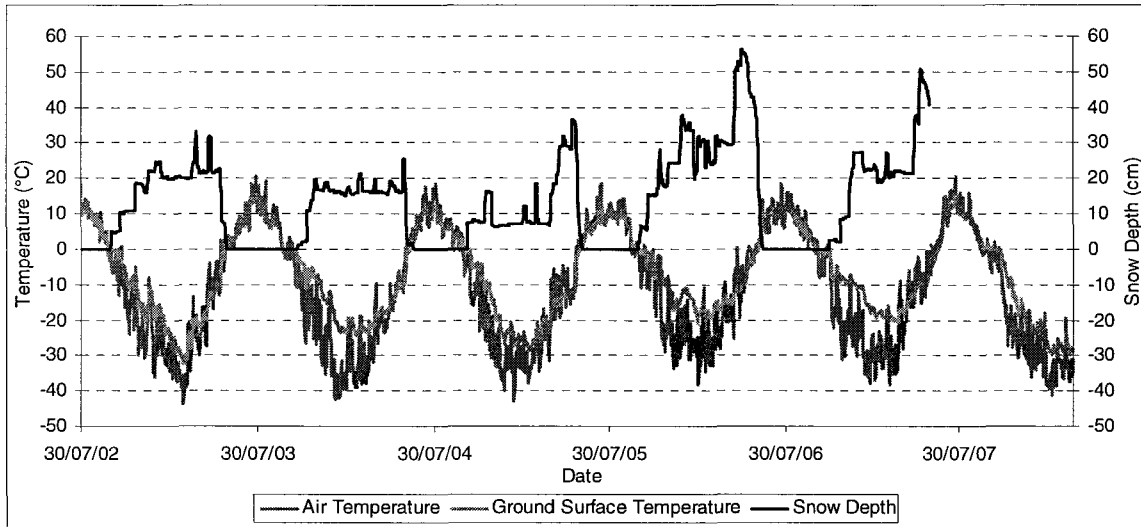


Figure 4.40: Air and ground surface temperatures, and snow depths at Baker Lake BH4 between July 2002 and March 2008.

Table 4.14: Summary table of on-site data at Baker Lake BH4, including FDD_a, FDD_s, TDD_a, TDD_s, SDD, n_f and n_t.

Year	FDD _a	FDD _s	n _f	SDD	Year	TDD _a	TDD _s	n _t
2002-03	4777	3793	0.79	4339	2003	1018	904	0.89
2003-04	5311	3491	0.66	3478	2004	827	703	0.85
2004-05	5107	3939	0.77	3003	2005	925	831	0.90
2005-06	4131	2709	0.66	7282	2006	1001	871	0.87
2006-07	4471	2818	0.63	<i>M</i>	2007	862	778	0.90
2007-08	<i>M</i>	4019	<i>M</i>	<i>M</i>	2008	<i>M</i>	<i>M</i>	<i>M</i>
CV	0.10	0.16	0.10	0.42	CV	0.09	0.10	0.02

The coefficient of variation (CV) is presented to show the relative variability over the monitoring period. Missing values are represented by *M*.

The MAAT ranged between -8.7 and -12.2°C from 2002 to 2007. The MAGST ranged between -5.1 and -8.7°C from 2002 to 2008 at BH4. The MAGST for BH2 was significantly warmer ranging between -0.1 and -2.0°C from 2002 to 2006. The surface offset at BH4 ranged between 2.4 and 4.7°C over the corresponding years, and that at BH2 ranged between 7.7 and 10.5°C (Table 4.15). The greater surface offset values at

BH2 are due to the deep snow drift that persists late into the summer. The enhanced buffering effect of the deep snow drift is evident in the BH2 ground surface temperatures (Fig. 4.41).

Table 4.15: Summary table of continuously logged on-site data at Baker Lake BH2 and BH4, including the MAAT, MAGST, surface offset, TOP, TTOP, and the thermal offset. Note the large differences in MAGST and surface offsets at BH2 and BH4.

Date	MAAT (°C)	MAGST (°C)		Surface Offset (°C)		TOP (m)	TTOP (°C)	Thermal Offset (°C)
		BH2	BH4	BH2	BH4	BH4	BH4	BH4
2002-03	-10.4	-0.1	-8.0	10.3	2.4	2.2	-7.7	0.3
2003-04	-12.2	-2.0	-7.5	10.2	4.7	<i>M</i>	<i>M</i>	<i>M</i>
2004-05	-11.4	-0.9	-8.5	10.5	2.9	<i>M</i>	<i>M</i>	<i>M</i>
2005-06	-8.7	-1.0	-5.1	7.7	3.7	2.2	-6.2	-1.1
2006-07	-9.7	-1.9	-5.4	7.8	4.3	<i>M</i>	<i>M</i>	<i>M</i>
2007-08	<i>M</i>	<i>M</i>	-8.7	<i>M</i>	<i>M</i>	<i>M</i>	<i>M</i>	<i>M</i>

Missing values are represented by *M*.

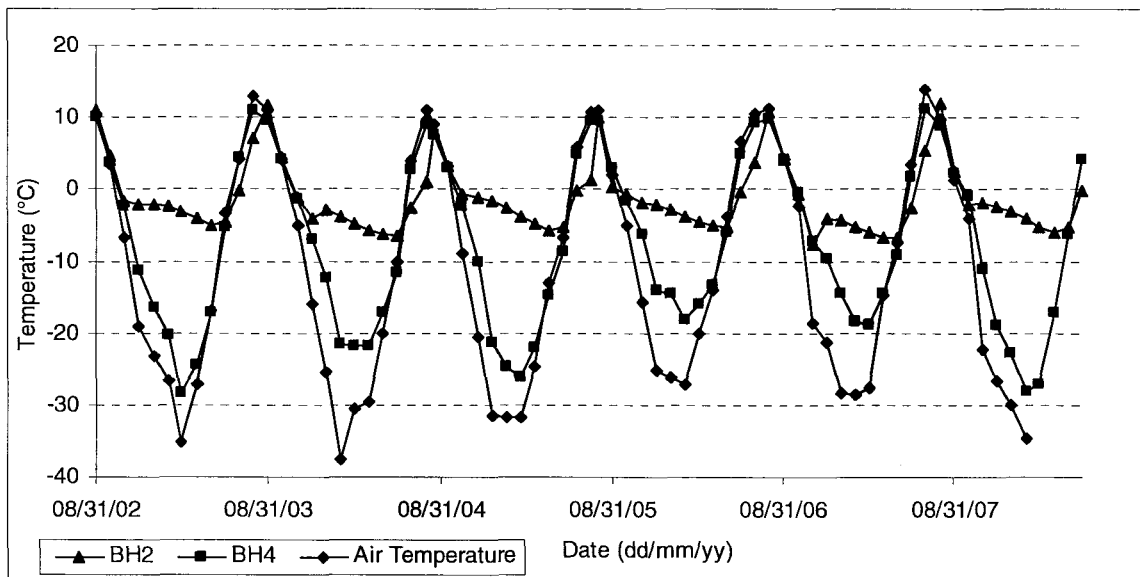


Figure 4.41: Monthly average air and ground surface temperatures at BH2 and BH4 from 2002 to 2008 at Baker Lake, Nunavut.

At BH4 values of FDD for the air ranged between 4131 and 5311, and that of the ground surface ranged between 2709 and 4019 from 2002 to 2008 (Table 4.14). Values of n_f ranged between 0.63 and 0.79. TDD of the air ranged between 827 and 1018, and that of the ground surface ranged between 703 and 904 from 2003 to 2007. Values of n_t

ranged between 0.85 and 0.90. The inter-annual variability in n_t is less than n_f , and the relationship between the air and the ground surface is stronger during the thawing season.

The FDD and TDD for the air were recalculated to correspond with the freezing and thawing seasons at the ground surface of BH2 (Table 4.16). The seasons used for calculating n-factors varied between the two sites because each was defined based on both the air and ground surface temperatures remaining above or below 0°C at the same time. The re-calculated FDD for the air ranged between 4140 and 5326, and that of the ground surface ranged between 713 and 1280, resulting in a range of n_f between 0.14 and 0.29. The re-calculated TDD for the air ranged between 470 and 809, and those for the ground surface ranged between 389 and 730, with n_t varying between 0.76 and 1.04. The inter-annual variability in these values is due to the variability in the timing and depth of the large snow drift.

Table 4.16: Summary table of on-site data at Baker Lake BH2, including FDD_a, FDD_s, TDD_a, TDD_s, n_f and n_t .

Year	FDD _a	FDD _s	n_f	Year	TDD _a	TDD _s	n_t
2002-03	4794	713	0.15	2003	701	730	1.04
2003-04	5326	1070	0.20	2004	470	389	0.83
2004-05	5122	723	0.14	2005	515	434	0.84
2005-06	4140	781	0.19	2006	643	581	0.90
2006-07	4490	1280	0.29	2007	809	618	0.76
2007-08	<i>M</i>	924	<i>M</i>	2008	<i>M</i>	<i>M</i>	<i>M</i>
CV	0.10	0.25	0.30	CV	0.22	0.25	0.12

The coefficient of variation (CV) is presented to show the relative variability over the monitoring period. Missing values are represented by *M*.

TOP, TTOP and the thermal offset were derived for two years at BH4 (Table 4.15). TTOP was -7.7°C during 2002-03, and -6.2°C in 2005-06. TOP was approximately 2.2 m during both years. The corresponding thermal offsets were 0.3 and -1.1°C. In 2005-06 the MAGST was warmer than TTOP resulting in a negative offset.

Latent heat effects at this borehole are limited. The zero-curtain effect observed in the spring is weak, sometimes not occurring at all. During freeze-back in autumn it lasts between 10 and 20 days near the end of September or beginning of October. The apparent thermal diffusivity within the active layer is low compared to deeper measurements, approximately $0.4 \times 10^{-6} \text{ m}^2\text{s}^{-1}$ compared to $5.8 \times 10^{-6} \text{ m}^2\text{s}^{-1}$ below the active layer, indicating that there are more latent heat effects in the near surface.

The MAGTs in the near surface at BH4 show slight warming towards the surface (Fig. 4.42), but the borehole is too shallow to observe the geothermal gradient. The depth of ZAA would be at approximately 17.8 m, based on the amplitude and the apparent thermal diffusivity between 2.0 and 2.5 m depth. The thickness of the permafrost at this site is expected to be between 200 and 400 m, based on a standard geothermal rate of $1^\circ\text{C}/30\text{-}60 \text{ m}$. The MAGTs calculated from manual measurements between 1997 and 2007 follow a similar trend to MAAT, but no statistically significant warming or cooling trends exist (Fig. 4.43). There is, however, a statistically significant ($p < 0.01$; $r^2 = 0.69$) relationship between the September to August MAGT at 3 m and the June to May MAAT, based on a 3 month phase lag from the ground surface to 3 m (Fig. 4.44 A). The r^2 value indicates that air temperature is important, but that variability in snow cover may influence the response of the ground to changes in air temperatures. The best-fit equation was used to hind-cast MAGTs using the hind-cast ECCS MAATs, and a significant warming trend of 0.3°C per decade occurred between the mid-1970's and 2007 ($p < 0.01$; Fig. 4.44 B).

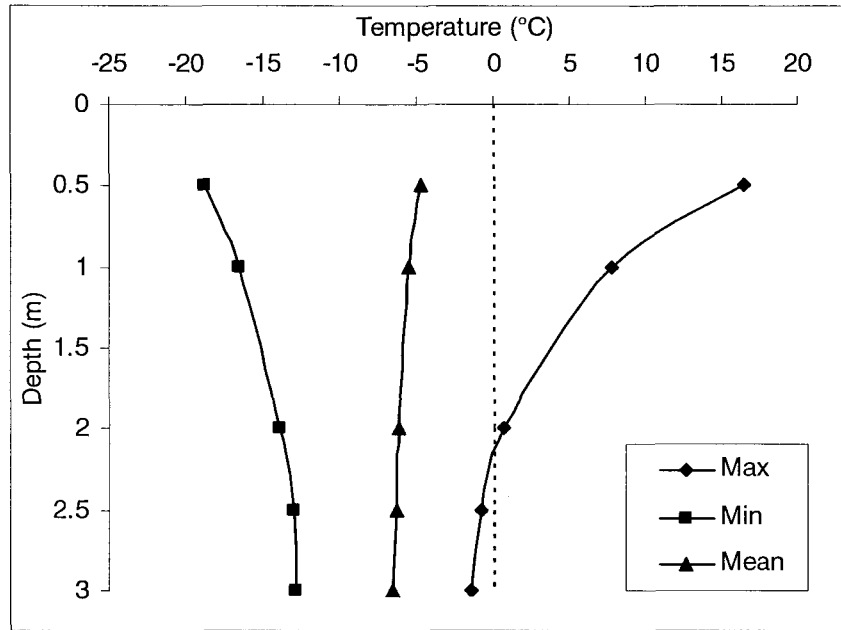


Figure 4.42: Temperature envelope at Baker Lake BH4, Nunavut, 2005-06.

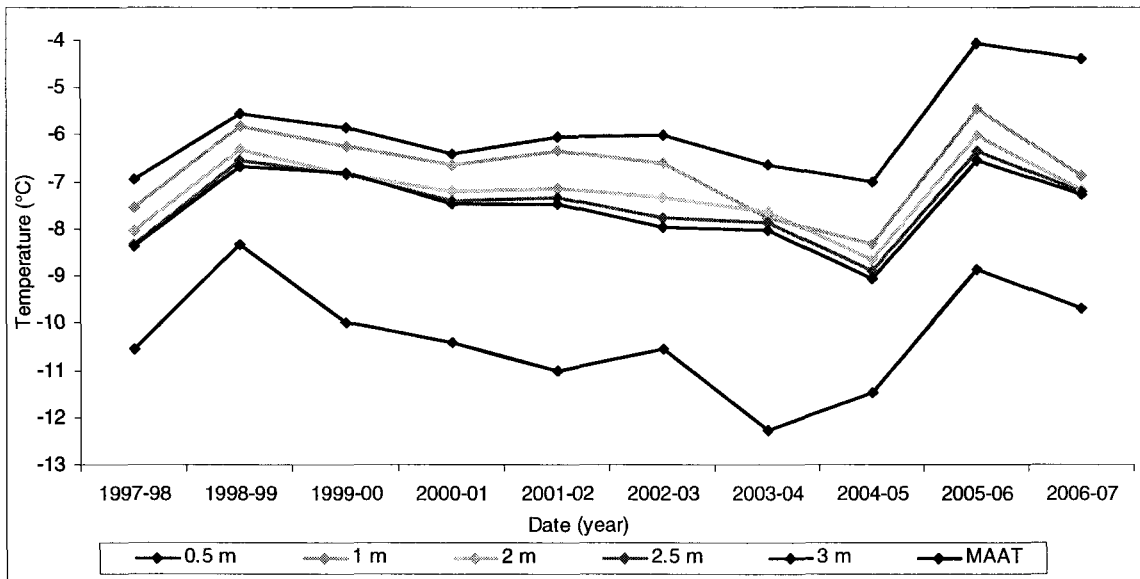


Figure 4.43: Changes in MAGTs from manual measurements at Baker Lake BH4 and MAAT from correlated ECCS data between 1997 and 2007 (Environment Canada, 2009).

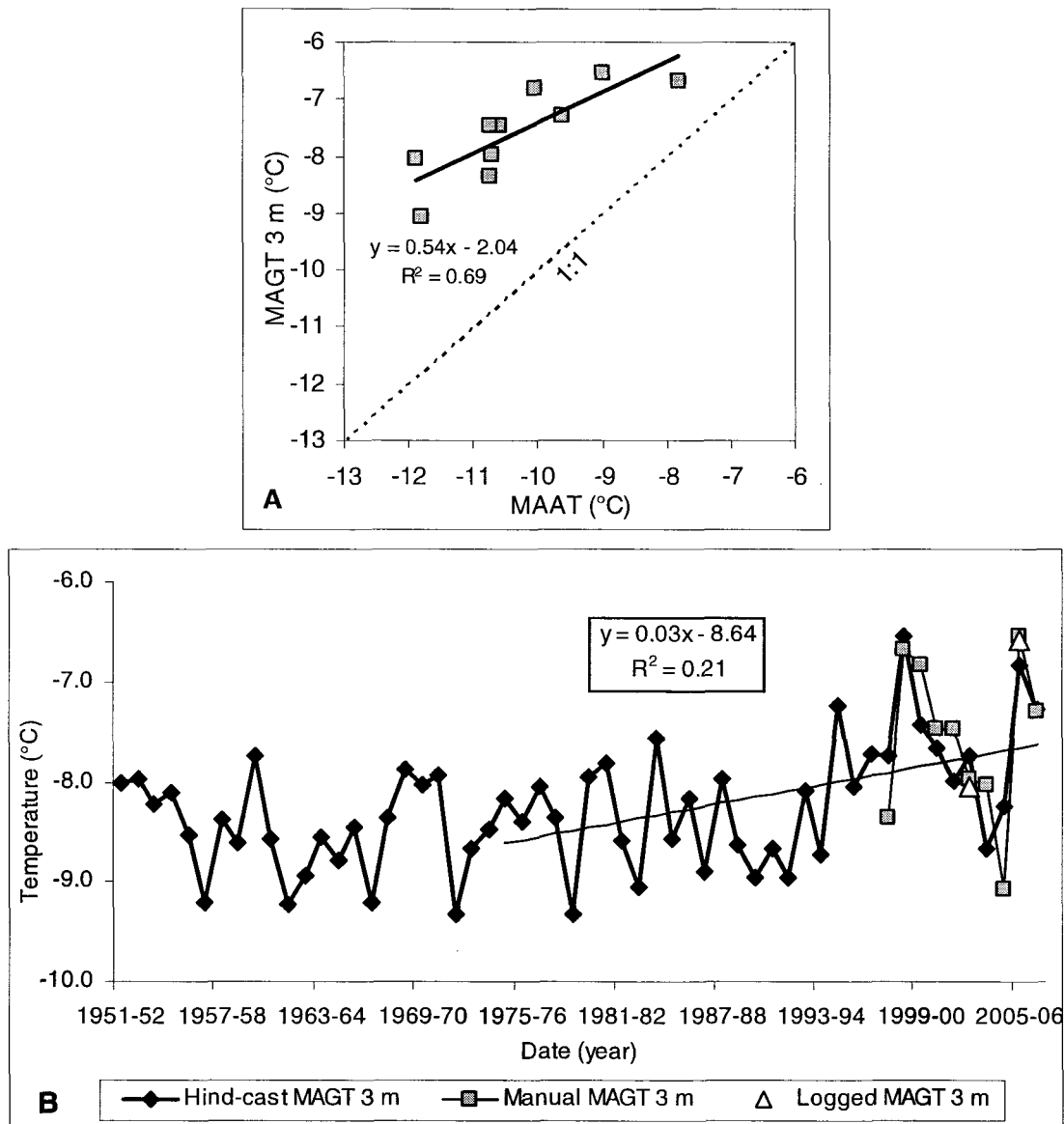
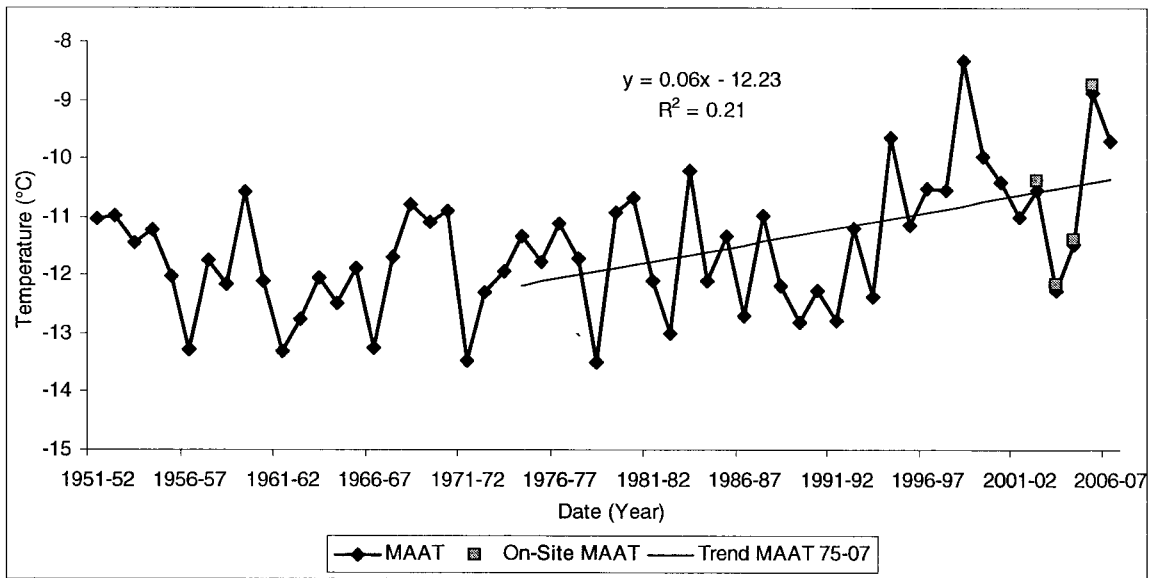


Figure 4.44: A) Relationship between MAGTs at 3 m, based on the September 1 to August 31 year, and MAAT, based on the June 1 to May 31 year, between 1997 and 2007 at Baker Lake BH4. The three month lag was decided based on the apparent thermal diffusivity and phase lags between the ground surface and 3 m depth. The correlation is significant at $p < 0.01$. B) Hind-cast 3 m MAGTs based on the best-fit equation from 1951 to 2007, plotted with MAGTs from manual and continuous measurements. The warming trend is significant at $p < 0.01$.

MAATs at Baker Lake show a statistically significant ($p < 0.01$) warming trend between 1975 and 2007 (Fig. 4.45). MAATs warmed at approximately 0.6°C per decade. Average seasonal air temperatures warmed variably over the monitoring period (Fig.

4.46). Winter air temperatures warmed with significance from the beginning of the record in 1951 until 2007 by 0.4°C per decade ($p < 0.01$). Winter air temperatures are the most inter-annually variable of all the seasons. Spring and summer air temperatures warmed by about 0.2°C per decade since 1950, but the trends are not statistically significant. The warming trend in autumn air temperatures began around 1984 at a rate of 1.3°C per decade, and the trend is statistically significant ($p < 0.05$).



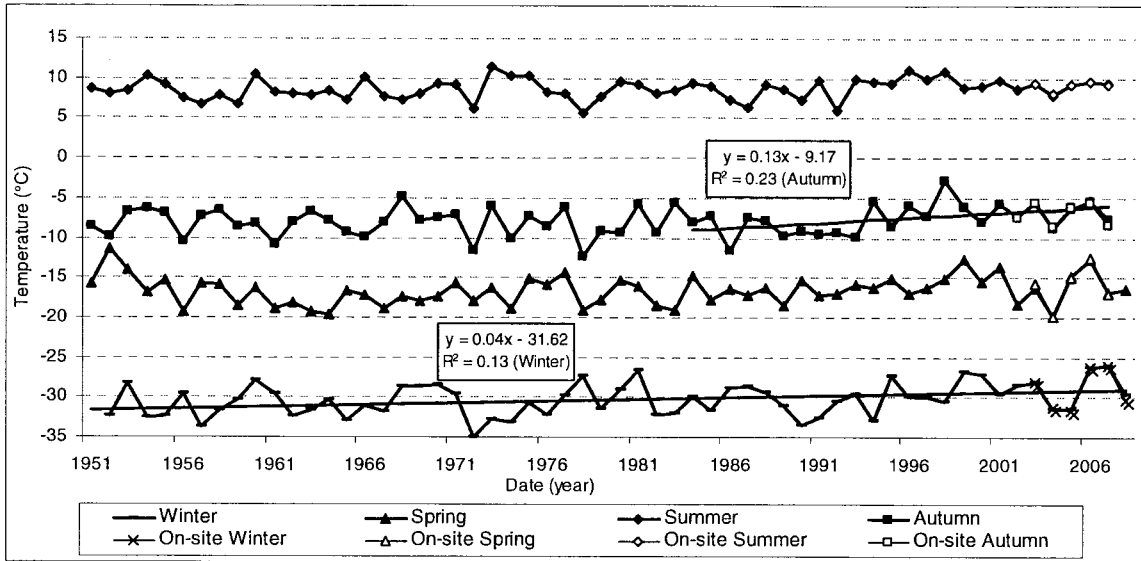


Figure 4.46: Trends in the seasonal average air temperatures at Baker Lake, Nunavut, between 1952 and 2008, derived from correlated ECCS data (Environment Canada, 2009). Statistically significant warming trends are observed in both the winter ($p < 0.01$), over the entire record, and autumn ($p < 0.05$) between 1984 and 2007.

4.3.1 Influence of a snow-fence induced snow drift at Baker Lake, Nunavut

A comparison between Baker Lake BH2, beneath the large snow drift, and BH4, representing natural conditions for the local area, illustrates the significant microclimatic effect that snow may have on air-to-ground temperature relations. The MAGSTs have warmed by 4 to 8°C at BH2 since the snow-fence was installed in 1981 (Table 4.15), as indicated by the difference between MAGSTs at BH2 and BH4. The surface offset has increased at BH2 to 7.7 and 10.5°C, compared to that at BH4 of 2.4 to 4.7°C (Table 4.15). Hinkel and Hurd (2006) also observed very large surface offsets and warming of the ground surface in Barrow, Alaska, at a snow-fence site. In terms of n-factors, n_f is strongly affected with an average of 0.19 at BH2 and 0.70 at BH4 (Tables 4.14 and 4.16). Values of n_f are similar despite the shortened thaw season at BH2 (Tables 4.14 and 4.16). The zero curtain effect at BH2 is visible in Fig. 4.47 and represents the length of the

snow melt period. Once the snow has melted, the ground surface temperature warms rapidly to almost the same temperature as the air (Fig. 4.47). The rapid increase in temperature is likely due to the darkened surface from dead vegetation beneath the snow drift (Fig. 4.37).

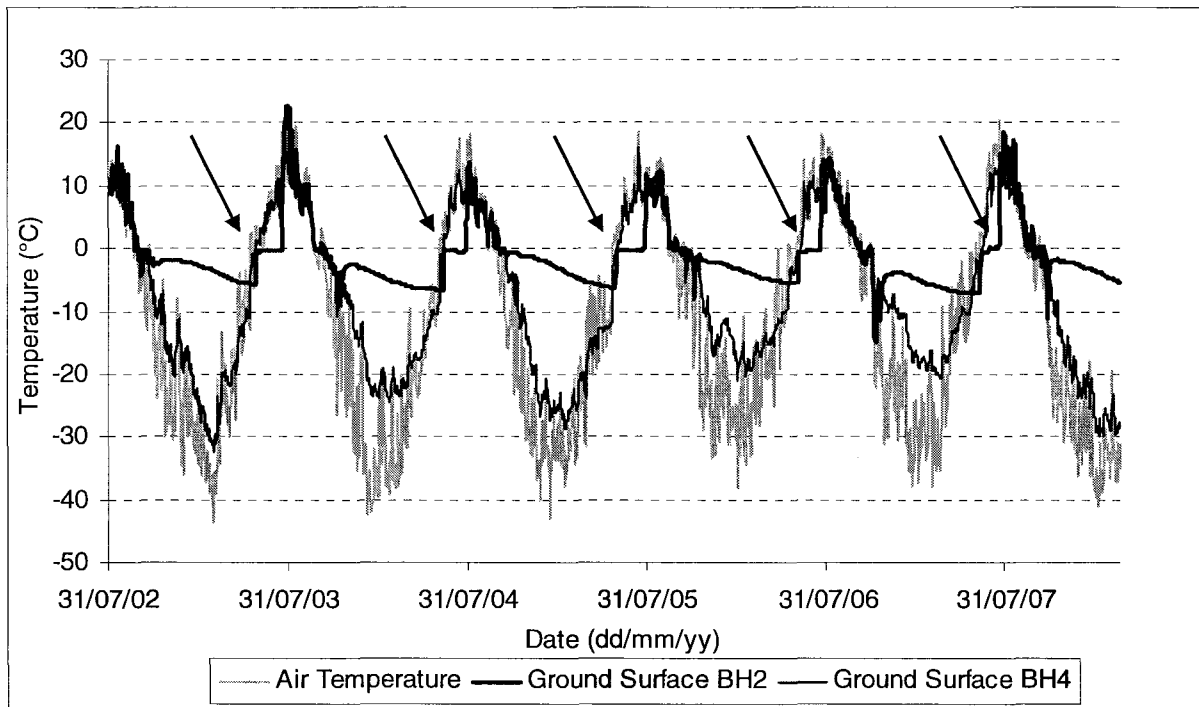


Figure 4.47: Air and ground surface temperature at Baker Lake BH2 and BH4, illustrating the extended zero-curtain in the spring during snow-melt at BH2 (indicated by the arrows), the damped ground temperatures in the winter compared to BH4 due to the snow drift, and the similarities between air and ground surface temperatures at both sites once the snow melt has finished.

The snow drift at Baker Lake presents an example of the effects that extreme amounts of snow can have on the ground thermal regime. Permafrost temperatures warmed throughout the profile due to the snow drift. The ground temperature amplitude is much greater at BH4 than at BH2 (Fig. 4.48). The difference is observed in the minimum temperatures due to the damping effect of the snow drift, which acts to reduce

the cooling of the ground surface during the winter at BH2. The maximum temperatures reached in the profiles are relatively similar (Figs. 4.47 and 4.48).

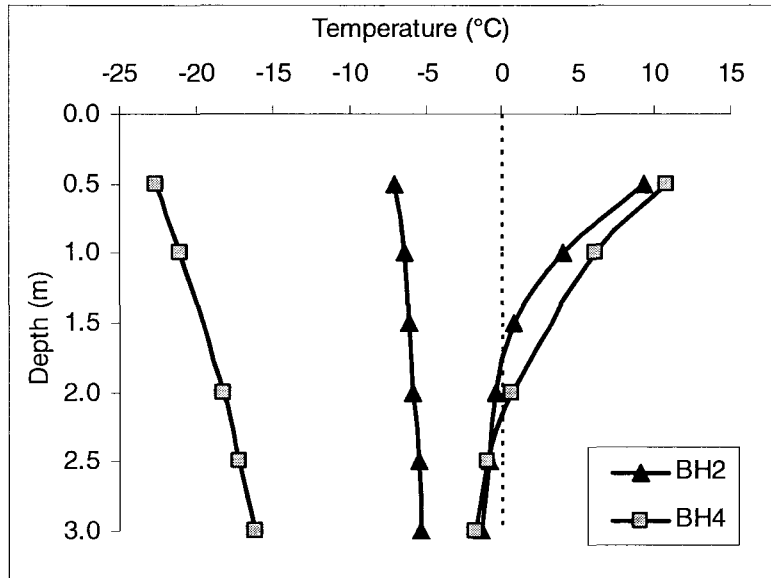


Figure 4.48: Temperature envelopes at Baker Lake BH2 and BH4, taken from manual measurements between 1997 and 2005 (absolute maxima and minima shown), showing the significant effect of the deep snow drift on minimum ground temperatures at BH2.

The length of the thaw season at BH2 is much shorter than at BH4. The deep snow drift persists longer into the summer, shortening the time that the ground surface is exposed to mild air temperatures. The thaw depths at BH2 were usually, but not invariably, shallower than at BH4 (Fig. 4.49) due to the shortened thaw season. The variability of thaw depths over the 9 years is greater at BH4 with a range of 0.9 m compared to BH2 with a range of 0.3 m (Fig. 4.49). Shallower thaw depths produced by the late-lying snow have also been observed near Barrow, Alaska (Hinkel & Hurd, 2006). Thermokarst development was also observed in Alaska beneath the large snow drift (Hinkel & Hurd, 2006), but this is not occurring at Baker Lake.

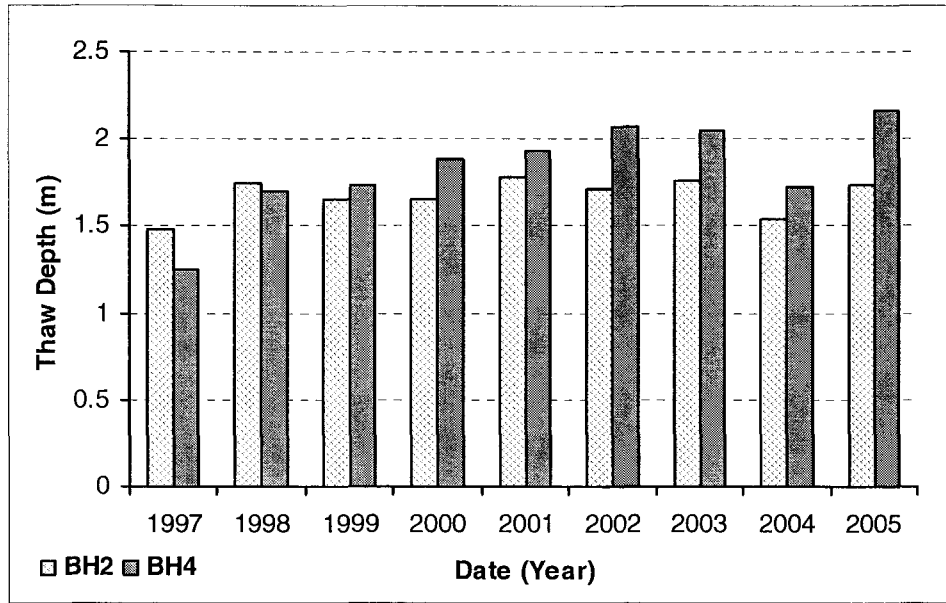


Figure 4.49: Thaw depths at Baker Lake BH2 and BH4 between 1997 and 2005. Most years BH2 thaw depths were shallower than BH4. Thaw depths were calculated by linear interpolation of manually collected borehole temperature data.

4.4 SIXTY MILE, YUKON

The permafrost thermal monitoring site at Sixty Mile is in the extensive discontinuous permafrost zone of the Yukon Territory close to the Alaska border at 63°54'N and 140°48'W (Fig. 1.1). This is an alpine tundra site, at an elevation of 1460 m, located on fractured bedrock and with sparse vegetation (Fig. 4.50). The borehole, angled at 50°, was drilled in August 2007 and was instrumented with a 50 m long cable to a vertical depth of 38.3 m with a logger recording temperatures at various depths three times per day (Fig. 4.51). A weather station was set up at the time of installation recording air temperature and relative humidity, wind speed and direction, precipitation, snow depth, incoming solar radiation, and shallow ground temperatures within the active layer. The ground temperature logger failed during the first year of monitoring, 39 days

after installation. The length of the records and depths of the thermistors are given in Table 4.17. The closest ECCS is in Dawson City at $64.2^{\circ}2'N$ and $139^{\circ}7'W$.

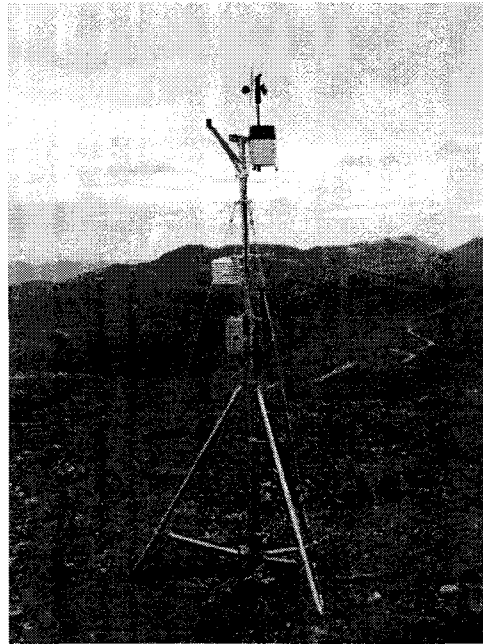


Figure 4.50: Photograph of the weather station at Sixty Mile, Yukon Territory, taken on July 17, 2008.

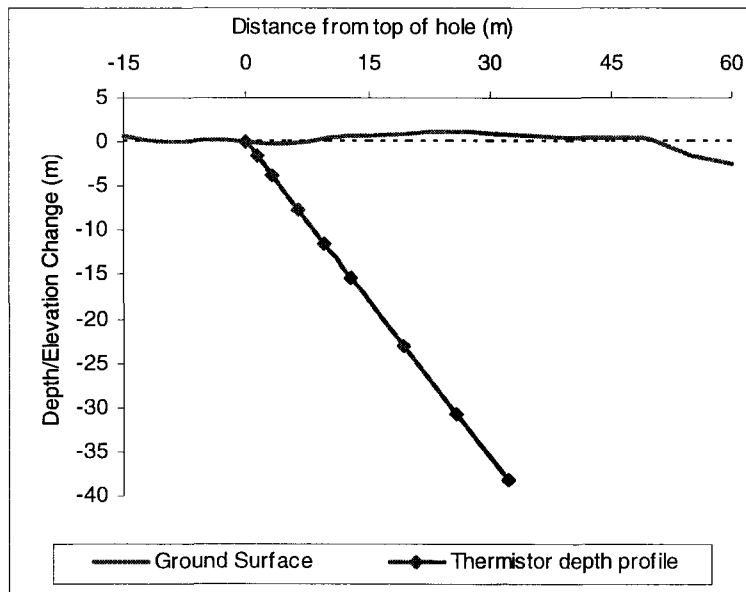


Figure 4.51: Depth profile of the Sixty Mile borehole showing the location of the thermistors in relation to the overlying terrain. Ground surface terrain was determined based on a leveling survey.

Table 4.17: Summary table of the data used in the analysis of the Sixty Mile borehole and the vertical depths of the thermistors from the surface.

Sixty Mile	
Manual Borehole Data	N/A
Logger Borehole Data	Aug 21-Sept 28/07, July 17/08 - Sept 3/09
Air Temperature	Aug 21/07 - Sept 3/09
Ground Surface Temperature	Aug 21/07 - Sept 3/09
10 and 25 cm	Aug 20/07 - Sept 3/09
50 cm	Aug 20-Dec 4/07, July 17/08 - Sept 3/09
Snow	2007-09
Air Temperature (ECCS)	N/A
Thermistor Depths (m)	1.5, 3.8, 7.7, 11.5, 15.3, 23.0, 30.6, 38.3

Snow depths at the Sixty Mile borehole site are higher than expected given its location on a plateau near the peak of a mountain. SDD were 6385 and 9175 over the two winters between 2007 and 2009. The snow accumulated in late September and melted completely by the end of April during both years (Fig. 4.52). It reached a maximum depth of about 60 cm near the end of October or beginning of November. It then decreased gradually over the rest of the season. During the first winter, 2007-08, snow depths decreased more dramatically than during the second winter, presumably because of wind scouring.

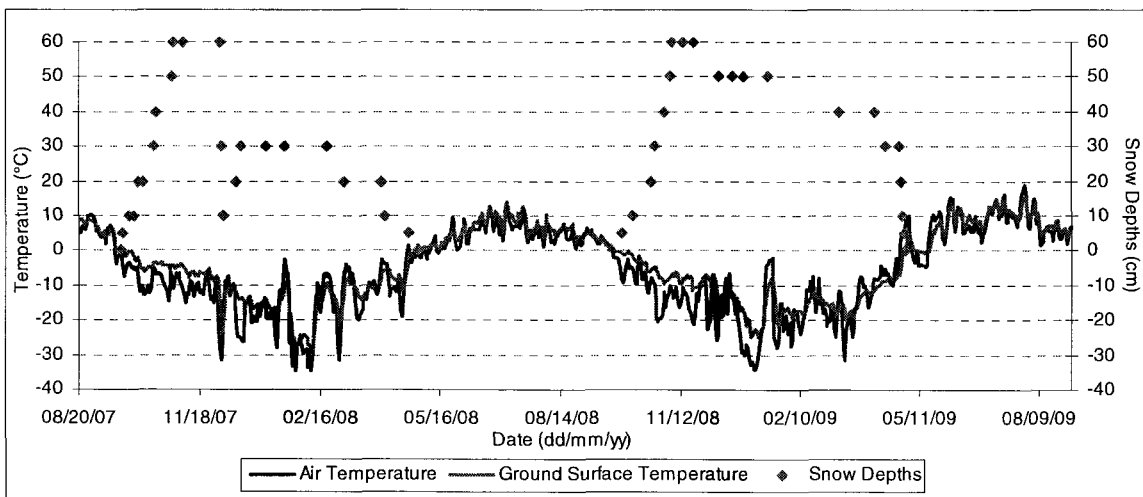


Figure 4.52: Air and ground surface temperatures with snow depths at Sixty Mile, Yukon, between August 20, 2007 and September 2, 2009.

The air and near surface temperature data is complete for two years at the Sixty Mile borehole site (Fig. 4.52). MAATs were -6.0 and -6.1°C during the 2007-08 and 2008-09 years, respectively, and MAGSTs were -4.1°C over both years, giving a surface offset of 1.9°C . TOP was located at 2.3 m during the thaw season of 2008-09. TTOP was interpolated as -4.7°C and the thermal offset is -0.5°C . The zero-curtain in the spring and autumn in the near surface at 0.10, 0.25, and 0.50 m depths lasted between a few days to two weeks.

FDD for the air were 2890 and 3183 during the two freezing seasons monitored to date, and FDD for the ground surface were 2347 and 2532, respectively. As a result, values of n_f were 0.81 and 0.80. TDD were calculated for the 2008 thaw season and measured 682 in the air and 833 at the ground surface, resulting in an n_t value of 1.2.

The ground temperature record from the Sixty Mile borehole that can be regarded as stable following re-equilibration after drilling is slightly longer than one year. The sensor at 1.5 m is within the active layer, and temperatures follow a similar path to the ground surface but are damped and lagged (Fig. 4.53). The temperature at 11.5 m appears to have been colder during August 2009 than in August 2008 (Fig. 4.54). The range in temperatures at the ground surface is about 40°C , which is reduced to 6.5°C at 3.8 m, and to 0.3°C at 15.3 m (Fig. 4.55). Based on the apparent thermal diffusivity between 11.5 and 15.3 m, the depth of ZAA is at approximately 16.6 m. Below ZAA, the temperature profile does not show warming or cooling with depth (Figs. 4.54 and 4.55).

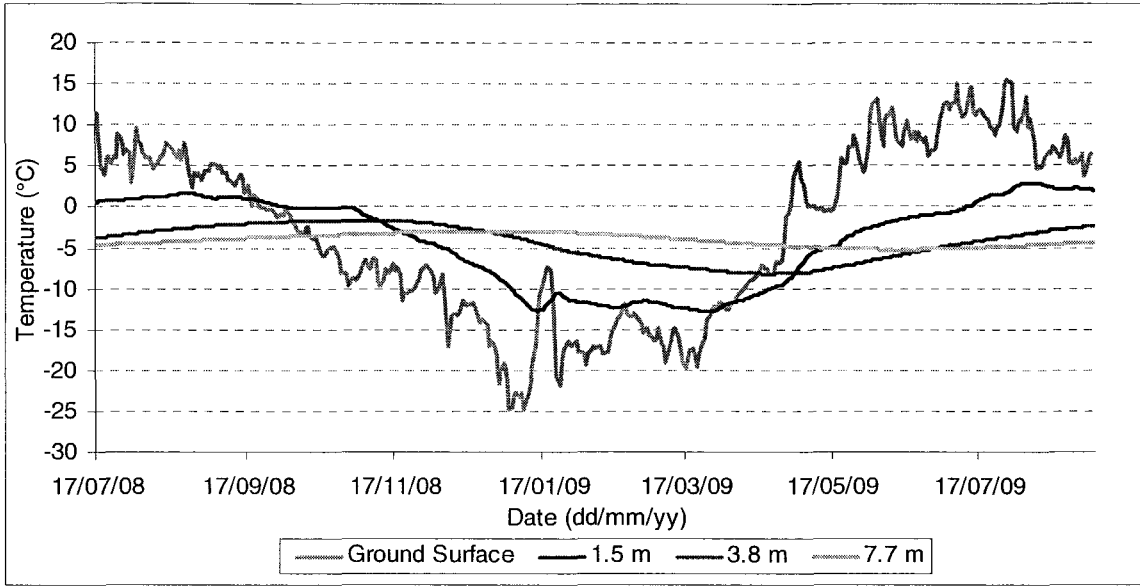


Figure 4.53: Shallow ground temperatures at the Sixty Mile borehole between July 17, 2008 and September 3, 2009. Attenuated patterns from the ground surface can be seen in the 1.5 m record.

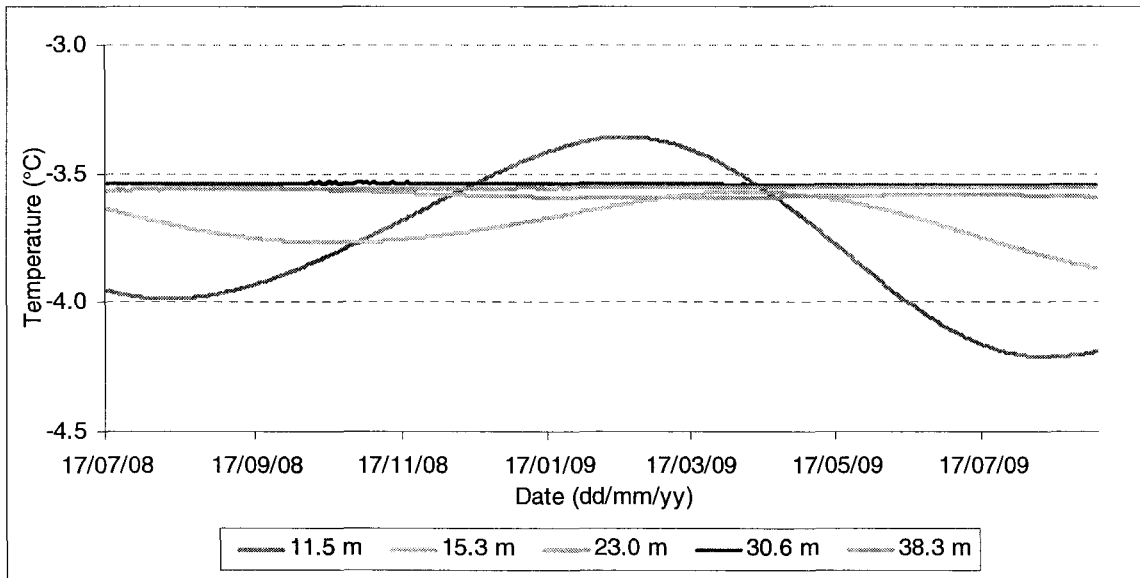


Figure 4.54: Deeper ground temperatures from the Sixty Mile borehole between July 17, 2008 and September 3, 2009. The temperatures at 11.5 m were colder in August 2009 than the previous year. Below ZAA, at 16.6 m, the temperatures are very similar, all about -3.6°C.

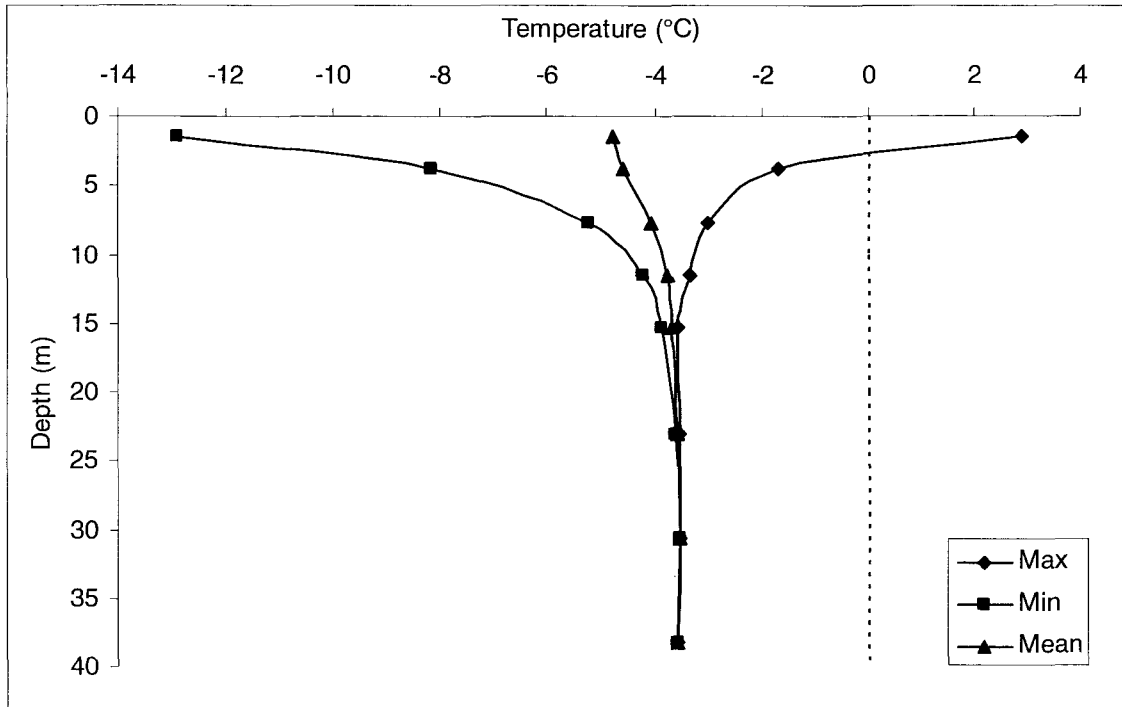


Figure 4.55: Temperature envelope at the Sixty Mile borehole for the 2008-09 year. The thermal profile below the depth of ZAA is virtually constant with depth, not showing cooling or warming.

4.5 RED CREEK, YUKON

The permafrost thermal monitoring site at Red Creek is located in the continuous permafrost zone of the Yukon Territory at 65°9'N and 138°21'W and 780 m elevation (Fig. 1.1). This is a hummocky tundra site with scattered stunted black spruce trees in the bottom of a broad river valley (Fig. 4.56). The borehole reaches 7 m and was drilled using the water-jet technique in August 2007. The ground is composed mainly of sands, silts and gravels, and with a moderate amount of segregated ice; these observations were made by observing the sediment that washed out of the hole and the movement of the drill-stem during water-jet drilling. Temperatures are being recorded three times per day at various depths (Table 4.18). Ground surface and near-surface temperatures, as well as snow depths were recorded hourly from the date of installation. Unfortunately the air

temperature sensor failed upon installation during the first year, and halfway through the second year. The closest ECCS is in Dawson at 64°2'N and 139°7'W, but some data are also available from Eagle Plains at 66°22'N and 136°43'W. The length of the records are given in Table 4.18.



Figure 4.56: Photograph of the Red Creek borehole, Yukon Territory, taken on July 19, 2008.

Table 4.18: Summary table of the data used in the analysis of the Red Creek borehole and the depths of the thermistors from the surface.

Red Creek	
Manual Borehole Data	N/A
Logger Borehole Data	Oct 3/07 - Sept 4/09
Air Temperature	N/A
Ground Surface Temperature	Aug 25/07 - Sept 4/09
10, 25, and 50 cm	Aug 25/07 - Sept 4/09
Snow	2007-2009
Thermistor Depths (m)	0.5, 1.0, 1.5, 2.0, 3.0, 4.0, 7.0

During the winter of 2007-08 snow cover thicknesses were generally between 25 and 35 cm, and remained within this range for the majority of the season. An estimate of SDD was 3760 for this year. The height of the iButton covered with snow was used as the daily snow thickness in calculating SDD. Snow arrived in early October and melted at the end of April, and the maximum depth was reached near the end of December. The

last day of snow melt corresponded with the ground surface temperature rising above 0°C on April 28, 2008 (Fig. 4.57). During the winter of 2008-09 snow began to accumulate in mid-October, and depths were between 30 and 50 cm by early November. An approximate value for SDD is 5680, considerably higher than during the previous year, but is still probably underestimating the actual value due to a gap in iButton sensors between 30 and 50 cm. The snow persisted at depths of at least 30 cm until the end of April. The ground surface was free of snow on May 3, 2009 (Fig. 4.57). The deeper snow in 2008-09 corresponded with higher near-surface temperatures in the ground than the previous year (Fig. 4.57).

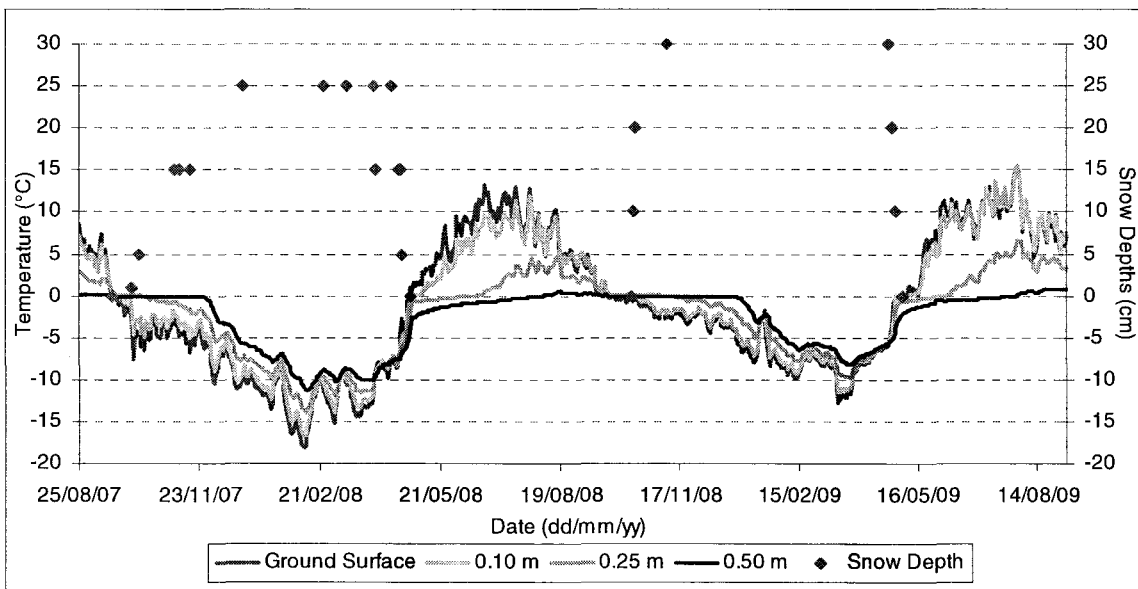


Figure 4.57: Temperatures at the ground surface, 10, 25, and 50 cm deep, and snow depths at Red Creek, Yukon, from August 28, 2007 to July 19, 2008.

The MAGST was -2.4°C in 2007-08 and increased to -0.2°C in 2008-09. TOP was interpolated at just below 1 m in the summer of 2008, and TTOP was approximately -1.7°C. The zero-curtain effect at 0.10 m and 0.25 m began just after snow melt in the spring of both years, though it lasted longer in the spring of 2008 than 2009 (Fig. 4.57).

The zero-curtain effect in the near-surface is weaker in autumn, lasting a few days to 2 weeks at 0.10 m, and about 3 to 5 weeks at 0.25 m in 2007 and 2008, respectively. At 0.5 m depth the zero-curtain lasts at least 3 months during freeze-back, indicating large amounts of unfrozen moisture and low thermal gradients. FDD for the ground surface totaled 1891 in 2007-08, and 1114 in 2008-09. TDD for the 2008 summer measured 975.

Temperatures at 0.5 m vary between the borehole and the air temperature station. The 0.5 m readings from the borehole are slightly warmer than the 0.5 m readings from the Hobo data-logger at the undisturbed site near the air temperature station, located only a few meters from the borehole (Fig. 4.58). During both the 2008 and 2009 thaw seasons the ground thawed sooner and warmed more at 0.5 m depth at the borehole than at the undisturbed site. During drilling, in August 2007, probing was done to assess the depth of the frost table around the borehole. The depth ranged from 0.43 to 0.58 m, indicating that the 0.5 m readings at the borehole are possibly a result of the natural variation in thaw depths in the area. The difference may also be due to the variability in frozen and unfrozen moisture, or the thermistors may be at slightly different depths, or there may be an influence from the iron pipe.

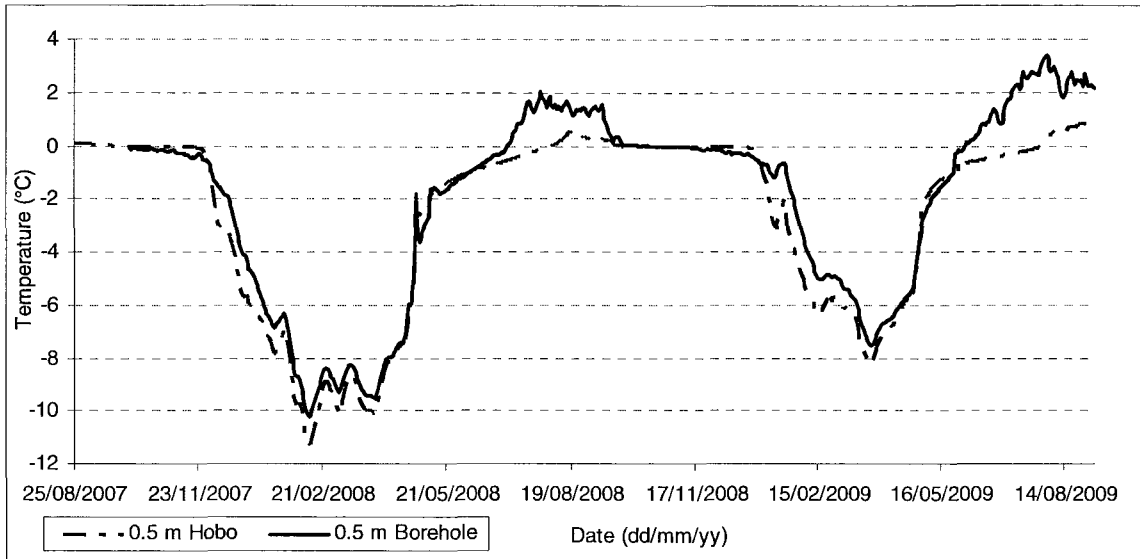


Figure 4.58: Ground temperatures at 0.5 m at Red Creek between August 2007 and August 2009: one reading is from the borehole, and the other is from the hobo logger beneath the air temperature station, located a few meters from the borehole. The difference is either a part of the natural variation in the area, or the sensors are at slightly different depths, or the sensor is being affected by the steel casing in the borehole.

This borehole site lies within the southern margin of the continuous permafrost zone. The annual minimum temperature wave takes about 3 months to travel from 0.5 m to 7 m (Fig. 4.59). The ground temperature range diminishes fairly rapidly with depth, and at 7 m the ground temperature ranges by about 1.3°C over the 290 days on record. The average apparent thermal diffusivity over the two years of monitoring is $0.8 \times 10^{-6} \text{ m}^2\text{s}^{-1}$ between 4 and 7 m. This value was used to predict an approximate depth of ZAA of 12.2 m.

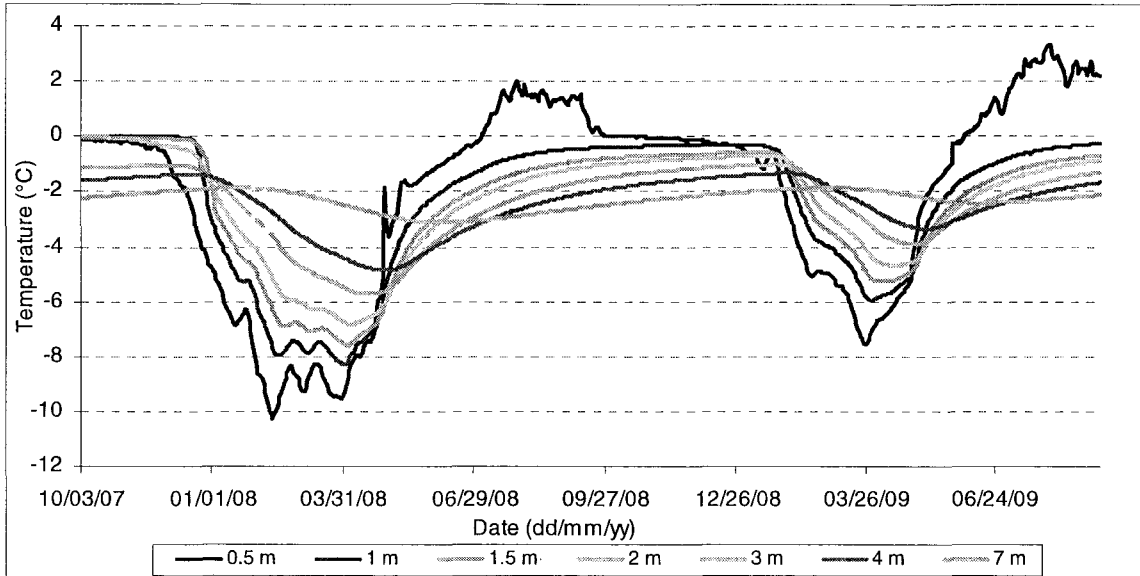


Figure 4.59: Ground temperature time series at Red Creek, Yukon, between October 3, 2007 and September 4, 2009.

The thermal profile in the 2007-08 year shows slight warming with depth, but cools with depth the following year (Fig. 4.60). The 2008-09 year was warmer than the previous year in the minimum, maximum and mean temperatures at all depths, and the amplitude of the temperature envelope was smaller (Fig. 4.60). Based on the standard geothermal gradient of 1°C warming per 30-60 m, the permafrost at this site would be between 100 and 200 m thick.

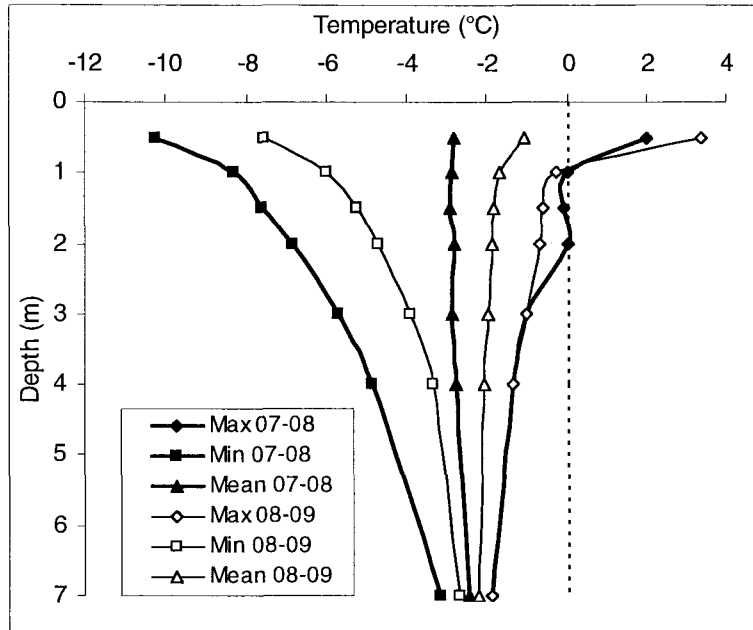


Figure 4.60: Temperature envelopes at Red Creek, Yukon, for the years October 3, 2007 to October 2, 2008, and September 1, 2008 to August 31, 2009. There is considerable inter-annual variability in ground temperatures between the two years.

4.6 ALPINE BURWASH – KLUANE RANGE, YUKON

The permafrost thermal monitoring site at Alpine Burwash is located at 61°27'N and 139°24'W within the sporadic discontinuous permafrost zone of the Yukon Territory, and is at an elevation of 1840 m (Fig. 1.1). The borehole was drilled in August 2008 and there is just over one year of data available for analysis. The area around the borehole is primarily low growing alpine tundra type vegetation with areas of gravelly scree slopes (Fig. 4.61). The hole is on a 50° angle into a southwest facing slope near the top of a ridge and reaches a vertical depth of 42.9 m (Fig. 4.62). The length of the records and depths of the thermistors from the surface are given in Table 4.19. The borehole has a logger recording ground temperatures 3 times per day, and a weather station recording every hour. There are also sensors recording near surface ground temperatures at depths

of 2, 25, 50, 60, and 75 cm. The closest ECCS is at Burwash Landing at 61°22'N and 139°3'W at an elevation of 807 m, more than 1000 m lower than the borehole site.



Figure 4.61: Photograph of the Alpine Burwash borehole during drilling, taken on August 16, 2008.

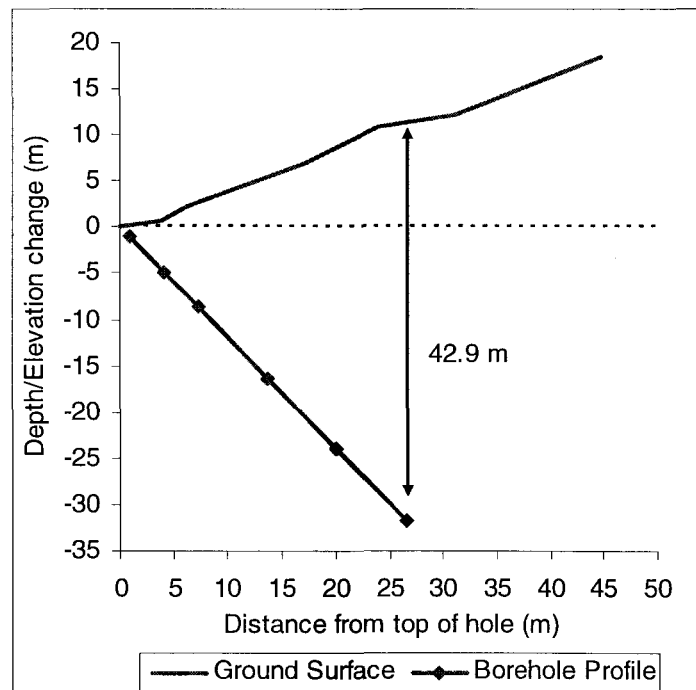


Figure 4.62: Depth profile of the Alpine Burwash borehole showing the location of the thermistors in relation to the overlying terrain. Ground surface terrain was determined based on a leveling survey, and depths of thermistors are based on vertical distance from the ground surface.

Table 4.19: Summary table of the data used in the analysis of the Alpine Burwash borehole and the vertical depths of the thermistors from the surface.

Alpine Burwash - Kluane Range	
Manual Borehole Data	N/A
Logger Borehole Data	Aug 18/08 - Sept 14/09
Air Temperature	Aug 18/08 - Sept 14/09
Ground Surface Temperature	Aug 18/08 - Sept 14/09
60 cm	Sept 21/08 - Sept 14/09
Snow	2008-2009
Thermistor Depths (m)	1.0, 5.6, 11.3, 21.9, 32.6, 42.9

Snow depths at this site were shallow throughout the winter of 2008-09, remaining around an average of 10 cm for most of the season (Fig. 4.63). Near the end of February snow depths reached maxima of between 30 and 40 cm for a few weeks, and then decreased gradually until the end of April, when the last of the snow melted. During the period of deeper snow, smoothing out of the ground surface temperature line occurred (Fig. 4.63), whereas for the majority of the winter the ground surface temperature followed the air temperature fluctuations quite closely. FDD were calculated for the ground surface and the air over the winter. The ground surface temperature data was taken from the undisturbed secondary air temperature site located about 3 m upslope from the borehole, and approximately 10 m upslope from the weather station where air temperatures were recorded. FDD of the ground surface were 2356, and those of the air were 2416, resulting in an n_f of 0.98. The n_f value was close to 1.0 because of the minimal amounts of snow persisting at the site during winter.

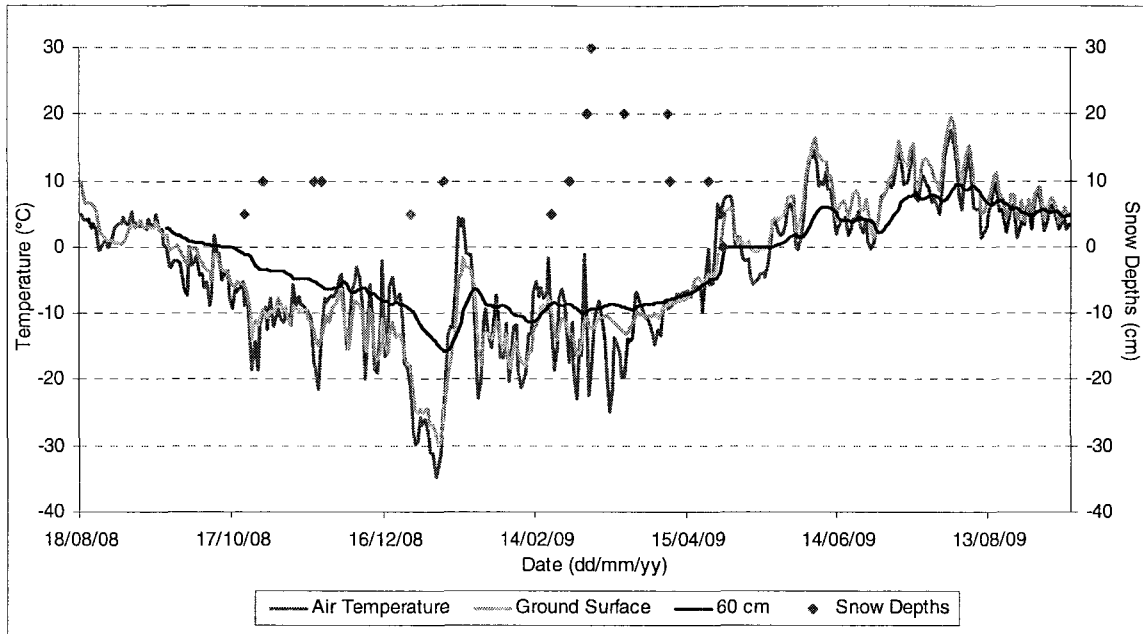


Figure 4.63: Daily air, ground surface, and 60 cm temperature, and snow depths at Alpine Burwash, Kluane Range, from August 18, 2008 to September 14, 2009. The ground surface temperature follows air temperature closely throughout the year and is often warmer than the air in the summer. A zero-curtain effect is evident in the spring at 60 cm.

Borehole temperatures at depth were within 0.25°C of their final values within about 2 months of drilling, indicating that re-equilibration had occurred (Fig. 4.64). The thermal gradient in the borehole is negative with depth (Fig. 4.65). Given that the borehole was drilled on a 50° angle into a slope, the variability in topography around the borehole may be affecting the thermal gradient. Long-term monitoring of this borehole may reveal the cause of the gradient. If it is due to recent climate warming the gradient will change in the coming years, and if it is due to topographic effects the gradient will be maintained.

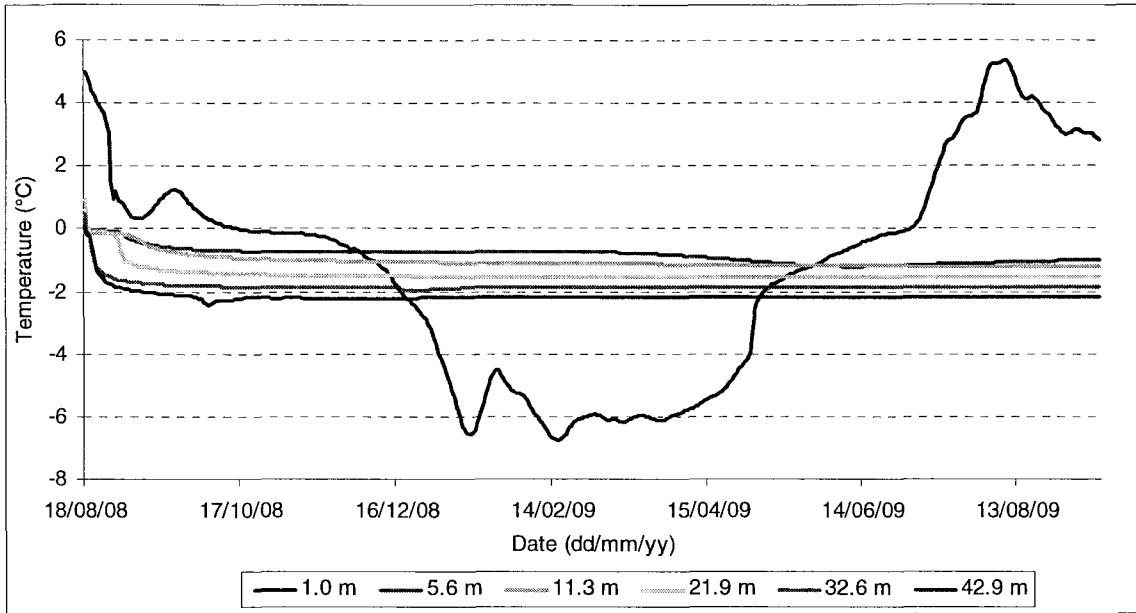


Figure 4.64: Daily ground temperatures at the Alpine Burwash, Kluane Range, borehole between August 18, 2008 and September 14, 2009. This graph shows, in particular, the process towards the re-equilibrating of ground temperatures near the beginning of the record.

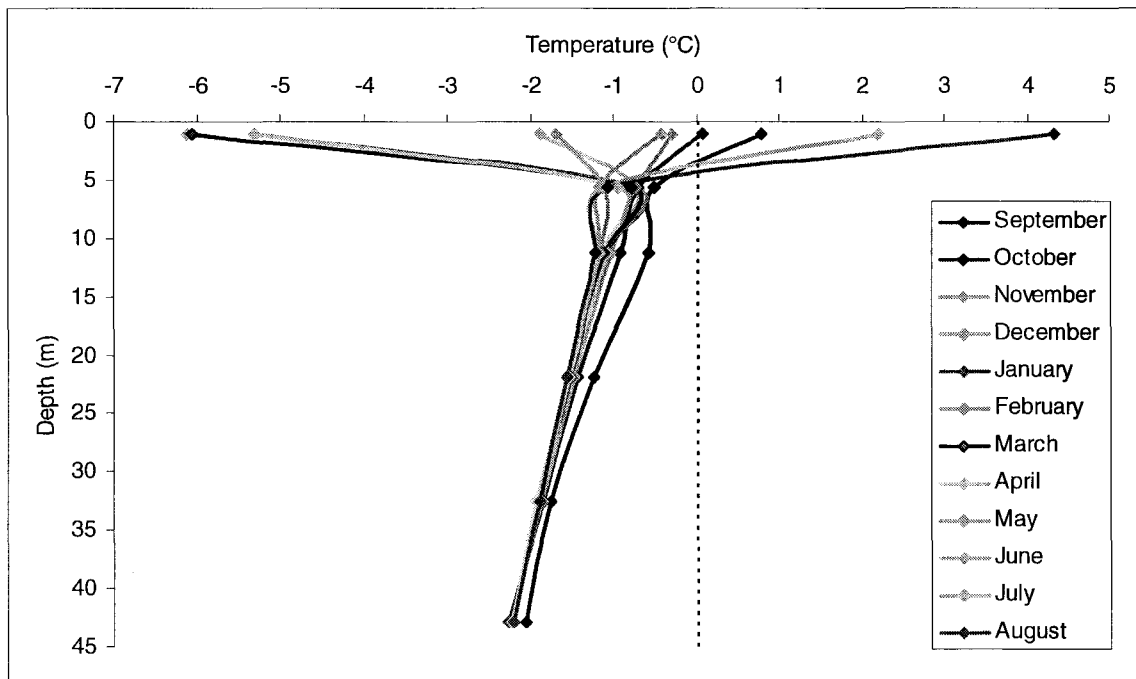


Figure 4.65: Monthly average temperature profiles from September 2008 to August 2009 at the Alpine Burwash – Kluane Range borehole. The September profile exhibits the strongest effects from the drilling, and each profile following shows part of the process towards re-equilibrating temperatures.

4.7 TABLE MOUNTAIN, NORTHWEST TERRITORIES

The permafrost thermal monitoring site at Table Mountain is located in the Northwest Territories at 63°36'N and 123°37'W, within the extensive discontinuous permafrost zone (Fig. 1.1). This site is in coniferous forest at the approach to a south-facing slope at 265 m elevation off the Norman Wells pipeline right-of-way (Fig. 4.66). The ground is composed of ice rich lacustrine deposits, mainly silty clay and clay with massive ice lenses.

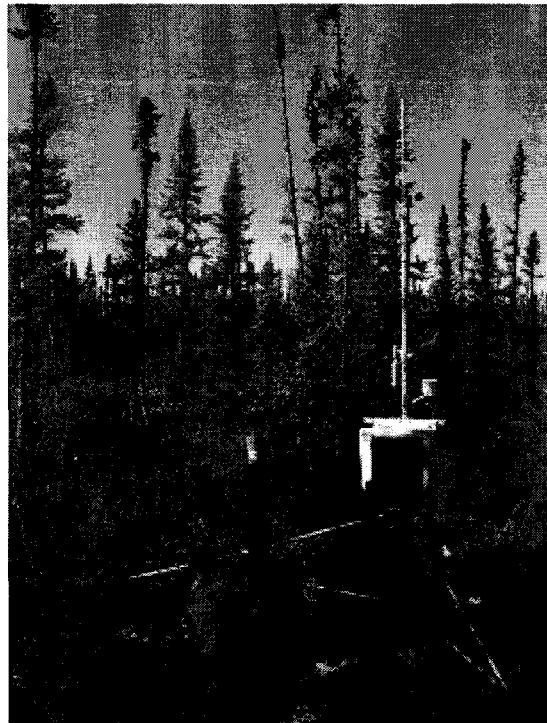


Figure 4.66: Photograph of the weather station and borehole at Table Mountain, taken in September, 2003 (photo is courtesy of the Geological Survey of Canada).

The borehole was drilled in 1985 to a depth of 20 m. Manual measurements were taken on a monthly or bimonthly basis from 1985 to 1995, and less frequently since then. An automatic data logger was attached to the ground temperature cable in 1995 reading temperatures to a depth of 17 m, and a weather station was set up in 2003 to record air temperature, snow depths and wind speed. The length of the records and depths of the

thermistors from the surface are given in Table 4.20. This borehole site is maintained by the Geological Survey of Canada. The closest ECCS is in Fort Simpson at 61°45'N and 121°14'W, which is approximately 230 km from the borehole site.

Table 4.20: Summary table of the data used in the analysis of the Table Mountain borehole and the depths of the thermistors within the borehole.

Table Mountain	
Manual Borehole Data	1985-2007
Logger Borehole Data	1995-2007
Air Temperature	2001-2008
Ground Surface Temperature	2002-2006
Snow	2003-2005
Air Temperature (ECCS)	1963-2008
Thermistor Depths (m)	1, 2, 3, 4, 6, 8, 12, 17

There are two years of on-site snow data at Table Mountain between 2003 and 2005 (Fig. 4.67). Both years had similar characteristics, with maximum depths of 85 and 74 cm, average depths of 42 and 44 cm, and SDD of 8559 and 8959. During both years the snow arrived in mid-to-late October and melted in early-to-mid May. More snow accumulated during the first winter between 2003 and 2004, and the effect is seen in the ground surface temperature fluctuating less than in the following year.

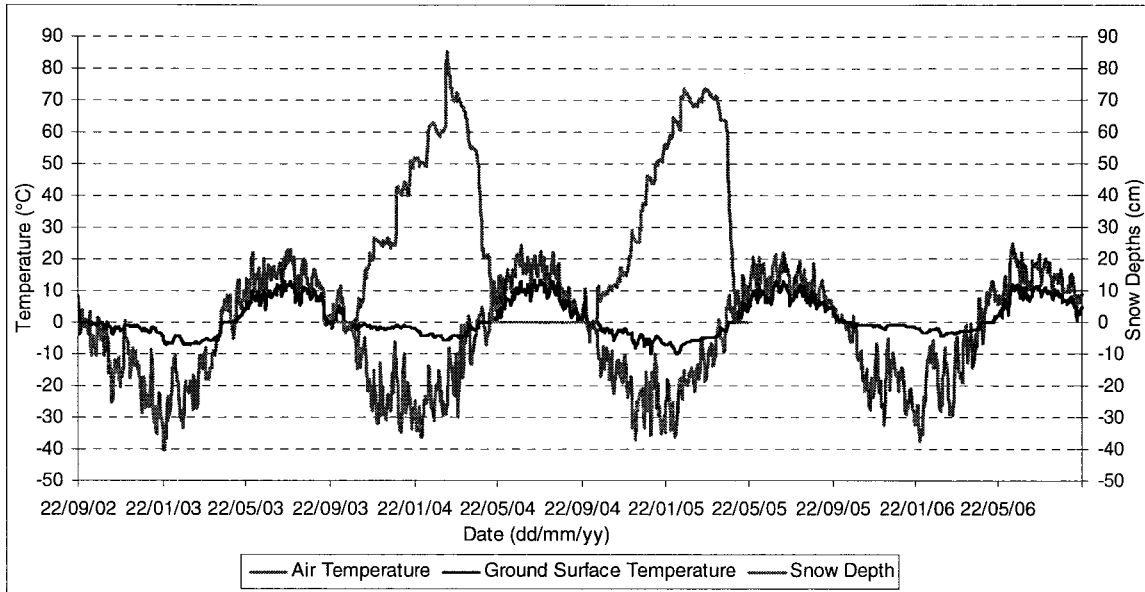


Figure 4.67: Daily air temperature, ground surface temperature, and snow depth trends at Table Mountain, NWT, between September 2002 and September 2006.

The MAAT ranged between -3.6 and -5.6°C from 2001 to 2008, and the MAGST ranged between 0.2 and 1.7°C between 2002 and 2006, remaining above zero the entire time (Table 4.21). The surface offset ranged between 4.6 and 6.4°C , due mainly to the persistent snow pack that acts as a buffer between the air and the ground surface during the winter months. The effects of the insulating snow-pack can be seen in Fig. 4.67, where minimum air temperatures reached -40°C , but the minimum ground surface temperature was only -10°C .

Table 4.21: Summary table of continuously logged on-site data at Table Mountain, including the MAAT, MAGST, surface offset, TOP, TTOP, and the thermal offset.

Date	MAAT (°C)	MAGST (°C)	Surface Offset (°C)	TOP (m)	TTOP (°C)	Thermal Offset (°C)
1995-96	-5.5*	<i>M</i>	<i>M</i>	1.7	<i>M</i>	<i>M</i>
1996-97	-5.1*	<i>M</i>	<i>M</i>	1.9	-0.3	<i>M</i>
1997-98	-2.6*	<i>M</i>	<i>M</i>	1.9	-0.2	<i>M</i>
1998-99	-3.4*	<i>M</i>	<i>M</i>	1.9	-0.3	<i>M</i>
1999-00	-4.0*	<i>M</i>	<i>M</i>	2.0	-0.3	<i>M</i>
2000-01	-4.1*	<i>M</i>	<i>M</i>	1.9	-0.3	<i>M</i>
2001-02	-5.3	<i>M</i>	<i>M</i>	<i>M</i>	<i>M</i>	<i>M</i>
2002-03	-3.6	1.0	4.6	2.0	-0.2	-1.2
2003-04	-5.0	1.4	6.4	2.0	-0.2	-1.7
2004-05	-4.8	0.2	5.0	<i>M</i>	<i>M</i>	<i>M</i>
2005-06	-3.6	1.7	5.3	1.9	-0.2	-1.9
2006-07	-4.4*	<i>M</i>	<i>M</i>	1.9	-0.2	<i>M</i>
2007-08	-5.6	<i>M</i>	<i>M</i>	<i>M</i>	<i>M</i>	<i>M</i>

* Values of MAAT were calculated using correlated ECCS data (Environment Canada, 2009). Missing data is represented by *M*.

FDD at the ground surface ranged between 378 and 946, and for the air they ranged between 3141 and 3591 (Table 4.22). The ground surface had greater inter-annual variability in relative terms, likely due to the variability of snow depth and duration. Values of n_f were low and ranged between 0.14 and 0.28, providing evidence of the strong effects of snow at this site.

Table 4.22: Summary table of on-site data at Table Mountain, including FDD_a, FDD_s, TDD_a, TDD_s, SDD, n_f and n_t .

Year	FDD _a	FDD _s	n_f	SDD	Year	TDD _a	TDD _s	n_t
2002-03	3141	668	0.21	<i>M</i>	2003	1891	1069	0.57
2003-04	3591	506	0.14	8559	2004	1659	984	0.59
2004-05	3396	946	0.28	8960	2005	1713	1066	0.62
2005-06	<i>M</i>	378	<i>M</i>	<i>M</i>	2006	<i>M</i>	<i>M</i>	<i>M</i>
CV	0.07	0.39	0.33	0.03	CV	0.07	0.05	0.04

The coefficient of variation (CV) is presented to show the relative variability over the monitoring period. Missing data is represented by *M*.

TDD at the ground surface ranged between 984 and 1069, and for the air they ranged between 1659 and 1891 (Table 4.22). Both the ground surface and the air exhibit little inter-annual variability. Values of n_t ranged between 0.57 and 0.62, indicating a

more consistent relationship than during the winter. The low n_t values are due to shading of the ground surface by vegetation, and the latent heat requirements due to the presence of soil moisture.

TOP ranged between 1.7 and 2.0 m between 1995 and 2007 (Table 4.21). TTOP ranged between about -0.2 and -0.3°C over the same period (Fig. 4.68). The thermal offset was calculated for three years and ranged between 1.2 and 1.9°C . Although the MAGST is above 0°C , permafrost exists at Table Mountain due to the high ice content and latent heat effects in the permafrost causing a sizeable thermal offset to exist. TTOP warmed by 0.1°C per decade between 1996 and 2007, and the trend is statistically significant (Fig. 4.68; $p < 0.01$).

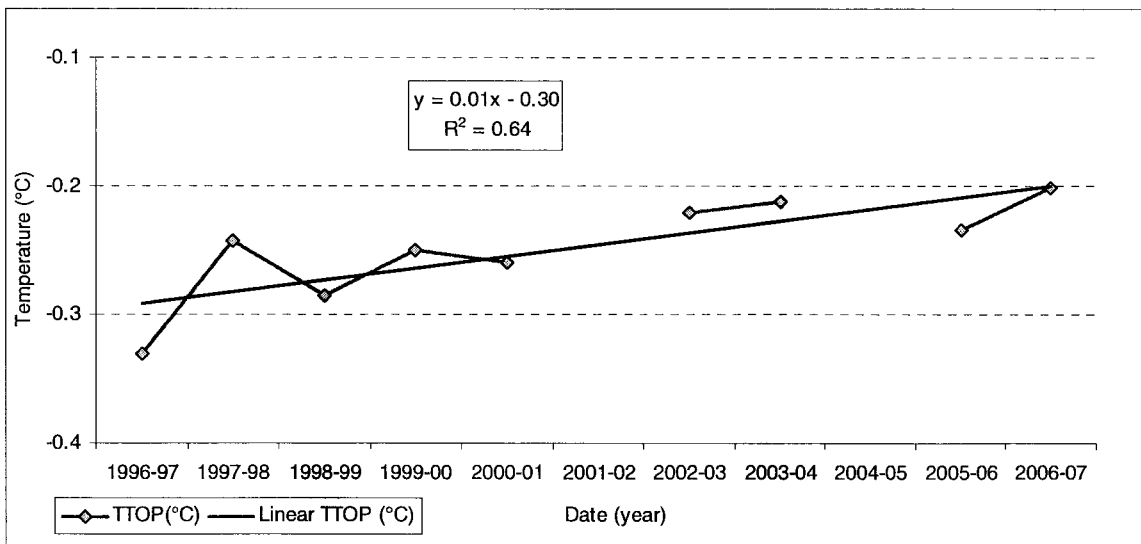


Figure 4.68: TTOP at Table Mountain, NWT, between 1996 and 2007. The warming trend of 0.1°C per decade is considered significant at $p < 0.01$.

The zero-curtain in the spring lasts between 2 and 3 weeks, starting just after air temperatures rise above 0°C and ending abruptly once all of the snow has melted (Fig. 4.67). During freeze-back in autumn the zero-curtain is shorter than in the spring.

The entire thermal profile at Table Mountain, as seen in the temperature envelope (Fig 4.69), is just below 0°C. All temperatures between 2 m and 17 m remain between 0 and -1°C throughout the year. The near-surface temperature range at 1 m is highly variable from year-to-year. From 1995 to 2007 the annual ground temperatures at 1 m depth ranged between 1.6 and 9.1°C, and remained within the active layer throughout monitoring. These differences are likely due to inter-annual variations in snow cover, seasonal air temperature variability, and soil moisture contents.

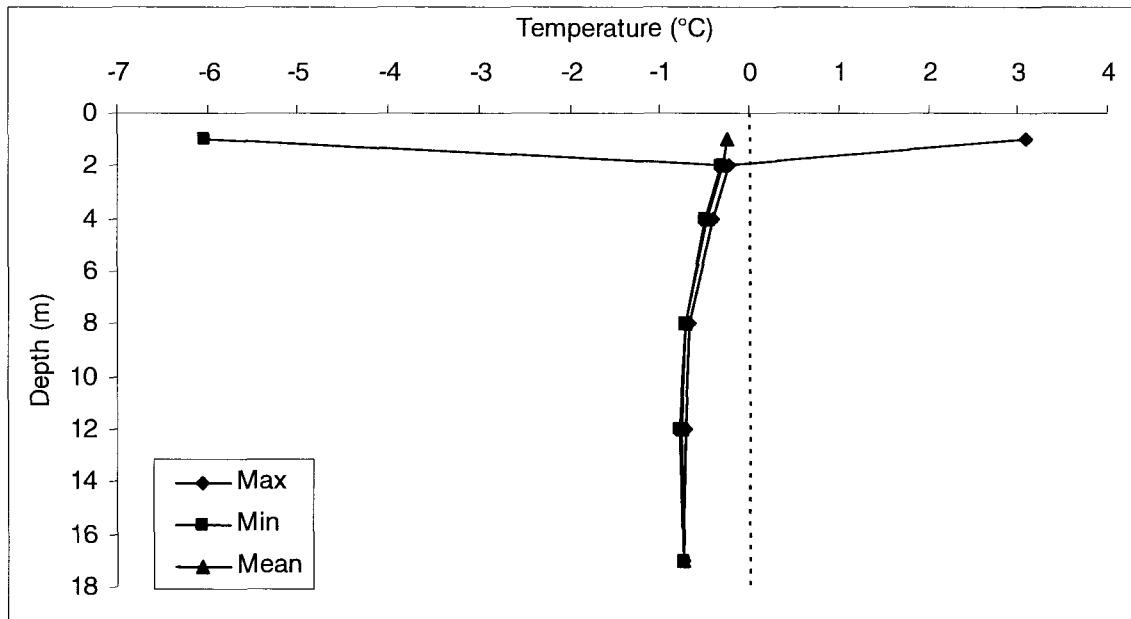


Figure 4.69: Temperature Envelope at Table Mountain, NWT, in 1998-99. The entire thermal profile below 2 m depth remains between -1 and 0°C.

The depth of ZAA at this site is very shallow at just below 2 m. This shallow depth is due to the high amounts of unfrozen moisture present in the ice-rich lacustrine deposits at temperatures very close to 0°C, and the large latent heat effects that accompany this. The thermal profile cools with depth, indicating that warming is occurring from the surface downwards, probably because of changing climatic conditions at the site in recent years. The temperature at 17 m is approximately 0.5°C colder than at

2 m. Warming of the ground temperatures through time occurred in the MAGTs below the depth of ZAA (Fig 4.70). The warming trends at both 2 m and 17 m are statistically significant ($p < 0.001$) because, even though the warming is slight, it has been consistent since the beginning of monitoring.

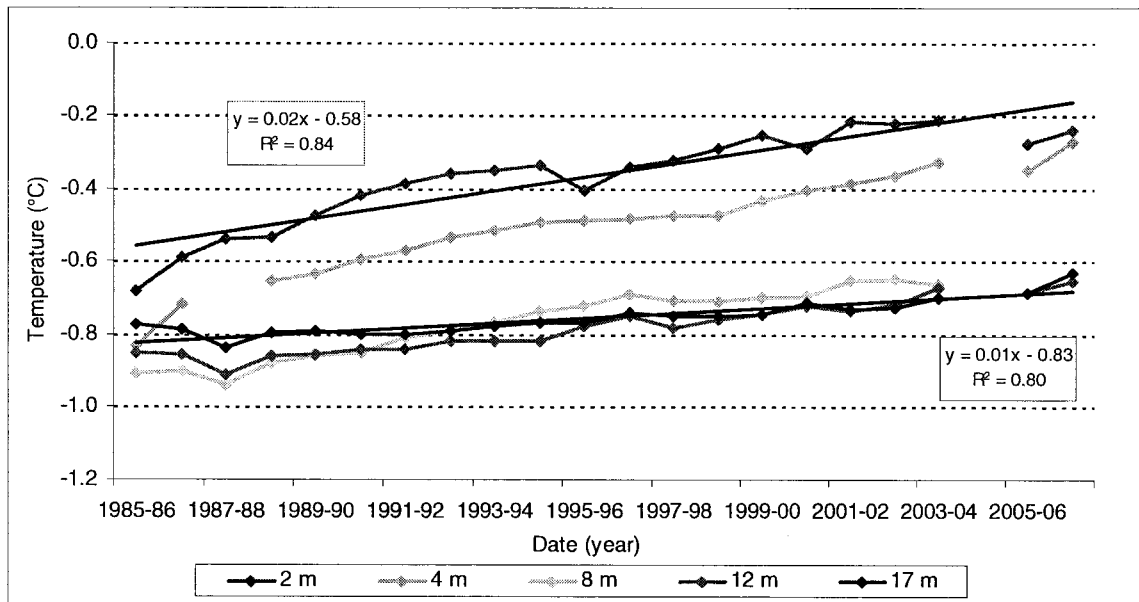


Figure 4.70: MAGTs at Table Mountain, NWT, at all depths below ZAA between 1985 and 2007, showing a gradual warming trend at all depths. The warming at 2 m and 17 m are significant at $p < 0.001$.

The thickness of the permafrost at this site can be estimated using the standard geothermal gradient of 1°C per 30-60 m. In 1988-89 the temperature at 17 m was -0.8°C , and under equilibrium conditions TTOP would be -1.2°C . Therefore, the permafrost at this site should be between 35 and 70 m thick. There are observations that permafrost in the region is probably less than 50 m thick, and a deep hole that was drilled nearby went through the base of permafrost at about 32 m (S. Smith, personal communication, November 2009). Consequently, the shallower value of ~ 35 m is more likely to be correct.

The record of on-site air temperature measurements is not long enough to determine if there was a trend, so temperatures from the Fort Simpson ECCS were utilized. Hind-cast MAATs warmed by about 0.6°C per decade since 1964 (Fig. 4.71; $p < 0.001$). MAAT ranged around -6.5°C at the beginning of the record, and in more recent years it is around -4.0°C.

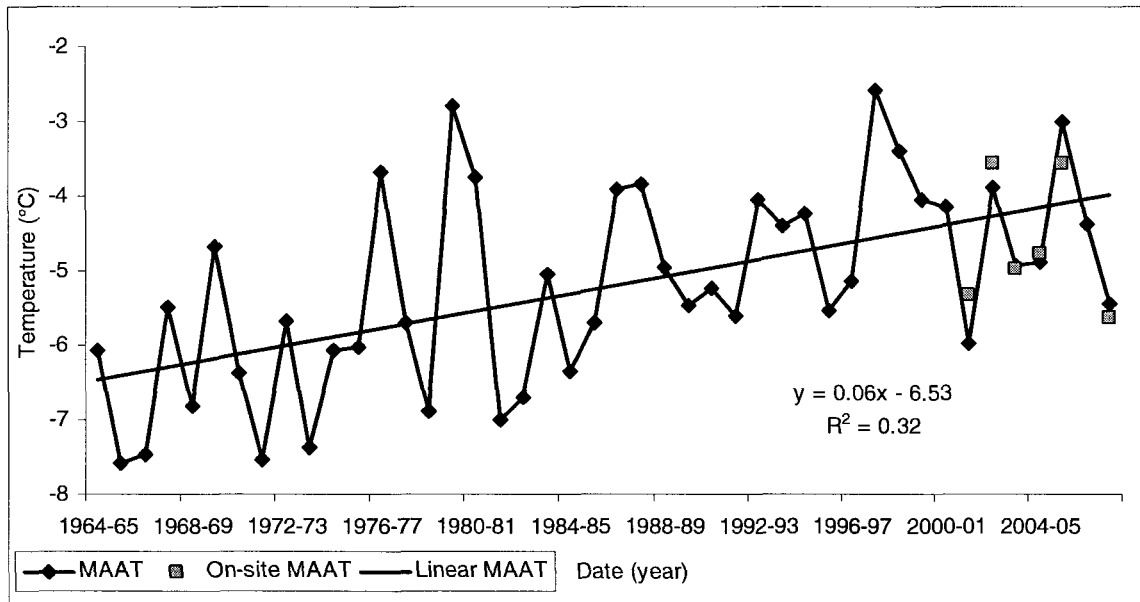


Figure 4.71: MAATs at Table Mountain, NWT, calculated from Fort Simpson ECCS data (Environment Canada, 2009) between 1964 and 2008, and the on-site measured values between 2001 and 2008. The warming trend is significant at $p < 0.001$.

From a seasonal perspective, average winter air temperatures warmed the most since 1964, by about 1.2°C per decade (Fig. 4.72; $p < 0.001$). Spring air temperatures increased by about 0.5°C per decade over the same period, but the trend is not statistically significant. Winter and spring air temperatures are the most variable from year-to-year. Summer air temperatures varied the least of all the seasons, and warmed with significance by 0.3°C per decade ($p < 0.01$; Fig. 4.72). Autumn air temperatures warmed by 0.4°C per decade, but the trend is not statistically significant.

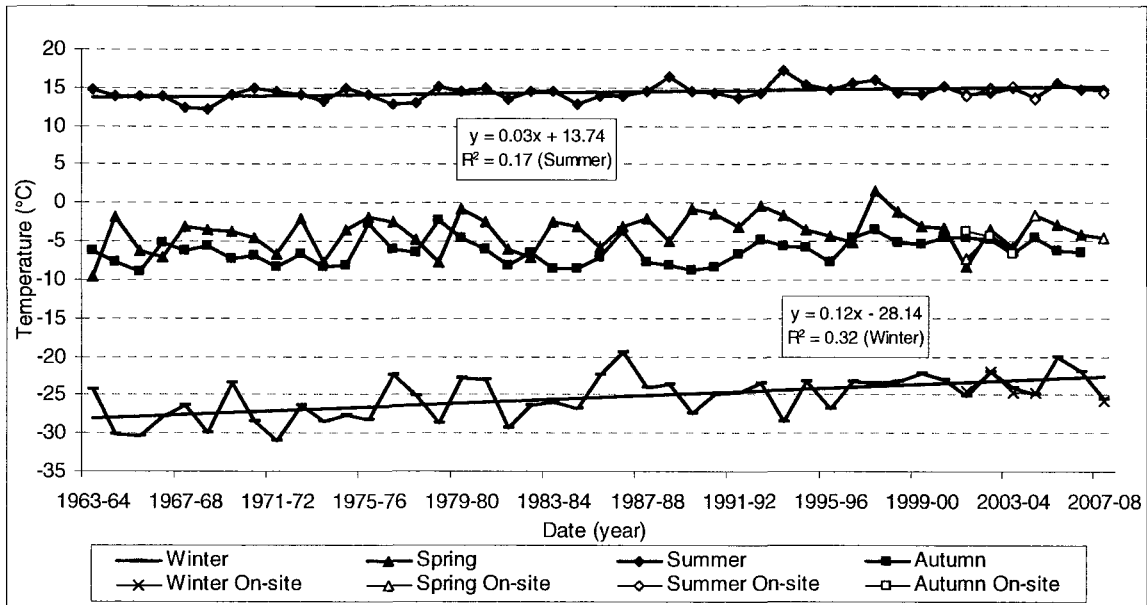


Figure 4.72: Seasonal average air temperatures at Table Mountain, NWT, from correlated Fort Simpson ECCS data (Environment Canada, 2009) between 1963 and 2008, and on-site measured air temperatures from 2001 to 2008. Warming trends in the winter and autumn are significant at $p < 0.001$ and $p < 0.01$, respectively.

4.8 WRIGLEY, NORTHWEST TERRITORIES

The permafrost thermal monitoring site at Wrigley is located at $63^{\circ}15'35''\text{N}$ and $123^{\circ}25'11''\text{W}$ in the extensive discontinuous permafrost zone of the Northwest Territories (Figs. 1.1 and 4.73). This borehole is 20 m deep in a coniferous forest with a few scattered birch trees, and is located to the west of the Norman Wells pipeline, on a flat approach to a north-facing slope at approximately 195 m elevation (Google Earth, 2009). Permafrost here is ice-rich with approximately 50% visible ice content, and the ground is composed of silt and clay. This borehole was drilled in 2001 and was instrumented with an automatic data-logger measuring temperatures down to 16.5 m three times per day. Air and ground surface temperatures were recorded from the date of installation, and a weather station was set up in 2002 adding the collection of snow depth and wind speed data. The length of the records and depths of the thermistors from the

surface are given in Table 4.23. This borehole site is maintained by the Geological Survey of Canada. The closest ECCS is in Fort Simpson at 61°45'N and 121°14'W, approximately 200 km from the borehole site.

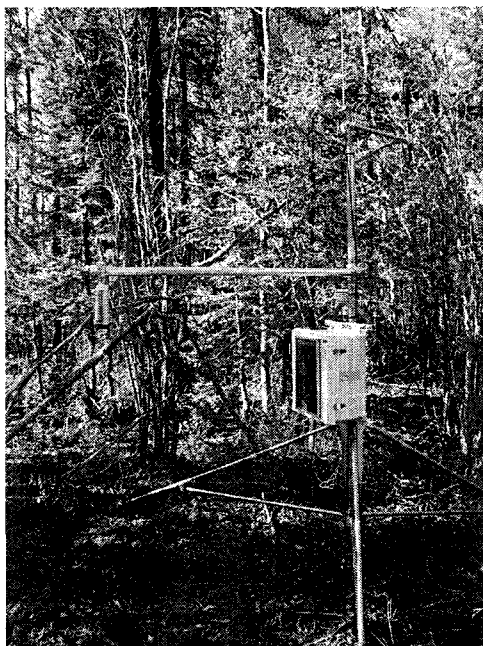


Figure 4.73: Photo of weather station at Wrigley borehole site, taken in August, 2002 (photo is courtesy of the Geological Survey of Canada).

Table 4.23: Summary table of the data used in the analysis of the Wrigley borehole and the depths of the thermistors within the borehole.

Wrigley	
Manual Borehole Data	N/A
Logger Borehole Data	2003-2008
Air Temperature	2001-2008
Ground Surface Temperature	2001-2006, 2007-2008
Snow	2002-2005
Air Temperature (ECCS)	1963-2008
Thermistor Depths (m)	0.5, 1.5, 2.5, 3.5, 5.5, 7.5, 11.5, 16.5

Snow accumulates at this site and persists for the entire winter. The maximum wind speed recorded at the site was 3.8 m/s, and the average between September 2002 and April 2006 was 1.6 m/s, limiting the redistribution of snow. There are three complete years of snow data for this site between 2002 and 2005, and all but the end of the season

in 2006 (Fig. 4.74). In 2002-03 there was the least amount of snow with an average of 25 cm, and the following years had averages of 32 and 44 cm. The maximum snow depth also increased each year from 50 to 66 to 73 cm, and SDD increased from 5113 to 7811 to 9243. Snow accumulated on the ground soon after air temperatures dipped below 0°C, so the ground had little time to cool in response to the decreasing air temperatures prior to this accumulation.

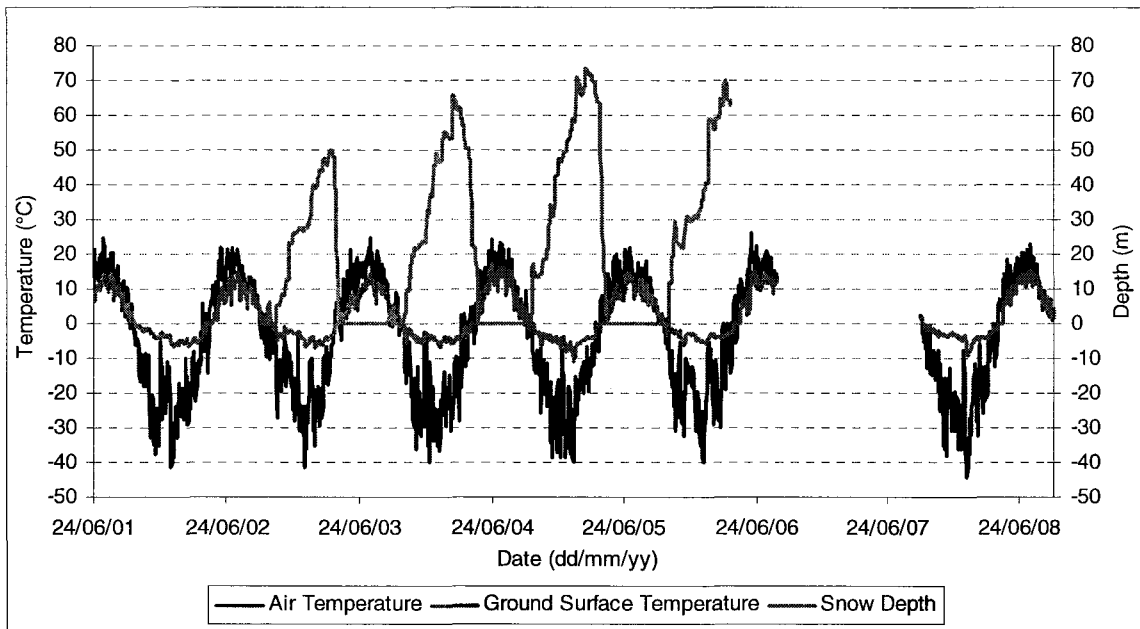


Figure 4.74: Air and ground surface temperatures, and snow depths at Wrigley, NWT, between June 2001 and September 2008. Air temperatures reach much colder temperatures than the ground surface in the winter, likely due to the deep snow that accumulates and persists throughout the winter.

The MAAT ranged between -3.3 and -5.6°C from 2001 to 2008, and the MAGST ranged between 0.8 and 1.7°C, remaining above 0°C for the entire monitoring period (Table 4.24). The surface offset ranged between 4.5 and 7.3°C. The deep snow cover at this site acts as a buffer between the air and the surface during the winter producing ground surface temperatures that are much warmer than those in the air. The inter-annual variability in snow depth and duration contributes to some of the variability in the offset.

In the summer the coniferous trees shade the ground from direct radiation, leaving the air warmer than the surface, but the difference is not great enough to counteract the large temperature differences during the winter.

Table 4.24: Summary table of continuously logged on-site data at Wrigley, including the MAAT, MAGST, surface offset, TOP, TTOP, and the thermal offset.

Date	MAAT (°C)	MAGST (°C)	Surface Offset (°C)	TOP (m)	TTOP (°C)	Thermal Offset (°C)
2001-02	-5.4	1.0	6.4	1.9	-0.4	-1.4
2002-03	-3.3	1.2	4.5	<i>M</i>	<i>M</i>	<i>M</i>
2003-04	-4.8	1.7	6.5	<i>M</i>	<i>M</i>	<i>M</i>
2004-05	-4.7	0.8	5.6	1.6	-0.3	-1.1
2005-06	-3.4	1.7	5.1	1.7	-0.3	-2.0
2006-07	-4.2	<i>M</i>	<i>M</i>	1.9	-0.3	<i>M</i>
2007-08	-5.6	1.7	7.3	1.9	-0.2	-1.9

Missing data is represented by *M*.

FDD of the air ranged between 2999 and 3798, and that of the ground surface ranged between 656 and 854 (Table 4.25). The inter-annual variability is almost the same, in relative terms, between the ground surface and the air. Values of n_f are low, ranging between 0.19 and 0.26, and are a result of the deep snowpack.

Table 4.25: Summary table of on-site data at Wrigley, including FDD_a, FDD_s, TDD_a, TDD_s, SDD, n_f and n_t .

Year	FDD _a	FDD _s	n_f	SDD	Year	TDD _a	TDD _s	n_t
2001-02	3661	744	0.20	<i>M</i>	2001	<i>M</i>	<i>M</i>	<i>M</i>
2002-03	2999	665	0.22	5112	2002	1622	1051	0.65
2003-04	3521	738	0.21	7812	2003	1861	1140	0.61
2004-05	3347	854	0.26	9243	2004	1673	1282	0.77
2005-06	3146	656	0.21	<i>M</i>	2005	1694	1252	0.74
2006-07	<i>M</i>	<i>M</i>	<i>M</i>	<i>M</i>	2006	<i>M</i>	<i>M</i>	<i>M</i>
2007-08	3798	725	0.19	<i>M</i>	2007	<i>M</i>	<i>M</i>	<i>M</i>
CV	0.09	0.10	0.11	0.28	CV	0.06	0.09	0.11

The coefficient of variation (CV) is presented to show the relative variability over the monitoring period. Missing data is represented by *M*.

TDD of the air ranged between 1622 and 1861, and that of the ground surface ranged between 1051 and 1282 (Table 4.25). The TDD of the air were highest in 2003, yet this is not reflected in the ground surface TDD of the same year, indicating that there

must be other factors affecting the ground surface during the thaw season, possibly soil moisture or shading from vegetation. Values of n_t ranged between 0.61 and 0.77.

TTOP at Wrigley had little inter-annual variation, and ranged between -0.2 and -0.4°C between 2001 and 2008 (Table 4.24). TOP varied from 1.9 to 2.4 m over the same period. The thermal offset ranged between -1.1 and -1.9°C, and the slight variations were due to differences in MAGST from year-to-year, since TTOP varied very little.

The zero-curtain effect is prominent in the spring and lasts between 2 and 3 weeks, beginning about 4-6 days after the start of snow melt, and ending abruptly once the snow has melted completely. The zero-curtain in autumn is variable from year-to-year, in some years being absent, and in others lasting for 2 to 3 weeks. This is likely due to a combination of the timing of air temperatures dropping below 0°C and snow accumulating on the ground, and the soil moisture content.

The apparent thermal diffusivity within the active layer, between 0.5 and 1.5 m, is approximately $2.9 \times 10^{-8} \text{ m}^2\text{s}^{-1}$. This low value limits the propagation of the surface temperature wave, and is due to the presence of large quantities unfrozen moisture. The temperature wave at 0.5 m depth would take about 115 days to reach 1.5 m.

The entire MAGT profile within the permafrost at Wrigley is within 1 degree of 0°C (Fig. 4.75) and it cools with depth, indicating that it is in the process of warming, and is not in equilibrium with the current climate. The MAGT at 16.5 m depth was at least 0.3°C colder than at 3.5 m over the monitoring period. Large amounts of unfrozen moisture are present at this site due to its warm temperatures and fine-grained soils. This unfrozen moisture limits the reaction that the ground has to climate change due to required changes in latent heat. This site is not a sensitive indicator of climate change at

present as large amounts of energy would be required to thaw the soil in order to warm the entire profile above 0°C.

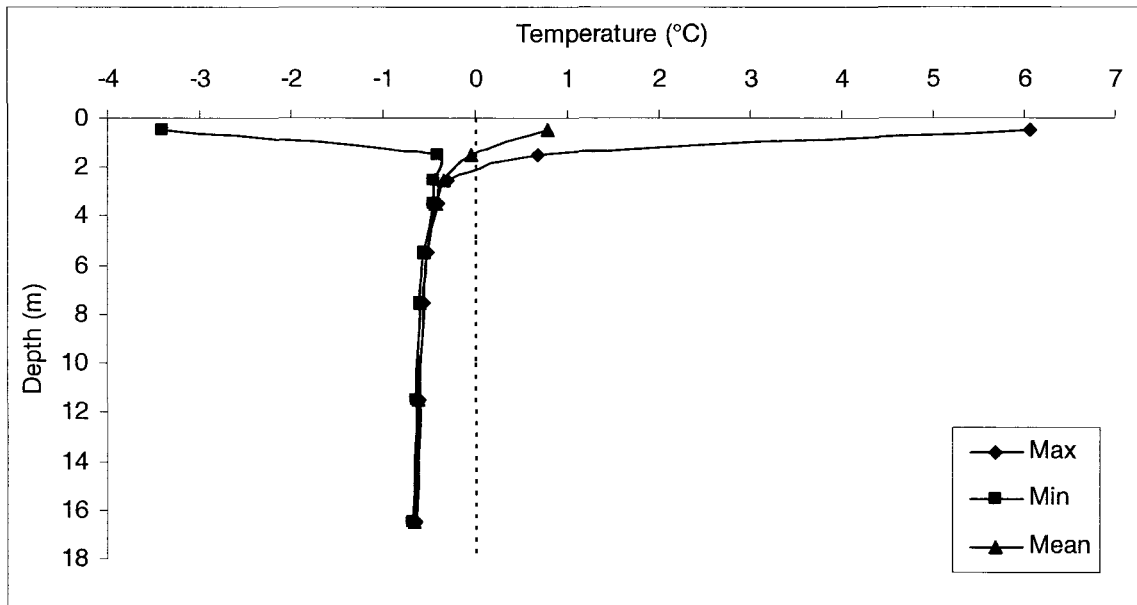


Figure 4.75: Temperature envelope at Wrigley, NWT, for 2005-06. Data shows shallow depth of ZAA and warm temperatures lying between 0 and -1°C throughout the profile below this depth. A curve toward warmer temperatures near the surface is evident.

The temperature at 16.5 m is -0.6°C, which was used to calculate that under equilibrium conditions the temperature at 1.5 m would be -1.2°C. However due to climate warming, it has averaged -0.3°C. If the temperature at TTOP were -1.2°C in the past, the thickness of the permafrost at this site would be 35 to 70 m.

Ground surface temperatures range annually by about 24.6°C, which diminished to about 9.4°C at 0.5 m, 1.4°C at 1.5 m, and 0.15°C at 2.5 m depth. The depth of ZAA is at approximately 2.6 m, which is significantly shallower than typical ZAA depths of 10-20 m (Williams and Smith, 1989; Gruber et al., 2004; Isaksen et al., 2007). The depth of ZAA is just below the base of the active layer. This shows the impact that unfrozen moisture at temperatures close to 0°C has on the propagation of surface temperatures.

Over the five years of monitoring, maximum ground temperatures in the summer reached slightly higher temperature values each year at 0.5 and 1.5 m depth. In addition, the MAGT at 2.5 m showed a warming trend of 0.3°C per decade, and the MAGT at 3.5 m showed a warming trend of 0.2°C per decade; both of these trends are statistically significant (Fig. 4.76; $p < 0.01$ and $p < 0.05$, respectively).

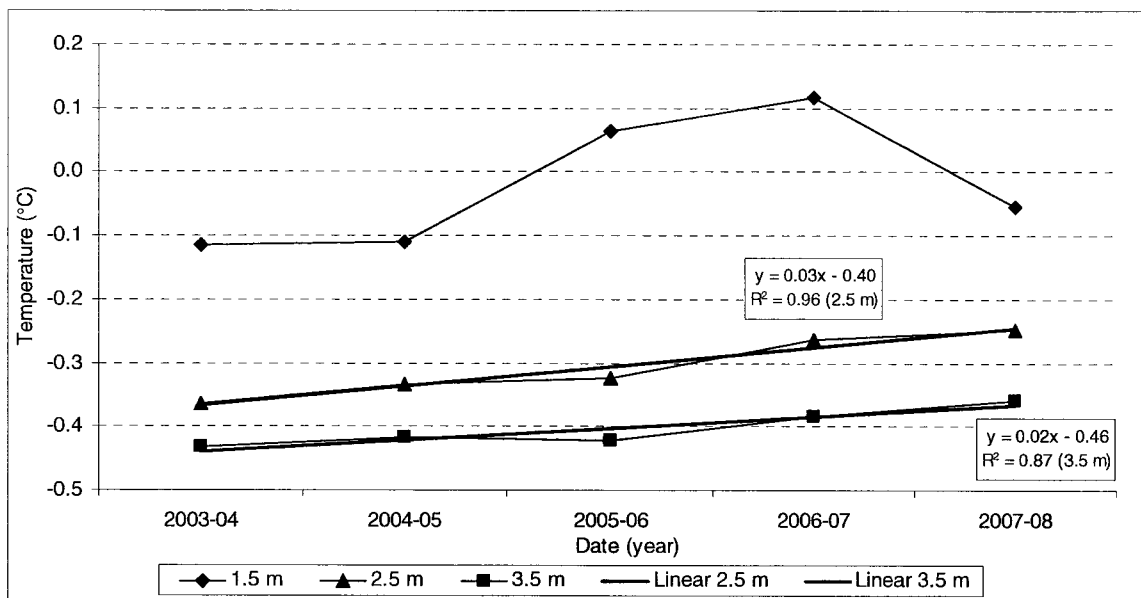


Figure 4.76: MAGTs at 1.5, 2.5, and 3.5 m depth at Wrigley, NWT, between 2003 and 2008. The warming trends at 2.5 and 3.5 m are significant at $p < 0.01$ and $p < 0.05$, respectively.

A supra-permafrost talik may form during the coming years due to warming from the surface, as indicated by the curve toward warmer temperatures at the top of the profile (Fig. 4.75). The ground at this site is very resistant to temperature changes due to high latent heat effects from frozen and unfrozen moisture, and it will take a significant amount of time to warm the deeper ground layers.

The six years of on-site air temperature monitoring do not give an indication of warming since the record is too short. The MAAT record was hind-cast using the Fort Simpson Environment Canada Climate Station data (Environment Canada, 2009). The

regional climate has warmed linearly since the beginning of the climate record in 1964, and the trend is statistically significant ($p < 0.001$; Fig. 4.77). At the beginning of the record the MAAT fluctuated around -6.5°C , whereas in more recent years it fluctuates around -4.0°C , i.e. an increase of about 2.5°C over the past 40 years, or 0.6°C per decade. The air temperature trends at this site are similar to those at Table Mountain since both hind-cast sets of values are based on the Fort Simpson ECCS.

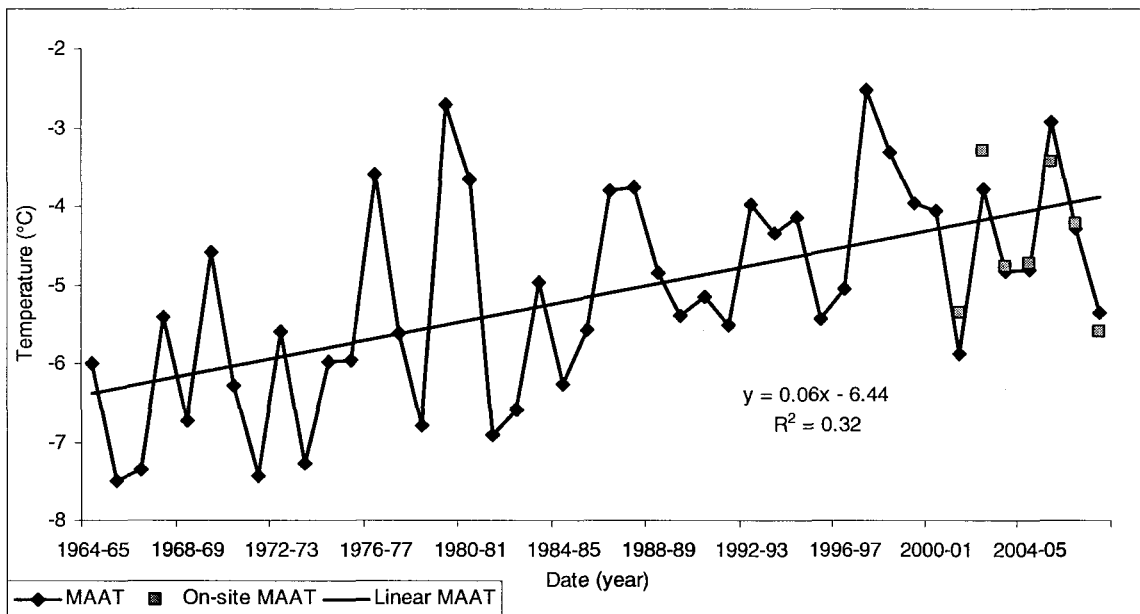


Figure 4.77: MAAT at Wrigley, NWT, hind-cast from Fort Simpson ECCS (Environment Canada, 2009), between 1964 and 2008, showing a warming trend over the period. On-site measured MAAT have been plotted for 2001-2008 to show the accuracy of the method. The warming trend is significant at $p < 0.001$.

From a seasonal perspective, winter air temperatures are the most inter-annually variable and have warmed the most. The warming trend is statistically significant ($p < 0.001$) at a rate of 1.2°C per decade, with an overall warming of about 5°C since 1963 (Fig. 4.78). Summer air temperatures are the least variable inter-annually, and have also shown a statistically significant ($p < 0.01$) warming trend of 0.3°C per decade (Fig. 4.78). Spring and autumn air temperatures are slightly less variable from year-to-year

than winter, and have also warmed. Spring air temperatures warmed by 0.4°C per decade, and autumn warmed by 0.3°C per decade, but neither of these trends are statistically significant.

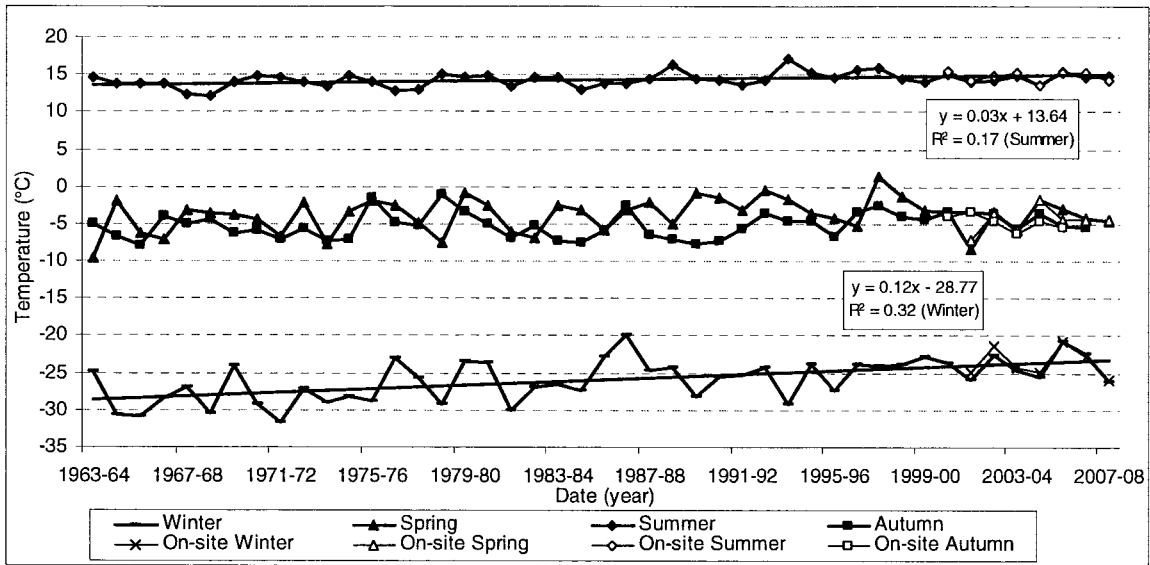
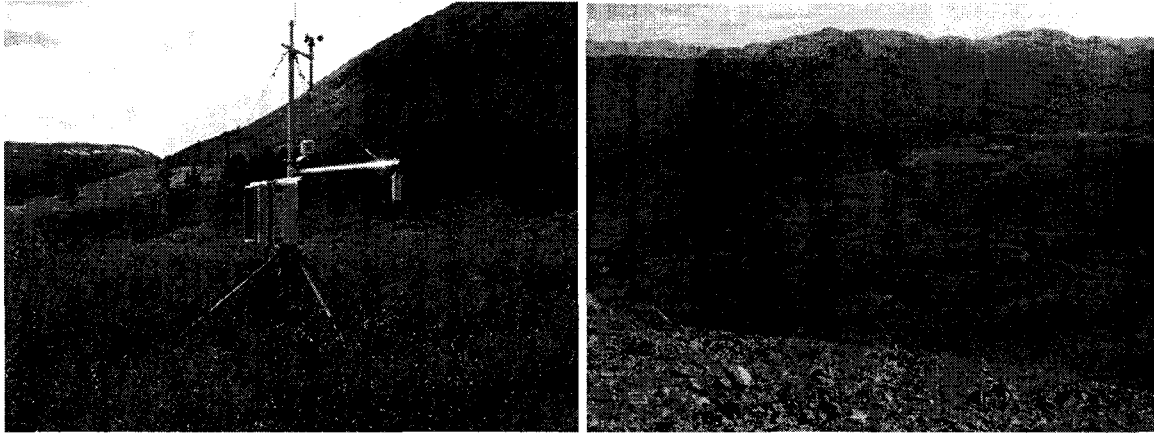


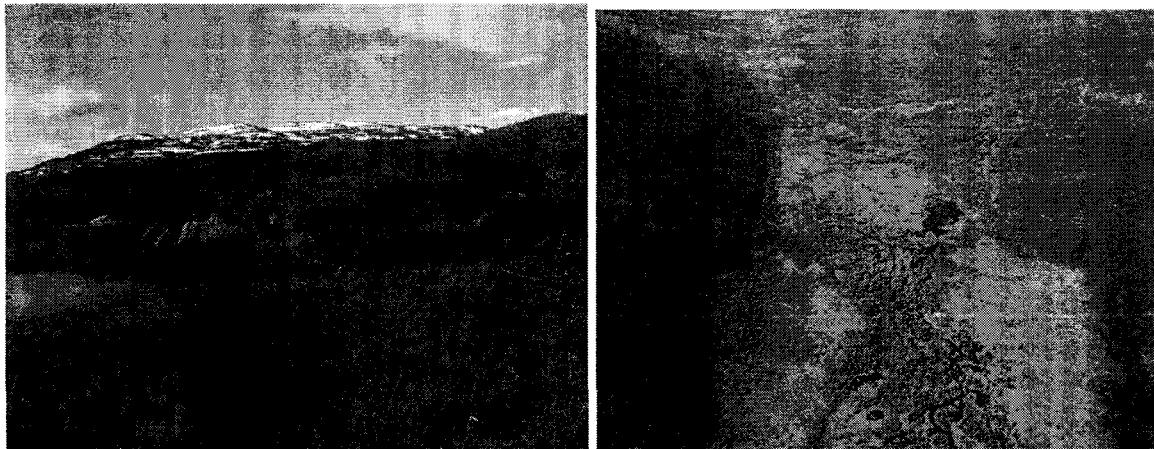
Figure 4.78: Seasonal average air temperatures at Wrigley, NWT, from correlated Fort Simpson ECCS data (Environment Canada, 2009) from 1963 to 2008, and on-site seasonal averages between 2001 and 2008. The warming trends in winter and summer were significant at $p < 0.001$ and $p < 0.01$, respectively.

4.9 WOLF CREEK, YUKON

Two permafrost thermal monitoring sites are located in the Wolf Creek basin southwest of Whitehorse in the sporadic discontinuous permafrost zone of the Yukon Territory (Fig. 1.1). Both were water-jet drilled in 2004. The first at Wolf Creek is the Aggradational Permafrost Mound (APM) site, located at 60°28'N and 135°11'W (Fig. 4.79), and the second is Palsa 25, located at 60°29'N and 135°13'W (Fig. 4.80). The closest ECCS is in Whitehorse at 60°42'N and 135°4'W, at an elevation of 706 m.



A **B**
 Figure 4.79: Photographs of the Wolf Creek Aggradational Permafrost Mound (APM) borehole site. Photo A is a view of weather station from the ground level, and B, is a view of the thermokarst valley where the borehole is located (red circle) (photos are courtesy of A.G. Lewkowicz, 2007).



A **B**
 Figure 4.80: Photographs of Wolf Creek Palsa 25 borehole site. Photo A is of Palsa 25 from the ground, the borehole is located a little to the left of the centre of the palsa, and B is of the fen and palsa valley from the air (photos are courtesy of A.G. Lewkowicz, 2006).

The APM site is on a valley floor with numerous other aggradational mounds interspersed with thermokarst lakes. The borehole reaches a depth of 15.3 m and a weather station was set up adjacent to it. There is a gap in the weather station data from 2006-07 when the logger failed. The Palsa 25 borehole is 6.85 m deep and goes through a 2 m high palsa located in a fen in the bottom of a valley. Snow depths and ground surface temperatures are monitored at Palsa 25, and air temperature is recorded on a palsa

approximately 500 m to the north. The length of the records and depths of the thermistors from the surface are given in Table 4.26. Both of these boreholes are instrumented with automatic data loggers recording three times per day. The vegetation at both sites is classified as alpine shrub tundra.

Table 4.26: Summary table of the data used in the analysis of the Wolf Creek boreholes and the depths of the thermistors.

Wolf Creek	Aggradational Permafrost Mound	Palsa 25
Manual Borehole Data	N/A	N/A
Logger Borehole Data	2004-05, 2006-08	2004-2008
Air Temperature	2004-2008	2001-2008
Ground Surface Temperature	2005-2008	2004-2008
25 cm	2005-2008	N/A
Snow	2004-06, 2007-08	2006-2008
Air Temperature (ECCS)	N/A	N/A
Thermistor Depths (m)	0.3, 0.8, 1.8, 3.8, 6.8, 9.8, 15.3	0.5, 1, 1.5, 2, 3, 3.9, 5, 6.9

4.9.1 Wolf Creek Aggradational Permafrost Mound

The vegetation at the APM site is approximately 1 m high, allowing snow to be trapped during winter. There are three years of snow data at this site between 2004 and 2008 (Fig. 4.81). SDD ranged between 2739 and 8609 (Table 4.27), average snow depths ranged between 8 and 24 cm, and the maximum snow depth ranged between 34 and 65 cm. The snow characteristics at this site appear to have high inter-annual variability.

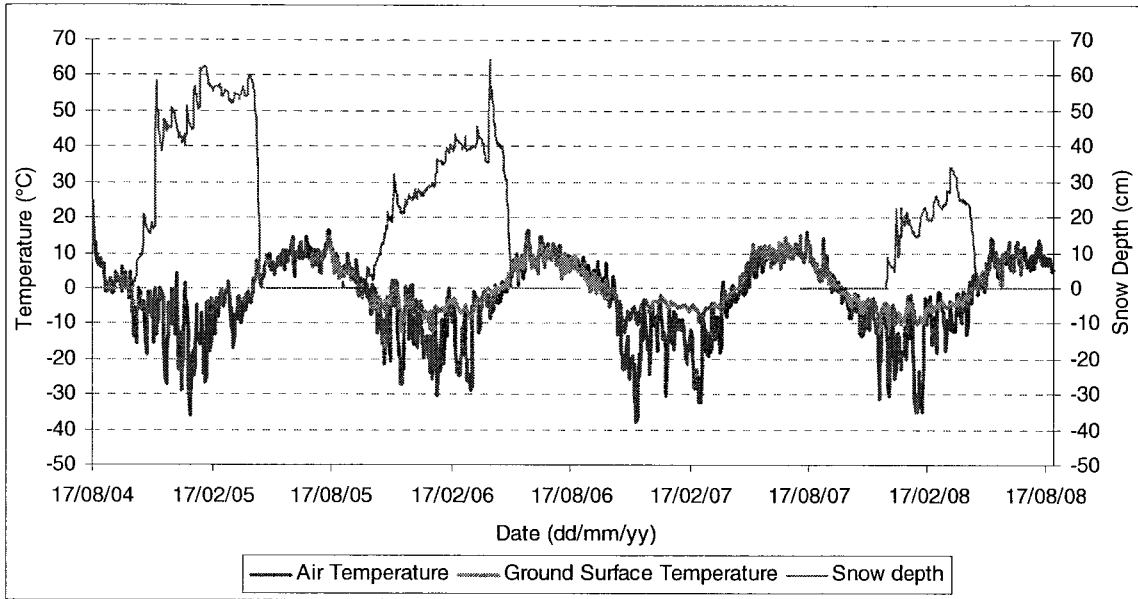


Figure 4.81: Air and ground surface temperatures with snow depths at the Wolf Creek APM site between August 2004 and August 2008.

Table 4.27: Summary table of on-site data at Wolf Creek APM, including FDD_a, FDD_s, TDD_a, TDD_s, SDD, n_f and n_t.

Year	FDD _a	FDD _s	n _f	SDD	Year	TDD _a	TDD _s	n _t
2004-05	<i>M</i>	<i>M</i>	<i>M</i>	8609	2004	<i>M</i>	<i>M</i>	<i>M</i>
2005-06	2085	928	0.45	6618	2005	<i>M</i>	<i>M</i>	<i>M</i>
2006-07	2604	996	0.38	<i>M</i>	2006	1010.9	941.4	0.93
2007-08	2204	1083	0.49	2739	2007	1052.2	1161.3	1.10
CV	0.12	0.08	0.13	0.50	CV	0.03	0.15	0.12

The coefficient of variation (CV) is presented to show the relative variability over the monitoring period. Missing data is represented by *M*.

The MAAT ranged from -1.4 to -4.3°C, and the MAGST ranged from 0 to 0.4°C between 2004 and 2008 (Table 4.28). The MAGST remained above 0°C each year, yet permafrost exists due to the large amounts of frozen and unfrozen moisture present at this site. The surface offset ranged between 3.0 and 4.7°C.

Table 4.28: Summary table of continuously logged on-site data at Wolf Creek APM, including the MAAT, MAGST, surface offset, TOP, TTOP, and the thermal offset.

Date	MAAT (°C)	MAGST (°C)	Surface Offset (°C)	TOP (m)	TTOP (°C)	Thermal Offset (°C)
2004-05	-1.4	<i>M</i>	<i>M</i>	<i>M</i>	<i>M</i>	<i>M</i>
2005-06	-2.9	0.1	3.0	<i>M</i>	<i>M</i>	<i>M</i>
2006-07	-4.3	0.4	4.7	<i>M</i>	<i>M</i>	<i>M</i>
2007-08	-3.5	0.0	3.5	1.7	-0.7	-0.7

Missing data is represented by *M*.

FDD of the air ranged between 2085 and 2604, and that of the ground surface ranged between 928 and 1082 (Table 4.27). Values of n_f ranged between 0.38 and 0.49. The highest value for n_f occurred during 2007-08, the year with the least amount of snow on record. TDD were calculated for 2 years, 2006 and 2007, and the values for the air were 1011 and 1052, and for the ground surface they were 941 and 1161. Values of n_t were 0.9 and 1.1 for those two thaw seasons.

TOP was interpolated at 1.7 m, and TTOP was -0.7°C in the 2007-08 year, resulting in a thermal offset of -0.7°C (Table 4.28). The permafrost at this site is warm with a MAGST of 0°C or warmer each year. The apparent thermal diffusivity is at its lowest within the active layer with an average of $2.3 \times 10^{-8} \text{ m}^2\text{s}^{-1}$, compared to an average of $3.5 \times 10^{-7} \text{ m}^2\text{s}^{-1}$ within the permafrost. The temperature wave at 0.3 m would take about 120 days to reach TOP. The low apparent thermal diffusivity and extended phase lags are due to the high latent heat effects that result from warm temperatures and high volumes of frozen and unfrozen moisture.

A zero-curtain at the ground surface is observed during thaw in the spring, but is not evident during freeze-back in autumn. It tends to last between one to two weeks near the end of April and beginning of May. The soil surface at the borehole is usually dry in the summer, explaining the lack of zero-curtain effect in autumn, and the high

temperatures reached at the ground surface during summer. There is, however, a strong zero-curtain effect observed at 0.25 m depth from the ground temperature sensor a few meters from the borehole, and lasts between one and two months in both autumn and spring (Fig. 4.82).

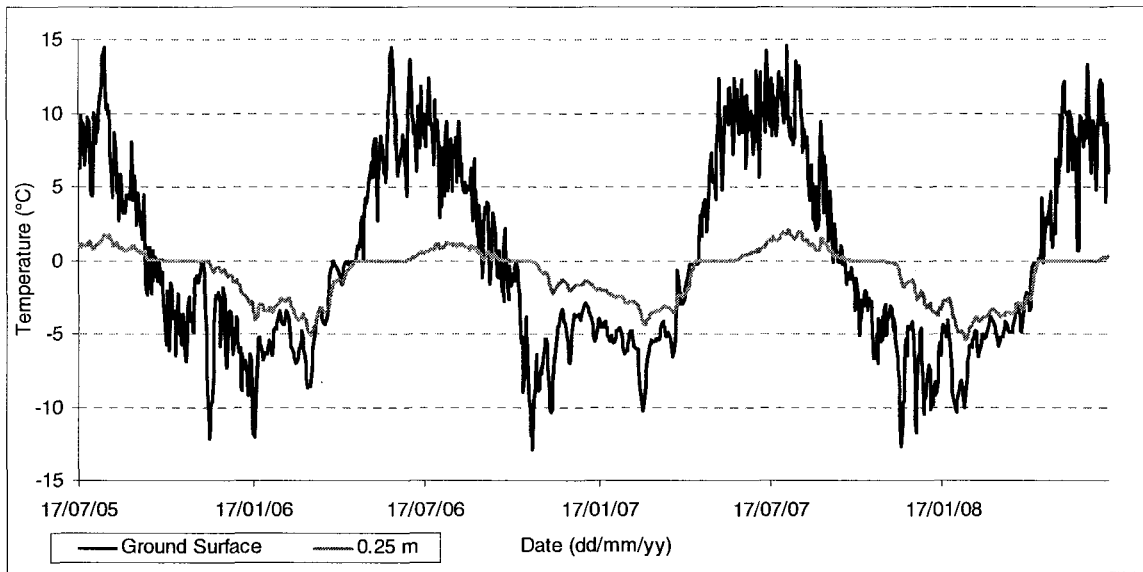


Figure 4.82: Ground surface and 25 cm temperature trends at Wolf Creek APM site, between July 2005 and July 2008. The graph shows a more pronounced zero-curtain effect at 25 cm than at the surface.

The temperature envelope at this site shows the effects of high volumes of frozen and unfrozen moisture (Fig. 4.83). The maximum temperatures at all depths below TTOP remain between 0 and -1°C. The MAGT profile warms very slightly with depth below about 4 m, and above 4 m there is a curve toward warmer temperatures, indicating warming from the surface downwards. The depth of ZAA is at approximately 6.9 m with a mean annual temperature of about -0.5°C. The permafrost at this site would be between 24 and 39 m thick based on the standard geothermal gradient of 1°C/30-60 m.

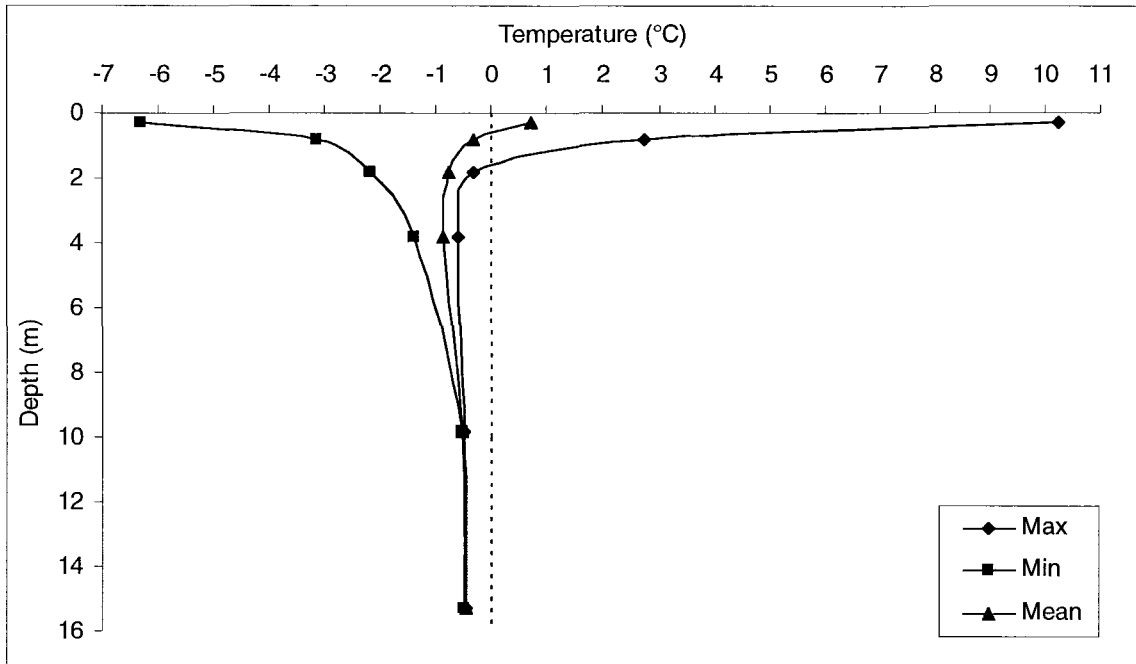


Figure 4.83: Temperature envelope at Wolf Creek APM between June 1, 2007 and May 31, 2008.

4.9.2 Wolf Creek Palsa 25

There are 2 years of snow data at the Palsa 25 site, from 2006 to 2008 (Fig. 4.84). Palsa 25 is elevated from the valley floor and could be prone to wind scouring, but the vegetation reaches approximately 1 m height and, as a result, traps snow. During the 2006-07 winter maximum snow depths reached between 57 and 67 cm, and the following year they reached between 30 and 40 cm. The MAAT of 2006-07 was colder than the following year, but due to the thinner snow pack during 2007-08, the ground surface reached colder temperatures than during the previous winter.

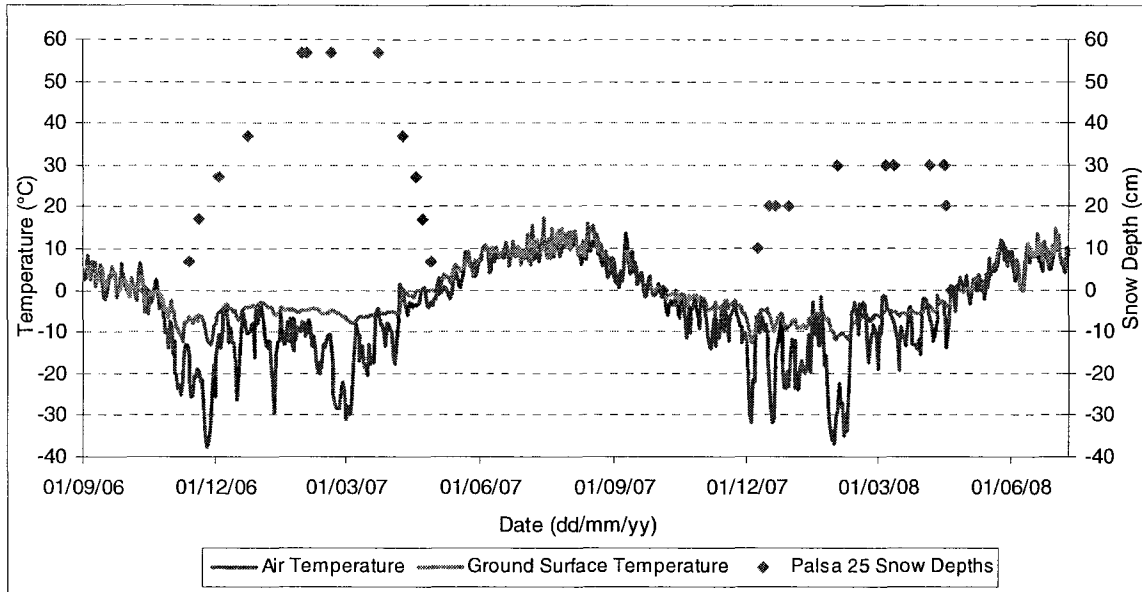


Figure 4.84: Air and ground surface temperatures and snow depths from Palsa 25 in Wolf Creek, Yukon, between September 2006 and July 2008.

The MAAT ranged between -4.2 and -2.0°C from 2001 to 2008 in the palsa valley (Table 4.29). The air temperature record is too short to observe any long term trends. The MAGST ranged between 0.1 and 1.2°C from 2004 to 2008, remaining above 0°C each year. The surface offset for the 4 years of ground surface monitoring ranged between 3.3 and 4.7°C .

Table 4.29: Summary table of continuously logged on-site data at Wolf Creek Palsa 25, including the MAAT, MAGST, surface offset, TOP, TTOP, and the thermal offset.

Date	MAAT ($^{\circ}\text{C}$)	MAGST ($^{\circ}\text{C}$)	Surface Offset ($^{\circ}\text{C}$)	TOP (m)	TTOP ($^{\circ}\text{C}$)	Thermal Offset ($^{\circ}\text{C}$)
2001-02	-4.1	M	M	M	M	M
2002-03	-2.1	M	M	M	M	M
2003-04	-2.0	M	M	M	M	M
2004-05	-2.2	1.2	3.4	M	M	M
2005-06	-3.5	0.2	3.7	1.4	-0.5	-0.7
2006-07	-4.2	0.6	4.8	1.3	-0.7	-1.3
2007-08	-3.7	0.1	3.7	1.3	-0.8	-0.8

Missing data is represented by *M*.

FDD of the air ranged between 1799 and 2524, and that of the ground surface between 574 and 1132 from 2004 to 2008 (Table 4.30). Inter-annual differences in

ground surface FDD are linked to snow conditions. Values of n_f ranged between 0.32 and 0.49, and the highest n_f occurred in the most recent year when snow depths were shallower than 40 cm.

Table 4.30: Summary table of on-site data at Wolf Creek Palsa 25, including FDD_a, FDD_s, TDD_a, TDD_s, SDD, n_f and n_t .

Year	FDD _a	FDD _s	n_f	SDD	Year	TDD _a	TDD _s	n_t
2004-05	1799	574	0.32	<i>M</i>	2005	1080	1082	1.00
2005-06	2227	997	0.45	<i>M</i>	2006	931	1056	1.13
2006-07	2524	977	0.39	6457	2007	992	1200	1.21
2007-08	2291	1132	0.49	3330	2008	<i>M</i>	<i>M</i>	<i>M</i>
CV	0.14	0.26	0.18	0.45	CV	0.07	0.07	0.10

The coefficient of variation (CV) is presented to show the relative variability over the monitoring period. Missing data is represented by *M*.

TDD of the air ranged between 931 and 1080, and that of the ground surface ranged between 1056 and 1200 (Table 4.30). Values of n_t ranged between 1.0 and 1.2 from 2005 to 2008.

There are three years of data for TOP and TTOP between 2005 and 2008 (Table 4.29). During this time TOP varied little, ranging from 1.3 to 1.4 m, and TTOP ranged from -0.5 to -0.8°C. Since MAGST was more variable than TTOP, the thermal offset varied more, from -0.7 to -1.3°C.

The zero-curtain effect within the active layer was more pronounced during autumn than spring (Fig. 4.85). At 0.5 m it lasted up to a maximum of 1 week during spring, and 3 to 6 weeks during autumn. At 1 m, it lasted between 2 and 4 months in autumn. The latent heat effects that cause the zero-curtain to occur also affect the apparent thermal diffusivity within the active layer. The apparent thermal diffusivity is approximately $2.5 \times 10^{-8} \text{ m}^2\text{s}^{-1}$ in the near surface.

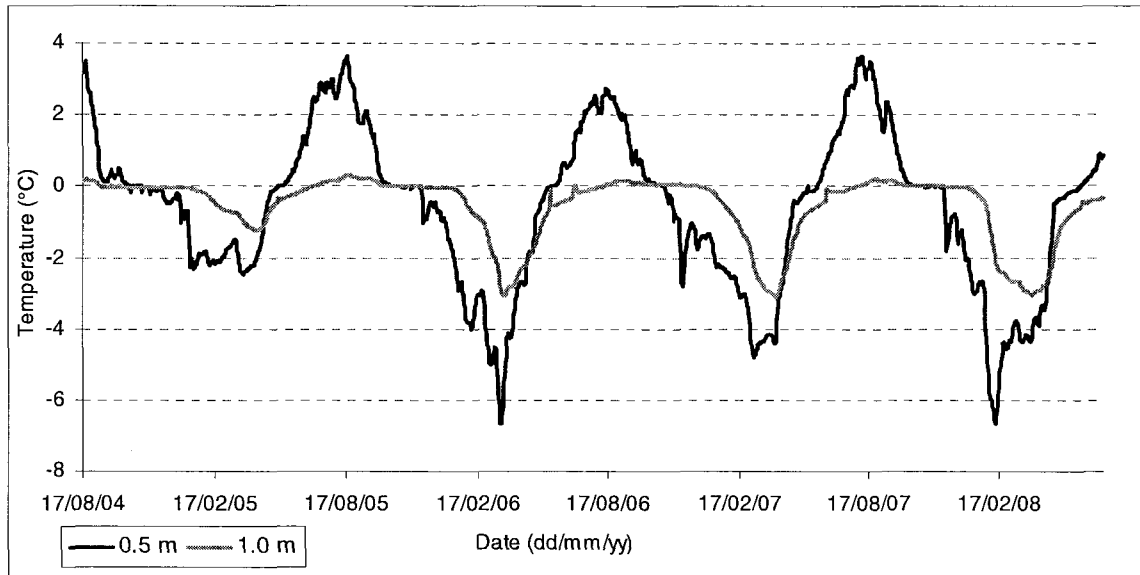


Figure 4.85: Ground temperature trends at 0.5 and 1 m from Palsa 25, Wolf Creek, Yukon Territory. Trends show the differences in the strength of the zero-curtain effect during autumn and spring between 2004 and 2008.

Within the permafrost, the ground warms to just below 0°C and remains there until cooling occurs at the start of the freezing season (Fig. 4.86). This indicates the influence of high amounts of frozen and unfrozen moisture at this site causing significant latent heat effects, preventing the ground from thawing. During the freezing season ground temperatures cool faster than they are able to warm because once re-frozen the conductivity is high and heat can leave the ground more rapidly than when thawed. The MAGT profile at Palsa 25 is within 1°C of 0°C (Fig. 4.87). The thermal profile warms with depth until it reaches the bottom of the permafrost at 6.9 m depth. The amplitude diminishes rapidly and the depth of ZAA is at approximately 4.6 m. This shallow depth is due to large amounts of unfrozen moisture present in fine-grained soils that are very close to 0°C.

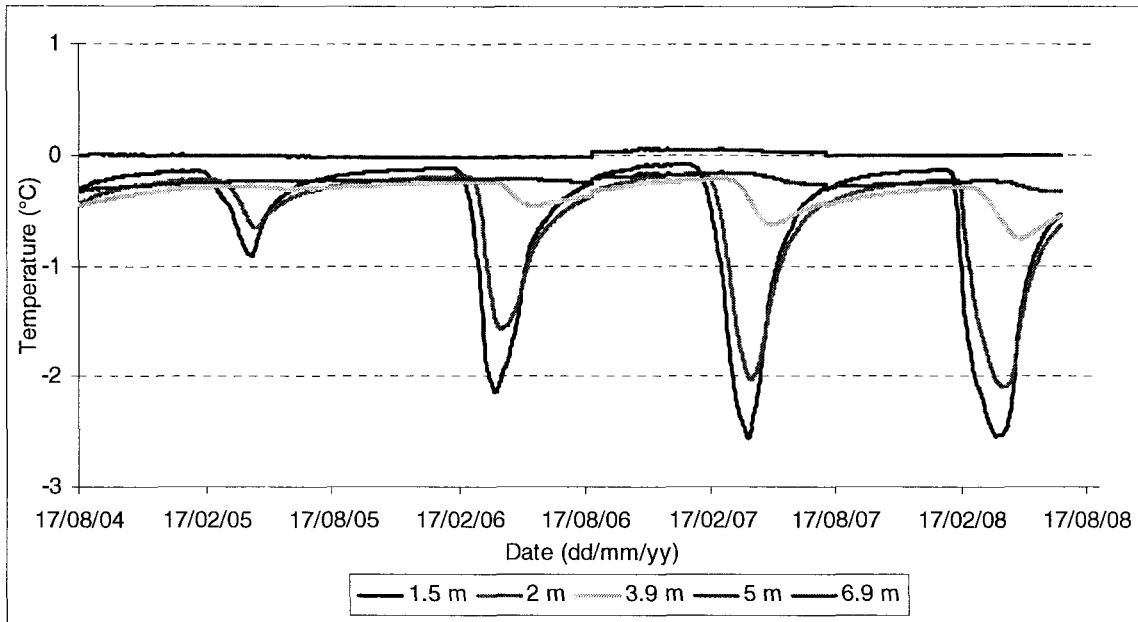


Figure 4.86: Ground temperature time series in borehole at Wolf Creek Palsa 25 below the active layer between August 2004 and July 2008. During the thawing season the ground temperatures warm to just below 0°C, and remain there until cooling occurs during the freezing season. Thawing of the material does not occur due to the high moisture content creating high latent heat requirements.

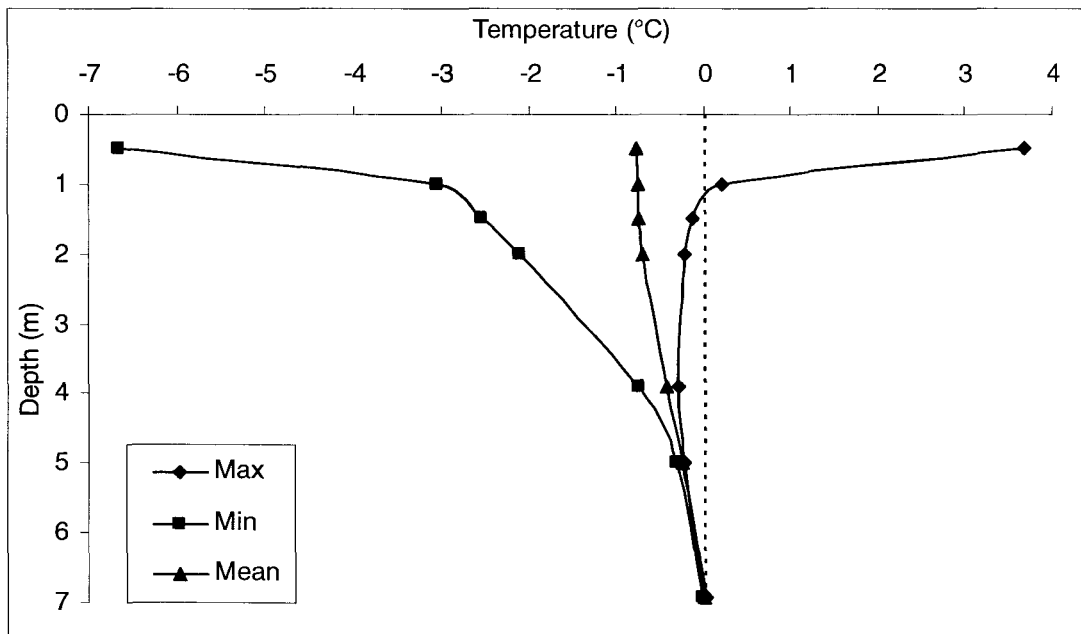


Figure 4.87: Temperature envelope at Palsa 25, Wolf Creek, Yukon, for the year 2007-08. The borehole goes to the base of the permafrost at approximately 6.9 m depth.

5. DISCUSSION

This section will discuss 1) inter-site comparisons in the context of major influences on permafrost, such as air temperatures, the thermal diffusivity, and snow characteristics, and 2) changes in air and permafrost temperatures that have occurred over time. Intra-site comparisons for Alert and Baker Lake were covered in the results sections.

5.1 INTER-SITE COMPARISONS

5.1.1 MAAT

Macroclimate, itself influenced by latitude, is a primary control on determining the presence of permafrost and its characteristics (Smith and Riseborough, 2002). In general, colder MAATs result in colder permafrost temperatures (Table 5.1; Fig. 5.1). Fig. 5.1 shows the strong relationship between MAATs and MAGTs across the range sites in this study. The relationship has an r^2 value of 0.96, and is significant at $p < 0.001$. The strength of this relationship illustrates the influence of macroclimate on permafrost conditions.

Table 5.1: Table of average values of MAAT, MAGST, and MAGT over the monitoring period at all sites, the depth that the MAGT represents, and if the permafrost is considered cold (C) or warm (W).

Thermal Monitoring Site	Cold vs. Warm	MAAT (°C)	MAGST (°C)	MAGT* (°C)	Depth (m)
Alert BH3 (A3)	C	-16.0	-12.5	-14.6	14.6
Alert BH4 (A4)	C	-16.5	-14.5	-15.1	9.1
Alert BH5 (A5)	C	-15.4	-14.3	-14.9	15.2
Iqaluit (IQ)	C	-7.8	-5.6	-7.2	5.0
Baker Lake BH4 (BL4)	C	-10.3	-7.2	-7.6	3.0
Sixty Mile (SM)	C	-6.1	-4.1	-3.5	23.0
Red Creek (RC)	C	<i>M</i>	-1.3	-2.3	7.0
Alpine Burwash (AB)	C	-4.4	-3.6	-2.0	32.6
Table Mountain (TM)	W	-4.2	1.1	-0.8	12.0
Wrigley (W)	W	-4.5	1.4	-0.7	16.5
Wolf Creek APM (WC APM)	W	-3.0	0.2	-0.4	15.3
Wolf Creek Palsa 25 (WC P25)	W	-3.1	0.5	-0.2	5.0

*The MAGT represents conditions below ZAA when possible, and if the borehole is too shallow, it represents the MAGT at the deepest sensor in the borehole. Missing data is represented using *M*.

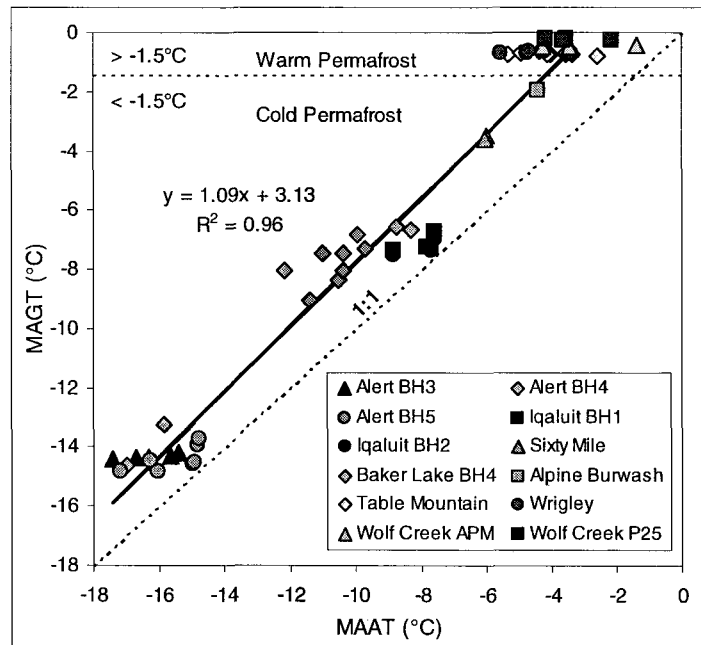


Figure 5.1: Relationship between MAGTs and MAATs from all of the boreholes, with the exception of Red Creek due to missing air temperature data and Baker Lake BH2 where snow conditions are anthropogenically affected. MAAT is the primary determinant of the permafrost temperature. Warm permafrost sites have MAGTs between 0 and -1.5°C, and cold permafrost sites are those that are below -1.5°C. This correlation is significant at $p < 0.001$.

MAGTs at Alert BH5 and the Iqaluit boreholes have the closest relation to MAAT, as illustrated in Fig. 5.1 where they lie very close to the 1:1 line. Fig. 5.1 also shows that on average, the differences between MAAT and MAGT increase with warmer MAATs. The MAAT to MAGT relation in this study differs when compared to the findings of Burgess and Smith (2000) at boreholes in the Mackenzie Valley, although their study sites encompass a smaller and warmer range of temperatures. In their study the relation between MAAT and MAGT was weaker, which correlated with an r^2 value of 0.44, the differences between values were greater, and the warmer the MAAT, the smaller the difference between MAAT and MAGT. The differing results are likely due to the greater range in MAATs explored in the current study and the important influence on the best-fit line of low snow accumulation at the Alert sites.

The presumption, made by Riseborough and Smith (1998), that the higher the MAAT the greater the thaw depth is generally true (CALM, 2009), although many characteristics of the ground in the discontinuous zone, such as high ice content or a thick peat layer at the surface, may maintain shallow thaw depths at sites where air temperatures are warm. Smith et al. (2009) found that thaw depth variability between sites was high due to variations in organic cover and moisture contents. The data from this research show that thaw depths increase as MAATs increase at bedrock sites, but not in the sediment sites (Fig. 5.2). There is a significant correlation between thaw depths and MAAT at the bedrock sites with an r^2 value of 0.84 ($p < 0.01$; Fig. 5.2).

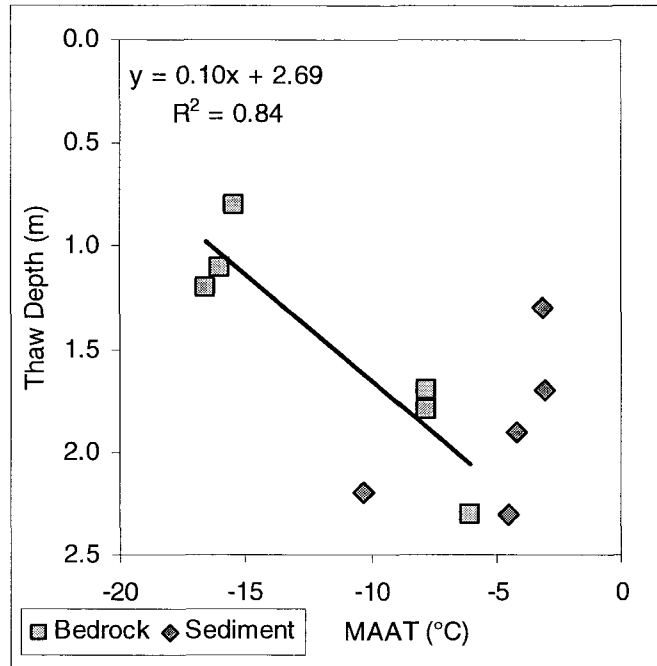


Figure 5.2: Relationship between average MAAT with thaw depth at both the bedrock and sediment sites. The linear relation is significant ($p < 0.01$) for bedrock (shown on graph), but not for the sediment sites.

5.1.2 MAGT

For the purpose of this work, cold permafrost is classified as having MAGTs below -1.5°C , and warm permafrost is classified as having MAGTs warmer than -1.5°C , but remaining below 0°C (Wu et al., 2002). This threshold was selected based on the likelihood of large amounts of unfrozen moisture being present in the ground which may occur at temperatures above -1.5°C . The differentiation between the two types of permafrost is important because they will respond differently to changes in surface conditions. Warm permafrost is influenced thermally by annual changes in unfrozen moisture, is more susceptible to thaw, and is usually within the discontinuous permafrost zone (Fig. 2 in Smith et al., submitted 2010), but can occasionally be located in the continuous zone where it is newly aggraded, or in areas of flooding or high snow cover.

Cold permafrost, on the other hand, tends to have little or no unfrozen moisture, requires very long term climatic change to thaw, and is usually within the continuous permafrost zone, but does occasionally extend into the discontinuous zone (Fig. 2 in Smith et al., submitted 2010). However, ground temperatures at cold permafrost sites are more responsive to changes in climate due to minimal amounts of unfrozen moisture.

Four of the ground thermal monitoring sites in this thesis are considered 'warm' permafrost: Wrigley, Table Mountain, and the two Wolf Creek boreholes, the APM and Palsa 25 (Table 5.1 and Fig. 5.1). MAGTs at these sites are all warmer than -1°C , and MAGSTs are above 0°C (Table 5.1). Wrigley and Table Mountain are within the extensive discontinuous permafrost zone and the Wolf Creek sites lie within the sporadic discontinuous permafrost zone (Fig. 1.1).

The other six thermal monitoring sites are considered 'cold' permafrost (Table 5.1; Fig. 5.1), although the temperatures in the ground and the site characteristics are far more varied than at the warm permafrost sites. The warmest of the 'cold' permafrost sites is Alpine Burwash, an alpine site in the discontinuous permafrost zone of the Western Yukon, with ground temperatures of about -2.0°C . The coldest is Alert BH2, a coastal site (though further from the coast than BH1) on the northernmost tip of Ellesmere Island in the continuous permafrost zone, with ground temperatures of approximately -15.4°C . All but two of the cold permafrost sites are within the continuous permafrost zone, the exceptions being Alpine Burwash and Sixty Mile, which are both high elevation alpine sites nominally in the sporadic and extensive discontinuous permafrost zones, respectively.

5.1.3 Apparent Thermal Diffusivity

The apparent thermal diffusivity calculated for the warm and cold permafrost sites differs by at least one order of magnitude: values are greater at colder permafrost sites due to higher thermal conductivities where moisture is absent or frozen, and where there is a lack of latent heat effects from phase change (Table 5.2; Fig. 5.3). The near-surface apparent thermal diffusivity is also an order of magnitude lower than deeper in the profiles (Table 5.2; Fig. 5.3), which is likely due to latent heat effects in the active layer at each site. Hanson and Hoelzle (2005) also observed lower thermal diffusivities near the ground surface, and higher values with a greater degree of variability between them with depth. Among the cold permafrost sites, Red Creek stands out as having the lowest values of apparent thermal diffusivity deeper in the profile and the shallowest depth of ZAA (Table 5.2). It differs from the other cold permafrost sites in that it is in ice-rich fine-grained material, whereas the other sites are in bedrock or coarse-grained sediment with little ice. It is the warmest of the sites in the continuous permafrost zone and its ground temperatures during the thawing season are within the range where unfrozen moisture can be present (Williams and Smith, 1989). This is discussed further below. Baker Lake also stands out as having the highest apparent thermal diffusivity near the base of the borehole at 3 m, which is possibly associated with the granitic bedrock outcrop that begins near the bottom of the borehole (GTN-P, 2009).

Table 5.2: Table of average apparent thermal diffusivities at thermal monitoring sites and the depth of ZAA. There are clear differences between the near-surface and deeper within the permafrost, and between the cold and the warm permafrost sites. The division between shallow and deep was decided based on the difference in apparent thermal diffusivity values. There is usually at least one order of magnitude difference above and below a depth of about 2 m.

Site	Shallow (m^2s^{-1})	Min Deep (m^2s^{-1})	Max Deep (m^2s^{-1})	Depth of ZAA (m)
Alert BH3	2.3×10^{-7}	1.7×10^{-6}	3.4×10^{-6}	19.9
Alert BH4	6.9×10^{-7}	1.2×10^{-6}	1.7×10^{-6}	18.2
Alert BH5	6.9×10^{-7}	1.5×10^{-6}	2.8×10^{-6}	23.8
Baker Lake BH4	3.5×10^{-7}	1.3×10^{-6}	5.8×10^{-6}	17.8
Iqaluit BH1	5.2×10^{-7}	1.4×10^{-6}	1.5×10^{-6}	18.8
Iqaluit BH2	6.4×10^{-7}	1.0×10^{-6}	1.7×10^{-6}	21.4
Sixty Mile	4.6×10^{-7}	1.3×10^{-6}	1.9×10^{-6}	16.6
Red Creek	3.5×10^{-7}	0.7×10^{-6}	1.0×10^{-6}	12.2
Wrigley	2.9×10^{-8}	1.2×10^{-7}	5.8×10^{-7}	2.6
Wolf Creek APM	2.3×10^{-8}	1.2×10^{-7}	3.5×10^{-7}	6.9
Wolf Creek P25	4.6×10^{-8}	2.3×10^{-7}	4.6×10^{-7}	4.6

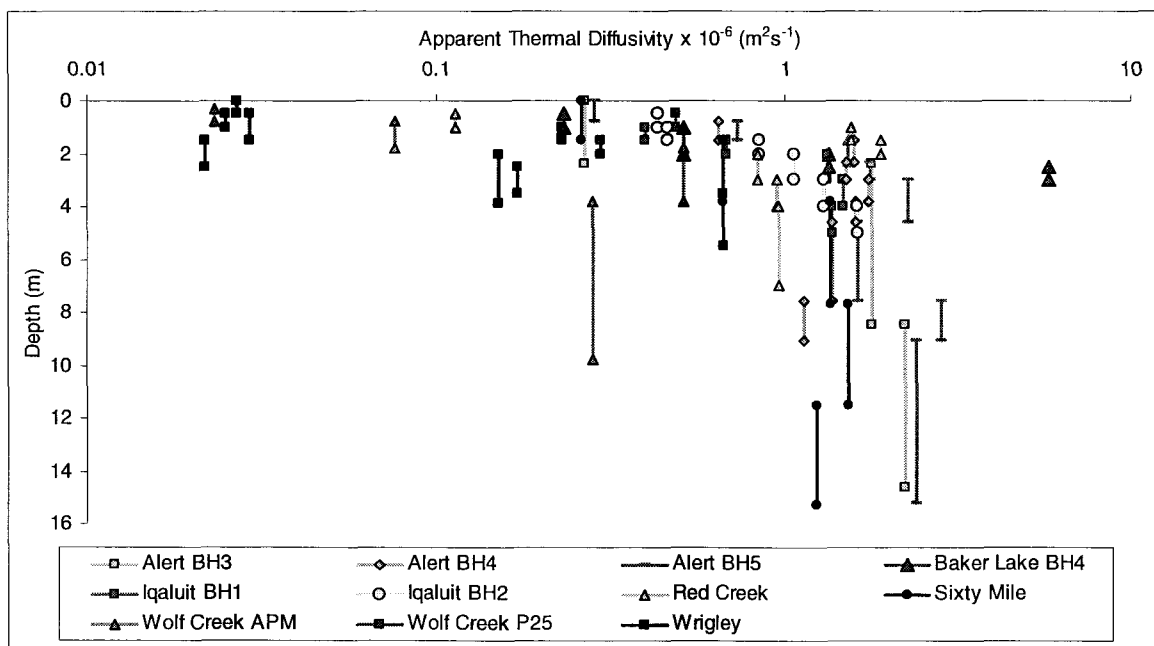


Figure 5.3: The apparent thermal diffusivity ($\times 10^{-6} \text{ m}^2\text{s}^{-1}$) is plotted on a logarithmic scale against depth at each borehole. The apparent thermal diffusivity generally increases with depth at each site, and the order of magnitude difference between cold and warm permafrost sites is evident. The vertical bars represent the range of depths over which the diffusivity calculations were made.

The depth of ZAA is greater at the cold permafrost sites because of the higher apparent thermal diffusivity (Fig. 5.4 and Table 5.2). The depth of ZAA generally increases with decreasing MAGTs, although it appears that eventually a maximum depth of ZAA will be reached. The depth of ZAA at the warm permafrost sites, with MAGTs higher than -1.5°C , have depths shallower than the expected range of 10 to 20 m (Williams and Smith, 1989; Gruber et al., 2004; Isaksen et al., 2007), whereas the cold permafrost sites are within this range or deeper. The relationship indicates that where unfrozen moisture is present, as in the case of the warm permafrost sites, the apparent thermal diffusivity is lower, and the depth of ZAA is shallower.

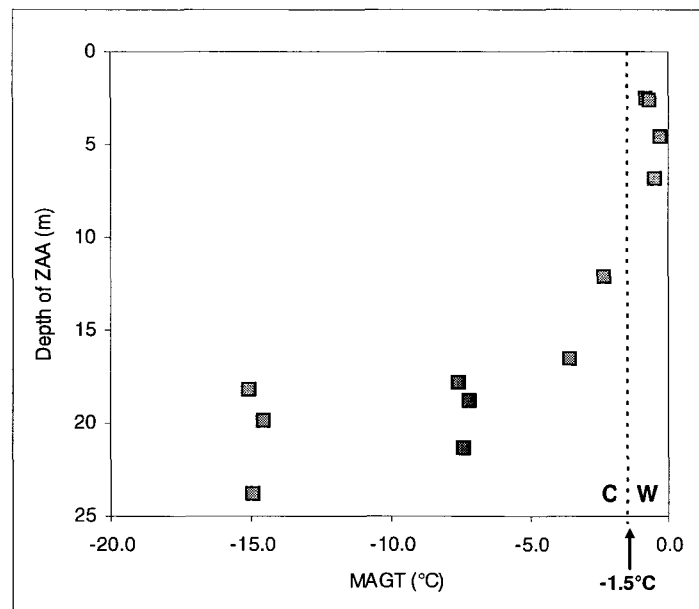


Figure 5.4: The relationship between MAGTs from each site, at either a depth below ZAA or the greatest depth for shallower sites, and the calculated depth of ZAA. Cold (C) and warm (W) permafrost sites are on either side of the -1.5°C line.

5.1.4 n_t

Values of n_t are affected by numerous factors during the thaw season, mainly surface shading by vegetation or canopy cover and soil moisture at the surface. The near-

surface thermal diffusivity and subsurface conditions have also been identified as important to n_t (Karunaratne and Burn, 2004). The forested, ice-rich sites at Wrigley and Table Mountain have the lowest average values of n_t , with values 0.69 and 0.59, respectively (Table 5.3). This agrees with Taylor's (2000) findings that the lowest values of n_t occur at forested sites, although there are no un-forested sites with similar climatic conditions for comparison in the present study. The highest values of n_t (greater than 1.0) occur at the sites with the least amount of vegetation: the Alert boreholes, Iqaluit, and Sixty Mile (Table 5.3). Taylor (2000) also observed the highest values of n_t occur in open areas with good sun exposure. The high values are due to the lack of vegetation, dry surface and subsurface conditions, and the long hours of direct insolation, allowing the ground surface to heat more than the air.

Table 5.3: Average values of n_f , SDD, and n_t at all sites, and the length of the record in years used to obtain each average value.

Site	n_f (no. of years)	SDD (no. of years)	n_t (no. of years)
Alert BH3	0.80 (7)	10529 (6)	1.7 (5)
Alert BH4	0.91 (7)	3079 (6)	2.2 (5)
Alert BH5	0.96 (7)	194 (3)	2.2 (5)
Iqaluit	0.84 (3)	M	1.3 (3)
Baker Lake BH2	0.19 (5)	M	0.87 (5)
Baker Lake BH4	0.70 (5)	4526 (4)	0.88 (5)
Sixty Mile	0.81 (2)	7780 (2)	1.2 (1)
Alpine Burwash	0.98 (1)	2210 (1)	M
Red Creek	M	4720 (2)	M
Table Mountain	0.21 (3)	8759 (2)	0.59 (3)
Wrigley	0.21 (6)	7389 (3)	0.69 (4)
Wolf Creek APM	0.44 (3)	5989 (3)	1.0 (2)
Wolf Creek Palsa 25	0.41 (4)	4894 (2)	1.1 (3)

The sites APM and Palsa 25 at Wolf Creek both have n_t values close to 1.0. This is an unexpected result, since the sites are moderately vegetated. The high values are attributed to the shrub vegetation at the site and the low albedo of the ground surface.

The borehole at the APM site in particular is in a small clearing, exposing the surface to direct insolation. These sites are both raised above the fen on the valley floor, and are not necessarily representative of the surrounding region. The ground surfaces are composed primarily of peat, which has low thermal conductivity in the summer, especially when dry. Karunaratne (2002) observed a similar situation with n_t values above 1.0 where surfaces were dry and had a low albedo. Latent heat transfer occurs more effectively than sensible heat transfer, so once the moisture has evaporated from the ground surface the heat is not efficiently conducted downward due to the low thermal conductivity of the dry peat, causing the surface to warm significantly. It is possible that cold air drainage at the sites in the Wolf Creek basin (Lewkowitz and Ednie, 2004) has an impact on their n_t values through advection of heat as a result of changing air temperatures during the night.

The thermal monitoring site at Iqaluit is very close to the coast of Frobisher Bay, and the latter likely acts as a moderator for changes in air temperature over the land due to coastal advection. The bare ground surface at Iqaluit is warmed through long periods of direct insolation, but the surface warming does not automatically raise the temperature of the air above due to cool air moving in from the coast. Hence, the coastal effect maintains cooler air temperatures, while the ground surface is being heated by direct insolation, resulting in n_t values that are higher than 1.0.

The n_t values at Baker Lake are lower than 1.0, ranging from 0.85 to 0.90 at BH4. This site differs from the other arctic sites in that it has low growing tundra vegetation resulting in surface shading, and is likely moist after snow-melt, resulting in cooler ground surface temperatures than the air during the summer.

5.1.5 n_f

Snow significantly affects air to ground temperature relations where it accumulates early and persists for the entire season, insulating the ground surface from extremely cold air temperatures during the winter. The sites most affected by snow are the four classified as warm permafrost, followed by Baker Lake BH4 and Alert BH3. Although Baker Lake BH2 is the most affected by snow of all the sites, it has been omitted from this discussion because it is an anthropogenic effect. Due to the missing air temperature data, the significance of snow at Red Creek could not be determined. The four warm permafrost sites, Wrigley, Table Mountain, Wolf Creek APM and Palsa 25 (Figs. 4.67, 4.74, 4.81, and 4.84), have the lowest values of n_f ranging between 0.21 and 0.44 (Table 5.3). A given number of SDD is a more important indicator of the insulating effect of snow where air temperatures are warmer, which agrees with the findings of Riseborough and Smith (1998) that n_f is a function of both snow depths and MAAT (discussed in detail below). At Alert BH3, one of the coldest sites in this study, although significant amounts of snow accumulate ($SDD > 10000$ cm days), the n_f value is still 0.80.

At the cold permafrost sites, where less vegetation is present, snow characteristics are more variable from site-to-site. Snow accumulates throughout the winter and remains on the ground at some sites, while at others it is prone to scouring and is cleared or redistributed periodically throughout the season. Alert BH3 is like the former (Fig. 4.11), while at Alert BH5 the snow barely rests on the ground before it is blown away, and this effect is reflected in the high values of n_f (Table 5.3). Alpine Burwash is another site with a very high n_f value reflecting the thin snow cover that is redistributed throughout the season (Fig. 4.63).

Riseborough and Smith (1998) show n_f as a function of snow depth and MAAT (Fig. 5.5). Values of n_f decrease as snow depth increases, but snow depths have a greater effect on the MAGST at sites with warmer MAATs. They identify the increased sensitivity to snow depths as being due to the thickness of the active layer: complete re-freezing of the active layer must take place before the ground surface temperature can decrease, and active layers are expected to be thicker where MAATs are warmer. Following Riseborough and Smith (1998), n_f and SDD are plotted for all of the boreholes (Fig. 5.5), excluding Red Creek and Iqaluit due to missing data. In general the study sites follow the pattern that snow depths affect n_f more in warmer permafrost areas and less in colder permafrost areas. However, there are exceptions, such as the alpine sites at Sixty Mile and Alpine Burwash, which appear similar to the Alert sites, as if they were very cold locations with MAATs below -12°C , although MAATs actually range between -4.4 and -6.1 at these sites (Fig. 5.5).

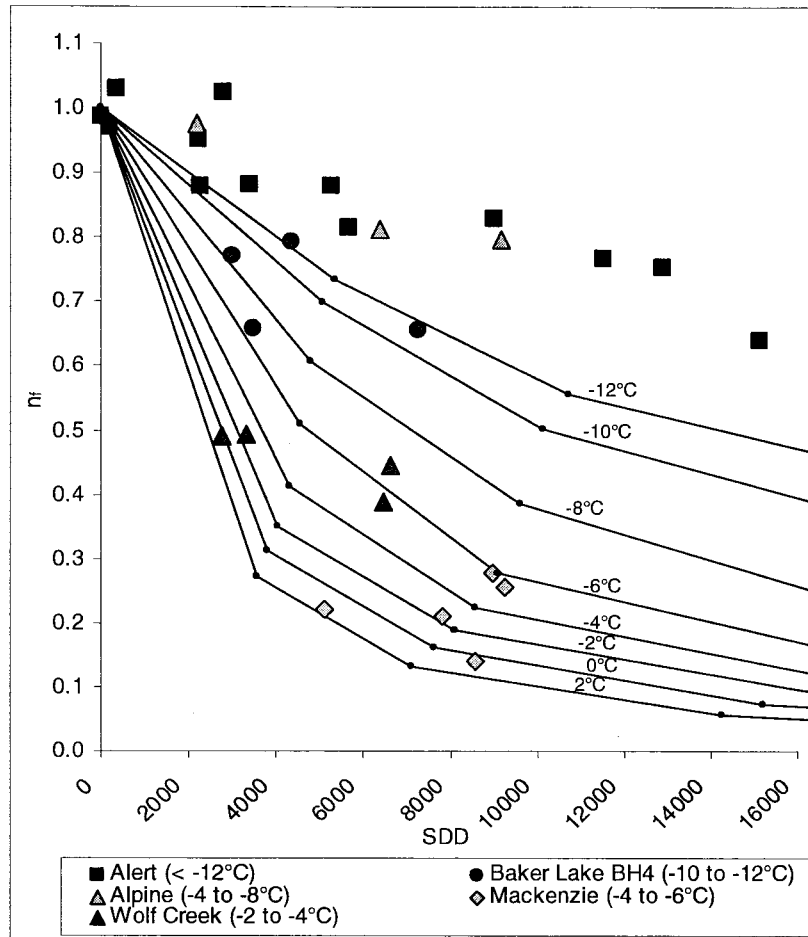


Figure 5.5: The relation between SDD and n_f for individual years for sites Alert, Baker Lake BH4, Sixty Mile, Alpine Burwash, Table Mountain, Wrigley, and Wolf Creek APM and Palsa 25. They are grouped based on the range of MAATs at each site. The dependence of n_f on snow cover are derived from Riseborough and Smith (1998) based on different MAAT ranges to observe how the sites from this study fit with their modeled expectations. Average snow thicknesses from Riseborough and Smith (1998) were converted to SDD (Riseborough, personal communication, January 2010).

The relationship between SDD and n_f does not appear to depend only on MAAT and the thickness of the active layer, but also on the substrate material and moisture content, both frozen and unfrozen, at the site. The Alert and alpine boreholes are all largely in bedrock, which reduces or eliminates the likelihood of latent heat effects, and the active layer cools rapidly allowing the surface temperatures to fall, resulting in higher values of n_f (Fig. 5.5), although the same would be expected for low ice content coarse-

grained sediment sites. Riseborough and Smith (1998) did not consider the moisture content of the ground, nor the differences in substrate between bedrock and sediment, in their model calculations, explaining why the sites in this study do not fit with their modeled results.

5.1.6 Moisture Content

The four warm sediment permafrost sites, Table Mountain, Wrigley, and the two at Wolf Creek, all have high latent heat effects due to frozen and unfrozen moisture present in the ground resulting in temperatures that are somewhat insensitive to changes in climate. Red Creek stands apart from the continuous cold permafrost sites in that it is in sediment with greater moisture content and latent heat effects are evident throughout the profile. During the thawing season the ground temperature wave levels off when nearing 0°C and a zero-curtain effect is evident within the permafrost, indicating that latent heat is being absorbed in the summer and is released during refreezing (Fig. 5.6 A). This summer warming pattern within the permafrost at Red Creek is very similar to that at Wolf Creek Palsa 25 and APM (Fig. 5.6 B and C), although the ground is colder and there is a wider range of annual temperatures. This pattern in permafrost temperatures indicates that the latent heat effects related to phase change, due to the presence of frozen and unfrozen moisture in the permafrost, limit the summer thaw. A similar pattern was observed in Barrow, Alaska (Figure 2A in Hinkel et al., 2001), where permafrost with high frozen and unfrozen moisture contents experience a zero-curtain effect throughout the thawing season in the upper portions of the permafrost.

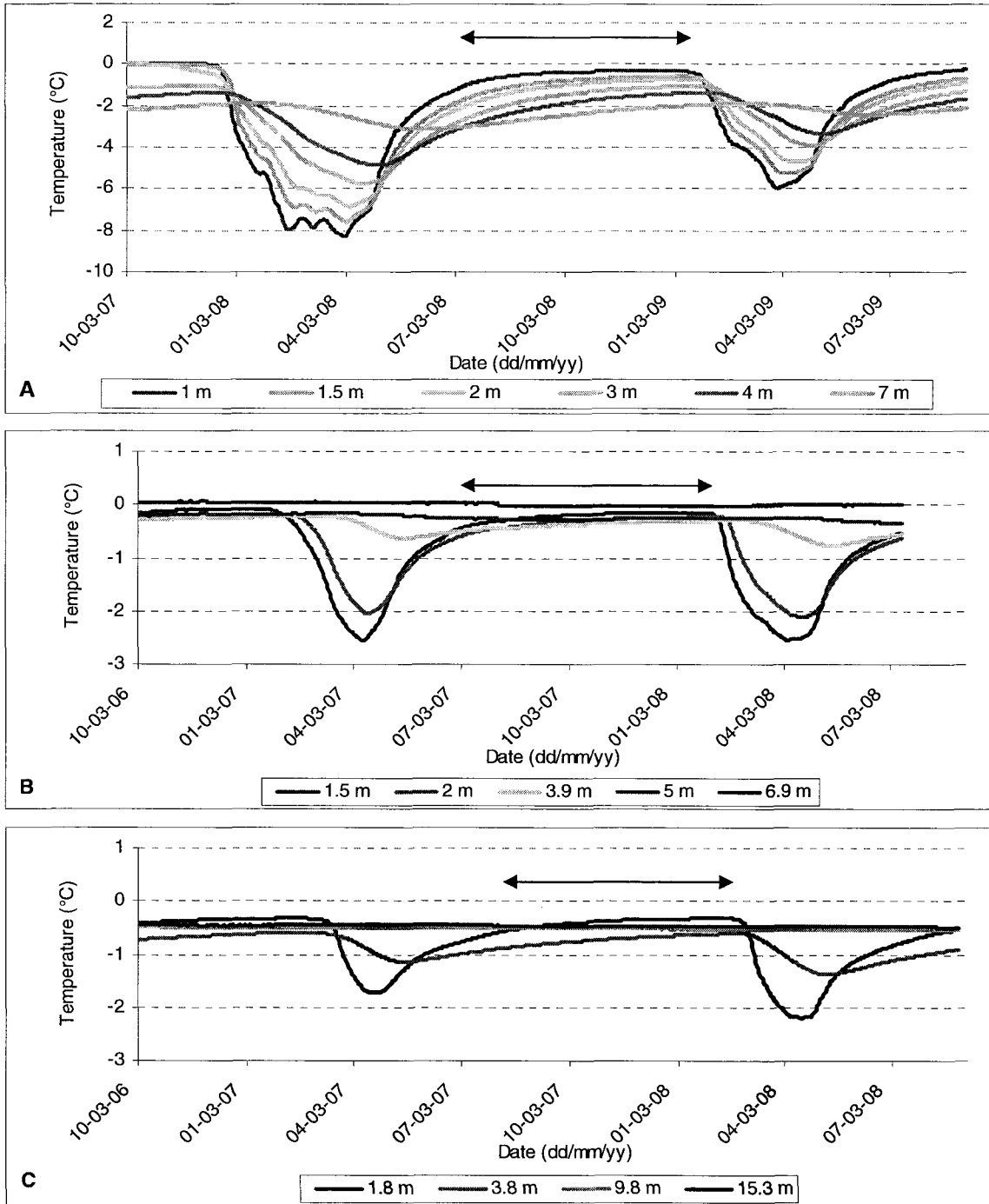


Figure 5.6: Permafrost temperatures at A) Red Creek between 2007 and 2009, B) Wolf Creek Palsa 25 between 2006 and 2008 and C) Wolf Creek APM between 2006 and 2008 showing similar warming tendencies that indicate latent heat effects during the thawing season, indicated by the arrows. Note: The scale of the temperature axis at Red Creek differs from the Wolf Creek sites.

The bedrock sites have low potential to contain significant amounts of frozen or unfrozen moisture, and therefore have short durations of zero-curtain effects during spring and autumn. Of the Alert sites, BH3 has the most defined effect lasting only 12 days at most in autumn. Iqaluit, Baker Lake, and the alpine sites also show very short zero-curtain periods, indicating that any moisture in the active layer freezes quite quickly in bedrock or at sites with coarse-grained sediment and low ice content, allowing ground temperatures to then fall further.

The sediment sites that have higher moisture/ice content, in contrast, generally have long zero-curtain effects (Figs. 4.57, 4.82, and 4.85). The zero-curtain effect tends to last longer at depths closer to TOP indicating the presence of moisture causing latent heat exchange during freezing and thawing periods. At Red Creek the zero curtain at 0.25 m lasts between 4-7 weeks in both the spring and autumn, and at 0.5 m depth (at the climate station a few metres from the borehole) it lasts almost the entire thawing season beginning in May, and continuing into the early part of winter until December (Fig. 4.57). At Wrigley and Table Mountain the permafrost is isothermal (Figs. 4.69, 4.70, 4.75, and 4.76). At these two sites there are short near-surface zero-curtain effects lasting up to a few weeks in spring and autumn. The zero-curtain at Wolf Creek APM and Palsa 25 is evident at each depth in the profile during the thaw season where ground temperature increases until just below 0°C, then remain there until cooling occurs in autumn (Fig. 5.6 B and C).

5.1.7 Site Typology

The annual range in air temperatures is generally greater than the annual range in ground temperatures due to the buffering above the surface and in the near-surface. The

relationship between the annual ground temperature range and annual air temperature range at the study sites illustrates the variability of buffering effects due to site-specific characteristics (Fig. 5.7). Air temperature ranges were calculated using the coldest and warmest monthly average air temperatures, and ground temperature ranges were calculated using absolute values measured three times daily for sites with sensors located between 0.8 and 1.5 m depth. The temperature ranges were selected at ~1.0 m in the ground and from the monthly mean air temperatures in order to filter out any minor fluctuations that may occur.

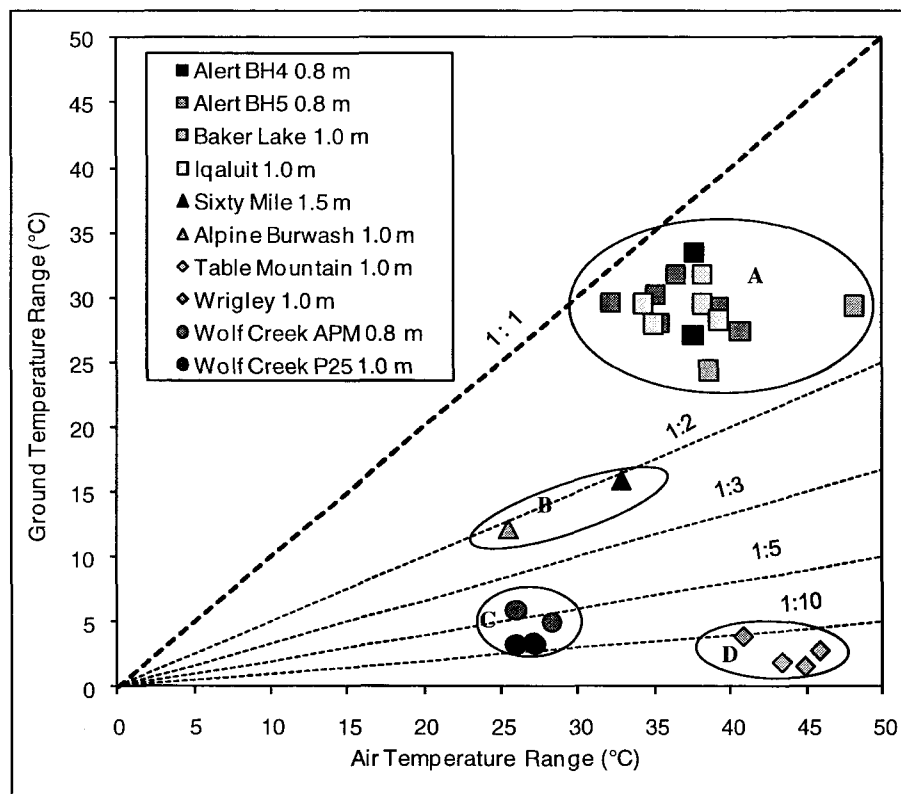


Figure 5.7: Relationship between the annual range in monthly average air temperatures and ground temperatures near 1.0 m depth. Clusters of sites with similar conditions are as follows: A) Arctic continuous permafrost; B) Alpine tundra; C) High elevation discontinuous permafrost mounds; D) Mackenzie valley ice rich isothermal permafrost.

The points fall into four distinct clusters due to variable conditions between the sites, which include the range in air temperatures, the snow depth and duration, the moisture content in the ground, the type of substrate, and the type and height of vegetation. These conditions determine how much buffering there is between air and ground surface temperatures, and the apparent thermal diffusivity. The air and ground temperature ranges at the arctic continuous permafrost sites (Alert, Baker Lake and Iqaluit; Fig. 5.7, cluster A) are the most similar to one another, and the cluster is situated closest to the 1:1 line, and is above the 1:2 line. This cluster has the least buffering between the air and the ground for numerous reasons. Air temperature ranges reach about 38°C, while those in the ground are about 30°C (Fig. 5.8). Temperatures are able to propagate at these sites efficiently because the ground is cold with little to no moisture and the substrate is generally bedrock (or coarse-grained sediment with low ice content), which results in high apparent thermal diffusivities. Also, snow depths are generally low, and have a lesser influence on buffering during winter due to the cold temperatures (as observed in the n_f section), and there is very little vegetation allowing the surface to reach higher temperatures in the summer. Within cluster A, Baker Lake (Fig. 5.9) is furthest from the 1:1 line which is likely due to the differences in vegetation characteristics and substrate at the site; the vegetation is thicker than at the other sites, there is about 15 cm of peat at the surface, and the substrate is till composed of coarse gravels and sand with low ice content.

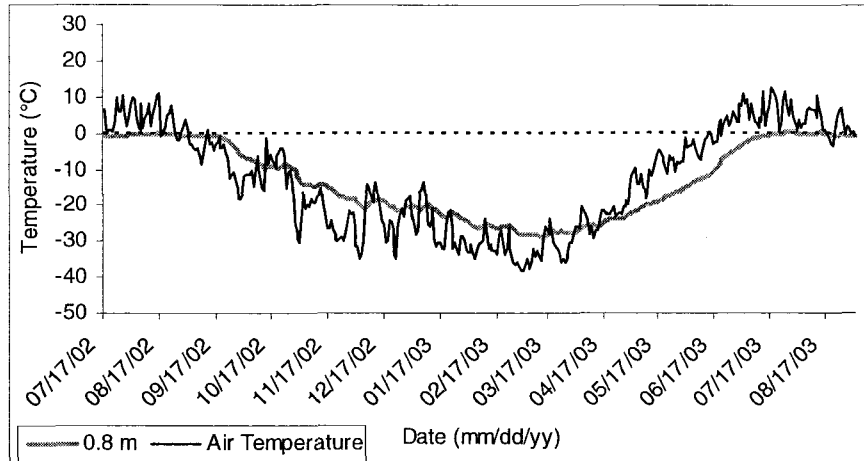


Figure 5.8: Range of temperatures at Alert BH5 for both the air and the ground at 0.8 m between July 17, 2002 and September 2, 2003.

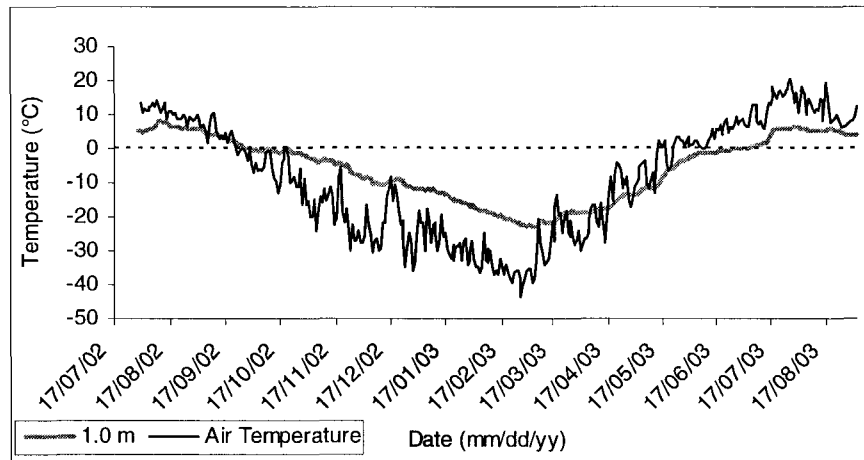


Fig. 5.9: Range of temperatures at Baker Lake BH4 for both the air and the ground at 1.0 m between July 17, 2002 and September 2, 2003.

The alpine tundra sites (Sixty Mile and Alpine Burwash; Figs. 5.7, cluster B, and 5.10) have lower ranges in air temperature due to the moderating effects of the alpine environment. In general, summer temperatures remain cooler at high elevations due to environmental lapse rates, and winter temperatures remain warmer than lower elevation sites likely due to air temperature inversions common in the mountainous regions of the Yukon (Wahl et al., 1987). The two points lie close to the 1:2 line, indicating that the range is diminished by half in the ground. These two sites have high apparent thermal

diffusivities due to the bedrock substrate with little to no moisture, and the buffering is minimal due to low growing tundra vegetation and moderate to low snow cover.

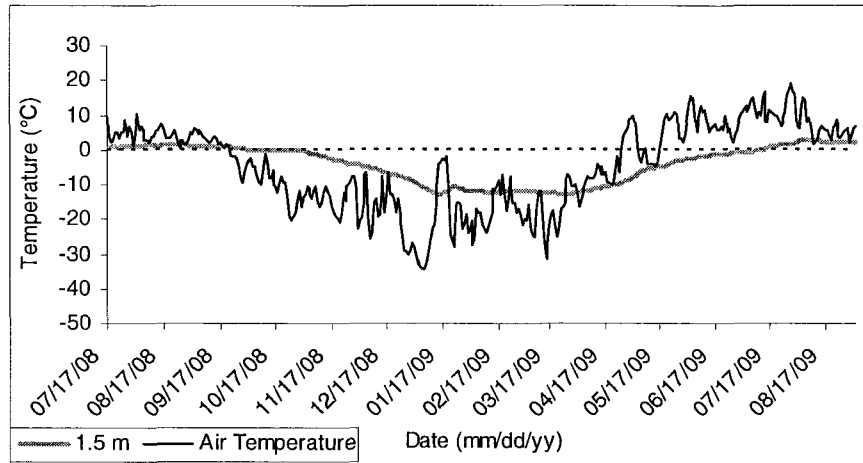


Figure 5.10: Range of temperatures at Sixty Mile for both the air and the ground at 1.5 m between July 17, 2008 and September 2, 2009.

The high elevation discontinuous permafrost mound sites (Wolf Creek APM and Palsa 25; Figs. 5.7, cluster C, and 5.11) are controlled by an alpine climate, similar to the alpine tundra sites, and exhibit a small range of air temperatures. The range in ground temperatures diminishes significantly at these sites lying close to the 1:5 or 1:10 line. These sites have low apparent thermal diffusivities due to the high ice and unfrozen moisture content in this isothermal permafrost in surficial deposits. Also, the vegetation and snow depths are moderate, creating greater buffering above the ground surface, and with the milder MAATs the snow has a greater influence on air-to-surface interactions.

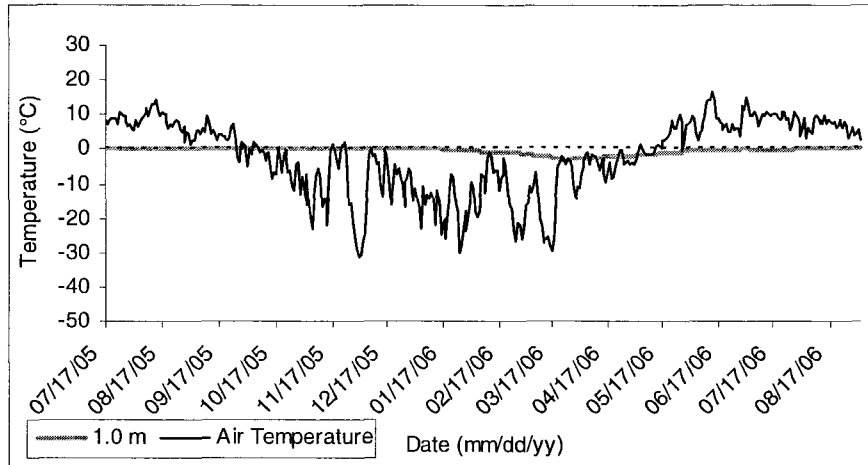


Figure 5.11: Range of temperatures at Wolf Creek Palsa 25 for both the air and the ground at 1.0 m between July 17, 2005 and September 2, 2006.

The final cluster, the Mackenzie Valley ice-rich warm permafrost sites are at or below the 1:10 line (Wrigley and Table Mountain; Figs. 5.7, cluster D, and 5.12), illustrating the greatest difference between ranges in air and ground temperatures. The continental climate creates large air temperature ranges that are as great, or greater, than those for cluster A, although the range in ground temperatures is the lowest of all the clusters. The strong buffering above the surface is caused by high amounts of vegetation, with both sites located in forests, and the high amounts of snow that accumulates and persists for the entire winter. Within the ground the apparent thermal diffusivity is low due to high amounts of ice and unfrozen moisture in the fine-grained warm permafrost.

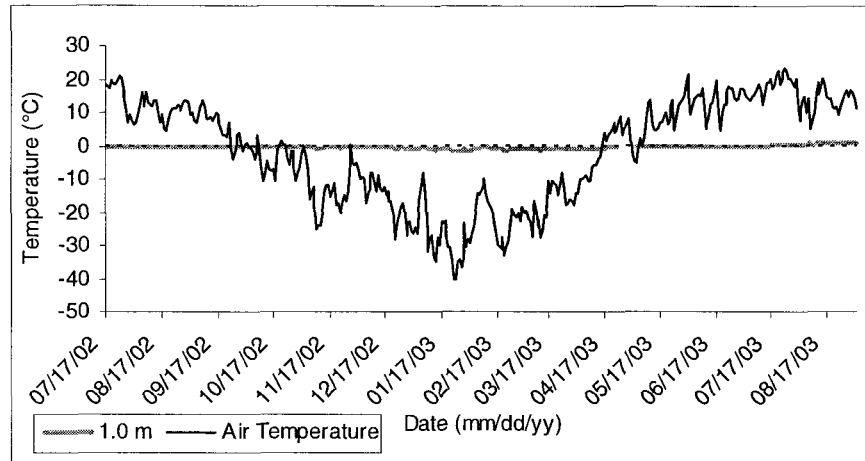


Figure 5.12: Range of temperatures at Table Mountain for both the air and the ground at 1.0 m between July 17, 2002 and September 2, 2003.

5.2 CHANGES OVER TIME

5.2.1 Response of the ground to air temperature trends

Ground temperatures have increased significantly at most of the permafrost thermal monitoring sites examined in this thesis over the long-term. Ground temperatures at four of the five boreholes at Alert (excluding BH3) have increased significantly since 1978 (Figs. 4.26, 4.27, 5.13 A-D) following increases in MAATs in recent decades (Fig. 5.14). The warming at each of these boreholes varied in magnitude due to variations in the characteristics of the snow-pack (Table 4.8). Permafrost temperatures at Iqaluit also increased, though the trend began more than a decade later in the early 1990's (Figs. 4.32, 4.34, 4.34, and 5.13 E), following the regional climatic warming trend (Fig. 5.14). During the period of thermal monitoring at Baker Lake there was no warming trend evident, but when the 3 m MAGT record was hind-cast to 1951, an increasing trend appeared between the mid-1970's and 2007 (Fig. 4.44 B). Permafrost temperatures increased at the Table Mountain thermal monitoring site, but the warming at

this site differs in magnitude from the previous two. Even though the permafrost at Table Mountain is within 1 degree of 0°C and latent heat effects are evident, the permafrost has warmed significantly ($p < 0.001$) since the beginning of monitoring in the mid-1980's (Figs. 4.70 and 5.13 F).

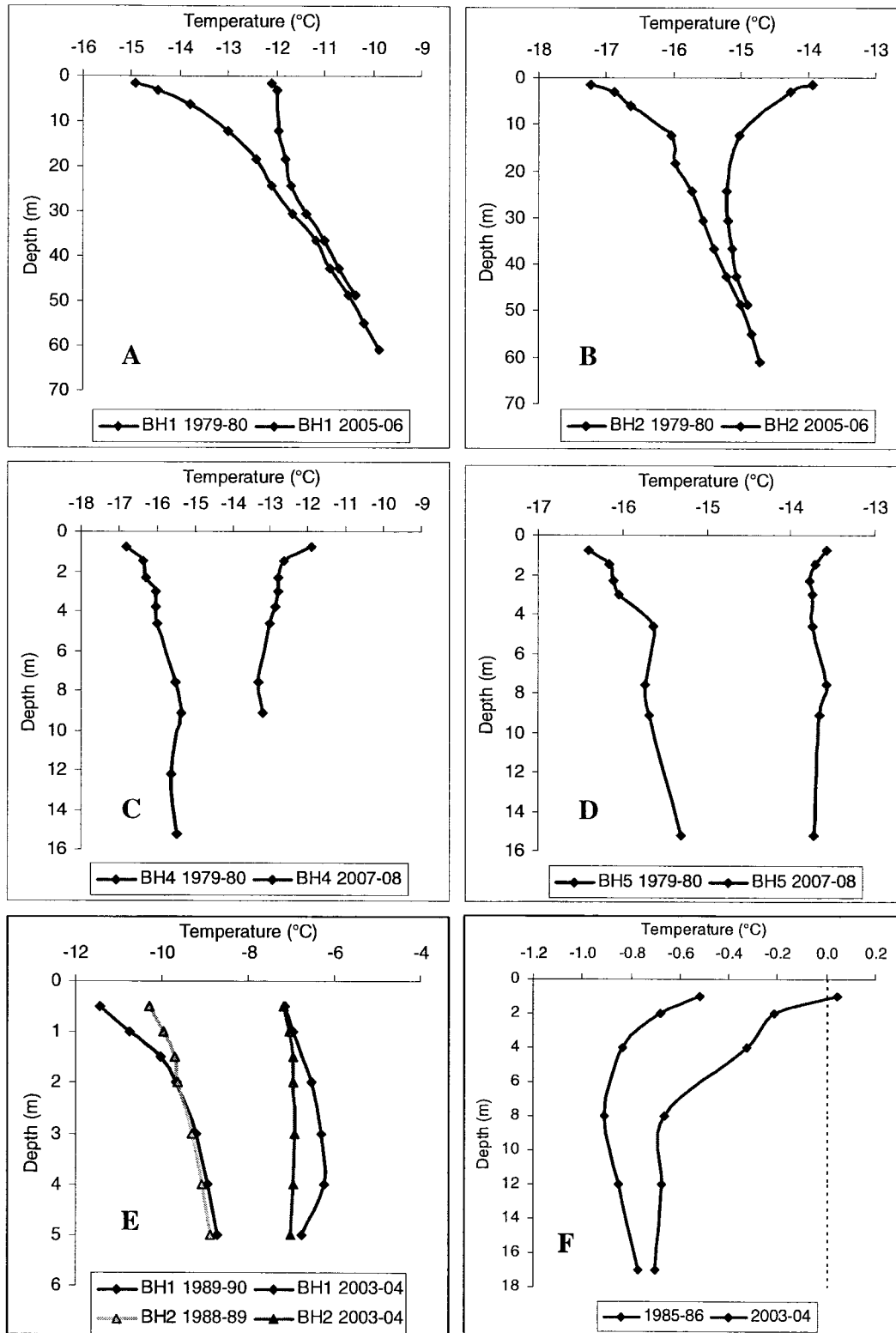


Figure 5.13: MAGT profiles at all sites that warmed over the monitoring period: A – Alert BH1; B – Alert BH2; C – Alert BH4; D – Alert BH5; E – Iqaluit BH1 and BH2; F – Table Mountain. Note: All axes and dates differ from one another.

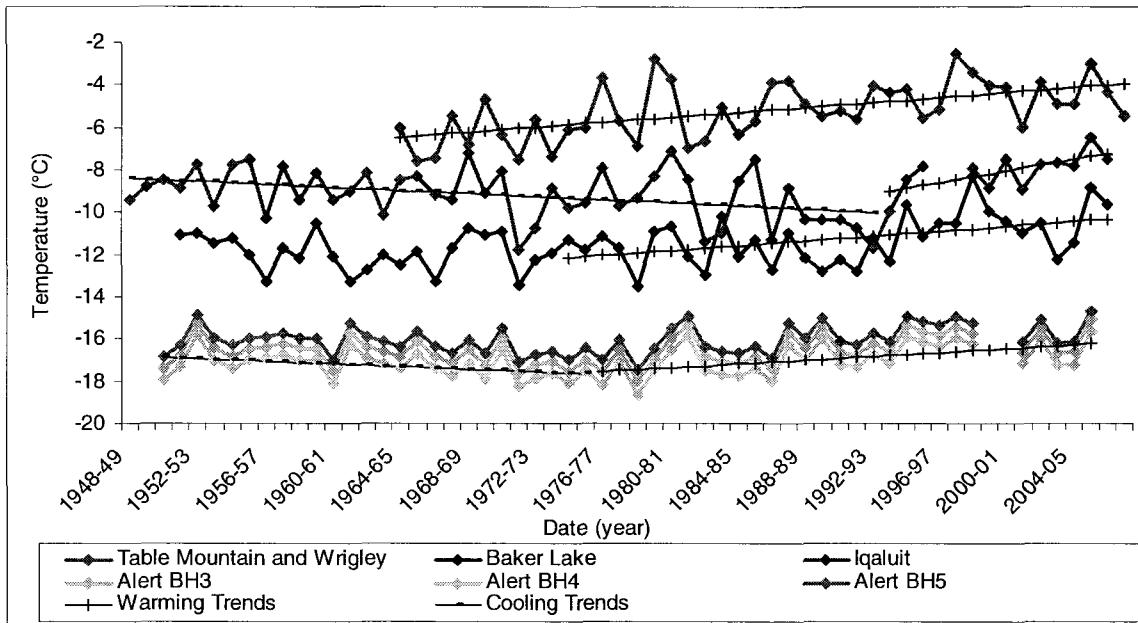


Figure 5.14: MAAT trends at Table Mountain and Wrigley, Baker Lake, Iqaluit and Alert BH3, BH4 and BH5, all from correlated ECCS data (Environment Canada, 2009). Straight lines show the timing of statistically significant warming and cooling trends at the sites. Note: Hind-cast values of MAAT at Table Mountain and Wrigley are within 0.2°C of one another, so only Table Mountain values have been plotted on this graph.

The magnitude of the response in the ground varies among the sites that have warmed, due primarily to the magnitude and direction of the air temperature trend, as well as varying site-specific factors. The Alert BH4 and BH5 sites accumulate the least amount of snow in winter and lack a surface buffer layer, and therefore the permafrost has warmed the most at these sites compared to that at BH3, where snow depths are greater. The increases in ground temperatures at Alert can therefore be attributed to the significant autumn and winter warming trends observed in the region beginning in the 1970's (Fig. 4.25).

The increasing trend in MAGTs at Table Mountain has been very slight but continuous over the monitoring period, on the order of 0.1 to 0.2°C per decade (Fig. 4.70). The significant increasing trend in MAAT of 0.6°C per decade since the mid

1960's (Figs. 4.71 and 5.14) is reduced by the latent heat effects acting at this site where permafrost temperatures are very close to 0°C, as well as the surface buffering from vegetation, the organic mat, and continuous snow during winter. A difference in the increasing of air temperatures in this region is that it is occurring mainly in the summer and winter (Fig. 4.72), as opposed to autumn and winter warming at the other sites.

At Iqaluit, air and permafrost temperatures are closely linked (Figs. 4.30, 4.32, and 4.33). The MAGT has increased by almost the same amount as the MAAT since the early 1990's which is later than the warming trends observed at the other study sites (Fig. 5.14). The warming at this site has been stronger than at any of the other sites with MAATs increasing at a rate of 1.4°C per decade, and winter and autumn average air temperatures increasing by 2.3°C per decade (Figs. 4.35 and 4.36). The timing of the climatic trends at Iqaluit correspond to observations made in northern Quebec by Allard et al. (1995; 2002), where decreasing air and permafrost temperatures occurred into the early 1990's, followed by increases since then (Fig. 5.14). Intense climatic cooling was also observed by Hansen et al. (1996) from 1965 to 1995 in the region between Hudson Bay and Greenland, occurring mostly in the winter and spring. Allard et al. (1995) concluded that the cooling trend was due mainly to significant winter cooling, as opposed to year-round cooling. Winter average air temperatures at Iqaluit, from correlated ECCS data (Environment Canada, 2009), decreased by about 0.6°C per decade between the late 1940's and the early 1990's, but the inter-annual variability in winter temperatures was too high to be statistically significant, whereas the spring average temperatures decreased significantly by 0.7°C per decade over the same period. Air temperatures over the winter

and spring (December to May) decreased significantly between 1948 and 1993 by 1.3°C per decade ($p < 0.05$; Fig. 5.15).

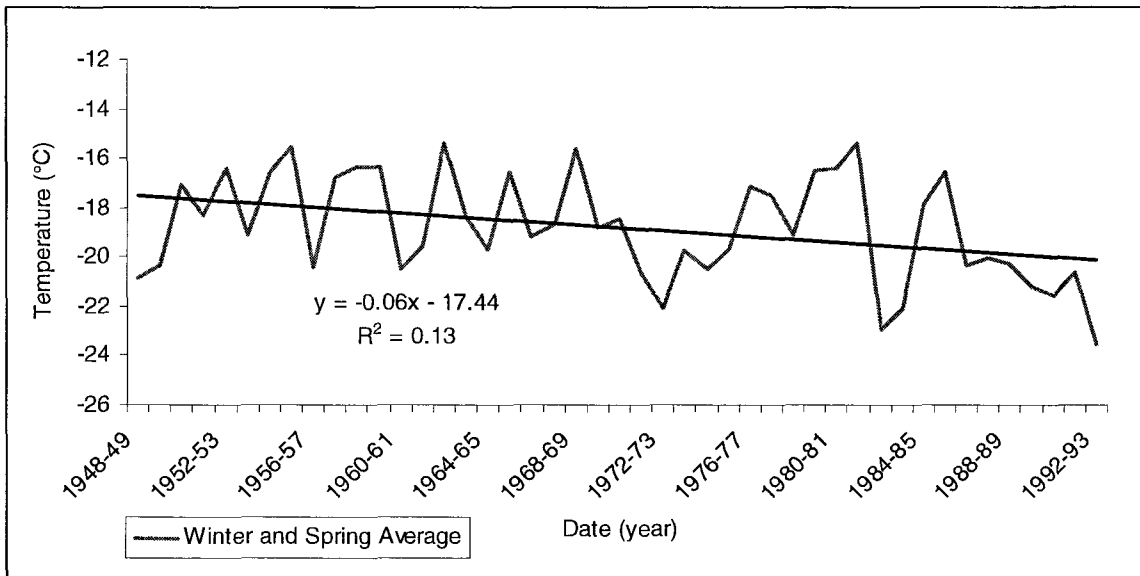


Figure 5.15: December to May average temperatures at Iqaluit between 1948 and 1993 showing the decreasing trend of 1.3°C per decade. The trend is significant at $p < 0.05$.

The MAAT record at Baker Lake does not show a distinct increasing or decreasing trend prior to the 1970's, although warming did begin about the same time as at Alert, in the mid-1970's (Fig. 5.14). The MAGTs at Baker Lake follow a similar pattern to the MAAT over the ground temperature monitoring period between 1997 and 2007 (Figs. 4.43 and 4.44). The measured ground temperature record at Baker Lake is too short to determine a trend, but the hind-cast record of MAGTs at 3 m show a significant warming trend of 0.3°C per decade since the mid 1970's ($p < 0.01$; Fig. 4.44 B). South of Baker Lake in Northern Manitoba, Camill (2005) found a significant winter warming trend of approximately 0.4°C per decade during the latter half of the 20th century at 4 of the 5 sites for which climate records were analyzed. These trends are similar to that observed for Baker Lake (Fig. 4.45).

Overall, the results indicate that the winter warming observed at all of the sites with long time series may be the primary contributor to permafrost warming, particularly at sites with characteristically low snow. The sites with the least amount of snow accumulation at Iqaluit and Alert BH4 and BH5, in combination with winter average air temperatures increases, have also shown the greatest degree of permafrost warming.

5.2.2 Seasonal Correlations

The method used by Popova and Shmakin (2009) was tested using the sites with longest time series of ground temperature data. The goals of the method were to determine 1) which season had the greatest statistical influence on ground temperatures at a site, and 2) how much of an effect previous years had on ground temperatures. The method was tested on the five boreholes at Alert and the one at Table Mountain. Summer ground temperature data was de-trended at the closest depth to 10 m, and was correlated with de-trended seasonal average air temperatures from the nearest ECCS station (Environment Canada, 2009). The correlations were conducted three times for each season: with no lag (or the season within the previous year); a one year lag; and a two year lag. Only 3 of the 72 correlations were statistically significant ($p < 0.05$; Table 5.4).

Table 5.4: Table of r^2 values from seasonal correlations at the five boreholes at Alert and the one at Table Mountain. All correlations were tested for statistical significance, and only 3 of the 72 tests were considered statistically significant at $p < 0.05$ (bold and highlighted in grey). Note: the 0 year lag is the most recent seasonal average from the previous year, and lag 1 and 2 are from 1 and 2 years prior to that.

Season	Lag (Years)	Alert BH1 12.2 m			Alert BH2 12.2 m			Alert BH3 8.5 m		
		R ²	n	Significant (Y/N)	R ²	n	Significant (Y/N)	R ²	n	Significant (Y/N)
Spring	0	0.12	22	N	0.05	21	N	0.03	21	N
	1	0.05	23	N	0.08	22	N	0.03	21	N
	2	0.12	23	N	0.20	22	Y, p=<0.05	0.04	21	N
Summer	0	0.08	22	N	0.02	21	N	0.14	21	N
	1	0.02	23	N	0.00	22	N	0.00	21	N
	2	0.11	23	N	0.02	22	N	0.02	21	N
Autumn	0	0.05	22	N	0.08	21	N	0.03	22	N
	1	0.04	23	N	0.14	22	N	0.04	22	N
	2	0.04	23	N	0.05	22	N	0.03	22	N
Winter	0	0.07	21	N	0.00	20	N	0.10	21	N
	1	0.13	22	N	0.05	21	N	0.14	21	N
	2	0.61	22	N	0.04	21	N	0.08	21	N
Season	Lag (Years)	Alert BH4 9.1 m			Alert BH5 9.1 m			Table Mountain 12.0 m		
		R ²	n	Significant (Y/N)	R ²	n	Significant (Y/N)	R ²	n	Significant (Y/N)
Spring	0	0.40	10	N	0.01	22	N	0.01	20	N
	1	0.01	11	N	0.01	22	N	0.08	20	N
	2	0.34	11	N	0.01	22	N	0.17	20	N
Summer	0	0.03	10	N	0.18	21	N	0.20	20	Y, p=<0.05
	1	0.21	11	N	0.01	22	N	0.10	20	N
	2	0.13	11	N	0.01	22	N	0.00	20	N
Autumn	0	0.01	10	N	0.18	23	Y, p=<0.05	0.01	20	N
	1	0.14	11	N	0.11	23	N	0.05	20	N
	2	0.00	12	N	0.01	23	N	0.02	20	N
Winter	0	0.01	10	N	0.13	22	N	0.08	20	N
	1	0.24	10	N	0.11	22	N	0.03	20	N
	2	0.24	11	N	0.11	22	N	0.00	20	N

The first statistically significant relationship was between the summer ground temperatures at Alert BH2 and spring air temperatures with a two year lag (Fig. 5.16 A). Even though this was statistically significant, the lag between the seasons is too long for a physically-based relationship given the apparent thermal diffusivity at the site, and is therefore considered spurious. The second relationship at Alert BH5 is between autumn air temperatures during the previous year (or no lag) and the summer ground

temperatures, and is physically possible, but very weak (Fig. 5.16 B). The last significant relationship was at Table Mountain between summer air temperatures with no lag and the summer ground temperatures and appears to be spurious because it is a negative correlation (Fig. 5.16 C). This relationship is affected by measurement error due to the extremely small residuals associated with the ground temperatures.

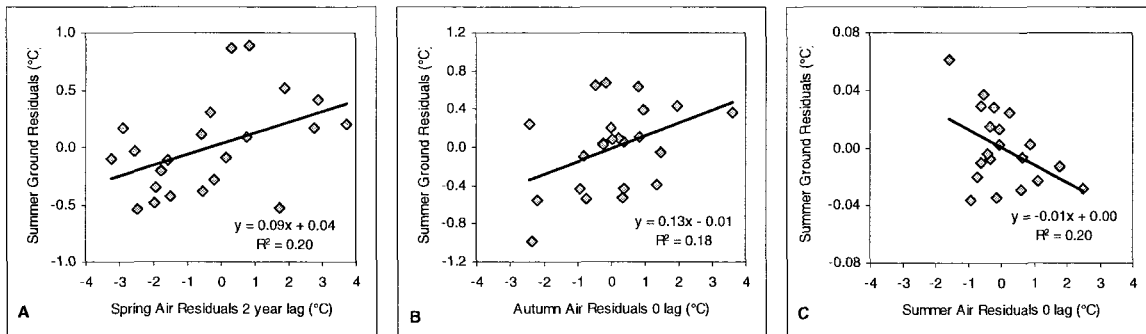


Figure 5.16: The three significant correlations between the residuals of (A) summer ground temperatures and 2 year lagged spring air temperatures at Alert BH2; (B) summer ground temperatures and autumn air temperatures, no lag, at Alert BH5; and (C) summer ground temperatures and summer air temperatures, no lag, at Table Mountain. The correlations are significant at $p < 0.05$.

Popova and Shmakin (2009) found that spring air temperatures had the greatest statistical influence on summer ground temperatures between 5 and 10 m depth.

However, they did not examine the relationships through physically based modeling which would be a better method to test for seasonal influences on ground temperatures.

The application of the method to the current study suggests that it is not useful at the Canadian sites.

5.3 LIMITATIONS OF THE STUDY

This thesis was heavily based on previously collected data, and as a consequence several limitations were encountered during the analyses:

1. The data for this thesis were collected from many different sources over various time spans.
2. The equipment used at the sites and the methods of data collection were outside the control of this study.
3. The depths of thermistors were determined long before the start of this research, so detailed analysis of active layer processes could not be conducted at most sites.
4. Equipment/instrument failures, in particular the missing air temperature data from Red Creek, limited the interpretation of air-to-permafrost interactions.

5.4 FUTURE RECOMMENDATIONS

Recommendations for research to be undertaken in the future:

1. Continued monitoring of sites with shorter time series in order to collect enough data to test for long-term trends in the future.
2. Further investigations into seasonal influences on permafrost temperatures.
3. After a few years of data collection at Red Creek, comparisons can be made between this cold sediment permafrost site containing high amounts of ice and the warmer permafrost sites also containing high amounts of ice and unfrozen moisture.

4. Most of the study sites in the continuous permafrost zone are in bedrock, while all of the sites in the discontinuous permafrost zones, except for the alpine ones, are in sediment. A follow-up study should be done comparing a number of sites with similar macro- and micro-climatic conditions, but with differing substrates to test the importance of substrate on ground temperature characteristics.
5. The usefulness of snow depth-days (SDD) should be examined further through an investigation into the difference between a long snow-cover season with shallow snow depths and a short one with deep snow. The same SDD value may reflect entirely different circumstances, and would have an effect on the relations between air and ground temperatures.
6. MAGTs are closely linked to MAATs at Iqaluit, but unfortunately the borehole only reaches 5 m depth. The installation of a deep borehole at this site would provide a clearer indication of climate changes that have occurred in the past.

6. CONCLUSION

This study has demonstrated the wide range of permafrost and climatic conditions that exist across northern Canada, has explained some of the determining factors involved in controlling these conditions, and has shown that significant changes have occurred at sites over monitoring periods of the past 20 to 30 years. Permafrost conditions are determined by the macro-climate of the region, the micro-climate at the site, and the type and conditions of the substrate. This study is one of the first to attempt to investigate climate-to-permafrost temperature relationships in the continuous and discontinuous permafrost zones at a range of ground temperatures from 0 to -15°C with varying environmental conditions. The outcomes of the three main objectives of this thesis are as follows:

1. Relations between climate and permafrost:
 - a. The MAAT is the primary determinant of permafrost temperatures. There is a strong relationship between MAAT and MAGT (Fig. 5.1).
 - b. The presence of moisture in the ground, both frozen and unfrozen, strongly affects the rate at which temperatures propagate with depth. For example, the zero-curtain was longest and most significant at sites with high ice contents and MAGTs close to 0°C. There is a distinction between the effects of moisture in bedrock and sediment sites, as well as between cold and warm permafrost. The permafrost sites in this thesis that are considered cold or bedrock show limited latent heat effects and are more temperature sensitive to changes in climate. In contrast, the permafrost sites that are considered warm or in ice-rich sediment in this study may be

significantly affected by latent heat effects (Fig. 5.6), resulting in enhanced buffering between climate and permafrost. However, the characteristics of the sites in this research mean that it is not possible to separately explore the influences of temperature and substrate.

- c. The ground temperatures at the bedrock sites in this study, both the alpine tundra and the arctic sites, are more closely linked to climate year round than the sites with high latent heat effects, and therefore may be expected to respond more rapidly, in terms of temperature, to changes in climate.

2. Trends in annual and seasonal climate and their impacts on permafrost conditions:

- a. MAATs increased at all of the sites with longer time series in recent decades (Fig. 5.14). The earliest observed warming began in the mid 1960's at Wrigley and Table Mountain, Northwest Territories (+0.6°C/decade; Figs. 4.71 and 4.77), followed by warming in the mid 1970's at Alert and Baker Lake, Nunavut (+0.4 and +0.6°C/decade, respectively; Figs. 4.23 and 4.45), and since the early 1990's, with the most rapid warming of all the sites, at Iqaluit, Nunavut (+1.4°C/decade; Fig. 4.35). Cooling occurred at Alert, Nunavut, between the early 1950's and the mid 1970's (-0.3°C/decade; Fig. 4.23), and at Iqaluit, Nunavut, between the late 1940's and the early 1990's (-0.4°C/decade; Fig. 4.35).
- b. All of the sites assessed for long-term seasonal air temperature trends increased significantly during the winter (December, January, and February) in recent decades. The greatest magnitudes of winter warming occurred at Iqaluit since 1993 (+2.3°C/decade; Fig. 4.36), followed by

Table Mountain and Wrigley since 1964 ($+1.2^{\circ}\text{C}/\text{decade}$; Figs. 4.72 and 4.78), Baker Lake and Alert since 1951 and 1970, respectively ($+0.4^{\circ}\text{C}/\text{decade}$; Figs. 4.46 and 4.25, respectively). Significant warming also took place during autumn (September, October, and November) at Baker Lake ($+1.3^{\circ}\text{C}/\text{decade}$; Fig. 4.46), Iqaluit ($+2.3^{\circ}\text{C}/\text{decade}$; Fig. 4.36), and Alert ($+0.9^{\circ}\text{C}/\text{decade}$; Fig. 4.25), and during the summer (June, July, and August) at Table Mountain and Wrigley ($+0.3^{\circ}\text{C}/\text{decade}$; Figs. 4.72 and 4.78). The only site where significant seasonal cooling in air temperatures occurred was at Iqaluit during spring (March, April, and May) between 1948 and 1992 ($-0.7^{\circ}\text{C}/\text{decade}$; Fig. 4.36).

- c. Increases in permafrost ground temperatures were observed at Alert, Baker Lake, Iqaluit, and Table Mountain in recent decades (Fig. 5.13). Ground temperatures at all of the Alert boreholes, except BH3, increased between 1978 and 2008 at depths close to or greater than ZAA ($+0.2$ to $+0.6^{\circ}\text{C}/\text{decade}$; Fig. 4.27). Permafrost temperatures at both of the Iqaluit boreholes are closely related to air temperatures, more so than all of the other thermal monitoring sites in this thesis, and increased at 5 m depth between 1988 and 2004 ($+1.6$ to $+1.9^{\circ}\text{C}/\text{decade}$; Figs 4.32 and 4.33). Hind-cast 3 m MAGTs at Baker Lake increased since the mid-1970's ($+0.3^{\circ}\text{C}/\text{decade}$; Fig. 4.44 B). At Table Mountain, ground temperatures increased at all depths between 2 and 17 m between 1985 and 2007 ($+0.2$ and $+0.1^{\circ}\text{C}/\text{decade}$, respectively; Fig. 4.70). The permafrost warming at this site was slight but consistent over the period and is important because

it must represent a progressive change in unfrozen moisture in the fine-grained, ice rich permafrost at the site.

- d. Using the data available in this thesis it was not possible to determine the direct impacts of seasonal air temperature trends on permafrost temperatures. This was either due to the inadequacy of the data to assess these relations, or because the permafrost temperatures are influenced by a portion of all of the seasons, and one particular season cannot be singled out as the primary influence.

3. The effects of snow-pack characteristics on ground surface and permafrost temperatures:

- a. From the results in this thesis it seems that after MAAT, local snow characteristics are the most important site condition in determining air-to-permafrost relations, followed by moisture within the active layer.
- b. Snow has a greater influence on winter ground temperatures in regions where MAATs are warmer (Fig. 5.5). However, the influence of snow on ground temperatures also varies with substrate, the thickness of the active layer, and the presence of moisture in the ground, both frozen and unfrozen.
- c. The influence of deep snow was demonstrated at Alert BH3, which receives the most snow of the four boreholes at Alert (Fig. 4.11 and Table 4.8), where ground temperatures increased the least of all the boreholes in the area over the 30 year record (Figs. 4.26 and 4.27). The lack of permafrost warming at Alert BH3 indicates that the winter increases in air

temperatures at Alert may be the dominant cause of warming permafrost temperatures at the other boreholes.

- d. The effects of deep and late-lying accumulations of snow were observed at Baker Lake BH2 (beneath snow drift) where minimum and mean annual ground temperatures warmed (Figs. 4.47 and 4.48), the surface offsets increased (Table 4.14), and the active layer remained thin (Fig. 4.49) in relation to BH4 (natural conditions).

REFERENCES

- ACIA, 2005. *Arctic Climate Impact Assessment*. Cambridge University Press, 1042p.
URL: <http://www.acia.uaf.edu>
- Allard, M., B. Wang, and J.A. Pilon (1995). Recent Cooling along the Southern Shore of Hudson Strait Quebec, Canada, Documented from Permafrost Temperature Measurements. *Arctic and Alpine Research*, 27: 157-166.
- Allard, M., R. Fortier, C. Duguay, and N. Barrette (2002). A Trend of Fast Climate Warming in Northern Quebec Since 1993. Impacts on Permafrost and Man-made Infrastructures. *American Geophysical Union*, Fall Meeting, abstract B11E-03.
- Bassett, G.W. and Z. Lin (1993). Breaking Global Temperature Records After Mt. Pinatubo. *Climate Change*, 25: 179-184.
- Brown, J., O.J. Ferrians, Jr., J.A. Heginbottom, and E.S. Melnikov (1997). Circum-Arctic map of permafrost and ground-ice conditions. *U.S. Geological Survey in Cooperation with the Circum-Pacific Council for Energy and Mineral Resources*, Circum-Pacific Map Series CP-45, scale 1:10,000,000, Washington, DC.
- Brown, R.J.E. (1960). The distribution of Permafrost and its relation to air temperature in Canada and the U.S.S.R. *Arctic*, 13, 3: 163-177.
- Brown, R.J.E. (1978). Influence of climate and terrain on ground temperatures in the continuous permafrost zone of northern Manitoba and Keewatin District, Canada, in *Proceedings, Third International Conference on Permafrost, July, Edmonton, Canada*. National Research Council of Canada, Ottawa, 1: 15-21.
- Burgess, M.M. and D.W. Riseborough (1990). Observations on the thermal response of discontinuous permafrost terrain to development and climate change – an 800 km transect along the Norman Wells pipeline, in *Proceedings, 5th Canadian Permafrost Conference*, Université Laval, Quebec City, Quebec, Nordicana 54: 291-297.
- Burgess, M.M. and S.L. Smith (2000). Shallow ground temperatures, in *The Physical Environment of the Mackenzie Valley, Northwest Territories: a Base Line for the Assessment of Environmental Change*, Edited by L.D. Dyke and G.R. Brooks. Geological Survey of Canada, Bulletin 547: 89-103.
- Burn, C.R. (2004). The Thermal Regime of Cryosols, in *Cryosols: Permafrost-Affected Soils*, Edited by J.M. Kimble. Springer, Germany: 391-413.

- Burn, C.R. and C.A.S. Smith (1988). Observations of the “Thermal Offset” in Near-Surface Mean Annual Ground Surface Temperatures at Several Sites near Mayo, Yukon Territory, Canada. *Arctic*, 40, 2: 99-104.
- CALM (2009). Circumpolar Active Layer Monitoring project: *Long-Term Observations of the Climate-Active Layer-Permafrost System*. URL: <http://www.udel.edu/Geography/calm/index.html> Site and data accessed November 2009.
- Camill, P. (2005). Permafrost Thaw Accelerates in Boreal Peatlands During late-20th Century Climate Warming. *Climate Change*, 68:135-152.
- Eley, J. (2005). Climate permafrost stations data sets 1985-2004. Climate Research Branch, Environment Canada.
- England, J. (1976). Postglacial isobases and uplift curves from the Canadian and Greenland High Arctic. *Arctic and Alpine Research*, 8: 61–78.
- Environment Canada (2009). Canada’s National Climate Archive online data. URL: http://climate.weatheroffice.ec.gc.ca/climateData/canada_e.html
- French, H.M. (2007). *The Periglacial Environment*, 3rd Edition, John Wiley and Sons Ltd., West Sussex, England.
- French, H.M. and O. Slaymaker (1993). Canada’s Cold Land Mass. *Canada’s Cold Environments*, Edited by H.M. French and O. Slaymaker. McGill-Queen’s University Press, Montreal and Kingston: 3-27.
- Goodrich, L.E. (1978). Some results of a numerical study of ground thermal regimes, in *Proceedings, Third International Conference on Permafrost, July, Edmonton, Canada*. National Research Council of Canada, Ottawa, 1: 29-34.
- Goodrich, L.E. (1982). The influence of snow cover on the ground thermal regime. *Canadian Geotechnical Journal* 19: 421–432.
- Google Earth 5.0.1, (2009). 63°15’35”N and 123°25’11”W.
- Gruber, S., L. King, T. Kohl, T. Herz, W. Haeberli, and M. Hoelzle (2004). Interpretation of Geothermal Profiles Perturbed by Topography: the Alpine Permafrost Boreholes at Stockhorn Plateau, Switzerland. *Permafrost and Periglacial Processes*, 15: 349-357.
- GTN-P (2009). Global Terrestrial Network for Permafrost. URL: http://www.gtnp.org/index_e.html

- Hansen, J., R. Ruedy, M. Sato, and R. Reynolds (1996). Global surface air temperature in 1995: Return to pre-Pinatubo level. *Geophysical Research Letters*, 23, 13: 1665-1668.
- Hanson, S. and M. Hoelzle (2005). Installation of a shallow borehole network and monitoring of the ground thermal regime of a high alpine discontinuous permafrost environment, Eastern Swiss Alps. *Norsk Geografisk Tidsskrift – Norwegian Journal of Geography*, 59: 84-93.
- Harris, C., D.V. Muhl, K. Isaksen, W.Haerberli, J.L. Sollid, L. King, P. Holmlund, F. Dramis, M. Guglielmin and D. Palacios (2003). Warming Permafrost in European Mountains. *Global and Planetary Change*, 39: 215-225.
- Heginbottom, J.A., M.A. Dubreuil and P.A. Harker (1995). Canada – Permafrost, in *National Atlas of Canada, 5th Edition*, National Atlas Information Service. Natural Resources Canada, Ottawa, MCR 4177.
- Hinkel, K.M. (1997). Estimating seasonal values of thermal diffusivity in thawed and frozen soils using temperature time series. *Cold Regions Science and Technology*, 26.
- Hinkel, K.M., F. Paetzold, F.E. Nelson, and J.G. Bockheim (2001). Patterns of soil temperature and moisture in the active layer and upper permafrost at Barrow, Alaska: 1993-1999. *Global and Planetary Change*, 29: 293-309.
- Hinkel K.M. and J.K. Hurd Jr. (2006). Permafrost destabilization and thermokarst following snow fence installation, Barrow, Alaska, U.S.A. *Arctic, Antarctic and Alpine Research*, 38: 530-539.
- IPCC (2007). *Climate Change 2007: Synthesis Report*. Working group contributions to the Fourth Assessment Report, Valencia, Spain, November 12-17. URL: <http://www.ipcc.ch/ipccreports/ar4-syr.htm>
- Isaksen, K., J.L. Sollid, P. Holmlund and C. Harris (2007). Recent warming of mountain permafrost in Svalbard and Scandinavia. *Journal of Geophysical Research*, 112.
- Ishikawa, M. (2002). Thermal regimes and the snow-ground interface and their implications for permafrost investigation. *Geomorphology*, 52: 105-120.
- Jessop, A.M., T.J. Lewis, A.S. Judge, A.E. Taylor and M.J. Drury (1984). Terrestrial Heat Flow in Canada. *Tectonophysics*, 103: 239-261.
- Jorgenson, M.T., C.H. Racine, J.C. Walters and T.E. Osterkamp (2001). Permafrost degradation and ecological changes associated with a warming climate in central Alaska. *Climatic Change*, 48: 551-579.

- Jorgenson, M.T., Y.L. Shur, and E.R. Pullman (2006). Abrupt increase in permafrost degradation in Arctic Alaska. *Geophysical Research Letters*, 33.
- Judge, A. (1973). The prediction of Permafrost Thicknesses. *Canadian Geotechnical Journal*, 10, 1.
- Karunaratne, K.C. (2002). N-factors and the Relations between Air and Surface Temperature in Discontinuous Permafrost near Mayo, Yukon Territory. MSc Thesis, Carleton University.
- Karunaratne K.C. and C.R. Burn (2003). Freezing n-factors in discontinuous permafrost terrain, Takhini River, Yukon Territory, Canada, in *Proceedings, Eighth International Conference on Permafrost, July 20-25*, Edited by M. Phillips, S.M. Springman and L.U. Arenson. University of Zurich, Switzerland: 519-524.
- Karunaratne, K.C. and C.R. Burn (2004). Relations between air and surface temperature in discontinuous permafrost terrain near Mayo, Yukon Territory. *Canadian Journal of Earth Sciences*, 41: 1437-1451.
- Karunaratne, K.C., S.V. Kokelj and C.R. Burn (2008). Near-Surface Permafrost Conditions near Yellowknife, Northwest Territories, Canada, in *Proceedings, Ninth International Conference on Permafrost, June 29-July 3*, Edited by D.L. Kane and K.M. Hinkel. University of Alaska, Fairbanks, Alaska, USA: 907-912.
- Klene, A.E., F.E. Nelson, N.I. Shiklomanov, and K.M. Hinkel (2001). The N-Factor in Natural Landscapes: Variability of Air and Soil-Surface Temperatures, Kuparuk River Basin, Alaska, USA. *Arctic, Antarctic, and Alpine Research*, 33, 2: 140-148.
- Kwong, Y.T. and T.Y. Gan (1994). Northward migration of permafrost along the Mackenzie highway and climate warming. *Climate Change*, 26: 399-419.
- Lachenbruch, A.H. and B.V. Marshall (1986). Changing Climate: Geothermal Evidence from Permafrost in the Alaskan Arctic. *Science*, 234: 689-696.
- Lewkowicz, A.G. (2008). Evaluation of Miniature Temperature-loggers to Monitor Snowpack Evolution at Mountain Permafrost Sites, Northwestern Canada. *Permafrost and Periglacial Processes*, 19: 323-331.
- Lewkowicz, A.G. and M. Ednie (2004). Probability Mapping of Mountain Permafrost Using the BTS Method, Wolf Creek, Yukon Territory, Canada. *Permafrost and Periglacial Processes*, 15: 67-80.

- Lunardini, V.J. (1978). Theory of n-factors and correlation of data, in *Proceedings, Third International Conference on Permafrost, July, Edmonton, Canada*. National Research Council of Canada, Ottawa, 1: 40-46.
- Nelson, F.E. and K.M. Hinkel (2003). Methods for Measuring Active-Layer Thickness, in *A Handbook on Periglacial Field Methods*, Version 20040406. Edited by O. Humlum and N. Matsuoka. Available on-line at:
http://www.unis.no/35_staff/staff_webpages/geology/ole_humlum/periglacialhandbook/handbookmain.htm
- Osterkamp, T.E. (2005). The recent warming of permafrost in Alaska. *Global and Planetary Change*, 49: 187-202.
- Osterkamp, T.E. (2007). Characteristics of the recent warming of permafrost in Alaska. *Journal of Geophysical Research*, 112.
- Osterkamp, T.E. (2008). Thermal State of Permafrost in Alaska during the Fourth Quarter of the Twentieth Century, in *Proceedings, Ninth International Conference on Permafrost, June 29-July 3*, Edited by D.L.Kane and K.M. Hinkel. University of Alaska, Fairbanks, Alaska, USA: 1333-1338.
- Osterkamp, T.E. and V.E. Romanovsky (1999). Evidence for Warming and Thawing of Discontinuous Permafrost in Alaska. *Permafrost and Periglacial Processes*, 10: 17-37.
- Outcalt, S.I. and K.M. Hinkel (1996). The Response of Near-Surface Permafrost to Seasonal Regime Transitions in Tundra Terrain. *Arctic and Alpine Research*, 28, 3: 274-283.
- Outcalt, S.I., F.E. Nelson and K.M. Hinkel (1990). The Zero-Curtain Effect: Heat and Mass Transfer Across an Isothermal Region in Freezing Soil. *Water Resources Research*, 26, 7: 1509-1516.
- Popova, V.V. and A.B. Shmakin (2009). The Influence of Seasonal Climatic Parameters on the Permafrost Thermal Regime, West Siberia, Russia. *Permafrost and Periglacial Processes*, 20: 41-56.
- Pullman, E.R., M.T. Jorgenson and Y. Shur (2007). Thaw Settlement in Soils of the Arctic Coastal Plain, Alaska. *Arctic, Antarctic and Alpine Research*, 39, 3: 468-476.
- Riseborough, D.W. (1990). Soil latent heat as a filter of the climate signal in permafrost, in *Proceedings, 5th Canadian Permafrost Conference*, Université Laval, Quebec City, Quebec, Nordicana 54: 199-205.

- Riseborough, D.W. (2008). Estimating Active Layer and Talik Thickness from Temperature Data: Implications from Modeling Results, in *Proceedings, Ninth International Conference on Permafrost, June 29-July 3*, Edited by D.L.Kane and K.M. Hinkel. University of Alaska, Fairbanks, Alaska, USA: 1487-1492.
- Riseborough, D.W. and M.M. Burgess (1996). Measurement Interval and the Accurate Assessment of Ground Temperature Trends. *Permafrost and Periglacial Processes*, 7: 321-335.
- Riseborough, D.W. and M.W. Smith (1998). Exploring the Limits of Permafrost, in *Proceedings, Permafrost: Seventh International Conference, Proceedings*, Edited by A.G. Lewkowicz and M. Allard. Yellowknife, Canada, Nordicana 55: 935-941.
- Romanovsky, V.E. and T.E. Osterkamp (1995). Interannual Variations of the Thermal Regime of the Active Layer and Near-Surface Permafrost in Northern Alaska. *Permafrost and Periglacial Processes*, 6: 313-335.
- Romanovsky, V.E. and T.E. Osterkamp (2000). Effects of Unfrozen Water on Heat and Mass Transport Processes in the Active Layer and Permafrost. *Permafrost and Periglacial Processes*, 11: 219-239.
- Smith, M.W. (1975). Microclimatic Influences on Ground Temperatures and Permafrost Distribution, Mackenzie Delta, Northwest Territories. *Canadian Journal of Earth Sciences*, 12: 1421-1438.
- Smith, M.W. and D.W. Riseborough (1996). Permafrost Monitoring and Detection of Climate Change. *Permafrost and Periglacial Processes*, 7: 301-309.
- Smith, M.W. and D.W. Riseborough (2002). Climate and the Limits of Permafrost: A Zonal Analysis. *Permafrost and Periglacial Processes*, 13.
- Smith, S.L., M.M. Burgess, and A.E. Taylor (2003). High Arctic permafrost observatory at Alert, Nunavut – analysis of a 23 year data set, in *Proceedings, Eighth International Conference on Permafrost, July 20-25*, Edited by M. Phillips, S.M. Springman and L.U. Arenson. University of Zurich, Switzerland: 1073-1078.
- Smith, S.L., M.M. Burgess, D.W. Riseborough, and F.M. Nixon (2005). Recent Trends from Canadian Permafrost Thermal Monitoring Network Sites. *Permafrost and Periglacial Processes*, 16: 19-30.
- Smith, S.L., S.A. Wolfe, D.W. Riseborough, and F.M. Nixon (2009). Active-Layer Characteristics and Summer Climatic Indices, Mackenzie Valley, Northwest Territories, Canada. *Permafrost and Periglacial Processes*, 20: 201-220.

- Smith, S.L., V.E. Romanovsky, A.G. Lewkowicz, C.R. Burn, M. Allard, G.D. Clow, K. Yoshikawa, and J. Throop (2010). Thermal State of Permafrost in North America – A Contribution to the International Polar Year. *Permafrost and Periglacial Processes*, submitted for review.
- Taylor, A.E. (1995). Field measurements of n-factors for natural forest areas, Mackenzie Valley, Northwest Territories, in *Current Research 1995-B, Geological Survey of Canada*: 89-98.
- Taylor, A.E. (2000). Relationship of ground temperatures to air temperatures in forests, in *The Physical Environment of the Mackenzie Valley, Northwest Territories: a Base Line for the Assessment of Environmental Change*, Edited by L.D. Dyke and G.R. Brooks. *Geological Survey of Canada, Bulletin*, 547: 111-117.
- Taylor, A.E., K. Wang, S.L. Smith, M.M. Burgess, and A.S. Judge (2006). Canadian Arctic Permafrost Observatories: Detecting contemporary climate change through inversion of subsurface temperature time series. *Journal of Geophysical Research*, 111.
- Taylor, A.E., M.M. Burgess, A.S. Judge, and V.S. Allen (2000). Deep Ground Temperatures, in *The Physical Environment of the Mackenzie Valley, Northwest Territories: a Baseline for the Assessment of Environmental Change*, Edited by L.D. Dyke and G.R. Brooks. *Geological Survey of Canada, Bulletin 547*: 105-109.
- Taylor, A.E., R.J.E. Brown, J. Pilon, and A.S. Judge (1982). Permafrost and the shallow thermal regime at Alert, N.W.T., in *The Roger J.E. Brown memorial volume: proceedings of the Fourth Canadian Permafrost Conference, Calgary, Alberta, March 2-6*, Edited by H.M. French. National Research Council of Canada, Ottawa: 12-22.
- Throop, J.L., S.L. Smith and A.G. Lewkowicz. (2008). Effect of a snow fence on the shallow ground thermal regime, Baker Lake, Nunavut, Canada, in *Extended Abstracts, Ninth International Conference on Permafrost, June 29-July 3*, Edited by D.L. Kane and K.M. Hinkel. University of Alaska, Fairbanks, Alaska, USA: 313-314.
- van Everdingen, R., ed. (2005). *Multi-language glossary of permafrost and related ground-ice terms*. Boulder, CO: National Snow and Ice Data Center/World Data Center for Glaciology.
- Wahl, H.E., D.B. Fraser, R.C. Harvey, and J.B. Maxwell (1987). Climate of Yukon. Climatological studies, Atmospheric Environment Services, Environment Canada, No. 40: 323 p.

- Williams, P.J. and M.W. Smith (1989). *The Frozen Earth: Fundamentals of Geocryology*. New York: Cambridge University Press.
- Woo, M., M. Mollinga, S.L. Smith (2007). Climate warming and active layer thaw in the boreal and tundra environments of the Mackenzie Valley. *Canadian Journal of Earth Sciences*, 44: 733-743.
- Wu, Q., Y. Zhu, and Y. Liu (2002). Evaluation model of permafrost thermal stability and thawing sensibility under engineering activity. *Cold Regions Science and Technology*, 34: 19-30.
- Zhang, Y., W. Chen, S.L. Smith, D.W. Riseborough, and J. Cihlar (2005). Soil temperatures in Canada during the twentieth century: Complex responses to atmospheric climate change. *Journal of Geophysical Research*, 110.

APPENDIX A

Resolution and Accuracy of Monitoring Equipment

Table A-1: Resolution and accuracy of monitoring equipment used at sites in this study.

Data Logging Instrument (use)	Sites where instrument is used	Accuracy	Resolution	Range
Hobo 12-bit temperature sensor (used for near surface ground temperatures with Onset HOBO Weather Stations)	Sixty Mile, Alpine Burwash	0.2°C or better from 0°C to 50°C	±0.03 from 0°C to 50°C	-40°C to +100°C
Hobo 12-bit Temperature RH Smart Sensor (used for air temperature with Onset HOBO Weather Stations)	Sixty Mile, Alpine Burwash	0.2°C at 0°C to 50°C	±0.02°C at 25°C	-40°C to +75°C
Hobo Temperature/External Temperature data logger: U23-004 (used for air, ground surface, and near surface temperatures)	Red Creek, Sixty Mile, Alpine Burwash, Wolf Creek APM and Palsa 25	±0.18°C at 25°C	0.02°C at 25°C	-40°C to +100°C
Thermochron iButton: DS1921G (used for snow depths)	Red Creek, Sixty Mile, Alpine Burwash, Wolf Creek APM and Palsa 25	±1°C between -30°C and 70°C, ±1.25°C outside this range	0.5°C	-40°C to +85°C
RBR Logger: XR-420 T8 (used for borehole temperature readings)	All sites in this study	±0.005°C	<0.00005°C	-40°C to +35°C
YSI thermistor cables	All sites in this study	±0.1°C*	±0.1°C*	
Vemco minilog (used for air and near surface temperatures)	Alert, Baker Lake, Table Mountain, Wrigley	±0.5°C*	±0.3°C*	
Campbell Scientific SR50M acoustic snow sensor	Alert, Iqaluit, Baker Lake, Table Mountain, Wrigley, and Wolf Creek APM	±1.0 cm	0.01 mm	

* Source: Smith et al., 2003, and Smith, personal communication 2010.

APPENDIX B

Correlations for air temperature Standardization between on-site weather station air temperatures and ECCS air temperatures.

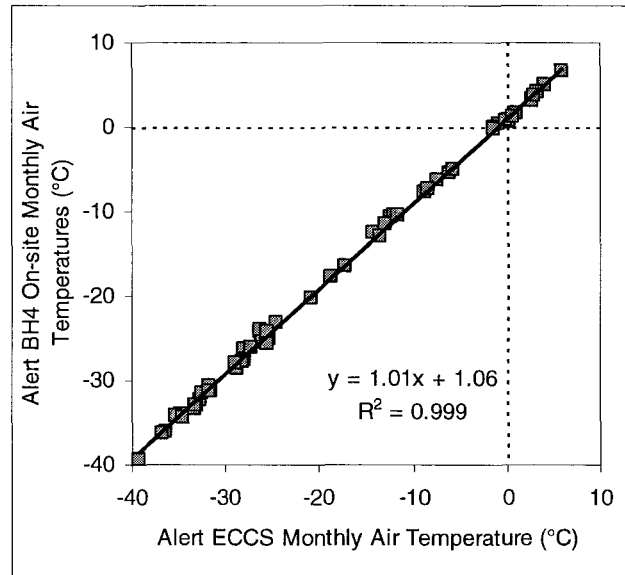


Figure B-1: Relationship between monthly average air temperatures at the Alert BH4 on-site weather station and the Alert ECCS (Environment Canada, 2009) from 2000 to 2006. The correlation is significant at $p < 0.001$.

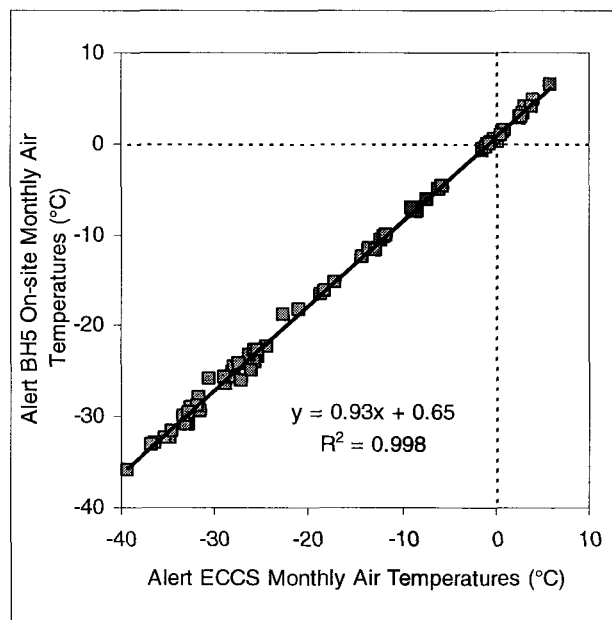


Figure B-2: Relationship between monthly average air temperatures at the Alert BH5 on-site weather station and the Alert ECCS (Environment Canada, 2009) from 2000 to 2006. The correlation is significant at $p < 0.001$.

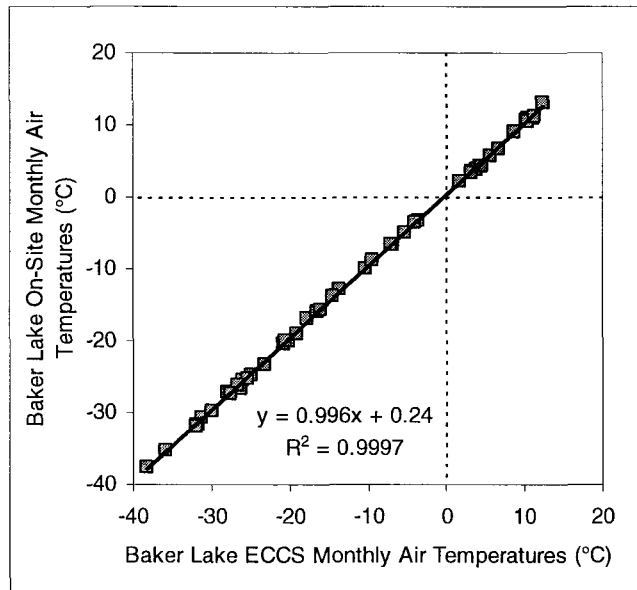


Figure B-3: Relationship between monthly average air temperatures at the Baker Lake on-site weather station and the Baker Lake ECCS (Environment Canada, 2009) from 2002 to 2006. The correlation is significant at $p < 0.001$.

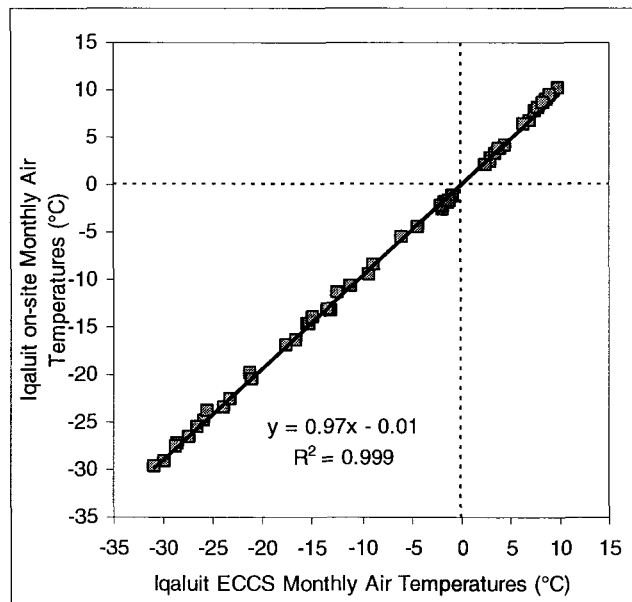


Figure B-4: Relationship between monthly average air temperatures at the Iqaluit on-site weather station and the Iqaluit ECCS (Environment Canada, 2009) from 2000 to 2004. The correlation is significant at $p < 0.001$.

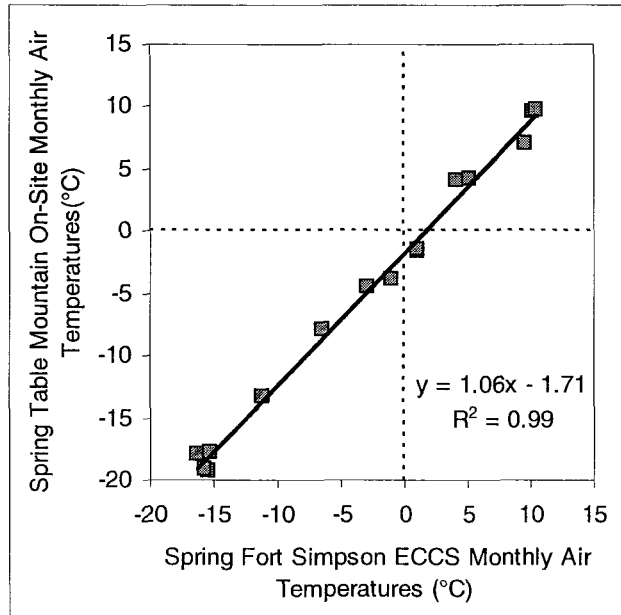


Figure B-5: Relationship between the average air temperatures during the spring months (March, April, and May) at the Table Mountain on-site weather station and the Fort Simpson ECCS (Environment Canada, 2009) from 2002 to 2008. The correlation is significant at $p < 0.001$.

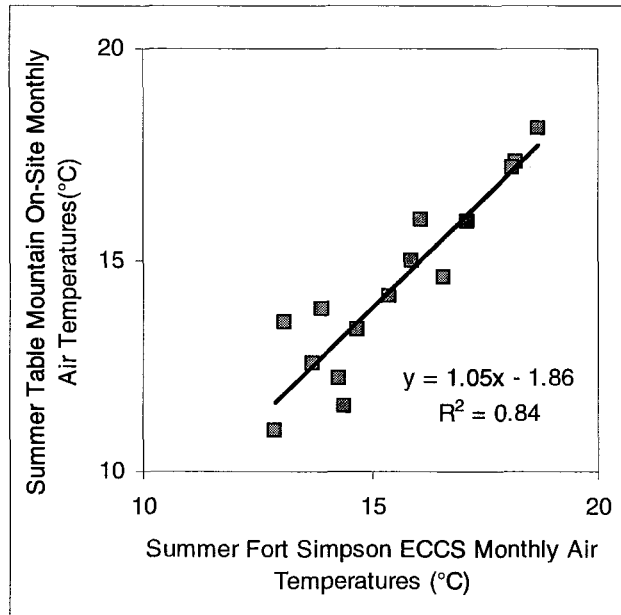


Figure B-6: Relationship between the average air temperatures during the summer months (June, July, and August) at the Table Mountain on-site weather station and the Fort Simpson ECCS (Environment Canada, 2009) from 2002 to 2008. The correlation is significant at $p < 0.001$.

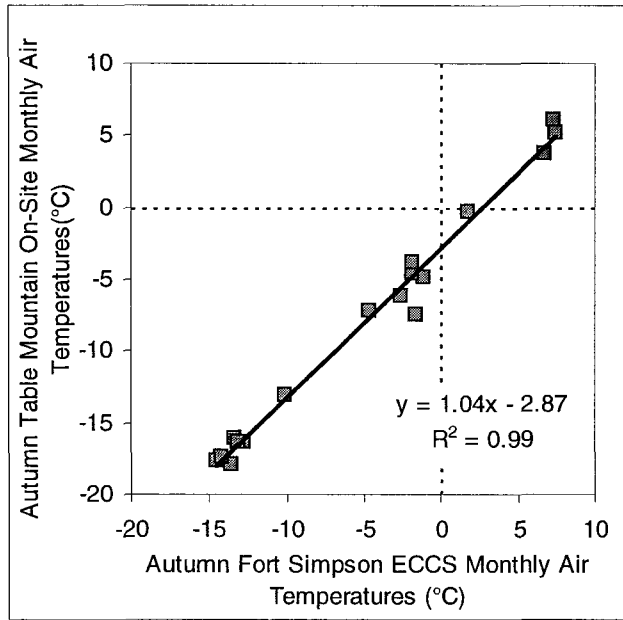


Figure B-7: Relationship between the average air temperatures during the autumn months (September, October, and November) at the Table Mountain on-site weather station and the Fort Simpson ECCS (Environment Canada, 2009) from 1999 to 2007. The correlation is significant at $p < 0.001$.

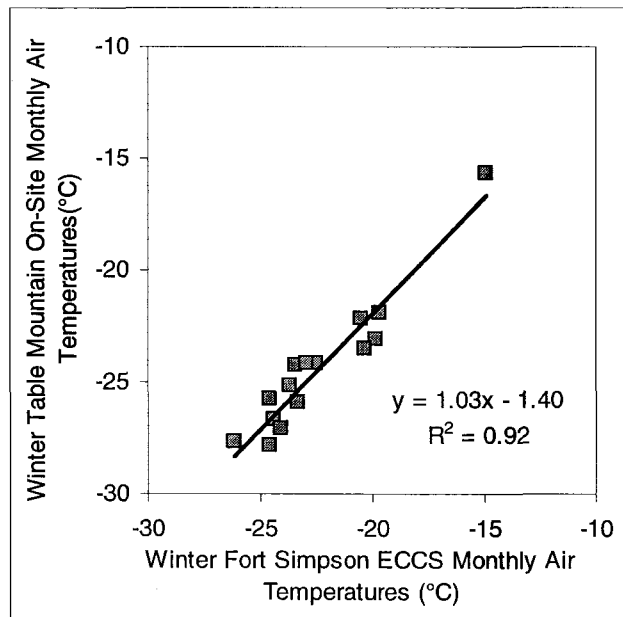


Figure B-8: Relationship between the average air temperatures during the winter months (December, January, and February) at the Table Mountain on-site weather station and the Fort Simpson ECCS (Environment Canada, 2009) from 1999 to 2008. The correlation is significant at $p < 0.001$.

APPENDIX C

The deviations used for MAGT standardization from manual data at Alert BH4, BH5, and Baker Lake BH4, and the MAGTs calculated using this method.

Table C-1: Table of average deviations from MAGT at Alert BH4 based on data from 2000 to 2002 and 2007 to 2008; these values are subtracted from the corresponding manual reading to obtain an expected MAGT for each reading.

10-day intervals	0.8 m	1.5 m	2.3 m	3.0 m	3.8 m	4.6 m	7.6 m	9.1 m
Aug 1-10	15.2	10.5	7.6	5.5	3.7	2.2	-1.0	-1.1
Aug 11-20	15.1	10.9	8.3	6.2	4.4	2.9	-0.5	-0.9
Aug 21-31	13.3	11.1	8.7	6.8	5.1	3.5	-0.1	-0.9
Sept 1-10	12.9	11.1	9.0	7.2	5.6	4.1	0.3	-0.6
Sept 11-20	11.8	10.9	9.1	7.5	6.0	4.6	0.7	-0.3
Sept 21-30	9.0	9.7	8.8	7.5	6.2	4.9	1.1	0.0
Oct 1-10	6.6	7.9	7.8	7.1	6.1	5.1	1.5	0.3
Oct 11-20	3.5	5.9	6.5	6.4	5.8	5.0	1.8	0.5
Oct 21-31	1.5	4.2	5.1	5.3	5.2	4.7	2.0	0.8
Nov 1-10	0.0	2.3	3.7	4.3	4.4	4.2	2.2	1.0
Nov 11-20	-3.2	0.1	2.1	3.1	3.6	3.7	2.2	1.2
Nov 21-30	-4.9	-1.9	0.3	1.7	2.6	3.0	2.2	1.3
Dec 1-10	-4.5	-3.0	-0.9	0.5	1.5	2.2	2.2	1.3
Dec 11-20	-5.7	-3.7	-1.8	-0.4	0.6	1.4	2.0	1.3
Dec 21-31	-6.3	-4.4	-2.5	-1.2	-0.1	0.7	1.8	1.3
Jan 1-10	-7.2	-5.4	-3.4	-1.9	-0.8	0.1	1.5	1.2
Jan 11-20	-8.2	-6.1	-4.1	-2.7	-1.5	-0.5	1.3	1.1
Jan 21-31	-9.7	-6.9	-4.9	-3.4	-2.1	-1.1	1.0	0.9
Feb 1-10	-9.4	-7.6	-5.6	-4.0	-2.7	-1.7	0.7	0.8
Feb 11-20	-9.9	-8.4	-6.3	-4.7	-3.3	-2.2	0.4	0.6
Feb 21-28/29	-10.1	-8.9	-6.8	-5.2	-3.8	-2.7	0.1	0.5
Mar 1-10	-10.9	-9.5	-7.4	-5.8	-4.3	-3.1	-0.2	0.3
Mar 11-20	-11.2	-10.2	-8.1	-6.4	-4.9	-3.7	-0.5	0.2
Mar 21-31	-11.8	-10.6	-8.6	-7.0	-5.5	-4.2	-0.8	0.0
Apr 1-10	-12.1	-10.2	-8.7	-7.3	-5.9	-4.7	-1.2	-0.2
Apr 11-20	-11.3	-9.6	-8.5	-7.3	-6.1	-5.0	-1.5	-0.3
Apr 21-30	-9.5	-8.7	-8.0	-7.1	-6.1	-5.1	-1.8	-0.5
May 1-10	-6.5	-6.4	-6.7	-6.5	-5.9	-5.1	-2.0	-0.7
May 11-20	-3.3	-4.1	-5.1	-5.4	-5.2	-4.8	-2.2	-0.8
May 21-31	0.1	-1.3	-3.1	-3.9	-4.2	-4.2	-2.3	-1.0
June 1-10	3.7	1.5	-0.9	-2.3	-3.0	-3.3	-2.3	-1.1
June 11-20	7.7	4.0	1.1	-0.7	-1.8	-2.4	-2.2	-1.2
June 21-30	11.3	6.6	3.2	1.0	-0.5	-1.4	-2.0	-1.3
July 1-10	13.3	8.4	5.0	2.7	0.9	-0.3	-1.7	-1.3
July 11-20	14.1	9.6	6.3	4.0	2.1	0.7	-1.4	-1.2
July 21-31	15.0	10.4	7.3	5.1	3.2	1.7	-1.0	-1.1

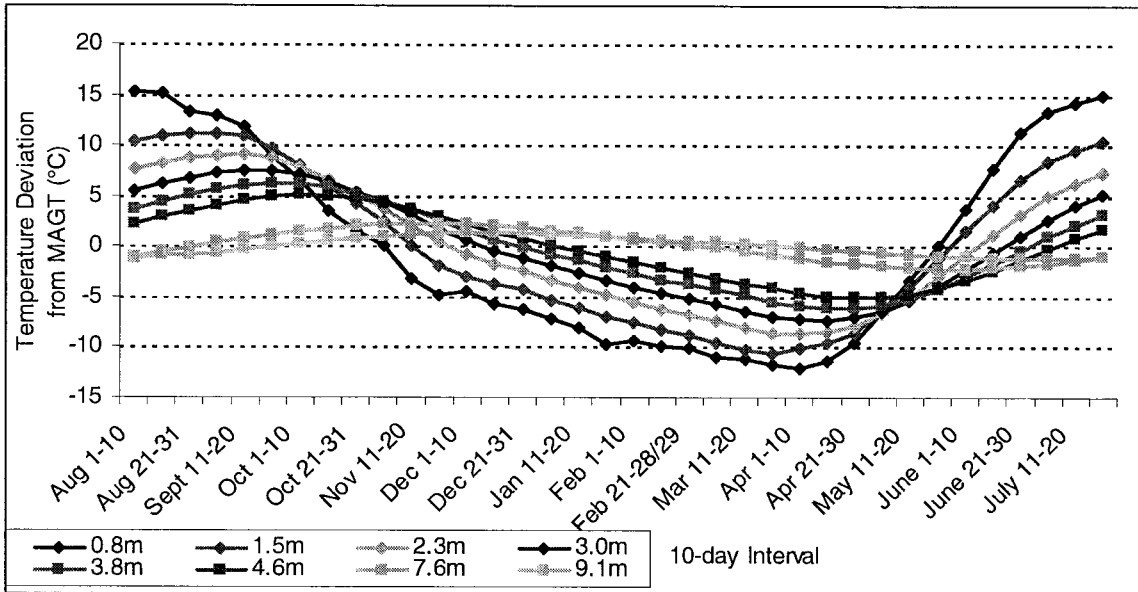


Figure C-1: The average deviations from the MAGT for each 10-day period at Alert BH4.

Table C-2: MAGTs at Alert BH4 calculated from discontinuous manual measurements between 1978 and 1988.

Year	0.8 m	1.5 m	2.3 m	3.0 m	3.8 m	4.6 m	7.6 m	9.1 m
1978-79	-15.9	-15.2	-15.1	-15.1	-14.8	-14.9	-15.4	-15.4
1979-80	-16.8	-16.4	-16.3	-16.0	-16.0	-16.0	-15.5	-15.4
1980-81	-14.7	-15.4	-15.5	-15.5	-15.6	-15.7	-15.6	-15.5
1981-82	-13.9	-14.3	-14.7	-14.7	-14.8	-14.9	-15.0	-15.0
1982-83	-14.0	-14.0	-14.2	-12.8	-14.5	-14.8	-15.2	-15.0
1983-84	-13.5	-15.3	-15.5	-15.7	-15.7	-15.8	-15.5	-15.1
1984-85	-18.1	-16.8	-16.3	-16.0	-15.8	-15.8	-15.6	-15.2
1985-86	-16.5	-16.5	-17.2	-16.6	-16.3	-16.3	-16.0	-15.5
1986-87	-12.0	-15.1	-15.4	-13.1	-12.7	-12.3	-16.2	-15.8
1987-88	-15.7	-15.2	-15.5	-15.4	-15.5	-15.6	-15.7	-15.3

Table C-3: Table of average deviations from MAGT at Alert BH5 based on data from 2000 to 2008; these values are subtracted from the corresponding manual reading to obtain an expected MAGT for each reading.

10-day intervals	0.8 m	1.5 m	2.3 m	3.0 m	4.6 m	7.6 m	9.1 m	15.2 m
Sept 1-10	13.8	11.2	9.0	7.4	4.6	0.8	0.0	-0.6
Sept 11-20	12.8	11.2	9.2	7.7	5.1	1.3	0.4	-0.6
Sept 21-30	10.1	10.3	9.1	7.8	5.4	1.7	0.7	-0.5
Oct 1-10	7.0	8.5	8.2	7.5	5.6	2.0	1.0	-0.5
Oct 11-20	4.4	6.2	6.8	6.6	5.4	2.3	1.3	-0.4
Oct 21-31	3.3	4.9	5.5	5.6	5.0	2.5	1.6	-0.3
Nov 1-10	-0.7	2.7	4.1	4.6	4.5	2.6	1.8	-0.2
Nov 11-20	-2.9	0.4	2.3	3.2	3.9	2.6	1.9	-0.1
Nov 21-30	-4.1	-1.1	0.8	1.9	3.0	2.5	2.0	0.0
Dec 1-10	-5.6	-2.4	-0.4	0.8	2.2	2.3	1.9	0.1
Dec 11-20	-6.2	-3.4	-1.5	-0.2	1.4	2.1	1.9	0.2
Dec 21-31	-7.0	-4.2	-2.3	-1.1	0.7	1.7	1.7	0.3
Jan 1-10	-8.0	-5.1	-3.2	-1.9	0.0	1.4	1.5	0.4
Jan 11-20	-8.5	-5.8	-3.9	-2.6	-0.7	1.0	1.3	0.4
Jan 21-31	-9.8	-6.8	-4.7	-3.4	-1.3	0.7	1.1	0.4
Feb 1-10	-10.3	-7.4	-5.5	-4.1	-1.9	0.4	0.8	0.5
Feb 11-20	-10.9	-8.1	-6.1	-4.7	-2.5	0.1	0.6	0.5
Feb 21-28/29	-11.4	-8.6	-6.7	-5.3	-3.0	-0.2	0.3	0.5
Mar 1-10	-13.1	-9.6	-7.3	-5.8	-3.5	-0.5	0.1	0.5
Mar 11-20	-13.8	-10.7	-8.3	-6.6	-4.1	-0.9	-0.2	0.4
Mar 21-31	-13.1	-10.8	-8.8	-7.3	-4.7	-1.2	-0.5	0.4
Apr 1-10	-11.4	-10.2	-8.8	-7.6	-5.2	-1.6	-0.8	0.4
Apr 11-20	-9.9	-9.3	-8.4	-7.4	-5.4	-1.9	-1.1	0.3
Apr 21-30	-7.3	-7.9	-7.6	-7.1	-5.5	-2.2	-1.4	0.2
May 1-10	-4.6	-6.0	-6.4	-6.3	-5.3	-2.4	-1.6	0.2
May 11-20	-1.3	-4.0	-5.0	-5.3	-5.0	-2.6	-1.8	0.1
May 21-31	2.0	-1.5	-3.2	-4.0	-4.3	-2.6	-1.9	0.0
June 1-10	5.3	1.0	-1.3	-2.5	-3.5	-2.6	-2.0	-0.1
June 11-20	8.1	3.3	0.6	-1.0	-2.6	-2.5	-2.0	-0.2
June 21-30	11.3	5.8	2.5	0.7	-1.5	-2.2	-1.9	-0.3
July 1-10	12.8	7.6	4.4	2.3	-0.4	-1.9	-1.7	-0.4
July 11-20	13.5	8.8	5.7	3.6	0.7	-1.6	-1.5	-0.4
July 21-31	14.2	10.5	8.1	6.3	3.8	1.3	1.3	1.9
Aug 1-10	14.3	10.4	7.6	5.7	2.7	-0.6	-0.9	-0.5
Aug 11-20	14.3	10.8	8.3	6.4	3.4	-0.1	-0.6	-0.5
Aug 21-31	14.2	11.2	8.8	7.1	4.2	0.5	-0.2	-0.5

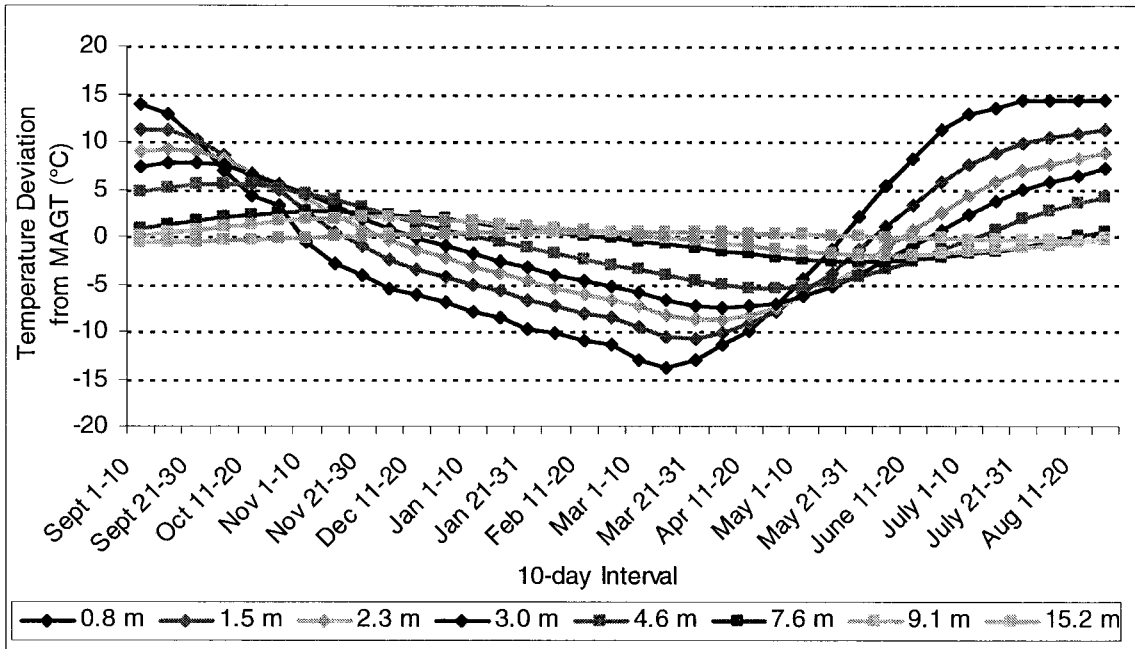


Figure C-2: The average deviations from the MAGT for each 10-day period at Alert BH5.

Table C-4: MAGTs at Alert BH5 calculated from discontinuous manual measurements between 1978 and 2000.

Year	0.8 m	1.5 m	2.3 m	3.0 m	4.6 m	7.6 m	9.1 m	15.2 m
1978-79	-16.3	-16.1	-15.9	-15.7	-15.4	-15.6	-15.7	-15.5
1979-80	-16.4	-16.2	-16.1	-16.1	-15.6	-15.7	-15.7	-15.3
1980-81	-15.6	-16.2	-16.1	-16.0	-15.5	-15.8	-15.8	-15.4
1981-82	-14.3	-14.8	-15.1	-15.1	-15.0	-15.4	-15.4	-15.2
1982-83	-14.8	-14.8	-15.3	-15.0	-15.0	-15.4	-15.4	-15.2
1983-84	-16.5	-16.2	-16.2	-16.1	-15.6	-15.6	-15.6	-15.1
1984-85	-16.4	-16.2	-15.9	-15.7	-15.1	-15.4	-15.3	-15.0
1985-86		-17.3	-17.1	-17.5	-15.6	-16.0	-15.9	-15.0
1986-87								
1987-88	-16.2	-15.1	-15.5	-15.8	-15.7	-15.6	-15.6	-15.3
1988-89	-15.2	-15.3	-15.2	-15.1	-15.0	-14.9	-15.0	-14.9
1989-90	-15.2	-15.2	-15.2	-15.1	-13.6	-15.1	-15.1	-14.8
1990-91	-16.3	-16.3	-16.2	-15.9	-15.6	-15.2	-15.2	-14.8
1991-92	-16.3	-16.1	-15.8	-15.7	-15.8	-15.1	-15.1	-14.8
1992-93	-16.5	-16.5	-16.2	-16.3	-16.4	-15.9	-15.8	-15.2
1993-94	-16.2	-16.0	-15.8	-15.7	-15.6	-15.5	-15.6	-15.2
1994-95	-18.1	-17.3	-16.7	-16.3	-15.8	-15.4	-15.5	-15.2
1995-96	-14.1	-14.7	-15.0	-15.1	-15.3	-15.4	-15.5	-15.1
1996-97								
1997-98	-14.7	-14.9	-15.0	-14.9	-14.8	-14.6	-14.6	-14.6
1998-99								
1999-00	-15.5	-16.0	-16.3	-16.3	-16.3	-15.6	-15.5	-14.7

Table C-5: Table of average deviations from MAGT at Baker Lake BH4 based on data from 2002 to 2003 and 2005 to 2006; these values are subtracted from the corresponding manual reading to obtain an expected MAGT for each reading.

10-day interval	0.5 m	1.0 m	2.0 m	2.5 m	3.0 m
Sept 1-10	11.5	10.4	7.2	6.0	5.2
Sept 11-20	10.1	9.4	7.2	6.1	5.3
Sept 21-30	5.7	6.8	6.8	6.1	5.4
Oct 1-10	4.3	5.9	6.6	6.1	5.5
Oct 11-20	3.7	5.6	6.4	6.1	5.6
Oct 21-31	2.9	5.1	5.9	5.9	5.6
Nov 1-10	1.0	3.6	4.7	5.2	5.3
Nov 11-20	-0.4	2.4	3.9	4.6	4.9
Nov 21-30	-3.0	0.0	2.2	2.8	3.1
Dec 1-10	-5.4	-2.4	0.1	0.9	0.8
Dec 11-20	-6.7	-4.1	-1.0	-0.2	0.0
Dec 21-31	-7.6	-4.7	-2.0	-1.1	-0.8
Jan 1-10	-7.5	-4.9	-2.3	-1.4	-0.7
Jan 11-20	-9.3	-6.5	-3.6	-2.8	-2.3
Jan 21-31	-11.5	-8.8	-5.4	-4.5	-4.3
Feb 1-10	-12.9	-10.4	-6.8	-5.8	-5.3
Feb 11-20	-14.0	-11.4	-7.9	-6.9	-6.3
Feb 21-28/29	-15.4	-12.6	-9.0	-7.9	-7.3
Mar 1-10	-15.1	-12.9	-9.4	-8.2	-7.1
Mar 11-20	-14.2	-11.9	-9.0	-7.8	-6.5
Mar 21-31	-11.9	-10.2	-8.0	-7.1	-5.7
Apr 1-10	-12.0	-10.1	-7.7	-6.7	-5.4
Apr 11-20	-10.0	-9.1	-7.3	-6.4	-5.2
Apr 21-30	-6.6	-6.6	-6.1	-5.6	-4.8
May 1-10	-5.2	-5.2	-5.1	-4.7	-4.2
May 11-20	-0.3	-2.3	-3.8	-3.8	-3.5
May 21-31	3.4	1.5	-1.1	-1.9	-2.1
June 1-10	6.4	4.0	1.1	0.0	-0.6
June 11-20	10.4	5.7	2.6	1.4	0.7
June 21-30	12.1	6.6	3.7	2.5	1.7
July 1-10	13.8	7.6	4.3	3.2	2.5
July 11-20	15.1	9.1	4.8	3.8	3.0
July 21-31	17.5	11.4	5.6	4.4	3.6
Aug 1-10	18.0	12.5	6.3	5.0	4.2
Aug 11-20	16.0	12.4	6.8	5.5	4.6
Aug 21-31	13.2	11.1	7.2	5.8	4.9

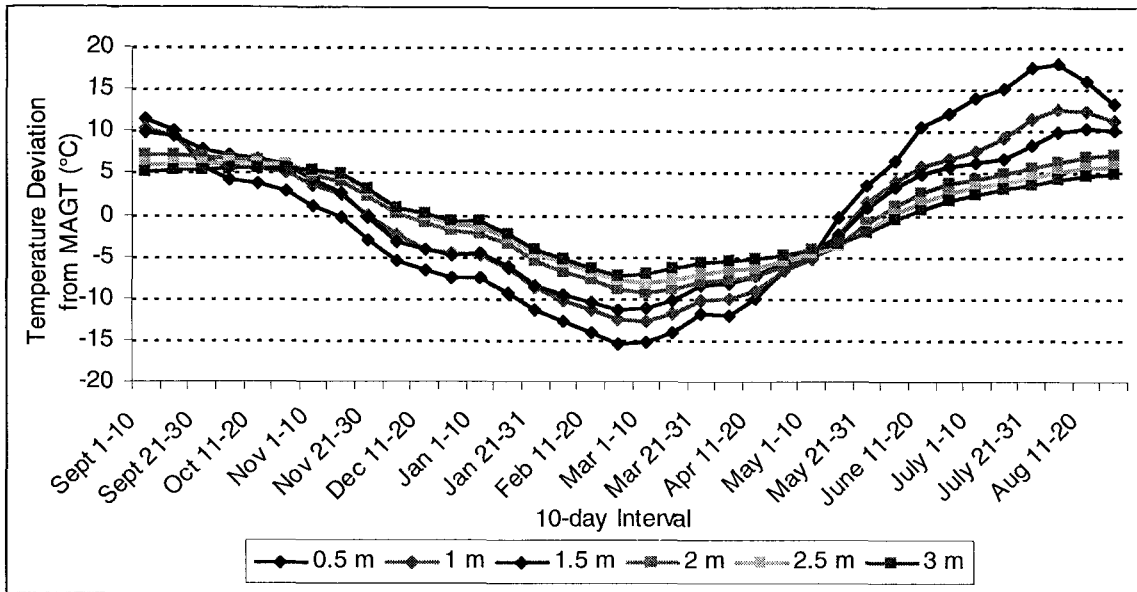


Figure C-3: The average deviations from the MAGT for each 10-day period at Baker Lake BH4.

Table C-6: MAGTs at Baker Lake BH4 calculated from discontinuous manual measurements between 1997 and 2005.

Year	0.5 m	1.0 m	2.0 m	2.5 m	3.0 m
1997-98	-7.6	-7.6	-7.8	-8.2	-8.2
1998-99	-5.4	-5.8	-6.3	-6.5	-6.6
1999-00	-3.5	-4.0	-5.1	-5.3	-5.5
2000-01	-6.8	-6.6	-7.0	-7.2	-7.2
2001-02	-2.3	-3.0	-4.8	-5.4	-5.7
2002-03	-5.1	-6.0	-6.9	-7.5	-7.8
2003-04	-2.5	-4.1	-5.1	-5.8	-6.3
2004-05	-7.8	-7.9	-6.8	-7.9	-8.1